

In Vitro Models of Glioblastoma Targeting Cancer Metabolism

by

Alexander Lincoln Wilding

BBiomedSc (Hons) (Monash University) 2006

**A thesis submitted in accordance with the requirements
for the degree of**

Doctor of Philosophy

at

Monash University

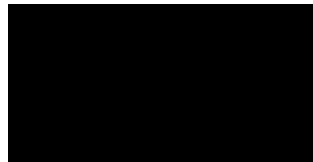
2014

Under the Copyright Act 1968, this thesis must be used only under the normal conditions of scholarly fair dealing. In particular no results or conclusions should be extracted from it, nor should it be copied or closely paraphrased in whole or in part without the written consent of the author. Proper written acknowledgement should be made for any assistance obtained from this thesis.

I certify that I have made all reasonable efforts to secure copyright permissions for third-party content included in this thesis and have not knowingly added copyright content to my work without the owner's permission.

In accordance with Monash University Regulation 17.2 Doctor of Philosophy regulations the following declaration is made:

I hereby declare that this thesis contains no material which has been accepted for the award of any other degree or diploma at any university or equivalent institution and that, to the best of my knowledge and belief, this thesis contains no material previously published or written by another person except where due reference is made.

A solid black rectangular box used to redact the author's signature.

Alexander Wilding

26th June 2014

Summary

Glioblastoma (GBM) is a highly lethal and incurable primary tumour of the brain and central nervous system (CNS). While the genetic alterations in GBM are highly heterogeneous, most tumours exhibit changes promoting activation of RTK signalling and inactivation of Rb and p53 signalling pathways. As with other cancer types, the metabolism of rapidly proliferating tumour cells in GBM is dramatically different to that of their normal, non-proliferating counterparts. The most notable alteration is that of 'aerobic glycolysis', the propensity to metabolise glucose to lactate, even in the presence of oxygen. These changes are believed to support the increased proliferation rate and resistance to therapy that typify this and other types of cancer.

Our understanding of how metabolic changes support tumour growth is still poor. Nevertheless, the conservation of these changes across diverse tumour types highlights their importance and suggests that cancer metabolism is a potential therapeutic target. In particular PKM2, an isozyme of the glycolytic enzyme pyruvate kinase is highly expressed in most cancers including GBM and appears to facilitate many metabolic features of cancer including aerobic glycolysis. Universal expression of PKM2 in cancer makes it an appealing target for therapy and both activators and inhibitors of PKM2 have been investigated as potential therapeutic options.

Using *in vitro* models, this thesis explores the effects of a number of compounds that target or otherwise modulate cell metabolism. It is hoped that an understanding of how these compounds affect cancer cell metabolism will contribute to the development of novel therapeutic strategies for the treatment of glioma, as well as other cancers.

In Chapter 3, a methodology is developed for assaying the anti-proliferative effects of combinations of drugs on glioma cells *in vitro*, comparing different approaches to assess antagonistic and synergistic drug interactions.

In Chapter 4 of this dissertation, the factors that regulate tetramer formation and catalytic activity of PKM2 were examined in glioblastoma cell lines. Novel methods for the detection of PKM2 complex formation, pyruvate kinase activity and glycolytic rate were developed. The ability of a novel PKM2 activator to induce PKM2 tetramer formation and catalytic activity was assessed. We then attempted to exploit the effects of the PKM2 activator to affect cell metabolism in an attempt to identify a therapeutic application of pharmacologic PKM2 activation.

In Chapter 5, investigating the effects of TORC1 inhibition using Temsirolimus on PKM2 tetramer formation led to the observation that TORC1 inhibition results in rapid inhibition of glycolysis and a reversal of the Crabtree effect. While the precise target could not be identified, glucose metabolism appeared to be at the level of hexokinase or glucose transport, as both glycolysis and the PPP were affected. We then go on to demonstrate that this block in glucose metabolism induces a striking sensitivity to oxidative stress as would be encountered by glioma cells exposed to IR therapy.

In Chapter 6, the multi-kinase inhibitor Sorafenib was identified as exhibiting rapid and potent inhibitory effects on mitochondrial function in glioma cells leading to a reliance on glycolysis for ATP production. Detailed analysis of mitochondrial respiratory function the utility of simultaneous inhibition of respiration and glycolysis using Sorafenib and the glycolysis inhibitor 2-deoxyglucose as a therapeutic strategy is then evaluated *in vitro* and *in vivo*.

Table of Contents

List of abbreviations.....	vi
Chapter 1 – Introduction.....	1
Chapter 2 - Materials and Methods.....	87
Chapter 3 - Development of a Synergy Drug Screen	103
Chapter 4 - Regulation of Pyruvate Kinase in Glioma.....	143
Chapter 5 - Inhibition of Glucose Metabolism by Temsirolimus	179
Chapter 6 - Inhibition of Respiration with Sorafenib.....	197
Chapter 7 – General Discussion	225

List of abbreviations

2-DG	2-deoxyglucose
3-BrP	3-bromopyruvate
5,10-mTHF	5,10-Methylenetetrahydrofolate
AA	Antimycin A
AC	Activated carbon
ADP	Adenosine diphosphate
AMP	Adenosine monophosphate
AMPK	AMP-activated protein kinase
ANOVA	Analysis of variance
ATP	Adenosine triphosphate
BCA	Bicinchoninic acid
bFGF	Basic fibroblast growth factor
BLLB	Biotin labelling lysis buffer
BN-PAGE	Blue native polyacrylamide gel electrophoresis
bp	Base pair
CI	Combination index
CNS	Central nervous system
CoA	Coenzyme A
CoQ	Coenzyme Q ₁₀ , ubiquinone
DCA	Dichloroacetate
DHODH	Dihydroorotate dehydrogenase
DMEM	Dulbecco's Modified Eagle Medium
DMSO	Dimethyl sulfoxide
DNA	Deoxyribonucleic acid
DNP	2,4-dinitrophenol
DSB	Double stranded break
DTT	Dithiothreitol
ECAR	Extracellular acidification rate

EDTA	Ethylenediaminetetraacetic acid
EGF	Epidermal growth factor
EGFR	Epidermal growth factor receptor
EGFRvIII	Epidermal growth factor receptor variant 3
Em	Emission wavelength
Ex	Excitation wavelength
FAD	Flavin adenine dinucleotide
FBP	Fructose 1,6-bisphosphate
FCCP	Carbonyl cyanide p-trifluoro-methoxyphenyl hydrazone
FCS	Fetal calf serum
FDA	Food and Drug Administration
FDG	Fluorodeoxyglucose
G ₁	Growth 1 phase of the cell cycle
G ₂	Growth 2 phase of the cell cycle
G6P	Glucose-6-phosphate
G6PDH	Glucose-6-phosphate dehydrogenase
GAP	GTPase-activating protein
GAPDH	Glyceraldehyde 3-phosphate dehydrogenase
GBM	Glioblastoma multiforme
GDP	guanosine diphosphate
GPDH	Glycerol-3-phosphate dehydrogenase
GSSG	Glutathione disulfide
GTP	guanosine triphosphate
HGF	Hepatocyte growth factor
HIF	Hypoxia-inducible factor
HK	Hexokinase
IC ₅₀	Half maximal inhibitory concentration
IGF	Insulin-like growth factor
IL-2	Interleukin 2

IR	Ionising radiation
k_i	dissociation constant
K_m	Michaelis–Menten kinetics - substrate concentration achieving half V_{max}
LDH	Lactate Dehydrogenase
M	Mitotic phase of the cell cycle
MAPK	Mitogen-activated protein kinase
MAPKK	Mitogen-activated protein kinase kinase
MAPKKK	Mitogen-activated protein kinase kinase kinase
MGMT	O ⁶ -alkylguanine DNA alkyltransferase
MOPS	3-(N-morpholino)propansulfonic acid
mRNA	Messenger RNA
MTIC	5-(3-methyltriazen-1-yl)imidazole-4-carboxamide
mTOR	Mammalian target of rapamycin
MTS	3-(4,5-dimethylthiazol-2-yl)-5-(3-carboxymethoxyphenyl)-2-(4-sulfophenyl)-2H-tetrazolium
NAD	Nicotinamide adenine dinucleotide
NADP	Nicotinamide adenine dinucleotide phosphate
ns	Not significant
O ⁶ -MeG	O ⁶ -methylguanine
OCR	Oxygen consumption rate
Oligo	Oligomycin
oxPPP	Oxidative arm of the pentose phosphate pathway
PBS	Phosphate buffered saline
PCV	Procarbazine/CCNU/vincristine
PDGF	Platelet derived growth factor
PDH	Pyruvate dehydrogenase
PDK	Pyruvate dehydrogenase kinase
PEP	Phosphoenolpyruvate
PET	Positron emission tomography

PFK	Phosphofructokinase
P _i	Inorganic Phosphate
PI	Propidium Iodide
PI-3,4,5-P ₃	Phosphatidylinositol (3,4,5)-trisphosphate
PI3K	Phosphoinositide 3-kinase
PI-4,5-P ₂	Phosphatidylinositol (4,5)-disphosphate
PK	Pyruvate kinase
PMS	Phenazine methosulfate
PPP	Pentose phosphate pathway
PTP	Permeability transition pore
PVDF	Polyvinylidene fluoride
r ²	R-squared - coefficient of determination
RCR	Respiratory control ratio
RNA	Ribonucleic acid
RNAi	RNA interference
ROS	Reactive oxygen species
Rot	Rotenone
RTK	Receptor Tyrosine Kinase
S	Synthesis phase of the cell cycle
SDS-PAGE	Sodium dodecyl sulfate polyacrylamide gel electrophoresis
shRNA	short hairpin RNA
SOD	Superoxide dismutase
SSB	Single stranded break
TCA	Tricarboxylic acid cycle
TMPD	N,N,N',N'-tetramethyl-p-phenylenediamine
TMZ	Temozolomide
VDAC	Voltage dependent anion channel
VEGF	Vascular endothelial growth factor
V _{max}	Michaelis–Menten kinetics - maximum reaction rate

WHO	World Health Organisation
ΔG	Gibbs energy
$\Delta\Psi_m$	Mitochondrial membrane potential

Chapter 1 – Introduction

Table of Figures	5
Introduction to glioblastoma.....	6
Treatment of Glioblastoma	7
Ionising radiation	7
Temozolomide	8
Bevacizumab (Avastin).....	11
Targeted therapy	12
RTK-Ras-PI3K signalling.....	14
EGFR.....	16
c-Met.....	18
PI3K-Akt	19
TORC1	20
Ras-Raf-MAPK.....	22
Cancer Metabolism	23
Glycolysis.....	25
Mitochondrial respiration and the TCA cycle	27
Anaplerosis and cataplerosis.....	29
The electron transport chain.....	30
Mitochondrial reactive oxygen species.....	32
Relationship of glycolysis, fermentation and respiration	32

The Pasteur effect	33
The Crabtree effect	34
The Warburg effect	35
Why do cancer cells have increased glycolysis?.....	37
Warburg hypothesis	37
Suppression of ROS	37
Supply of biomolecules	38
Respiration is essential for proliferation	42
Regulation of Glucose Metabolism	43
Glucose transport	44
Hexokinase	45
Hexokinase isoforms.....	45
Regulation of hexokinase.....	46
Interaction of hexokinase with mitochondria	46
Akt interacts with hexokinase to regulate metabolism and apoptosis	47
Phosphofructokinase.....	48
Phosphofructokinase isoforms	48
Regulation of phosphofructokinase.....	49
Regulation by F2,6BP	49
TIGAR suppresses PFK1 activity to promote survival of glioma cells.....	50
Pyruvate Kinase	51
Pyruvate kinase isoforms.....	52

PK-L and PK-R	52
PK-M1 and PK-M2	52
Regulation of pyruvate kinase	53
Re-expression of PKM2 during carcinogenesis.....	55
Liver	55
Brain	56
Other tissues	57
Unique regulatory features of PKM2 support tumour growth.....	58
Oncogenic signalling inhibits PKM2	59
Serine phosphorylation of PKM2	60
PKM2 and redox balance	60
Serine metabolism	61
Regulation of PKM2 by A-Raf.....	62
PKM2 and aerobic glycolysis.....	62
Regulation of Pyruvate Metabolism.....	63
Pyruvate dehydrogenase	64
Lactate dehydrogenase.....	65
Hypoxia Inducible Factors	65
Akt-TORC1 and HIF signalling.....	67
Signalling Pathways Dysregulated in Glioma Affect Cell Metabolism.....	68
Akt.....	68
P53	69

Summary.....	70
References.....	73

Table of Figures

Figure 1.1 Interaction network of proteins frequently altered in GBM.	16
Figure 1.2. Glycolysis and branching pathways.	27
Figure 1.3. The Tricarboxylic Acid Cycle.....	28
Figure 1.4. The Tricarboxylate Transport System	29
Figure 1.5. The mitochondrial electron transport chain.....	31
Figure 1.6. Quantitative Principles of Metabolic Control.	41

Introduction to glioblastoma

Gliomas are a class of tumour that develop within the brain or less commonly in other parts of the central nervous system (CNS) which, based on histological morphology, appear to arise from astrocytic, oligodendroglial and ependymal (supportive, non-neuronal) lineages. Gliomas account for over 70% of all primary brain tumours. Of these, the most malignant histological subtype is glioblastoma multiforme (or simply glioblastoma, GBM), which accounts for 65% of all primary brain tumours (Ohgaki and Kleihues, 2005). While the incidence of primary brain tumours only makes up around 1.4% of all cancer cases in Australia, the mortality rate is disproportionately high, contributing to 2.8% of all cancer deaths in this country (Australian Institute of Health and Welfare, 2012)

Gliomas can be stratified into low grade (World Health Organisation, WHO grade I and II) and high grade (WHO grade III and IV) based on the degree of malignancy (Brat et al., 2008). Only WHO grade I gliomas are considered completely curable. While grade IV gliomas most frequently arise *de novo* (primary GBM) in older patients, grade II and III gliomas arising in younger patients can eventually progress to grade IV, so-called secondary GBM. The mortality rate of GBM is exceptionally high, with one and five year post diagnosis survival rates of only 28% and 2.9% respectively (Ohgaki and Kleihues, 2005).

GBM is highly aggressive, and is the most polymorphic of any known neoplasm. Necrotic foci surrounded by layers of proliferating endothelium forming so-called 'pseudopalisading necrosis' is the most distinguishing feature of glioblastoma (Rong et al., 2006, Louis et al., 2007). Microvascular proliferation and glomeruloid vascular structures are also typical histopathological features (Rojiani and Dorovini-Zis, 1996). As with all brain tumours WHO grade II and above, the boundaries of GBM are highly diffuse making complete surgical resection all but impossible (Crespo et al., 2012).

The standard of care treatment of GBM is a combination of tumour debulking surgery, radiation and alkylating agent based chemotherapy. While GBM is often initially responsive to these

treatments, tumours almost invariably recur within close proximity to the original tumour site and with acquired resistance to these therapies.

Growth of tumours within the confines of the intracranial cavity can rapidly lead to increased intracranial pressure and neurological dysfunction. Eventually, uncontrolled growth leads to herniation of the brain stem, leading to depression of respiratory function and death. Complications from surgery (such as cerebral haemorrhage and oedema) and radiation induced brain injury during the treatment of GBM are also major causes of death in GBM patients (Silbergeld et al., 1991)

Treatment of Glioblastoma

The current standard of care treatment for patients with newly diagnosed high grade gliomas includes surgical debulking of the tumour mass, followed by adjuvant chemotherapy and radiation. In the 1970s, radiation therapy following surgical tumour debulking was shown to have substantial clinical benefit, extending median survival time from 5.2 to 10.8 months (Kristiansen et al., 1981).

Ionising radiation

DNA damage is believed to be the primary target of ionising radiation (IR) used for the treatment of high grade gliomas. IR can affect DNA directly, or more often indirectly through radiolysis of water to produce free radicals (molecules, atoms or ions with unpaired valance electrons) that can then react with DNA to produce DNA radicals. These reactions ultimately result in chemical modification of DNA bases, single stranded breaks (SSBs) and double stranded breaks (DSBs) in the ribose-sugar backbone of DNA. Sensitivity of cells to DNA damage is increased dramatically during the G₂/M phase of the cell cycle. The elevated proliferation rate of cancer cells together with defects in DNA repair and cell cycle checkpoint control can explain much of the selective sensitivity of cancer cells over normal cells to the effects of ionising radiation.

Oxygenation is a major factor affecting sensitivity of cells to IR. Hypoxia is frequently observed in many tumour types including glioma and is considered a major hurdle to effective radiation therapy. Low oxygen tension leads to an intrinsic resistance to IR as well as cell adaptive responses. Radicals produced by radiolysis of water are relatively short lived, and can only damage DNA when formed in very close proximity to their target. However when present, redox reactions with molecular oxygen drive the formation of longer lived species which can then diffuse a greater distance to then form DNA radicals.

DNA radicals themselves are also highly reactive and short lived species. Reactions with radical-reducing species, typically reduced thiol moieties such as glutathione, results in “chemical repair” of the lesion, preventing the formation of SSBs and DSBs (Prise et al., 1998). However reactions with radical-oxidising species such as molecular oxygen results in “fixation” of the damage which can no longer be repaired by thiols. Thus sensitivity of a cell to IR is highly influenced by oxygen tension and the redox state of the cell (Chapman et al., 1973).

Temozolomide

In the decades following the introduction of IR therapy for GBM, improvements in radiation therapy as well as the introduction of alkylating agents has resulted in minor incremental improvements in survival time, however outcome remains dismal. The most notable advancement in glioma therapy has been the introduction of temozolomide, approved by the FDA for use in anaplastic astrocytoma (a grade III glioma) in 1999, and glioblastoma in 2005. Temozolomide was approved for use as frontline therapy in glioblastoma in response to a phase 3 clinical trial, which demonstrated that the addition of temozolomide to standard radiation therapy extended median survival time from 12.1 to 14.6 months (Stupp et al., 2005). This was the first phase 3 trial to show a clear improvement in survival with the use of nitrosurea based alkylating agents.

Temozolomide is an orally available pro-drug, stable in acid (enabling oral drug delivery), and is spontaneously hydrolysed to the active compound, MTIC at basic, physiologic pH. Monomethyl

triazeno imidazole carboxamide (MTIC) is an alkylating agent, stable only under basic conditions, which transfers its methyl group primarily to DNA nucleophiles (functional groups of DNA bases that donate electron pairs to electrophiles to form a chemical bond) (Newlands et al., 1997). The dependence on basic conditions for MTIC activation and stability was suggested to be a contributing factor for its efficacy against gliomas, which are typically more basic than normal brain white and grey matter (Vaupel et al., 1989) However one should note that different detection techniques have shown gliomas to be slightly basic, or amongst the most acidic of all tumour types (Vaupel et al., 1989).

Following FDA approval in response to the Stupp trial, a subsequent trial demonstrated that in terms of overall survival or progression free survival, the benefit of TMZ over the previous 'PCV regimen' (a combination of the alkylating agents procarbazine, CCNU (lomustine) and vincristine) is marginal at best (Brada et al., 2010) however TMZ is preferred because of significantly reduced adverse side effects and the ease of out-patient, oral drug delivery.

TMZ and other alkylating agents methylate multiple sites on DNA, however the ability to methylate guanine residues of DNA to O⁶-methyl guanine (O⁶-MeG) is considered to be the most biologically relevant action of this class of drug. While this lesion is not itself harmful to the cell, the mis-pairing properties of O⁶-MeG results in incorporation of a complementary thymine rather than cytosine during DNA replication.

The O⁶-MeG:T mismatch pair can be recognised by DNA mismatch repair systems, which remove the mismatched daughter strand thymine residue prior to reinsertion of the correct base. However, because the O⁶-MeG is still present on the template strand, another thymine is reinserted, and a futile cycle of excision and reinsertion ensues. This inability of mismatch repair systems to resolve the lesion results in prolonged G₂ arrest, double stranded DNA breaks and ultimately mitotic catastrophe and cell death (Mirzoeva et al., 2006).

O⁶-MeG lesions can be repaired in a single step reaction in which the methyl group is transferred from DNA to an acceptor cysteine residue in the protein O⁶-methyl guanine methyl transferase (MGMT) resulting in repair without excision. MGMT is a sacrificial enzyme, as transfer of the methyl moiety to cysteine results in permanent inactivation of the molecule. Exposure to temozolomide can deplete cellular levels of MGMT and thus resistance to alkylating agents is highly dependent on the level of MGMT expression.

MGMT is ubiquitously expressed in human tissues (Gerson et al., 1986). However in glioma, MGMT activity is frequently lost through epigenetic silencing of the MGMT gene promoter. Loss of MGMT activity is also observed in the normal brain tissue of glioma patients, suggesting that loss of activity is a predisposing risk factor to disease (Silber et al., 1996). Epigenetic silencing of MGMT is detectable in the tumours of 45% of newly diagnosed glioblastoma patients, and is associated with a favourable outcome whether treated with radiation alone or in combination with temozolomide. Survival is improved significantly by the use of temozolomide for tumours with silenced MGMT, but only marginally when MGMT silencing is absent (Hegi et al., 2005). In mouse xenograft models, treatment with TMZ results in induction of MGMT expression and acquired resistance to treatment in some but not all tumours (Kitange et al., 2009). Resistance to alkylating agents can also develop without expression of MGMT.

Alkylation therapy drives the acquisition of a hyper mutation phenotype in glioblastoma. The 'background' silent somatic mutation rate in TMZ treated tumours is over four times that seen in untreated tumours. This hypermutation phenotype is associated with loss of function mutations in DNA mismatch repair genes (TCGA-Consortium, 2008). Tumours with wildtype MSH6 (a mismatch repair gene) prior to treatment have acquired loss of function mutations upon recurrence following therapy (Yip et al., 2009). Cells deficient in DNA mismatch repair activity do not recognise the O⁶-MeG:T mismatch lesion caused by temozolomide and proceed through the cell cycle, without G₂

arrest, resulting in adenine-thymine pairs replacing guanine-cytosine pairs which accumulate as cells continue to proliferate (Friedman et al., 1997, Kaina et al., 1997).

Disruption of cell cycle control checkpoints also promotes resistance to alkylating therapy. Activation of Akt is frequently observed in GBM, and suppresses activation of the DNA damage signal transducers Chk2 and Cdc25C/Cdc2, allowing cells to bypass TMZ induced G₂ arrest and mitotic catastrophe (Hirose et al., 2005). The mutation rate of TP53 also increased from 37.5% to 58% in treated vs. untreated patient tumours (TCGA-Consortium, 2008) suggesting that TMZ treatment creates a selective pressure promoting TP53 loss of function.

Temozolomide resistance is a major barrier to effective glioma therapy and increases with tumour grade. Anaplastic astrocytoma (a type of grade III glioma) has a response rate to TMZ of 35% (Yung et al., 1999), while the response rate in glioblastoma (grade IV) is only 8% (Brada et al., 2001).

Bevacizumab (Avastin)

A recent addition to the number of approved therapies (in the USA) for the treatment of recurrent glioblastoma is the VEGF-A targeting monoclonal antibody bevacizumab. This agent acts as an angiogenesis inhibitor, intended to slow the growth of new blood vessels that ever expanding tumours require to sustain continued growth. Conversely it has also been proposed that inhibition of aberrant blood vessel formation can lead to normalisation of blood vessel formation supplying the tumour, reducing hypoxia (and thus increasing sensitivity to ionising radiation) and aiding the delivery of chemotherapeutic drugs (Jain, 2001). Bevacizumab was approved by the FDA for the treatment of recurrent GBM in 2009 based on Phase II clinical trials where radiologic imaging displayed partial responses in some patients (Cohen et al., 2009).

Unfortunately, GBM patients treated with bevacizumab frequently develop highly diffuse tumours that are non-enhancing by radiologic imaging suggesting that anti-angiogenic therapy increases the invasiveness of the tumour (Norden et al., 2008, Narayana et al., 2012). Further, the

supposed improvement in radiologic outcomes used to justify FDA approval of bevacizumab are not predictive of improved patient survival (Iwamoto et al., 2009). In animal models, bevacizumab therapy has been shown to increase intra-tumour hypoxia leading to an adaptive response mediated by hypoxia inducible factor 1 (HIF-1) that leads to increased invasiveness and tumourigenicity of glioma cells (Rapisarda et al., 2009, Kumar et al., 2013, Piao et al., 2013).

Subsequent trials of Bevacizumab have been mixed but generally indicate that progression free survival and overall survival in recurrent and newly diagnosed GBM is modestly improved by the addition of bevacizumab (Johnson et al., 2013, Narayana et al., 2012). Despite these disappointing outcomes, quality of life is substantially improved. This is likely as a result of reduced oedema, curtailing the need for prolonged steroid use (Nagpal et al., 2011) and its associated side effects that include hyperglycaemia, osteoporosis, immunosuppression, gastritis myopathy and insomnia (Deutsch et al., 2013).

Targeted therapy

Along with continued efforts to improve the efficacy of surgery, radiation and chemotherapy in GBM and other cancers, a great deal of research now focuses on the development of so-called ‘targeted therapies’, using small molecules or antibodies that target and disrupt the function of specific molecules or cellular components rather than broadly interfering with cell proliferation.

The treatment of any pathological growth in the body relies on exploiting differences in the biology of the pathologic cells compared to cells of the host body. Pathogenic bacterial cell growth is treated with antibiotics that may specifically target bacterial ribosomes (e.g. streptomycin) or enzymes involved in cell wall maintenance (e.g. penicillin), while chloroquine used treatment of malaria disrupts the function of the digestive vacuole. In each case, the biological target is found uniquely in the disease causing cells which are unrelated to the host.

However in the case of cancer, the pathologic cells originate from normal host cells that have acquired the hallmark features of cancer cells (reviewed in (Hanahan and Weinberg, 2011)) through mutation and evolution. Consequently, a unique target that can be exploited by therapy, that is completely absent from normal cells, rarely exists in the case of cancer. Instead, a therapeutic window can be achieved when cancer cells are *more* sensitive than normal cells to a particular treatment.

Chemotherapy and IR therapy, while generally not considered 'targeted therapy', target cancer cells over normal cells due to their differences in proliferation rate and cell cycle control i.e. chemotherapy and IR are particularly harmful to rapidly dividing cells, and cancer cells are typically rapidly dividing. The major limitation of chemotherapy and IR therapy is that other normal tissue types with high rates of proliferation are also sensitive to the damaging effects of these therapies.

An understanding of the specific genetic changes in any particular cancer is likely to highlight potential novel targets that can be exploited by targeted therapy, potentially with reduced toxicity to normal tissues that do not bear the same mutations. In recent years, our understanding of the genetic alterations that drive the formation of high grade gliomas has increased exponentially. These genetic alterations, which include mutation, rearrangement, amplification and deletion of genes, are highly heterogeneous, both across different patients and within cells of the same tumour.

The mutations and genetic alterations that drive the development high grade gliomas can be broadly divided into two categories; those that promote activation of pro-survival and proliferative signal transduction pathways, and those that inactivate mechanisms of cell cycle control and cellular senescence/apoptosis in response to DNA damage and other stressors.

The pro-survival PI3K-Akt pathway is one of the primary targets of activation in GBM, along with and to a lesser extent the Ras-Raf-MAPK pathway, both of which are major signal transducers of receptor tyrosine kinases (RTKs), while Rb and p53 signalling are most affected by pathway

inactivation. Systematic expression, gene amplification and sequence analysis of 601 selected genes in 91 matched tumour-normal pairs from GBM patients demonstrated that genetic alterations of RTKs and/or downstream signalling pathways could be identified in 88% of cases, while alterations of the highly overlapping Rb and p53 signalling pathways were identified in 78% and 87% of cases respectively.

Generally speaking, defects that arise due to loss of function mutations are difficult to target pharmacologically. A hypothetical 'activator of p53' is not going to do much for a cell that no longer expresses functional p53. On the other hand, the RTK-PI3K-Akt-mTOR and the RTK-Ras-Raf-MAPK signalling cascades activated in GBM present multiple drugable targets.

While these pathways are also important for proliferation and survival of normal, non-cancerous cells, hyper-activation of these pathways in cancer cells has been proposed to lead to a state of 'oncogenic addiction' (Weinstein and Joe, 2008), where the addicted cell becomes dependent on continuous activation of the signalling pathway. As a result, even temporary pathway inhibition can lead to induction of cell death, in experimental systems at least.

Figure 1.1 summarises many of the interaction of proteins known to be altered in glioma as expanded upon in the following sections.

RTK-Ras-PI3K signalling

Receptor tyrosine kinase (RTK) signalling is a major mechanism by which cells of multicellular animals communicate to regulate behaviours such as proliferation, survival and migration. Typically, growth factors produced by one cell bind to the appropriate RTK on another nearby cell. Activation of RTKs on the cell surface initiates a cascade of events via various second messenger systems that propagate and integrate various signals and stimuli within the cell, ultimately leading to a diverse range of effects including changes in gene transcription and translation and activity of many enzymes within the cell.

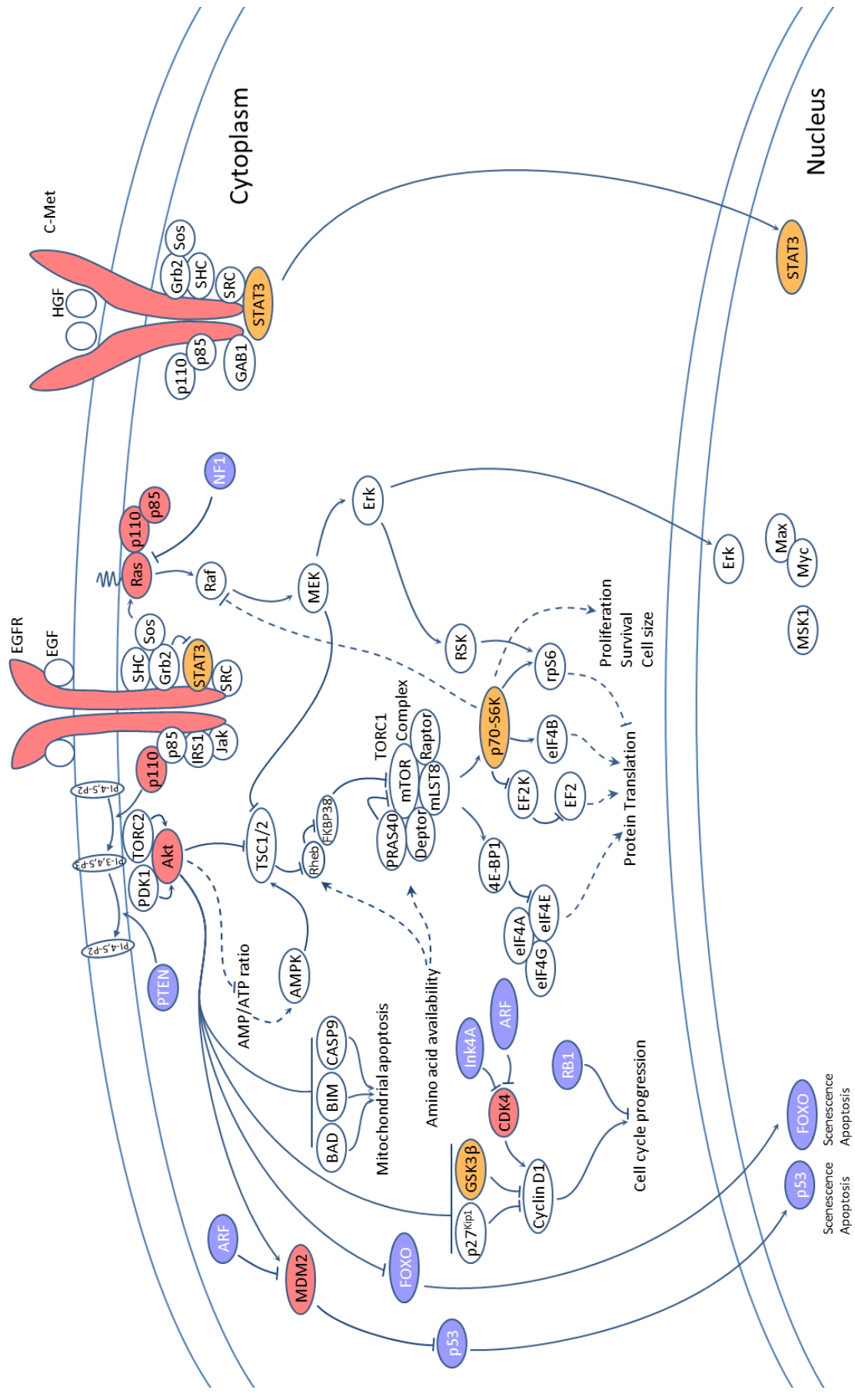


Figure 1.1 Interaction network of proteins frequently altered in GBM. Glioblastoma is characterised by frequent mutations within the highly overlapping PI3K-Akt, Ras-Raf-MAPK, p53 and RB1 signalling pathways. Elements in red represent proteins activated through gene mutation, amplification or over-expression, while those in blue represent proteins inactivated through mutation or deletion. Elements in orange have been observed with elevated activity/phosphorylation without genetic alteration or overexpression. Many of these interactions are described in detail in the main text.

Various mechanisms serve to limit the activation of RTKs and their downstream second messenger systems such that in normal cells, basal activation of RTKs is typically low and following ligand stimulation, activation is temporally restricted. However a frequent feature of cancer cells is chronic hyper-activation of RTKs, along with downstream signalling pathways. In GBM, activation of the RTK-PI3K-Akt-TORC1 and to a lesser extent the RTK-Ras-Raf-MAPK signalling pathways appear to be the most biologically relevant.

EGFR

Epidermal growth factor receptor (EGFR, ErbB1) is the prototypical member of the ErbB family of RTKs. EGFR is normally expressed in cells of epithelial, mesenchymal and neuronal origin and is involved in regulation of proliferation, differentiation and development (Yano et al., 2003).

EGFR signalling has been implicated in proliferation and differentiation of astrocytes (Kornblum et al., 1998), and survival and migration of post-mitotic neurons (Sibilia et al., 1998). EGFR is transiently expressed in astrocytes during development, whereas in the adult, expression is largely restricted to neuronal cells (Gomez-Pinilla et al., 1988). Following ischemic brain injury, EGFR is highly up-regulated in proliferating astrocytes near the injury site (Planas et al., 1998).

Polysomy of chromosome 7, which contains the *EGFR* gene is observed in 76% of GBMs, making it the most frequently observed amplification event observed in GBM (Lopez-Gines et al., 2005), while a frequency of 97% has been reported for primary GBMs (Crespo et al., 2011). The *EGFR* gene is also frequently amplified (42% of cases with *EGFR* amplification) in the form of small, circular extra-chromosomal elements known as 'double minutes'. Less frequently, (28% of cases with *EGFR*

amplification) the *EGFR* gene is reinserted into multiple locations of chromosome 7 (Lopez-Gines et al., 2010). *EGFR* amplification is rarely observed in low grade (grade I&II) gliomas (Ekstrand et al., 1991, Smith et al., 2001)), and is significantly less common in anaplastic astrocytoma (grade III glioma) than in GBM (Smith et al., 2001). Extremely strong concordance is observed between gene amplification and overexpression of EGFR.

More than half of GBMs with *EGFR* gene amplification also contain rearrangements of the *EGFR* gene leading to expression of aberrant EGFR proteins (Shinojima et al., 2003). The most common of these is EGFRvIII, a truncated mutant EGFR arising as a consequence of deletion of exons 2-7 of the *EGFR* gene. EGFRvIII is detected in ~45% of patients with identified *EGFR* amplification and ~8.5% of patients without (Shinojima et al., 2003).

The deletion of exons 2-7 causes an in-frame deletion, with the loss of amino acids 6-273 and insertion of a novel glycine into the protein product. This deletion results in the loss of most of the extracellular domain, and EGFRvIII is unable to bind any ligand, yet maintains a low level of constitutive activation (Gan et al., 2009). Unlike the wild type receptor, which is rapidly internalised and degraded in lysosomes following activation, EGFRvIII is only inefficiently internalised, and is recycled back to the cell surface rather than targeted to lysosomes resulting in constitutive, low level receptor signalling (Grandal et al., 2007).

High expression of EGFRvIII in the PTEN deficient glioblastoma cell line U87MG promotes tyrosine phosphorylation of PI3K signalling molecules to a much greater extent than STAT3 or MAPK pathways members (Huang et al., 2007). Expression of EGFRvIII also leads to the activation of multiple receptor tyrosine kinases including c-Met, PDGFR β independent of binding to their ligands (Pillay et al., 2009)

The prognostic value of these genetic rearrangements is disputed, with some studies showing *EGFR* amplification and/or presence of EGFRvIII is prognostic of reduced survival (Shinojima et al.,

2003), while others suggest no association (Waha et al., 1996, Heimberger et al., 2005). One recent study found EGFRvIII expression to be associated with improved survival in GBM patients (Montano et al., 2011)

c-Met

The receptor tyrosine kinase c-Met, along with its only known ligand hepatocyte growth factor/scatter factor (HGF/SF) is expressed in many epithelial cell types (Di Renzo et al., 1991). Within the brain, c-Met is expressed predominantly in neuronal cells of the hippocampus, cerebral cortex, cerebellum, septum and pons, while its ligand HGF is expressed in neuronal cells of the hippocampus, cerebral cortex, amygdala and granule cell layer of the cerebellum as well as in ependymal cells and glial cells (Jung et al., 1994, Honda et al., 1995)

HGF is a mitogenic, morphogenic and motogenic factor (Ma et al., 2003) and is believed to contribute to tissue repair following injury in a number of tissues including brain (Honda et al., 1995). Following ischemic brain injury in rats, both HGF and c-Met are dramatically up-regulated in reactive astrocytes localised to the infarct site (Nagayama et al., 2004). HGF has also been implicated as a chemo-attractant for the recruitment of neural stem cells to the injury site following spinal cord damage (Takeuchi et al., 2007).

Gene amplification of c-Met is present in only ~4% of GBMs, yet c-Met protein is present in all gliomas (Koochekpour et al., 1997). Further, c-Met is overexpressed in almost 30% of GBMs and this overexpression is associated with increased invasiveness, and reduced median survival time (Kong et al., 2009). In the absence of trans-activation from other RTKs (such as EGFRvIII), activation of c-Met is driven by binding of its ligand HGF/SF (hepatocyte growth factor/scatter factor), which is co-expressed with c-Met in gliomas with increasing grade (Koochekpour et al., 1997). While activating many of the same pathways as EGFR, c-Met signalling also promotes increased migration and invasion of glioma cells, expression of VEGF to promote vascularisation, and has recently been implicated in maintaining the stem cell like phenotype in glioma cells.

PI3K-Akt

Activation of signalling pathways downstream of RTKs begins with binding of growth factor ligands to their cognate receptors. Binding typically induces conformational changes and dimerisation/oligomerisation of the receptors, resulting in auto-activation of their kinase domains, and phosphorylation of intracellular tyrosine residues. These events create a range of docking sites for an array of second messenger molecules including members of PI3K-Akt and Ras-Raf-MAPK signalling pathways.

Tyrosine phosphorylation of the consensus sequence YXXM on the intracellular domains of RTKs creates a docking site for recruitment of Class IA phosphoinositide 3-kinases (PI3K). Binding of the p85 regulatory subunit of PI3K to the YXXM sequence relieves p85 inhibition of the p110 catalytic subunit. Localised in proximity to the plasma membrane, PI3K can then phosphorylate its substrate, the phospholipid PI-4,5-P₂ (phosphatidylinositol 4,5-bisphosphate) to PI-3,4,5-P₃ on the inner leaflet of the plasma membrane. This event facilitates recruitment of PH-domain containing proteins (which bind to PI-3,4,5-P₃) such as the serine/threonine kinase Akt, which is activated upon Thr308 phosphorylation by the PH-domain containing PDK1 (Lamming et al., 2012) and Ser473 phosphorylation by PDK2/TORC2 (Kumar et al., 2010, Sarbassov et al., 2005). Activating mutations of the Class IA PI3Ks are present in 15% of GBMs and occur exclusively in the p110 catalytic subunit, while mutations in Akt itself are infrequent.

Akt is considered to be the primary mediator of PI3K initiated signalling, with a broad range of downstream substrates. Phosphorylation by Akt inhibits activity of multiple pro-apoptotic proteins including Bim, Bad and Procaspase 9, as well as the FOXO family of pro-apoptotic transcription factors (Burgering and Medema, 2003). Akt phosphorylation of MDM2 promotes ubiquitination and degradation of p53 (Ogawara et al., 2002). Though a range of mechanisms Akt promotes the activation of TORC1 as outlined below.

The lipid phosphatase activity of PTEN (phosphatase and tensin homolog) limits Akt activation and downstream signalling by converting PI-3,4,5-P₃ back to PI-4,5-P₂. Chromosomal region 10q23, on which the human *PTEN* gene is located, is frequently associated with loss of heterozygosity in many human tumours. Loss of 10q has been found in 80% of GBMs (Chow and Baker, 2006), and biallelic loss, through mutation or deletion of the remaining *PTEN* gene occurs in 36% of GBMs (TCGA-Consortium, 2008). As a single event, *PTEN* loss does not result in increased phosphorylation of Akt and is insufficient to induce brain tumours in mice suggesting that *PTEN* loss must act in concert with other genetic aberrations to induce glioma. *PTEN* loss is not frequently observed in low grade gliomas, but is associated with progression to high grade malignancy suggesting that *PTEN* loss is a late event in GBM development. Thus the loss of *PTEN* appears to cooperate with other mutations, to enhance activation of proliferative growth signals in GBM.

TORC1

A major downstream target of Akt is the mTOR containing complex TORC1, which integrates growth factor signalling inputs with a diverse range of environmental stimuli including nutrient availability, energy status, redox state and oxygen tension. Activation of TORC1 promotes a plethora of cellular responses including increases in protein expression, ribosome biogenesis, changes in metabolism and suppression of autophagy and cellular senescence.

TORC1 is a large, dimeric protein complex, with each monomer consisting of one molecule of the mTOR (mammalian target of rapamycin), Raptor (regulatory associated protein of mTOR), PRAS40 (proline-rich AKT substrate 40 kDa), mLST8 (mammalian lethal with Sec-13 protein 8) and Deptor (DEP domain TOR-binding protein) (Russell et al., 2011). TORC1 functions as a serine/threonine kinase with catalytic activity contained within the mTOR subunit. Raptor promotes TORC1 complex formation and is essential for kinase activity. PRAS40 serves as a negative regulator of TORC1 in the absence of growth factor signalling, while the roles of mLST8 and Deptor are still poorly characterised.

Phosphorylation and activation of Akt leads to activation of the TORC1 complex through multiple mechanisms. A major substrate of Akt phosphorylation is tuberous sclerosis complex 2 (TSC2). In the absence of phosphorylation by Akt, TSC2 complexed with TSC1, acts as a GTPase activating protein (GAP) for the small GTPase Rheb (Ras homolog enriched in brain), converting it from its active GTP bound form to its inactive GDP bound form. When active, Rheb interacts with the mTOR inhibitory protein FKBP38, preventing its association with TORC1 and thus promoting TORC1 activity (Bai et al., 2007). Akt also promotes TORC1 activity more directly by phosphorylating PRAS Thr-246 initiating a cascade of events that leads to dissociation of the inhibitory protein from the TORC1 complex (Nascimento et al., 2010).

During nutrient deprivation or other causes of bioenergetics stress such as mitochondrial dysfunction, a fall in cellular ATP levels and a concomitant rise in AMP levels promotes activation of AMP-activated protein kinase (AMPK). When active, AMPK directly phosphorylates Raptor Ser792 leading to inactivation of TORC1 (Gwinn et al., 2008). AMPK also phosphorylates TSC2, which in concert with further phosphorylation by GSK3 β promotes increased TSC1/2 GAP activity and suppression of TORC1 (Inoki et al., 2006). Akt inhibits GSK3 β via direct phosphorylation (Cross et al., 1995), while Akt appears to inhibit AMPK indirectly by promoting increased ATP/AMP ratios (Hahn-Windgassen et al., 2005).

One of the most studied downstream targets of TORC1 is the serine/threonine kinase p70-S6K, activation of which promotes increased cell size, proliferation and survival, gene transcription and translation, reviewed in (Ruvinsky and Meyuhas, 2006). The other major downstream target of TORC1 is 4EBP1, which interacts with the translation initiation factor eIF4E to inhibit cap dependent translation. Phosphorylation of 4EBP1 by TORC1 inhibits this interaction resulting in increased cap dependent translation.

By integrating growth factor signalling with other environmental cues, TORC1 allows cells to grow and proliferate when only the appropriate growth signals and favourable environmental conditions are present.

Ras-Raf-MAPK

Along with activation of the PI3K-Akt pathway, RTK signalling also leads to activation of the Ras-Raf-MAPK pathway via the action of second messengers and adaptor molecules. Phosphotyrosine residues on the cytoplasmic tail of RTKs serve as docking sites for SH2 domain containing proteins including Grb2 which can then interact with proline rich residues of SOS via its two SH3 domains. SOS is a guanine exchange factor, which when co-localised with GDP-bound Ras, promotes exchange of GDP for GTP. Binding of GTP to Ras induces a conformational change facilitating recruitment and activation of the Raf family of serine/threonine kinases. Raf initiates activation of the MAPK signalling cascades, which promotes a diverse range of cellular responses in a cell type dependent manner including regulation of cell cycle progression, cellular senescence and apoptosis, and growth factor expression (McCubrey et al., 2007). Activated Ras can also recruit and activate the p110 catalytic subunit of PI3K independently of the p85 subunit to activate Akt signalling (Castellano and Downward, 2011).

Mutations in Ras genes are observed in ~30% of all human tumours. The most frequent targets of mutation are the tandem glycines at residues 12 and 13, followed by glutamic acid 61 (Fernandez-Medarde and Santos, 2011). These mutations disrupt interactions of Ras with their GTPase activating proteins (GAPs) leading to constitutive GTP binding, and activation of the Ras (Scheffzek et al., 1997). Mutations of Ras and Raf are rare in gliomas (Jeuken et al., 2007), yet on average, approximately 50% of Ras is in the activated GTP bound state in GBM, compared to 0.5-2.3% in normal brain (Guha et al., 1997).

Like activation of Akt, Ras activation can occur as a consequence of upstream signalling events such as RTK activation, or suppression of negative regulators. NF1 is a Ras GAP that promotes

inactivation of Ras. Functional loss of the Ras GAP protein NF1 through mutation and deletion was detected in at least 18% of all tumours. While germline mutation of NF1 predisposes children to development of astrocytoma (grade III glioma) (Listernick et al., 1997), loss of NF1 function from astrocytes promotes astrocytic proliferation but is insufficient to cause brain tumours in mice (Bajenaru et al., 2002). However NF1 mutation cooperates with other mutations, such as p53 or Rb1 inactivation to promote tumour formation in glioma mouse models.

Activation of Ras initiates a cascade of phosphorylation events, with phosphorylation of Raf (MAP kinase kinase kinase, MAPKKK) followed by phosphorylation of MEK1/2 (MAP kinase kinase, MAPKK) and ERK1/2 (MAP kinase, MAPK). Phosphorylation promotes activation of MAPK, which migrates into the nucleus to effect gene expression leading to increased cell survival and proliferation (Mebratu and Tesfaigzi, 2009). ERK1/2 can also phosphorylate and inactivate TSC2 such that activation of the MAPK signalling cascade also leads to activation of TORC1 independently of Akt (Ma et al., 2005). Expression of total and phosphorylated MAPK is significantly correlated with survival time in GBM (Mawrin et al., 2003).

Cancer Metabolism

The metabolism of many cancers is significantly different to that of normal tissues, creating the possibility that cancer metabolism is a potential alternative target for the treatment of cancer. The most studied of these changes is that of the metabolism of glucose, which is consumed at a much higher rate, and has different metabolic roles in tumour cells compared to normal cells. Only in recent years has the emerging role of pro-oncogenic signalling pathways on this and other metabolic changes in cancer come to light.

Understanding these metabolic changes in GBM and other cancers may prove useful for the development of novel therapeutic strategies. These metabolic effects are believed to be essential for proliferation by providing raw materials needed for macromolecule synthesis, cell growth and

proliferation. However the role of altered metabolism in cancer is still a matter of much speculation and debate.

Beginning with the studies of Otto Warburg over 80 years ago, biologists have had a growing understanding of the fundamental differences between the metabolisms of normal cells and tissues and cancerous cells and tissues. The precise nature of these changes, how they arise and what purpose they serve is a matter of ongoing investigation. However it is hoped that an improved understanding of these changes, together with new therapeutic tools with which to reverse or exploit them may lead to novel therapeutic strategies for the treatment of cancer.

The first recognised and most intensely studied metabolic change is that of dramatically increased glucose consumption and lactate production in cancer cells. By measuring glucose and lactic acid concentrations in arteries and veins, Warburg showed that normal tissues consume only a small fraction of available glucose (2-18%), and are typically not net producers of lactic acid *in vivo*. In contrast, Jensen sarcoma consumed on average 57% of available glucose and produced substantial amounts of lactate *in vivo* (Warburg et al., 1927).

Observations such as these have led to the development of imaging tools such as FDG-PET, for non-invasive diagnosis and evaluation of tumours. Radio-labelled glucose analogues such as ¹⁸F-Fluorodeoxyglucose (FDG) administered to a patient will be preferentially taken up by tissues with high glucose metabolism, creating a contrast between cancerous and non-cancerous tissue which can be visualised using positron emission topography (PET).

The mechanisms that lead to this profound increase in glucose metabolism, and the biological roles of this change are still being elucidated. There is an ever increasing appreciation of the role cell signalling pathways that are often perturbed in cancer, have on glucose metabolism. Further, the hypoxic microenvironment of solid tumours also likely plays an important role in the development of the glycolytic phenotype, through both stimulating an adaptive response via up-regulation of HIFs

and by exerting a selection pressure that favours the emergence of mutant cells with an acquired increased capacity for glucose metabolism.

The following sections will discuss glycolysis, mitochondrial respiration and their relationship in proliferating cells.

Glycolysis

Glucose is the most abundant and versatile organic carbon molecule in the bloodstream and is used as a nutrient and source of energy by practically all cell types in the body. The principle catabolic pathway for the breakdown of glucose is the Embden-Meyerhof-Parnas pathway, commonly known as 'glycolysis' in which the six carbon glucose molecule is oxidised to two, three carbon pyruvate molecules. This pathway, which occurs entirely in the cytoplasm, catalysed by ten distinct enzymes as outlined in **Figure 1.2**. Oxidation of one glucose molecule via glycolysis is concomitant with reduction of one NAD^+ to NADH and a net phosphorylation of two ADP to ATP .

While only generating a relatively small amount of ATP per glucose (relative to respiration) glycolysis is capable of supplying the cell ATP at a high rate. However NAD^+ consumed at the level of glyceraldehyde phosphate dehydrogenase (GAPDH) must be replenished in order for the process to continue. Catalysed by the enzyme Lactate Dehydrogenase (LDH), the pyruvate generated by glycolysis accepts electrons from NADH , becoming reduced to lactate and thus replenishing NAD^+ . Alternatively, NADH can be shuttled into the mitochondria where it is oxidised via the electron transport chain, allowing pyruvate to be oxidised further via mitochondrial respiration.

Beyond energy production, glycolysis also supplies precursors to a number of branching pathways. The oxidative arm of the pentose phosphate pathway originates at glucose-6-phosphate and is a major source of NADPH as well as ribose-5-phosphate. NADPH is a critical co-factor for driving many reductive anabolic processes as well as maintaining the redox state of the cell and



Figure 1.2. Glycolysis and branching pathways. Ten enzymes catalyse the conversion of glucose to pyruvate. The reactions of hexokinase, phosphofructokinase and pyruvate kinase are highly exergonic and considered essentially irreversible. Glucose-6-phosphate serves as the entry point for the oxidative arm of the pentose phosphate pathway (oxPPP) which is a major source of NADPH and ribose sugars for nucleotide synthesis. Activity of Glycerol-3-phosphate dehydrogenase redirects dihydroxyacetone phosphate into glycerol metabolism. 3-phosphoglycerate can be utilised for synthesis of serine which is subsequently consumed during folate metabolism. The end product of glycolysis, pyruvate, can either be reduced to lactate or oxidised to acetyl-CoA by lactate dehydrogenase or pyruvate dehydrogenase respectively. The later process results in entry into the TCA cycle in the mitochondria.

resistance to oxidative stress. The ribose-5-phosphate provides the sugar backbone for the *de novo* synthesis of purines and pyrimidines required for replication of DNA.

The glycolytic intermediate 3-phosphoglycerate is used as a precursor for the amino acid serine, which can then be used for *de novo* synthesis of ceramine, a major constituent of the lipid bilayer, while glyceraldehyde-3-phosphate can be reduced to glycerol-3-phosphate used for the production of phospholipids and triacylglycerol.

Mitochondrial respiration and the TCA cycle

The second ATP generating mechanism in the cell is mitochondrial respiration, in which substrates are fully oxidised to CO₂ via the tricarboxylic acid (TCA) cycle within the mitochondrial matrix. The TCA cycle (**Figure 1.3**) concomitantly reduces electron carriers (predominantly NAD) which feed electrons into the electron transport chain (ETC). The ETC facilitates the flow of electrons across a number of electron carriers before being finally transferred to molecular oxygen, reducing it to water. Energy from this electron flow is conserved with the pumping of protons across the inner mitochondrial membrane and out of the mitochondrial matrix to generate an electro-chemical gradient. This electro-chemical gradient can be used to perform work, predominantly the phosphorylation of ADP to ATP via the enzyme ATP-synthase.

Before entering the TCA cycle pyruvate is oxidised to acetyl-CoA by pyruvate dehydrogenase. The two carbon acetyl group of acetyl-CoA is then transferred to the four carbon oxaloacetate to

generate citrate by citrate synthase. Two carbons are subsequently lost through oxidation to CO₂ through one rotation of the TCA cycle to regenerate oxaloacetate.

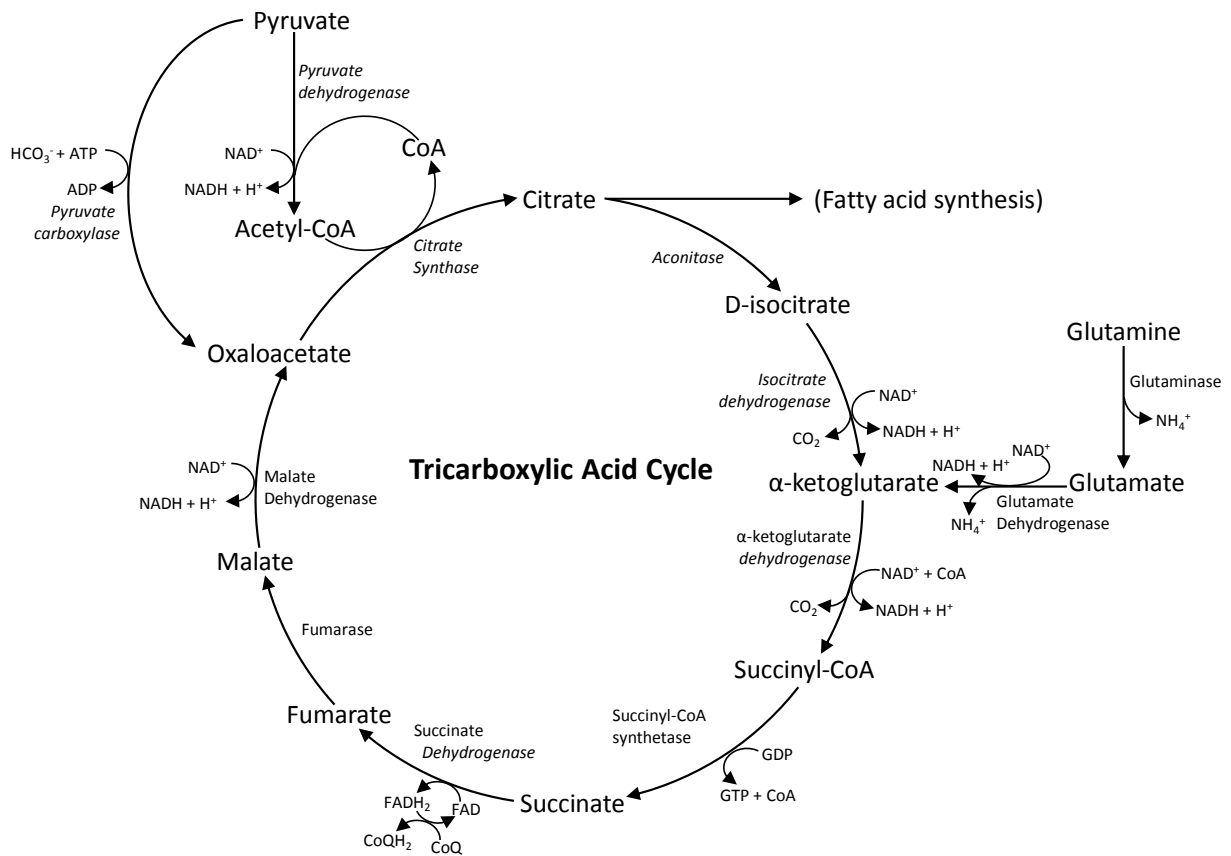


Figure 1.3. The Tricarboxylic Acid Cycle. The primary function of the TCA cycle is oxidation of pyruvate derived carbons to CO₂ and concomitant reduction of NAD⁺ to NADH. Citrate that leaves the TCA cycle (cataplerosis) for fatty acid synthesis requires replenishment of TCA cycle intermediates to prevent depletion of oxaloacetate. Anaplerosis is achieved through the action of glutamate dehydrogenase or pyruvate carboxylase.

Anaplerosis and cataplerosis

Like glycolysis, intermediates of the TCA cycle also serve as important precursors for anabolic pathways. Citrate from the TCA cycle can be shuttled from mitochondria to cytoplasm where it serves as a precursor for fatty acid synthesis. The tricarboxylate transport system (**Figure 1.4**) effectively uses citrate as a carrier for acetyl groups. Via the activity of malic enzyme, this process also supplies NADPH which provides the reducing power for fatty acid synthesis.

The process of extracting intermediates of the TCA cycle for biosynthetic processes is known as ‘cataplerosis’. As these processes ultimately lead to a depletion of oxaloacetate, the TCA cycle cannot be sustained without ‘anaplerosis’ i.e. reactions which replenish TCA cycle intermediates.

A key anaplerotic reaction is that of pyruvate carboxylase, which converts pyruvate and carbonic acid to oxaloacetate. Glutamine, the most abundant amino acid in the blood also serves as a key anaplerotic substrate, entering the TCA cycle via glutaminolysis.

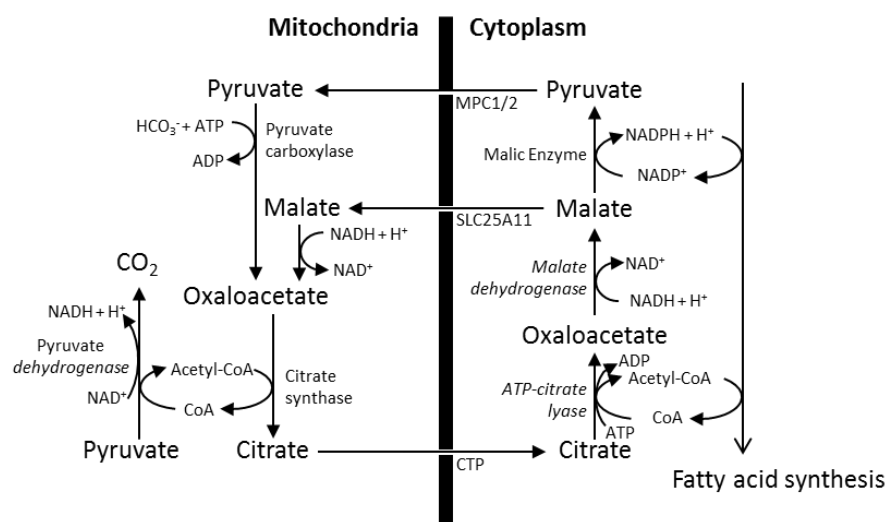


Figure 1.4. The Tricarboxylate Transport System facilitates transfer of acetyl-CoA in the form of citrate, from mitochondria to cytoplasm where it is used for fatty acid synthesis. Specific transporters facilitate transfer of pyruvate, malate and citrate across the inner mitochondrial membrane. This system allows acetyl-CoA produced in the mitochondria to be exported into the cytoplasm where it is utilised for fatty acid synthesis.

The electron transport chain

The electron transport chain (**Figure 1.5**) is a series of enzyme complexes and co-factors which accept electrons from various electron donors and transfer them, via a series of intermediates to the terminal electron acceptor, molecular oxygen. Much of the energy liberated from these redox reactions is conserved by the pumping of protons across inner mitochondrial membrane, out of the mitochondrial matrix.

NADH:ubiquinone reductase, (Complex I) accepts electrons from NADH and transfers them to coenzyme Q (CoQ) with concomitant pumping of protons out of the matrix. Succinate dehydrogenase, (Complex II) a component of the TCA cycle, oxidises succinate to fumarate, passing electrons first to the cofactor FAD then to CoQ

The lipid soluble coenzyme Q diffuses within the inner mitochondrial membrane and is oxidised by coenzyme Q : cytochrome c – oxidoreductase (Complex III) which transfers electrons to the protein cytochrome c, and pumps more protons out of the matrix. Finally, cytochrome c oxidase (complex IV) transfers electrons from cytochrome c to oxygen to produce water and pumps additional protons out of the matrix.

A number of other pathways also donate electrons to CoQ. The glycerol 3-phosphate dehydrogenase system transfers electrons from NADH in the cytoplasm to CoQ in the mitochondria. Dihydroorotate dehydrogenase (DHODH), an essential component of pyrimidine synthesis also transfers electrons to CoQ.

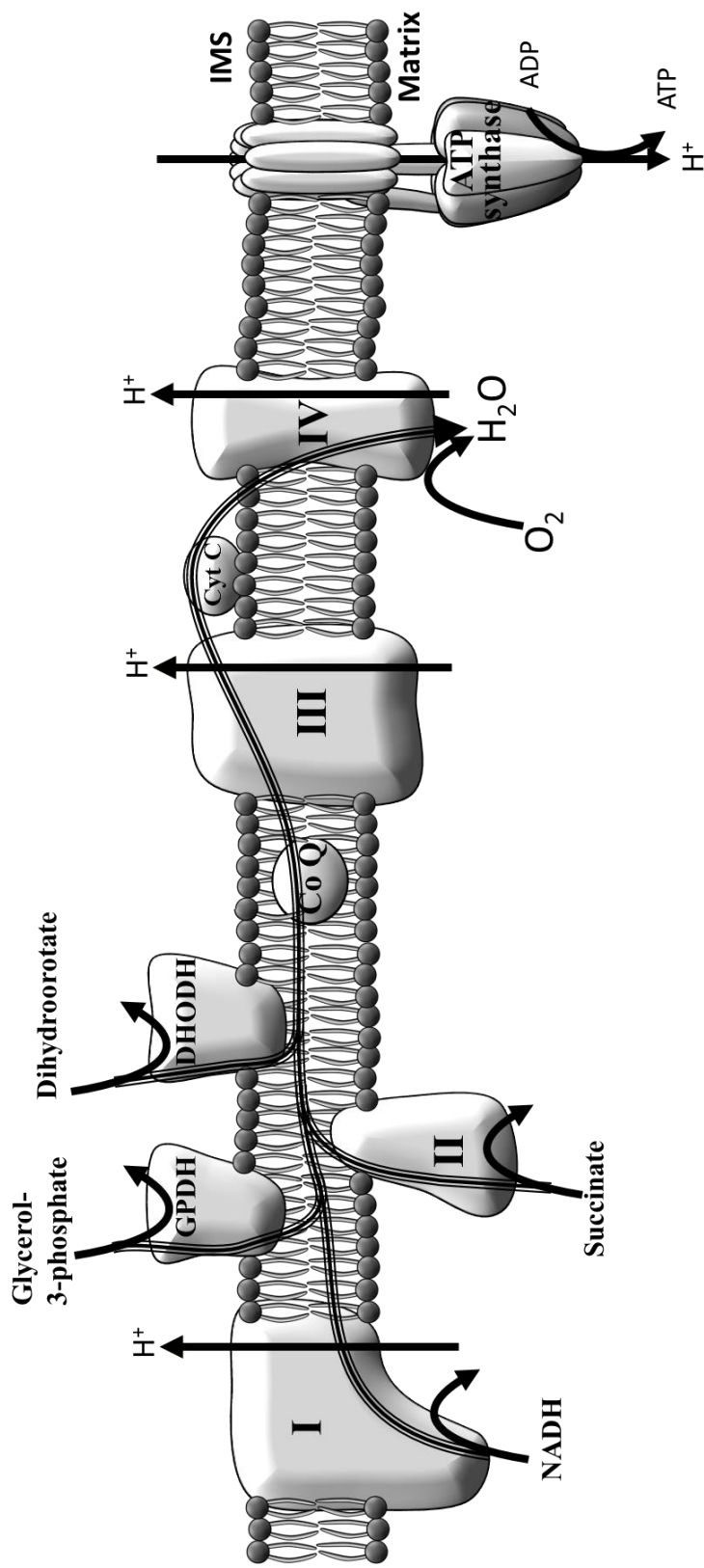


Figure 1.5. The mitochondrial electron transport chain. Embedded in the inner mitochondrial membrane, complex I, glycerol-3-phosphate dehydrogenase (GPDH) and dihydroorotate dehydrogenase (DHODH), transfer electrons from their respective substrates to coenzyme Q (Co Q). Catalysed by complex III, electrons from Co Q are transferred to cytochrome C, which is subsequently oxidised via complex IV which transfers electrons to molecular oxygen. During electron transport, protons (H⁺) are pumped out of the mitochondrial matrix by complexes I, III and IV to generate a proton gradient. The flow of electrons back through ATP synthase drives the phosphorylation of ADP to ATP.

Mitochondrial reactive oxygen species

The mitochondrial electron transport chain is imperfect, and at a number of locations, electrons are able to leak prematurely to molecular oxygen resulting in the formation of the highly reactive radical ion, super oxide (O_2^-). Super oxide is rapidly converted by superoxide dismutase (SOD) to the more stable, but still reactive molecule hydrogen peroxide (H_2O_2). Because of their reactivity, these and other volatile oxygen containing molecules (known collectively as reactive oxygen species, ROS) will readily undergo redox reactions with numerous cellular components and are thus potentially harmful to the cell when produced in excess or are not neutralised by antioxidant systems.

Under normal conditions, it is estimated that 1-2% of oxygen is converted to super oxide via the ETC. While the precise mechanisms are still being elucidated (reviewed in (Murphy, 2009)), in highly simplified terms single electron transfer to oxygen at complex I and III rather than two electron transfer at complex IV (which results in production of H_2O) leads to super oxide generation.

Various physiological states can dramatically increase superoxide production by the ETC including elevated matrix $NADH/NAD^+$ or inner membrane $CoQH_2/CoQ$ ratio together with a high $\Delta\Psi_m$. Such conditions can arise when supply of reducing equivalents are exceedingly high, such as during hyperglycaemia, or when supply of oxidising equivalents are low, such as during hypoxia. Dysfunction of the ETC, e.g. by loss of cytochrome c during apoptosis or pharmacologic inhibition of the ETC also results in conditions that yield high amounts of ROS.

Relationship of glycolysis, fermentation and respiration

As the two primary mechanisms for the production of ATP, the processes of glycolysis and respiration are intimately linked. Through a number of mechanisms, the activity of one pathway supports the activity of the other. During the preparatory phase of glycolysis, ATP is consumed by the hexokinase and phosphofructokinase, and the availability of ATP for these enzymes can be rate limiting for glycolysis. Hexokinase is often bound to the outer mitochondrial membrane, giving it privileged and rapid access to mitochondrially generated ATP to promote increased entry into

glycolysis. In this way respiration supports glycolysis. The final product of glycolysis is pyruvate, which is a major substrate for entry into the TCA cycle. Thus increased glycolysis can support high flux of the TCA cycle and respiration.

The Pasteur effect

However the activity of each pathway can also lead to the suppression of the other. The Pasteur effect is a phenomenon first observed in yeast over 150 years ago, where the presence of oxygen leads to the suppression of glycolysis (Pasteur, 1858). Similarly, a lack of oxygen, i.e. hypoxia promotes increased glycolysis.

Acutely, this effect is largely mediated through allosteric regulation of the rate limiting glycolytic enzyme phosphofructokinase 1 (PFK1). ATP and citrate (an intermediate of the TCA cycle) allosterically inhibit PFK1, leading to reduced glycolytic flux when the energy state of the cell is high, indicating that mitochondrial respiration is active, while ADP, AMP and P_i relieve this inhibition. This mechanism prevents excess and wasteful glycolytic flux when mitochondrial respiration is sufficient for energy production (Tejwani, 1978).

Hypoxia also leads to stabilisation and activation of the hypoxia inducible factors (HIF), transcription factors that promote gene expression of many glycolytic enzymes and increased glycolytic capacity. This allows for a more long term, adaptive response to hypoxia.

Hypoxia also leads to an active suppression of respiration. Complex IV has an extremely high affinity for O_2 , allowing isolated mitochondria to achieve half maximal respiration at only 0.02% O_2 (Gnaiger et al., 2000). Nevertheless, suppression of respiration in whole cells is observed even at 0.5% O_2 . Further, fibroblasts exposed to chronic hypoxia will maintain suppressed respiration for several hours following the reintroduction of oxygen, suggesting an active rather than passive suppression of respiration (Papandreou et al., 2006).

Suppression of respiration during hypoxia is dependent on Pyruvate dehydrogenase kinase 1 (PDK1), an enzyme up-regulated by HIF in response to hypoxia. PDK1 phosphorylates and inhibits pyruvate dehydrogenase, thus reducing entry of pyruvate into the TCA and suppressing respiration.

Without PDK1, continued TCA cycle flux ETC activity during hypoxia promotes conditions that favour production of ROS including high levels of reduced NAD and CoQ and high $\Delta\Psi_m$. Thus suppression of PDH by PDK1 protects cells by preventing the production of ROS during hypoxia (Kim et al., 2006).

The Crabtree effect

The addition of glucose to some cell types results in suppression of respiration. This phenomenon has been called the 'reverse Pasteur effect' or the Crabtree effect after its discoverer H.G. Crabtree who observed the effect specifically in cancer cells but not normal cells (Crabtree, 1929).

The most broadly (although far from universally) accepted explanation for the Crabtree effect is that of competition of both glycolysis and respiration for a common substrate, ADP. In cells with a high glycolytic capacity, the addition of glucose will cause rapid glycolysis and a depletion of ADP. Without a substrate for phosphorylation, H^+ flux through ATP synthase stops, increasing $\Delta\Psi_m$ and in turn inhibiting flux through the ETC and oxygen consumption.

In a cell free system containing coupled mitochondria, respiratory substrates (succinate or glutamate-malate) and an ADP regenerating system (yeast hexokinase, glucose, ATP), the addition of pyruvate kinase and PEP (as an ADP phosphorylating system, taking the place of glycolysis) resulted in a 75% reduction in respiration. This inhibition was partially alleviated by additional hexokinase or ATP and was completely reversed by uncoupling oxygen consumption from ATP synthase using the proton ionophores 2,4-dinitrophenol (DNP) (Gosalvez et al., 1974).

This effect is preserved in cancer cells *in vitro*. The addition of glucose to Ehrlich ascites cells stimulates a brief increase in respiration, owing to ADP production by the hexokinase reaction (Chance and Hess, 1959). This is followed by a sustained suppression of respiration, the classic Crabtree effect. By inhibiting pyruvate kinase with amino acid inhibitors (alanine, cysteine and phenylalanine), glycolysis is suppressed and this restores the respiratory rate to that prior to the addition of glucose (Gosalvez et al., 1975).

The Warburg effect

When both oxygen and glucose are supplied in sufficient quantities, most normal cells and tissues will preferentially use respiration as their primary source of ATP. On the other hand, cancer cells will preferentially use glycolysis (followed by fermentation) as their primary energy source even in the presence of oxygen. In other words, normal cells display a strong Pasteur effect, while in cancer cells the Crabtree effect is dominant.

This phenomenon, called 'aerobic glycolysis' or the 'Warburg effect' is named after its discoverer Otto Warburg, who demonstrated that the aerobic glycolytic ATP contribution of ascites cancer cells was 55%, while less than 1% in cells from normal liver and kidney (Warburg, 1956). While many normal tissues are dependent on oxygen supply to maintain viability, cancer cells can remain viable in the absence of either glucose or oxygen alone (Warburg et al., 1927). While Warburg fiercely defended the notion that this propensity for aerobic glycolysis is specific to cancer cells, numerous studies have shown that aerobic glycolysis is also present in non-cancerous cells and tissues, particularly those with a high proliferative rate. Crabtree demonstrated that non-malignant lesions induced by viral infection were frequently associated with an increase in aerobic glycolysis (Crabtree, 1928). Numerous other cells and tissues also have metabolism similar to that of tumours including retina, kidney medulla and bone marrow (Orr and Stickland, 1938), as well as leukocytes in the blood (Harrop and Barron, 1929). Using the same techniques as Warburg, (Crabtree, 1929) found an

extensive variability in respiration and glycolytic rate of experimental tumours some of which displayed high levels of respiration.

Rather than being a cancer specific phenomenon, several lines of evidence suggest that aerobic glycolysis is associated with proliferation of both tumorigenic and non-tumorigenic cells. In a set of hepatoma cell lines exhibiting a wide range of proliferation rates, the glycolytic rate is highly correlated with the proliferation rate and is always higher than that in normal, non-proliferating hepatic cells (Burk et al., 1967).

Rat thymocytes and lymphocytes are quiescent *in vitro* unless stimulated to proliferate with concanavalin A and/or IL-2 and have been used as a model system to study the metabolic differences between proliferating and non-proliferating cells.

Concanavalin A and IL-2 stimulation results in increased glucose consumption and lactate production, peaking at 20 times above resting levels and coinciding with a peak in DNA synthesis. Because lactate formation accounts for more than 95% of the glucose consumed, biomass accrual is not a contributing factor to increased glucose consumption (Wang et al., 1976).

Unstimulated thymocytes generate the vast majority (>95%) of their ATP from respiration in the presence of glucose and are not subject to the Crabtree effect (*i.e.* glucose induced suppression of respiration). Proliferation induced by mitogen stimulation results in a more than doubling of ATP turnover. This demand can met entirely from respiration of endogenous fuels in the absence of glucose and glutamine. The presence of glucose and glutamine causes a profound suppression of mitochondrial respiration in proliferating thymocytes, with almost two thirds (61%) of ATP production coming from glycolysis (Guppy et al., 1993).

Mitogen stimulation of these cells results in a dramatic increase in expression of multiple glycolytic enzymes, peaking at 48 hours, coinciding with the peak of cells in S-phase of the cell cycle

(Brand et al., 1988). PKM2 (the dominant PK isoform in thymocytes) mRNA increases 8-12 fold, and pyruvate kinase activity peaks 10 fold higher relative to resting cells (Netzker et al., 1992).

These studies demonstrate that increased glycolysis, and suppressed respiration in the presence of glucose is a feature of proliferating cells, and not solely of cancer cells.

Why do cancer cells have increased glycolysis?

Why is it that cancer cells and other proliferating cells in general exhibit elevated glycolysis? A range of theories have been proposed to explain why cancer cells or proliferating cells in general display increased glycolysis. Some of these are discussed below.

Warburg hypothesis

Otto Warburg postulated that cancer cells exhibited increased glycolysis as a consequence of defective mitochondrial function and also suggested that loss of mitochondrial dysfunction was a major driver of carcinogenesis. The 'Warburg Hypothesis' posited that various cellular insults, such as radiation, mutagens and transient hypoxia lead to cumulative and permanent damage of mitochondrial respiratory capacity, ultimately leading to the cancer phenotype (Warburg, 1956).

However cancer cells generally maintain mitochondrial respiratory capacity and will avidly consume oxygen to maintain ATP levels in the absence of glucose (Warburg et al., 1927). The efficiency of mitochondrial respiration of cancer cells is generally no lower than that of normal cells (Quastel and Bickis, 1959). While defects in mitochondrial function have been identified in some cancers, these are generally the exception rather than the rule. Thus defective mitochondrial respiration is not a prerequisite for cancer.

Suppression of ROS

It has been widely suggested that proliferating cells and cancer cells exhibit reduced respiration (and a compensatory increase in glycolysis) as a means of suppressing ROS levels in order to prevent

excessive oxidative stress and DNA damage. Indeed it is well known that excessive, supra-physiological levels of ROS, such as those encountered following ionising radiation therapy, inhibit proliferation and induce DNA damage.

However an extensive body of evidence demonstrates that moderate levels of ROS promote, rather than suppress proliferation of both normal and cancerous cells. (Kim et al., 2013, Chowdhury et al., 2010, Meng et al., 2008). Conversely, ROS scavengers can suppress proliferation (Havens et al., 2006).

In many cell types, NADPH oxidases are the primary source of proliferation stimulating ROS (Hole et al., 2013, Meng et al., 2008), however ROS derived from mitochondrial respiration has also been shown to be required for anchorage independent growth of KRas transformed cells (Weinberg et al., 2010).

Moderate levels of ROS inhibit protein tyrosine phosphatases (Meng et al., 2002) and activate kinases to promote tumour cell growth (Sauer et al., 2001). ROS are also required for entry into the S-phase of the cell cycle and increase throughout S-phase to peak at G₂/M phase (Havens et al., 2006).

Supply of biomolecules

One hypothesis is that high glucose consumption provides proliferating cells with the substrates required for biosynthesis and growth. Nucleic acids (*i.e.* DNA and RNA), lipids and protein make up the majority of the dry weight of the cell and cell replication requires a doubling in each of these constituents. As pointed out by Lunt *et al.*, glucose serves as a major source of carbon for *de novo* synthesis of nucleic acids, lipids and amino acids (Lunt and Vander Heiden, 2011). The five carbon sugar base of nucleotides is derived from ribose-5-phosphate, produced from glucose via the PPP and a number of the carbons of the nucleobase of nucleotides are also derived from glucose. Synthesis of fatty acids and cholesterol uses acetyl-CoA as a carbon source which is produced from

citrate derived from the TCA cycle, for which glucose via pyruvate, is a major carbon source. Finally, intermediates of glycolysis and the TCA cycle serve as precursors for synthesis of most of the non-essential amino acids. Thus in addition to being a source of energy for ATP production, glucose is a major source of carbons for macromolecule synthesis required for cell proliferation.

Indeed glucose is essential for continuous cell proliferation. In culture, cancer cells will not grow in culture media lacking glucose. However glucose can be replaced by alternative sugars such as fructose, galactose (Reitzer et al., 1979) or the nucleoside uridine (which acts as a source of ribose) (Wice et al., 1981, Linker et al., 1985), which can sustain proliferation rates that are only slightly lower than those in the presence of glucose. Unlike glucose, these alternative sugars are not metabolised via glycolysis to any significant degree but are instead utilised primarily via the pentose phosphate pathway for NADPH production and *de novo* nucleotide synthesis.

While glucose is essential, glycolysis itself is dispensable for proliferation. DS7 cells, which lack functional glucose-6-phosphate isomerase (the second enzyme of glycolysis), can only metabolise glucose via the oxPPP (Pouyssegur et al., 1980). These cells generate ATP entirely through mitochondrial respiration and surprisingly only have moderately impaired growth *in vitro* and maintain tumourigenicity of the parental cell line *in vivo* (Franchi et al., 1981).

These observations suggest that accrual of biomass and NADPH production via the glycolysis branching pathways, rather than ATP production via the glycolysis itself is why proliferating cells consume so much glucose. However almost all glucose taken up by cancer cells is released in the form of lactate or CO₂. Approximately 84% of 1-C¹³ glucose consumed by SF188 glioma cells *in vitro*, is released back into the culture media as 3-C¹³ lactate, and about 9% as 3-C¹³ alanine. 2-C¹³ glucose labelling experiments suggest that lactate production via the ox PPP (which would not be detectable by 1-C¹³ glucose labelling) accounts for an additional 5.8% of glucose consumed (DeBerardinis et al., 2007). This would mean over 98.5% of glucose carbon can be accounted for in fates not involving incorporation into biomass.

In a model called 'quantitative principles of metabolic control', by Newsholme *et al.*, suggested that maintaining a high flux through a core pathway such as glycolysis would allow branching pathways such as oxPPP to respond rapidly and dynamically to changes in demand for that pathway outlined in **(Figure 1.6)**. Activation of the oxPPP would theoretically cause concentrations of the pathway precursor, glucose-6-phosphate to fall, attenuating increased flux in response to pathway activation. This attenuation could be curtailed if flux through glycolysis (and therefore consumption of glucose-6-phosphate) is already very high.

The authors point out that the only alternative way to maintain the dynamic responsiveness of the oxPPP would be for enzymes upstream of glucose-6-phosphate i.e. hexokinase, to be subject to feedback inhibition by its product. Indeed this has proved to be the case. Glucose-6-phosphate is a potent inhibitor of hexokinase. This author is not aware of any study that has developed and tested a hypothesis based on 'quantitative principles of metabolic control' as the explanation as to why glycolysis is high in proliferating cells.

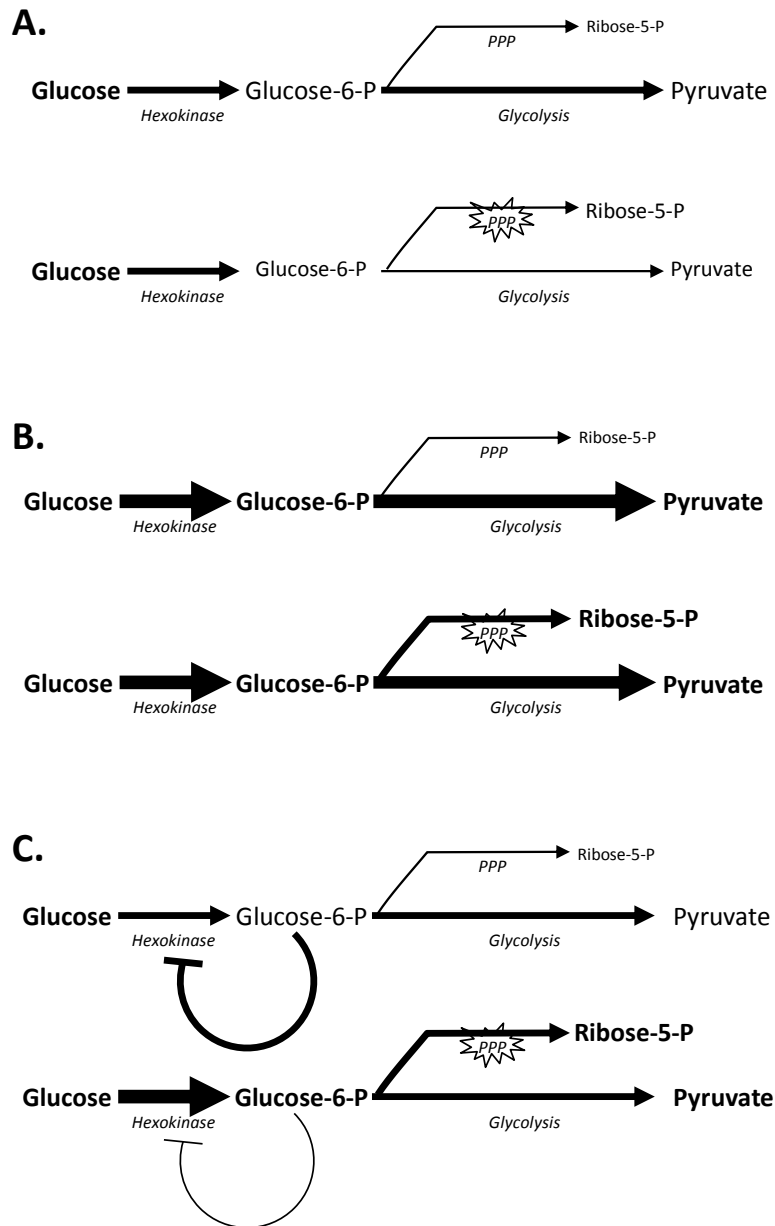


Figure 1.6. Quantitative Principles of Metabolic Control. **A.** In a system where flux through glycolysis is moderate and assuming no feedback control mechanisms, an increased flux capacity of the branching PPP pathway would lead to depletion of glucose-6-phosphate levels resulting in an increase in ribose-5-phosphate that is less than proportional to the activation of the pathway. **B. (Newsholme model)** In a system where flux through glycolysis is maintained at a high rate, stimulation of the PPP would only marginally increase the overall consumption rate of glucose-6-phosphate, allowing ribose-5-phosphate to increase proportionally to the increase in PPP flux capacity. **C. (Feedback model)** In a system where hexokinase is subject to feedback inhibition by glucose-6-phosphate, stimulation of the PPP resulting in consumption of glucose-6-phosphate would relieve inhibition on hexokinase allowing production of glucose-6-phosphate to increase to meet the change in demand.

Respiration is essential for proliferation

Respiration is absolutely essential for proliferation of normal and cancer cells alike. While moderate hypoxia can promote self-renewal in a number of cell types, anoxia is highly toxic to normal and cancer cells alike (Papandreou et al., 2005).

The reason for this is because a number of critical biosynthetic pathways involve the partial oxidation of glucose metabolites, in many cases transferring electrons to NAD^+ in the cytoplasm to produce NADH. In mammalian cells, the only effective mechanism for disposal of these excess reducing equivalents in order to replenish NAD^+ levels is through mitochondrial respiration. As is evident in **(Figure 1.2)**, oxidation of glucose intermediates via folate metabolism to produce $\text{N}^5, \text{N}^{10}$ methylene tetrahydrofolate (5,10-mTHF) requires the reduction of large amounts of NAD^+ . 5,10-mTHF is required as a methyl group donor for synthesis of purines and thymidine. The conversion of inosine monophosphate (IMP) to guanosine monophosphate (GMP) also involved the reduction of NAD^+ to NADH.

NADH from these biosynthetic processes in the cytoplasm is shuttled into the mitochondria via the malate-aspartate shuttle or the glycerol phosphate shuttle where reducing equivalents are transferred to molecular oxygen via the ETC. During pyrimidine synthesis, oxidation of dihydroorotate to orotate is catalysed by dihydroorotate dehydrogenase (DHODH), which in metazoan cells is located on the inner mitochondrial membrane and transfers reducing equivalents into the electron transport chain.

Mammalian cells cannot proliferate without a functional electron transport chain as they are unable to dispose of excess NADH or synthesise pyrimidines. Mammalian cells treated with ethidium bromide to deplete mitochondrial DNA will only proliferate *in vitro* if supplemented with exogenous pyruvate, which serves as an alternate electron acceptor to oxidise NADH via LDH, and uridine to support synthesis of pyrimidines (King and Attardi, 1989). Concentrations of pyruvate found in the blood are extremely low and therefore cannot support this function (Landon et al., 1962). *In vivo*,

mitochondrial respiration is indispensable for NAD^+ regeneration. Cancer cells lacking a functional ETC will not form tumours as subcutaneous xenografts (Franchi et al., 1981, Morais et al., 1994).

Some strains of yeast are capable of proliferating in anoxia by producing large quantities of glycerol (Pasteur, 1858). Reduction of the glycolysis intermediate dihydroxyacetone phosphate to glycerol-3-phosphate by glycerol-3-phosphate dehydrogenase (GPDH) oxidises NADH to NAD^+ . While the requisite enzymes are present in the human genome, little evidence suggest that a similar process occurs in the context of cancer. Glycerol is substantially elevated in the tumour tissue of patients with glioblastoma relative to normal peri-tumour tissue (Marcus et al., 2010). However gliomas have very low levels of GPDH compared to normal brain (Lowry et al., 1983). Ehrlich ascites tumour cells, a prototypical Warburg effect exhibiting cell line, are also deficient in GPDH (Boxer and Shonk, 1960) and instead produce glycerol-3-phosphate via a NADPH , rather than NADH dependent mechanism (Agranoff and Hajra, 1971).

While a number of theories exist as to why proliferation and cancer is associated with glycolysis, each has significant shortfalls, and the question as to why proliferating cells have increased glycolysis remains unanswered.

Regulation of Glucose Metabolism

The flux of glucose through glycolysis, along with its branching pathways is regulated by the cell by controlling the activity of several enzymes at several key points in the pathway. The reactions catalysed by hexokinase, phosphofructokinase and pyruvate kinase have large $-\Delta G$ (negative free energy change) and are considered irreversible at physiological conditions. These three enzymes are the major sites of glycolysis regulation. The remaining enzymatic reactions of glycolysis have relatively small changes in free energy, allowing the reactants to remain in constant equilibrium without enzyme regulation.

Regulating the activity of specific glycolytic enzymes allows the cell to increase the concentration of upstream glycolytic intermediates in order to redirect flux down the glycolysis branching pathways. The following section will discuss the regulatory features of these regulated enzymes, their importance to the metabolism of proliferating cells, and how they are altered in tumours with a focus on gliomas. These changes are mediated by both alterations in expression levels of the different isozymes, and by the actions of various signalling pathways that modify their function.

Additional functions of these and other glycolytic enzymes acting independently of their canonical role in metabolism have recently been uncovered and will be discussed.

Glucose transport

Because the plasma membrane is impermeable to glucose, uptake in most cell types via facultative diffusion is mediated by members of the GLUT transporter. GLUT1 is expressed in very high levels on both luminal and abluminal sides of the plasma membrane of endothelial cells within the brain, allowing glucose to rapidly cross the blood brain barrier. GLUT1 is also expressed to a lesser extent in astrocytes, while neurons express GLUT3 (Leino et al., 1997). GLUT3 has a significantly higher affinity for sugars than GLUT1, facilitating preferential uptake of glucose in GLUT3 expressing cells under conditions of reduced glucose availability (Gould and Holman, 1993).

Gliomas have high levels of GLUT1 and GLUT3. Glucose withdrawal has been shown to increase pro-tumourigenic phenotypes in glioma cells *in vitro* along with increased GLUT3 expression. Further, high GLUT3 expression is associated with poor clinical outcome (Flavahan et al., 2013). Glioma cells also frequently express high levels of VEGF, particularly in response to hypoxia which leads to increased GLUT1 expression in endothelial cells to facilitate enhanced glucose transport across the blood brain barrier (Yeh et al., 2008).

GLUT function can be modulated by its localisation as well as expression. Activation of GLUT4 in response to insulin is well characterised and involves the relocation of the transporter from

intracellular vesicles to the plasma membrane. While a range of stimuli have been shown to affect GLUT1 localisation in various cell types (including ATP levels, PI3K signalling and metabolic stress) the mechanisms of GLUT1 regulation are only poorly characterised (Leybaert, 2005).

Hexokinase

Hexokinase catalyses the phosphorylation of glucose to glucose-6-phosphate (G6P), using ATP as the phosphate donor. By adding a charged phosphate to the sugar, hexokinase traps the molecule within the plasma membrane, effectively committing the sugar to be metabolised by the cell. This reaction is required for practically all intracellular glucose utilising pathways.

Hexokinase isoforms

Four hexokinase genes arising from a single ancestral gene are present in the human genome. Glucokinase is a 50kDa monomeric enzyme with low affinity for glucose, its only sugar substrate, and is the primary hexokinase expressed in the liver. Hexokinase I, II and III (HK1, HK2 and HK3) are ~100kDa proteins, with homologous C and N terminal halves thought to have arisen from an ancient duplication and tandem ligation of a 50kDa glucokinase like ancestral gene (Printz et al., 1993). These three enzymes have ~250 fold higher affinity for glucose compared to glucokinase, and can also phosphorylate other sugars such as fructose (Wilson, 1995).

While expression of glucokinase is restricted to liver (which also expresses HK1), most other tissues express various mixtures of HK1 and HK2. Skeletal muscle expresses HK2 almost exclusively. Normal brain expresses high levels of HK1 while expression of HK2 is low (Katzen and Schimke, 1965).

While low grade meningiomas and astrocytomas maintain this expression pattern, high grade gliomas frequently express high levels of HK2 (Wolf et al., 2011). In U87MG cells, expression of HK2 but not HK1 or PKM2 is a key determinant of aerobic glycolysis. Knockdown of HK2 using shRNA

results in increased respiration, reduced glycolysis and increased sensitivity to hypoxia, radiation and temozolomide induced cell death (Wolf et al., 2011).

Other tissues such as kidney and the choroid layer of the eye express HK1 exclusively and only express HK2 following malignant transformation (Kamel and Schwarzfischer, 1975), suggesting that HK2 expression may be a common feature of cancer development.

Regulation of hexokinase

The most potent known allosteric regulator of hexokinase is its own reaction product G6P, which inhibits activity by competing with binding for ATP. The inhibition of hexokinase by G6P is antagonised or enhanced by levels of ATP and inorganic phosphate (P_i) in an isoform specific manner, possibly reflecting distinct roles in cellular metabolism. G6P inhibition of HK1 is antagonised by P_i , while P_i synergises with G6P inhibition of HK2 and HK3.

It has been suggested that HK2 primarily functions in a catabolic role. Periods of high energy demand would result in an increase in P_i /G6P ratio, which would lead to selective activation of HK1. HK1 is ubiquitously expressed in the body, and accounts for virtually all hexokinase activity in the brain. It has also been suggested that the regulatory features of HK2 favour anabolic metabolism, providing G6P for entry into the pentose phosphate pathway when energy levels are favourable and P_i levels are low (Wilson, 2003).

Interaction of hexokinase with mitochondria

A major component of the mitochondrial outer membrane is the voltage dependent anion channel (VDAC). VDAC forms a pore spanning the outer mitochondrial membrane and interacts with the adenine nucleotide transporter (ANT) embedded in the inner mitochondrial membrane to facilitate exchange of metabolites including ATP between cytoplasmic and mitochondrial compartments. HK1 and HK2 each possess an N-terminal VDAC targeting sequence that promotes their association with VDAC on the surface of mitochondria. This interaction promotes hexokinase

activity in two ways. First, this localisation provides hexokinase with immediate access to ATP exported from the mitochondria. Second, mitochondrial binding suppresses the inhibitory effect of G6P, however increasing G6P concentration eventually leads to dissociation from the mitochondria (Kurokawa et al., 1982).

Hexokinase binding also promotes the 'open' configuration of VDAC to facilitate exchange of metabolites across the outer mitochondrial membrane. This interaction is promoted by activation of Akt, which not only leads to enhanced mitochondrial metabolism, but also plays an important role in suppressing the mitochondria dependent apoptotic pathway (Robey and Hay, 2006).

Akt interacts with hexokinase to regulate metabolism and apoptosis

In response to pro-apoptotic stimuli, closure of VDAC and mitochondrial hyperpolarisation along with opening of the permeability transition pore (PTP) leads to release of cytochrome c, caspase activation and cell death. Many cancer cells suppress this pathway through increased expression of pro-survival Bcl-2 family member such as Bcl-2 and Bcl-XL, which counteract the pro-apoptotic Bcl-2 family members to prevent PTP opening. Like Bcl-2 and Bcl-XL, activated Akt can also prevent closure of VDAC, mitochondrial hyperpolarisation, opening of the PTP and cytochrome c release induced by exposure to ultraviolet light, etoposide, or Myc over-expression (Kennedy et al., 1999). Unlike Bcl-2 and Bcl-XL, prevention of apoptosis by activated Akt is dependent on glucose. Surprisingly, only the first step of glycolysis (i.e. the hexokinase reaction) is required for this protection, as 2-deoxyglucose (which can be metabolised by hexokinase but no further down glycolysis) also protected cells from apoptosis (Gottlob et al., 2001). Akt promotes localisation of the glucose transporter Glut1 to the plasma membrane and increases hexokinase activity (Rathmell et al., 2003). Akt also promotes hexokinase binding to the mitochondria, and this binding is required for the protective effects of Akt (Majewski et al., 2004). Overexpression of Glut1 and HK1 alone is also able to prevent mitochondrial dependent apoptosis and only in the presence of glucose (Rathmell et al., 2003). It has also been shown that upon activation, Akt physically interacts with HK2 to promote

phosphorylation of the enzyme and binding to VDAC and that this activity is required for Akt mediated protection of cardiomyocytes from ROS induced apoptosis (Miyamoto et al., 2008).

Phosphofructokinase

Hexose sugars such as glucose trapped within the cell by hexokinase mediated phosphorylation can continue to be metabolised via the glycolysis, or may be redirected into the oxidative arm of the pentose phosphate pathway. 6-phosphofructo-1-kinase (Phosphofructokinase 1, PFK1) is the third enzyme of glycolysis, catalysing the irreversible, ATP dependent phosphorylation of fructose-6-phosphate to fructose-1,6-bisphosphate. Situated in the glycolytic pathway, just distal to the bifurcation point with the oxidative PPP, activity of PFK1 is a major determinant of the relative flux through each of these alternate glucose utilising pathways.

Phosphofructokinase isoforms

The mammalian PFK1 enzyme is a homo-, or hetero-tetrameric complex consisting of a mixture of three different isozyme subunits encoded by three distinct genes; M type, L type and P type. Expression of each subunit is thought to reflect the activity of glycolysis and gluconeogenesis in different tissues. During embryonic development, early embryonic tissues express all three isoforms. In general, the isoform expression pattern shifts towards the adult pattern during gestation such that at birth, the distribution is similar to that seen in the adult (Davidson et al., 1983). M-type PFK1 is the dominant isoform in high glucose consuming tissues such as muscle and heart, while L-type is dominant in gluconeogenic tissues such as liver and kidney cortex and P-type is expressed in fibroblasts and rapidly dividing cells (Kahn et al., 1979), and is thought to favour aerobic glycolysis. Adult brain predominantly expresses M-type and to a lesser extent P-type PFK1, with the latter restricted to astrocytes (Almeida et al., 2004).

While there is no clear isozyme shift associated with oncogenesis, it has been demonstrated repeatedly that activity of PFK1 is elevated in cancer cells (Hennipman et al., 1988), presumably to

support increased aerobic glycolysis. For example, transformation of fibroblasts with oncogenic Ras, or Src results in increased PFK1 activity and glycolytic flux (Kole et al., 1991).

Regulation of phosphofructokinase

Positioned as a major regulator of glycolytic and PPP flux, PFK1 is subject to complex allosteric regulation. Overall, PFK1 activity is suppressed when the cellular energy state is high. ATP allosterically inhibits binding of the substrate fructose-6-phosphate, and citrate released from the mitochondria enhances this inhibition. ADP, AMP and P_i relieve PFK1 inhibition by ATP. These allosteric regulatory features allow for sparing of glucose from consumption by glycolysis when energy demands are satisfied by mitochondrial respiration. Allosteric inhibition of PFK1 is thought to be a major driver of the Pasteur effect (Tejwani, 1978).

PFK1 activity results in a decrease in upstream glycolytic metabolites including the hexokinase inhibitor glucose-6-phosphate, and an increase fructose-1,6-bisphosphate an allosteric activator of pyruvate kinase. Therefore, increases in PFK1 activity also promote activity of the other rate limiting enzymes of glycolysis.

Regulation by F2,6BP

A powerful allosteric activator of PFK1 is fructose-2,6-bisphosphate (F-2,6-BP). Levels of this metabolite, which is not part of glycolysis, are regulated by 6-phosphofructo-2-kinase/fructose-2,6-bisphosphatase (PFK-2/FBPase-2). PFK-2 is a bi-functional enzyme, constructed as a fusion protein of independent kinase and phosphatase domains (Bazan et al., 1989).

Allosteric activation of PFK1 by F-2,6-BP increases affinity for the substrate F6P, and relieves the inhibitory effects of ATP. A characteristic feature of proliferating cells is high intracellular F-2,6-BP concentration (Hue and Rider, 1987). This likely allows cancer cells to maintain high rates of glycolysis even in the presence of high ATP and may explain why cancer cells do not exhibit a strong Pasteur effect.

Levels of F2,6BP and hence activity of PFK1 is dictated by the balance between kinase and phosphatase activity of PFK-2/FBPase-2. Four isoforms of PFK-2/FBPase-2 are the product of four distinct genes, PFKFB1-4 with tissue specific expression patterns. PFKFB1, 2 and 4, have roughly equal kinase:phosphatase activity ratios (Chesney, 2006). PFKFB3, also termed 'inducible PFK2 (iPFK2)' because its expression is promoted by mitogenic, inflammatory and hypoxic stimuli (Minchenko et al., 2002), has almost no phosphatase activity, resulting in high F2,6BP levels in PFKFB3 expressing cells. Expression of PFKFB3 is dramatically elevated in many tumour types including tumours of the colon, breast, breast, ovary and thyroid (Atsumi et al., 2002), as well as high grade astrocytomas and glioblastomas (Kessler et al., 2008). PFKFB3, along with F2,6BP is transiently increased in proliferating normal lung fibroblasts (used as a model system for proliferating cells), specifically during S phase of the cell cycle (Atsumi et al., 2002). These results support the notion that increased F2,6BP levels, and therefore PFK1 activity, favours cell proliferation and tumour growth by promoting flux through glycolysis.

TIGAR suppresses PFK1 activity to promote survival of glioma cells

While there is strong evidence that increased activity of PFK1, supported by elevated PFK-2/FBPase-2 kinase activity and F2,6BP levels is conducive to cancer cell proliferation, there is also strong support that reduced F2,6BP levels and inhibition of PFK1 activity is favourable in cancer cells, by redirecting flux into the oxidative arm of the pentose phosphate pathway. Ectopic expression of the FBPase-2 domain results in depletion of F-2,6-BP and reduced PFK1 activity. While this results in reduced glycolysis and ATP content, inhibition of PFK1 also promotes increased flux through the oxidative PPP for NADPH production and increased resistance to oxidative stress (Boada et al., 2000).

TIGAR (TP53 induced glycolysis and apoptosis regulator) is a recently characterised p53 response factor with sequence homology to the FBPase-2 domain of PFK-2/FBPase-2, and displays FBPase-2 activity. Expression of TIGAR increases cellular antioxidant levels and suppresses ROS induced cell death by redirecting glucose flux from glycolysis to the PPP (Bensaad et al., 2006).

Expression of TIGAR is significantly elevated in glioblastoma relative to normal brain. Suppression of glycolysis in TIGAR expressing glioma cells promotes increased mitochondrial respiration in normoxic conditions, and suppressed ROS levels during hypoxia (Wanka et al., 2012). Ionising radiation results in up-regulation of TIGAR in U87MG glioma cells. Knockdown of TIGAR expression increases the glycolytic rate of these cells, reduces antioxidant levels, increases oxidative stress and sensitivity to ionising radiation (Pena-Rico et al., 2011). This evidence suggests that suppressed PFK1 activity is favoured in gliomas, and that this enhances tumour cell survival in a hostile environment.

Pyruvate Kinase

Pyruvate Kinase catalyses the final step of glycolysis, transferring the high energy phosphate group of phosphoenol pyruvate (PEP) to ADP yielding pyruvate and ATP. Like hexokinase and phosphofructokinase, the pyruvate kinase reaction has a large free energy change and is generally considered to be irreversible. Situated at the last step of glycolysis, regulation of pyruvate kinase activity not only influences flux through glycolysis, but also influences flux through the glycolysis branching pathways by affecting the concentration of glycolytic intermediates. Pyruvate kinase also has a complex relationship with respiration that is not completely understood.

Pyruvate kinase is of intense interest in the field of cancer metabolism. While a number of aspects remain controversial, it is clear that high expression of one particular pyruvate kinase isozyme, PKM2 is a near universal feature of cancer metabolism. As will be discussed in detail, expression of PKM2 is believed to be of fundamental importance in cancer cells because of its diverse array of regulatory features. These features afford the cancer cell a high degree of metabolic adaptability and control, facilitating survival and proliferation in the often harsh tumour environment.

Pyruvate kinase isoforms

In mammals, pyruvate kinase exists in four isoforms, encoded by two genes. These isoforms display diversity in the tissues in which they are expressed, their kinetic profiles, and mechanism of regulation. The *PK-L* gene gives rise to PK-R and PK-L through activation of tissue specific promoters. The *PK-M* gene gives rise to PK-M1 (PK M-type in older literature) and PK-M2 (PK K-type in older literature) through alternative splicing.

PK-L and PK-R

The *PK-L* gene possesses two promoters, ~500 bp apart, leading to inclusion of either exon 1 or exon 2 in the mRNA transcript. PK-L is generated by selective expression of exon 2 and is expressed in hepatocytes, kidney proximal tubules, and epithelial cells of the villi of the small intestines (Domingo et al., 1992). Expression of PK-L is highly responsive to nutrient status and insulin signalling allowing for regulation of pyruvate kinase activity in gluconeogenic tissues (Trempe et al., 1989).

PK-R is expressed exclusively in the erythrocyte lineage (Takegawa et al., 1983) through selective inclusion of exon 1. Inclusion of exon 1 in PK-R results in a protein 31 amino acids longer than PK-L. The function of this modification is unknown, but has been hypothesised to confer increased stability in erythrocytes (Muirhead, 1990) which were once believed to be incapable of protein synthesis (Kabanova et al., 2009).

PK-M1 and PK-M2

PKM1 and PKM2 are generated through mutually exclusive splicing of exon 9 and exon 10 of the *PKM* gene. These exons encode residues 380-435 (56 amino acids) of each isozyme respectively, with a difference of 23 amino acids. PKM1 is the predominant PK isoform in some adult tissues including muscle and brain and is expressed at lower levels in many other tissues.

PKM2 is the dominant isoform of pyruvate kinase in the embryo and in most adult tissues including kidney, intestine, stomach, spleen, lung, adipose tissue, testis, uterus, leukocytes (Imamura

and Tanaka, 1982), pancreatic islet cells (MacDonald and Chang, 1985), retina (Beemer et al., 1982), thyroid (Verhagen et al., 1985) and breast (Ibsen et al., 1982) and is highly expressed in most stromal tissue/fibroblasts (van Erp et al., 1991). It is also expressed at lower, yet still substantial levels in heart, brain and liver (Imamura and Tanaka, 1982, Bennett et al., 1975).

Expression of PKM2 in embryonic tissue is replaced other tissue specific isoforms as cells differentiate to their mature form. For example, myoblasts switch from PKM2 to PKM1 expression following differentiation to myotubes (Guguen-Guillouzo et al., 1977) as do neural progenitor cells differentiating into mature neurons (Venkatesan et al., 2011), and pro-erythrocyte differentiation to erythrocytes sees a progressive replacement of PK-M2 with PK-R (Takegawa et al., 1983). Many tissues maintain a mixture of different PK isoforms. When expressed in the same cell, mixtures of PK isoforms results in formation of hybrid tetramers. The nomenclature for these complexes describes their composition. For example a hybrid tetramer of one PKM1 and three PKM2 subunits would be denoted K₃M.

Selective expression of PKM1 or PKM2 isoforms is achieved through mutually exclusive inclusion of exon 9 (PKM1) or 10 (PKM2) in PKM transcripts, regulated by a process termed 'mutually exclusive splicing'. In tissues expressing PKM2, sequence specific repressors of splicing, hnRNPA1 and hnRNPA2 bind to the exon 9 splice site (EI9). Along with another splicing repressor, PTB which binds upstream of EI9, these proteins repress retention of exon 9, favouring the inclusion of exon 10 (David et al., 2010). Expression of hnRNPA1, hnRNPA2 and PTB are driven by the proto-oncogen c-Myc and have elevated expression in PKM2 expressing tumours. The exonic splicing enhancer SRSF3 also increases PKM2 by binding to exon 10 (Wang et al., 2012).

Regulation of pyruvate kinase

PKM2 and PK-L (and presumably PK-R) display sigmoidal enzyme kinetics with respect to PEP. These isozymes are allosterically activated by the upstream glycolysis intermediate fructose-1,6-bisphosphate (FBP). Binding of FBP induces a conformational change in these isozymes, promoting a

shift from the low PEP affinity 'tight' T-state, to the high PEP affinity 'relaxed' R-state (Jurica et al., 1998). This results in a reduced K_m for PEP (increased affinity), without affecting V_{max} or K_m for ADP. Uniquely, the PKM1 isoform displays no form of allosteric regulation and is 'locked' in the high PEP affinity R-state and displays hyperbolic kinetics, maintaining a high affinity for PEP, regardless of FBP or any other allosteric regulator (Ikeda et al., 1997). PKM2, PK-L are also allosterically inhibited by ATP and a number of amino acids, particularly alanine. PKM2 is allosterically activated by serine, while PK-L is not (Spellman and Fottrell, 1973). Phenylalanine is a non-competitive inhibitor of all pyruvate kinase isoforms.

Unlike the other pyruvate kinase isozymes which exist solely as tetramers, PKM2 is capable of switching between tetrameric and dimeric forms. Affinity for PEP is substantially lower in the dimeric form such that dimeric PKM2 is considered catalytically inactive at physiologically relevant PEP concentration (Feliu and Sols, 1976).

In the tetrameric form, pyruvate kinase associates with other glycolytic enzymes including phosphoglycerate kinase, glyceraldehyde phosphate dehydrogenase, and enolase in the 'glycolytic enzyme complex'. Formation of this complex is thought to increase glycolytic flux by reducing the diffusion distance between glycolytic enzymes (Mazurek et al., 1996). Along with reducing affinity for PEP, conversion to the dimeric form of PKM2 also results in dissociation from the glycolytic enzyme complex.

Both PKM2 and PK-L are regulated by phosphorylation through distinct mechanisms and for apparently different functions. In the liver, the hormone glucagon promotes phosphorylation of PK-L at an unknown site, most likely through activation of protein kinase A (Ishibashi and Cottam, 1978). Phosphorylation reduces the affinity of PK-L for both FBP and PEP, resulting reduced activity of the enzyme. Inhibition in response to glucagon is required to modulate the balance of gluconeogenesis and glycolysis in hepatocytes. PKM2 can also be inactivated by tyrosine phosphorylation through a protein kinase A independent mechanism (Eigenbrodt et al., 1977).

As will be discussed shortly, PKM2 is responsive to multiple stimuli present in cancer cells including phosphorylation and direct interaction with oncogenes, oxidation and allosteric regulation generally resulting in suppressed pyruvate kinase activity. While PK-L inactivation in liver is part of a coordinated metabolic shift towards glucose synthesis, the function of PKM2 inactivation in tumour cells appears to mediate a metabolic shift towards anabolism, by redirecting glycolysis intermediates into biosynthetic pathways.

Re-expression of PKM2 during carcinogenesis

The predominant view in the field of cancer metabolism is that neoplastic transformation of cells and tissues involves an isozyme switch from the tissue specific isoform (PK-L or PKM1) to PKM2. While it is certainly true that PKM2 is the dominant pyruvate kinase isoform expressed in cancer cells, it is less clear whether this is a consequence of isozyme switching, or simply due to the possibility that cancer cells generally arise from cell types that already express PKM2.

At present, there is a pervasive and erroneous tendency in the cancer metabolism field to purport that PKM1 is the predominant isoform in most adult tissues, while PKM2 expression is restricted to embryonic development and a small number of adult cell types. For example (Lv et al., 2011) stated that “PKM1 is expressed in most adult tissues, while PKM2 is exclusively expressed during embryonic development”, an assertion that is refuted by a plethora of experimental evidence.

Liver

Pyruvate kinase isoforms in the liver during normal function, regeneration and neoplastic transformation have been studied in far more detail than any other tissue type. In normal liver, PK-L expression is restricted to the parenchymal/hepatocyte cells, while stromal cells such as stellate and Kupffer cells, as well as the bi-potential ‘oval cells’ express PKM2. Following partial hepatectomy, all mature cell types of the liver re-enter the cell cycle in order to quickly recover hepatic function, reviewed in (Michalopoulos and DeFrances, 1997). During this period, a dramatic increase in PKM2

expression is observed. This was once believed to represent an isotype switch, from PK-L, in quiescent parenchymal cells, to PKM2, in proliferative parenchymal cells (Bonney et al., 1973).

Using percoll gradients to obtain highly pure cell populations, it was demonstrated that proliferating liver parenchymal cells do not in fact re-express PKM2, but maintain expression of only PK-L during proliferation, meaning the increase in PKM2 observed in whole liver preparations originates from non-parenchymal cells such as fibroblasts and Kupffer cells, which already express the M2 isoform (Miyanaaga et al., 1988).

Similarly, PK-L was shown to be replaced by PKM2 as the dominant pyruvate kinase isoform in hepatocellular carcinoma (HCC) animal models, with the authors concluding that this represented a shift towards PKM2 expression with malignant transformation (Reinacher and Eigenbrodt, 1981). These authors later revised their findings, showing that while transformed parenchymal cells lose PK-L expression, they do not gain expression of PKM2. Expression of PKM2 remained restricted to the stromal cell population and increased three fold in tumour bearing tissue (Reinacher et al., 1986).

More recently, immunohistochemistry evidence has supported a genuine shift in expression from PK-L to PKM2 within hepatocytes in premalignant hepatic foci of rats treated with the hepatocarcinogenic agent N-nitrosomorpholine (NNM) (Steinberg et al., 1999). The authors suggested that refinements in sample fixation may account for the discrepancy between this and the previous study.

Brain

Expression of pyruvate kinase isoforms has also been well studied in the brain, in both healthy and neoplastic tissue. As with most tissues, the embryonic brain primarily expresses PKM2. During maturation, a gradual shift in expression is observed such that in whole brain, PKM1 is the predominant isozyme, with lesser amounts of PKM2 (Bennett et al., 1975). Cortical grey matter, primarily composed of neuronal cell bodies, expresses PKM1 almost exclusively. In contrast, white

matter, primarily composed of axons, and glial cells, contains a mixture of M₄, K₃M and K₄ (van Veelen et al., 1978).

In human gliomas, the isozyme composition reverts back to predominant expression of PKM2. Surprisingly, the surrounding 'normal' brain tissue also frequently exhibited increased PKM2 expression despite no histological signs of neoplasm (Bennett et al., 1975). Like in the case of PK-L and PKM2 in the liver, high PKM1 expression in normal brain versus high PKM2 expression in glioma does not necessarily indicate a switch in expression in glioma cells, but may rather be a result of an expansion of the cell population that already expresses PKM2. Indeed the cells of the astrocytic lineage from which gliomas are thought to arise, already express high levels of PKM2 (van Erp et al., 1991).

Other tissues

Christofk *et al.* demonstrated that tumour development in a virally induced breast cancer mouse model is associated with a switch from PKM1 to PKM2 (Christofk et al., 2008a). This is in contrast to previous observations in human tissues showing that PKM2 is the predominant pyruvate kinase isoform in both normal and malignant breast tissue (Ibsen et al., 1982).

Bluemlein *et al.* recently used mass spectrometry for unbiased quantification of PKM isoforms (but not PK-L or PK-R) in a range of tumours and cell lines, along with equivalent normal tissue. As anticipated, PKM2 was the dominant PKM isoform in tumour tissue, however surprisingly for many, this was also the case for each normal tissue investigated (muscle and brain was not investigated). PKM2 in normal kidney, lung, liver and thyroid tissue accounted for at least 93% of total PKM suggesting that an isoform switch from PKM1 to PKM2 does not actually occur during tumourigenesis (Bluemlein et al., 2011). The authors did measure a consistent increase in the absolute expression level of PKM2 in tumour tissue compared to normal tissue except curiously in HCC, where expression remained low in two out of the three samples examined.

Unique regulatory features of PKM2 support tumour growth

While it remains questionable as to whether a shift in pyruvate kinase isoform expression really is a general feature of malignant transformation of cells, it is clear that tumour cells express PKM2 almost exclusively, and that expression is frequently much higher than in their non-cancerous counterparts (Koss et al., 2004). These tumour cells also express proportionally more catalytically inactive dimeric PKM2 (Mazurek et al., 2000), yet overall pyruvate kinase activity is still much higher in cancer cells compared to normal cells (Eigenbrodt et al., 1997). Glioma cells are an exception to this rule and maintain expression of moderate levels of PKM1 as well as high amounts of PKM2 (Mukherjee et al., 2013).

Numerous reports have also identified PKM2 of tumours as a distinct species to that of PKM2 of normal tissue, with altered regulatory characteristics and isoelectric point (Becker et al., 1986, Eigenbrodt et al., 1983).

High expression of PKM2 in cancer cells suggests that high pyruvate kinase activity is important for cell growth. Loss of pyruvate kinase activity through shRNA knockdown of PKM2 leads to impaired cell growth *in vitro*. Growth *in vitro* can be rescued equally well through re-expression of PKM2 or the unregulated PKM1 isozyme (Christofk et al., 2008a).

However tumours expressing high levels of PKM1 have never been observed, and once tumorigenic cells engineered to express PKM1 in place of PKM2 will fail to form tumours in mice (Christofk et al., 2008a). This indicates that the ability of pyruvate kinase activity to be down regulated is also critical for tumour formation. While in normal tissues PKM2 is mainly tetrameric, PKM2 in tumour cells is believed to be predominantly dimeric (Mazurek et al., 2005).

PKM2 expression and activity is increased in cancer cells and promotes cancer cell growth, making PKM2 inhibitors a potential rational therapeutic. The viability of cancer cells *in vivo* is also

dependent on the capacity of PKM2 activity to be down regulated, making PKM2 activators another potential rational therapeutic.

Justifying the potential therapeutic value of either PKM2 activators or PKM2 inhibitors will require an understanding of what role PKM2 regulation plays in cancer cell biology. There has been a great deal of progress in recent years in the understanding of the many regulators of PKM2 function, and how these regulatory features work for the benefit of the cancer cell. While theories as to how PKM2 expression benefits cancer cells, only recently have the tools (such as PKM2 activators and inhibitors) become available to test these theories.

The following sections will detail how PKM2 is regulated in the context of cancer and how this regulation serves to aid tumour growth.

Oncogenic signalling inhibits PKM2

The first evidence of PKM2 inhibition by oncogenic signalling was based on oncogenic viruses. The pp60^{src} phosphoprotein of the Rous sarcoma virus physically interacts with PKM2 resulting in phosphorylation of PKM2 tyrosine residues and reduced affinity for PEP (Presek et al., 1980, Presek et al., 1988). The E7 oncoprotein of HPV-16 (human papillomavirus type 16) also physically interacts with PKM2 to promote tetramer dissociation (Zwerschke et al., 1999).

Christofk *et al.* again showed that PKM2 binds to phospho-tyrosine peptides, and identified a peptide sequence that when tyrosine phosphorylated, interacted with PKM2 to promote dissociation of FBP and reduced enzyme activity. This interaction is dependent on residue Lys433, within the 56 amino acid segment unique to PKM2. Treatment of PKM2 expressing cells with the phosphatase inhibitor vanadate (to increase intracellular phospho-tyrosine levels), transfection with constitutively active cSrc (a non-receptor tyrosine kinase) or stimulation with IGF (insulin like growth factor) also resulted in reduced activity (Christofk et al., 2008b).

PKM2 can itself act as the PKM2 interacting phospho-tyrosine peptide. PKM2 can be phosphorylated on six tyrosine residues. Phosphorylation of Tyr105 but not the other five residues results in inhibition of PKM2 activity in a Lys433 dependent manner. A phosphorylated peptide derived from the sequence around Y105 of PKM2 induces release of FBP, dissociation of the tetramer and reduced pyruvate kinase activity. Pharmacologic inhibition of a range of tyrosine kinases including BCR-ABL, JAK2, FLT-3 and FGFR1 results in reduced PKM2 Tyr105 phosphorylation. Expression of the phosphorylation resistant mutant PKM2 Y105F reduces the tumourigenicity of cancer cells *in vivo*, demonstrating that tyrosine phosphorylation in response to oncogenic signalling is important for cancer cell biology (Hitosugi et al., 2009).

Serine phosphorylation of PKM2

PKM2 is also phosphorylated on serine residues, although very little is known about this modification. In high grade gliomas as well as medullary thyroid carcinomas, phosphorylation of PKM2 occurs exclusively on serine with no phosphorylation of tyrosine residues. Specific serine residues have not been identified (Weernink et al., 1990, Rijksen et al., 1988). Unlike tyrosine phosphorylation, which promotes dissociation of FBP, serine phosphorylation is inhibited by the presence of FBP (Weernink et al., 1992).

PKM2 and redox balance

PKM2 and PK-L are sensitive to inhibition by thiol oxidation of cysteine residues. Studies using enzymes from liver have shown that GSSG (glutathione disulphide, the oxidised form of glutathione), which accumulates in cells exposed to oxidative stress inhibits the activity of pyruvate kinase (Mannervik and Axelsson, 1980) while also stimulating activity of G6PDH to increase flux through the oxidative pentose phosphate pathway (Eggleston and Krebs, 1974). This reciprocal arrangement was hypothesised to aid in redirection into the PPP in order to counter oxidative stress (Ziegler, 1985).

Specifically, oxidation of Cys358, located in a region critical to catalytic activity results in inactivation of PKM2. While this residue is also present in PKM1, the isozyme is not sensitive to inhibition by thiol oxidation. Inactivation of PKM2 by oxidation of Cys358 is critical for redirecting flux into the oxPPP. Cells expressing the oxidation resistant mutant PKM2 C358S, or treated with a small molecule PKM2 activator maintain PKM2 activity and fail to redirect flux into the oxPPP resulting in reduced viability following exposure to oxidative stress (Anastasiou et al., 2011).

Serine metabolism

The amino-acid serine is synthesised from the glycolytic intermediate 3-phosphoglycerate, positioned several steps above that of pyruvate kinase. Serine catabolism to glycine and eventually NH_3 and CO_2 is a critical source of methyl groups for folate regeneration used in nucleotide synthesis. For many years it has been known that PKM2 is allosterically activated by serine (Spellman and Fottrell, 1973). For unknown reasons, PKM2 of tumours and placenta is more sensitive to serine activation than PKM2 of other PKM2 expressing tissues such as lung (Becker et al., 1986, Spellman and Fottrell, 1973).

Given that glycolytic intermediates upstream of pyruvate kinase are used for serine synthesis, and serine is an allosteric activator of PKM2, it had long been suspected that pyruvate kinase activity regulated serine metabolism. The first direct evidence that reduced pyruvate kinase activity promotes serine synthesis came from ^{13}C -glucose tracer experiments in PKM knockdown HCT116 cells (Chaneton et al., 2012). Loss of PKM1 and PKM2 expression in these cells promoted a dramatic increase in PEP, serine and glycine. Deprivation of serine reduces PK activity. The serine binding site of PKM2 is distinct from that of FBP and different mutants, H464A and S437Y specifically lose allosteric activation by serine and FBP respectively.

Small molecule activation of PKM2 induces profound dependence on exogenous serine in some cancer cell lines but not others. PKM2 activation results in negligible to no changes in metabolite levels in glycolysis, the PPP, the TCA cycle or of amino acids (Anastasiou et al., 2012, Kung et al.,

2012). However ¹⁵N-glutamine tracer experiments showed significantly reduced glutamine transamination for serine synthesis following PKM2 activation. This resulted in a profound dependence of A549 cells on exogenous serine to sustain proliferation, which could be partially substituted by glycine. This effect was highly cell line specific, as SW480 (colorectal adenocarcinoma) and H522 (lung cancer) cells were insensitive to PKM2 activation and serine withdrawal (Kung et al., 2012).

Regulation of PKM2 by A-Raf

The serine/threonine kinase A-Raf (but not B-Raf or c-Raf) interacts with PKM2, resulting in either activation or inactivation of PKM2 to promote growth depending on the cellular context. Transformation of immortalised fibroblasts with gag-A-Raf was associated with increased PKM2 tetramer and PK activity and glycolytic flux. Transformation of these cells was severely hampered by expression of the kinase inactive PKM2 K366M (Le Mellay et al., 2002).

More recently, the same lab reported that unlike in immortalised fibroblasts, expression of A-Raf in primary (rather than immortalised) mouse fibroblasts suppresses PKM2 tetramer formation, and reduced glucose consumption and lactate production (Mazurek et al., 2007). Dimeric PKM2 from A-Raf expressing cells was unresponsive to FBP, but was still sensitive to activation by serine. The authors noted that while primary fibroblasts consumed serine and produced glutamine, immortalised fibroblasts consumed glutamine and synthesised serine. The authors suggested that this opposing response in the two cell lines was as a consequence of differences in serine metabolism. While primary fibroblasts had high levels of serinolysis and glutamine production, the opposite was true for immortalised fibroblasts. Therefore A-Raf may have promoted tetramer formation in immortalised fibroblasts because of elevated serine levels.

PKM2 and aerobic glycolysis

Logically one would expect that inhibition of PKM2 catalytic activity would result in reduced glycolysis, and a compensatory increase in respiration. Indeed inhibition of PKM2 activity using

allosteric inhibitors resulted in increased oxygen consumption of Ehrlich ascites cells (Gosalvez et al., 1975). More recently, reducing the activity of pyruvate kinase was shown to facilitate increased mitochondrial respiration by promoting increased flux through the oxPPP this, providing NADPH to counter the production of mitochondrial ROS which would otherwise limit mitochondrial respiration (Gruning et al., 2011).

Contrary to these results, substituting expression of the highly regulated PKM2 isozyme with the unregulated (and thus more active) PKM1 isozyme results in increased oxygen consumption and reduced lactate production (Christofk et al., 2008a).

These disparate observations are difficult to reconcile. The observation that PKM2 but not PKM1 cooperates with HIF1 to promote expression of glycolytic enzymes could provide an explanation for this discrepancy. However increasing pyruvate kinase activity through exogenous PKM1 expression while maintaining endogenous PKM2 still results in increased respiration and reduced glycolysis. Similarly, cells expressing the phosphorylation resistant PKM2 Y105F mutant, or cells treated with a small molecule PKM2 activator also have suppressed aerobic glycolysis (Hitosugi et al., 2009, Anastasiou et al., 2012).

Regulation of Pyruvate Metabolism

Pyruvate formed at the end of glycolysis has a number of fates within the cell. In normal cells, most pyruvate enters the mitochondria where it is oxidised further by pyruvate dehydrogenase (PDH) to produce CO₂, NADH and acetyl-CoA which can then feed into the TCA cycle for complete oxidation to CO₂. The other major fate of pyruvate is its reduction to lactate by lactate dehydrogenase (LDH) which transfers reducing equivalents from NADH produced during glycolysis to regenerate the oxidised form NAD⁺. The relative activity of PDH and LDH therefore influence whether the pyruvate produced by glycolysis is used for fermentation or respiration.

Pyruvate can also be used for anaplerosis, carboxylated to the TCA cycle intermediates oxaloacetate or malate by pyruvate carboxylase or malate dehydrogenase respectively. Finally, alanine transaminase can catalyse the transfer of amine groups from glutamate to pyruvate to generate α -ketoglutarate and alanine.

Pyruvate dehydrogenase

The activity of pyruvate dehydrogenase is a major determinant of entry of pyruvate into the TCA cycle. The activity of this enzyme is primarily regulated via the action of pyruvate dehydrogenase kinase (PDK), which phosphorylates PDH on serine residues to inhibit enzyme activity. As discussed under 'The Pasteur Effect', inhibition of PDH during hypoxia is mediated through HIF1 dependent expression of PDK1. Other factors leading to increased HIF1 signalling will also lead to increased PDK expression, reduced PDH activity, and reduced entry of pyruvate into the TCA cycle.

Inhibitors of PDK have been investigated as potential therapeutic agents for cancer therapy. Dichloroacetate (DCA) is an inhibitor of PDK that has been used clinically to treat lactic acidosis in patients with mitochondrial disorders due to its ability to increase PDH activity and mitochondrial respiration.

Relative to normal brain most GBMs express extremely high levels of PDK2, a PDK isoform that is particularly sensitive to inhibition by DCA (Michelakis et al., 2010). Exposure of cancer cells but not normal cells to DCA *in vitro* has been shown to reduce lactate production and increase glucose oxidation which results in increased mitochondrial ROS production leading to mitochondrial K^+ efflux in turn promoting loss of $\Delta\Psi_m$ and enhanced apoptosis (Bonnet et al., 2007). DCA has been shown to be effective in preclinical models *in vivo* in multiple cancer types including glioma (Duan et al., 2013, Bonnet et al., 2007, Kumar et al., 2013) and small human studies have produced some favourable outcomes (Michelakis et al., 2010).

Lactate dehydrogenase

Lactate dehydrogenase (LDH) catalyses the reversible reduction of pyruvate to lactate, with concomitant oxidation of NADH to NAD⁺. In mammals, LDH is a homo- or hetero- tetramer composed of M or H subunits, products of the *LDHA* and *LDHB* genes respectively. While the LDH reaction is highly reversible, the H subunit is strongly inhibited by elevated pyruvate concentration, favouring oxidation of lactate to pyruvate, and promoting increased mitochondrial respiration. In contrast, the M subunit maintains high activity in the presence of pyruvate and is necessary for rapid fermentation of pyruvate generated through glycolysis (Dawson et al., 1964).

The shift towards expression of M subunit (i.e. LDHA) is a frequent occurrence in cancer. In primary brain tumours, increased ratio of M- to H- subunits is strongly associated with increased tumour grade (Sherwin et al., 1968, Yun, 1980).

Hypoxia Inducible Factors

While acute changes in energy metabolism in response to fluctuations in nutrient and oxygen availability can be achieved through allosteric regulation, cells also respond through changes in gene expression. Hypoxia results in increased expression of numerous genes associated with glucose metabolism. Mammalian cells exposed to chronic (96 hours) hypoxia results in increased activity of all ten glycolytic enzymes and lactate dehydrogenase. Pyruvate kinase activity was shown to increase over five fold in response to hypoxia (Robin et al., 1984). Microarray analysis of hypoxic murine fibroblasts also demonstrated up-regulation of genes for enzymes for eight of the ten steps of glycolysis, as well as lactate dehydrogenase and Glut 1 (Greijer et al., 2005). 89% (40 of 45) of genes up-regulated by hypoxia were dependent on a single hypoxia responsive transcription factor, HIF-1.

HIF complexes are master regulators of the cellular response to hypoxia. The heterodimeric transcription factors are composed of an oxia sensitive α subunit (HIF-1 α , HIF-2 α or HIF-3 α), and an

oxia insensitive β subunit (HIF-1 β , HIF-2 β or HIF-3 β). HIF-1 is composed of HIF-1 α and HIF-1 β . In the presence of oxygen, α subunits are rapidly degraded.

The stability and consequently activity of HIF α subunits is governed by the PHDs (prolyl hydroxylases) and FIH (factor interacting HIF), which hydroxylate HIF α , priming the enzyme for subsequent poly-ubiquitylation and proteosomal degradation (Harris, 2002). The PHDs and FIH utilise molecular oxygen as a substrate for hydroxylation of HIF α subunits.

The high K_m of PHDs and FIH for O_2 (100-250 μ M and 90 μ M respectively (Ehrismann et al., 2007)) allows the activity of these enzymes to respond dynamically across the spectrum of physiological oxygen concentrations without saturation. This enables cells to respond to hypoxia well before the oxygen concentration becomes limiting to mitochondrial respiration.

The effect of glucose on HIF-1 α stabilisation is dependent on cell type, but in numerous cancer cell lines, high glucose availability has been shown to increase stabilisation (Lu et al., 2005). In the absence of glucose, glutamine promotes HIF-1 α degradation (Dehne et al., 2010).

Stabilisation of HIF α subunits allows for interaction with the β subunit to form the HIF complex, which translocates to the nucleus to activate transcription of hypoxia responsive genes (Yamashita et al., 2001).

HIF1 transcriptional activity results in expression of genes involved in promoting glucose metabolism, including the glucose transporters GLUT1 and GLUT3, many glycolytic enzymes, and LDH (Iyer et al., 1998). HIF-1 α also drives expression of PDK1 (pyruvate dehydrogenase kinase 1), which phosphorylates and inhibits PDH (pyruvate dehydrogenase), to reduce entry of pyruvate into the TCA cycle (Kim et al., 2006). These responses are likely to be responsible for much of the active suppression of mitochondrial respiration that occurs during hypoxia (as discussed under 'The Pasteur Effect')

HIF1 activity also promotes a number of responses conducive to tumour growth not directly associated with metabolism. Stabilisation of HIF1 leads to expression of vascular endothelial growth factor (VEGF) promoting the neovascularisation required for continued growth (Forsythe et al., 1996) and promotes GLUT1 expression in endothelial cells of the blood brain barrier. HIFs have also been shown to play an important role in the maintenance of self-renewal and proliferative capacity in human embryonic stem cells (Forristal et al., 2010), indicating that HIFs may play a similar role in cancer cells.

Hypoxia and HIFs have been shown to repress differentiation in glioma cells (Pistollato et al., 2009) leading to increased expression of CD133, often used as a marker of increased tumourigenicity in glioma cells (Soeda et al., 2009, McCord et al., 2009). Cells isolated from the hypoxic core of gliomas display increased CD133 and MGMT expression and are more resistant to temozolomide compared to cells from the more normoxic periphery of the tumour (Pistollato et al., 2010).

Akt-TORC1 and HIF signalling

The Akt-TORC1 signalling axis also interacts with HIF1 signalling in a complex manner. In glioma cells, expression of HIF1 α is dependent on activation of Akt which can be induced by hypoxia. Overexpression of PTEN can block HIF1 α accumulation during hypoxia in glioma cells (Zundel et al., 2000), while activation of Akt even during normoxia can lead to increased HIF1 α as shown in prostate cancer cells (Zhong et al., 2000). Raptor, a component of the TORC1 complex interacts directly with HIF1 α to increase transcriptional activity (Land and Tee, 2007). HIF1 drives expression of Redd1 (Shoshani et al., 2002), which then inhibits TORC1 activity by increasing TSC1/2 activity (DeYoung et al., 2008). In this way, hypoxia stimulates activation of Akt, while limiting activation of downstream TORC1.

Signalling Pathways Dysregulated in Glioma Affect Cell

Metabolism

As discussed earlier mutations, gene amplification and gene expression changes occurring in RTK-Ras-PI3K, Rb and p53 signalling are highly enriched in glioblastoma cases. Many of the interactions of these signalling pathways and glucose metabolism have been discussed in the above sections. Below, additional effects of these signalling pathways on glucose metabolism is further elaborated.

Akt

In both normal and cancer cells, Akt activation promotes increased glycolysis independent of any effects on proliferation. Leukemic cells expressing a constitutively active mutant of Akt, (myrAkt) have increased glycolysis with no change in proliferation. Similarly, in glioma cell lines, glycolytic rate was poorly correlated with proliferative rate, but was associated with levels of phosphorylated Akt (Elstrom et al., 2004). Activated Akt promotes Glut1 localisation to the plasma membrane, increases the activity of and mitochondrial binding of hexokinase and activity and stability of PFK1 (Rathmell et al., 2003). As already discussed, the anti-apoptotic effect of Akt activation is dependent on its effects on glucose metabolism.

Beyond increased glucose consumption, cells with activated Akt are actually addicted to glucose, and dependent on glycolysis for survival. Glioma cells treated with the PI3K inhibitor LY294002 had a reduced glycolytic rate, but also became resistant to glucose starvation (Elstrom et al., 2004). RNAi knockdown of Akt, but not mTOR also improves survival during glucose starvation, suggesting this effect is not dependent on protein translation (Buzzai et al., 2005)

This dependence on glucose arises from an inability to activate fatty acid β -oxidation upon glucose withdrawal. Activation of AMPK with AICAR promoted β -oxidation to rescue Akt-driven, glucose starved cells. Similarly, supplying cells with methyl-pyruvate as an alternative mitochondrial

fuel source also maintained viability. The authors proposed that activation of Akt initiates a cascade of events that promote fatty acid synthesis and inhibits β -oxidation, leading to a loss of energy in the absence of glucose (Buzzai et al., 2005).

P53

The tumour suppressor p53 is a master regulator to cellular stress. Although well known to induce cellular senescence and cell death in response to a wide range of stimuli including genotoxic damage, nutrient stress and oncogene activation (Horn and Vousden, 2007), p53 activation in response to moderate levels of stress can actually lead to cellular responses that favour increased survival and resistance to stress (Kim et al., 2009). Reflecting this complexity on cell survival, p53 affects glucose metabolism at multiple levels in an apparent contradictory fashion.

A number of studies have demonstrated that p53 loss, or expression of dominant negative p53 mutants (DN-p53) leads to increased glucose uptake. In some cell types, this effect appears to be due to increased expression of GLUT family transporters (Schwartzberg-Bar-Yoseph et al., 2004). Loss of p53 was shown to relieve repression of the NF- κ B transcription factor to promote GLUT3 expression and increased glycolysis (Kawauchi et al., 2008). Other studies have observed increased glucose uptake independent of any change in GLUT expression (Smith et al., 2006).

Exposure of cells to ionising radiation leads to increased glucose uptake, reflecting its central role in nucleotide synthesis (for repair of damaged DNA) and NADPH production (maintenance of cellular anti-oxidant systems). Glucose uptake and hexokinase activity is dramatically enhanced in cancer cells lacking functional p53 in response to ionising radiation (Cheon et al., 2007, Chung et al., 2007).

P53 promotes ubiquitination and degradation of phospho glycerate mutase (PGM, catalysing the eight step of glycolysis) to suppress glycolysis. This increase in glycolysis and PGM expression is

necessary for immortalisation of mouse embryonic fibroblasts triggered by p53 loss (Kondoh et al., 2005).

These observations indicate that p53 activity inhibits glucose metabolism leading to reduced cell survival. However as discussed earlier, p53 also functions via TIGAR to suppress PFK1 activity, redirecting glucose flux down the pentose phosphate pathway to increase resistance to oxidative stress (Bensaad et al., 2006). Specific p53 mutations lead to gain-of-function activity that promotes tumour development and many tumours express high amounts of mutant p53. The hepatoma cell line AS-30D expresses high levels of p53 G103S/E256G, which binds to the HK2 promoter to drive increased expression of hexokinase (Mathupala et al., 1997).

Summary

Glioblastoma is a devastating disease with an exceptionally poor prognosis, high mortality rate and treatment options of only limited benefit. Like other cancer types, in glioma cells there is a shift in metabolism towards that which is characteristic of rapidly dividing cells, including increased glycolysis and suppressed respiration. While the mechanisms by which this occurs, and the survival and growth benefits that these changes confer are only partly understood, the near universality of altered metabolism in cancer highlights its fundamental importance.

As with other cancers, expression levels, isozyme composition and activity of multiple metabolic enzymes and their regulators are dramatically altered in glioma compared to normal brain tissue and mediate the changes in metabolism seen with cancer. These changes are not typically the result of genetic alteration of metabolic genes themselves, but as a consequence of altered cell signalling pathways which are a primary target of genetic alteration in cancer.

Activation of pro-oncogenic RTK-RAS-PI3K signalling in particular as well as perturbation in p53 promotes the coordinated increase in survival and proliferation and associated changes in metabolism necessary to support survival and proliferation of glioma cells.

Targeting of these signalling pathways for therapy has been a major focus of cancer research in recent years; however this strategy has been largely unsuccessful when applied in the clinic. The heterogeneity and diversity of driving mutations and the capacity for cancer cells to exhibit or acquire resistance, often through unrecognised mechanisms represents a target that is constantly moving and difficult to find.

On the other hand cancer metabolism, as a downstream effector of oncogenic signalling represents a much more conserved target. While there is a plethora of independent ways a cell can activate TORC1 activity, metabolic pathways present a number of relatively fixed potential targets.

Hexokinase is effectively the only entry point of glucose into cell metabolism, presenting an appealing target for inhibition. PKM2 is the dominant isoform of pyruvate kinase, and is highly expressed in practically all tumours. Even with an incomplete understanding of how high PKM2 expression supports tumour growth, this universality highlights the importance of this enzyme in cancer biology.

The overall aim of this thesis is to explore the utility of therapeutic interventions targeting cancer cell metabolism. While principally focused on glioma cell lines, the lessons learned are likely to be applicable across a range of cancer types.

In Chapter 3, a methodology is developed for assaying the anti-proliferative effects of combinations of drugs on glioma cells in vitro, comparing different approaches to assess antagonistic and synergistic drug interactions.

Because of its apparent critical role in regulating cancer metabolism, PKM2 is a sought after target for therapeutics. A novel PKM2 activator developed by Pfizer Inc. named WAY677099 was examined in Chapter 4. Specific aims were to:

- Identify factors and conditions regulating formation of the active tetrameric form (and hence catalytic activity) of PKM2 in glioma cell lines
- Assess the utility of a novel PKM2 activator WAY677099 to force PKM2 tetramer formation under conditions where it would otherwise be inactive
- Examine the effects of pharmacologic PKM2 activation on cell metabolism, particularly in regards to glycolysis and respiration
- Evaluate whether pharmacologic PKM2 activation can adversely affect the biology of cancer cells, thus leading to therapeutic potential of PKM2 activators.

While investigating factors influencing PKM2 activity, it was observed that two clinically approved anti-cancer therapeutic agents; temsirolimus and sorafenib, have potent effects on cell metabolism.

Sorafenib, which is currently approved for the treatment of HCC and RCC, and is currently undergoing evaluation for numerous other cancer types including glioma was found inhibit mitochondrial respiration in glioma cells as investigated in Chapter 5. Specific aims were to:

- Characterise in detail the specific effects of sorafenib on mitochondrial respiration
- Assess whether sorafenib treatment leads to a reliance on glycolysis for energy production and cell survival
- Evaluate the synergistic effect of sorafenib in combination with a glycolysis inhibitor to perturb cancer cell growth both *in vitro* and *in vivo*.

The TORC1 inhibitor temsirolimus was found to inhibit PKM2 and glycolytic flux in glioma cells, therefore this effect was examined further in Chapter 6. Specific aims were to:

- Characterise the inhibitory effect of temsirolimus on glycolysis and elucidate which stage of the pathway the drug is exerting its effect
- Demonstrate the inhibitory effect of temsirolimus on glycolysis
- Identify which step of glycolysis is inhibited by temsirolimus
- Evaluate the therapeutic implications of glycolysis inhibition by temsirolimus with regards to sensitisation to oxidative stress

References

- AGRANOFF, B. W. & HAJRA, A. K. 1971. The acyl dihydroxyacetone phosphate pathway for glycerolipid biosynthesis in mouse liver and Ehrlich ascites tumor cells. *Proc Natl Acad Sci U S A*, 68, 411-5.
- ALMEIDA, A., MONCADA, S. & BOLANOS, J. P. 2004. Nitric oxide switches on glycolysis through the AMP protein kinase and 6-phosphofructo-2-kinase pathway. *Nat Cell Biol*, 6, 45-51.
- ANASTASIOU, D., POULOGIANNIS, G., ASARA, J. M., BOXER, M. B., JIANG, J. K., SHEN, M., BELLINGER, G., SASAKI, A. T., LOCASALE, J. W., AULD, D. S., THOMAS, C. J., VANDER HEIDEN, M. G. & CANTLEY, L. C. 2011. Inhibition of pyruvate kinase M2 by reactive oxygen species contributes to cellular antioxidant responses. *Science*, 334, 1278-83.
- ANASTASIOU, D., YU, Y., ISRAELEN, W. J., JIANG, J. K., BOXER, M. B., HONG, B. S., TEMPEL, W., DIMOV, S., SHEN, M., JHA, A., YANG, H., MATTAINI, K. R., METALLO, C. M., FISKE, B. P., COURTNEY, K. D., MALSTROM, S., KHAN, T. M., KUNG, C., SKOUMBOURDIS, A. P., VEITH, H., SOUTHALL, N., WALSH, M. J., BRIMACOMBE, K. R., LEISTER, W., LUNT, S. Y., JOHNSON, Z. R., YEN, K. E., KUNII, K., DAVIDSON, S. M., CHRISTOFK, H. R., AUSTIN, C. P., INGLESE, J., HARRIS, M. H., ASARA, J. M., STEPHANOPOULOS, G., SALITURO, F. G., JIN, S., DANG, L., AULD, D. S., PARK, H. W., CANTLEY, L. C., THOMAS, C. J. & VANDER HEIDEN, M. G. 2012. Pyruvate kinase M2 activators promote tetramer formation and suppress tumorigenesis. *Nat Chem Biol*.
- ATSUMI, T., CHESNEY, J., METZ, C., LENG, L., DONNELLY, S., MAKITA, Z., MITCHELL, R. & BUCALA, R. 2002. High expression of inducible 6-phosphofructo-2-kinase/fructose-2,6-bisphosphatase (iPFK-2; PFKFB3) in human cancers. *Cancer Res*, 62, 5881-7.
- AUSTRALIAN INSTITUTE OF HEALTH AND WELFARE 2012. ACIM (Australian Cancer Incidence and Mortality) Books. AIHW: Canberra.
- BAI, X., MA, D., LIU, A., SHEN, X., WANG, Q. J., LIU, Y. & JIANG, Y. 2007. Rheb activates mTOR by antagonizing its endogenous inhibitor, FKBP38. *Science*, 318, 977-80.
- BAJENARU, M. L., ZHU, Y., HEDRICK, N. M., DONAHOE, J., PARADA, L. F. & GUTMANN, D. H. 2002. Astrocyte-specific inactivation of the neurofibromatosis 1 gene (NF1) is insufficient for astrocytoma formation. *Mol Cell Biol*, 22, 5100-13.
- BAZAN, J. F., FLETTERICK, R. J. & PILKIS, S. J. 1989. Evolution of a bifunctional enzyme: 6-phosphofructo-2-kinase/fructose-2,6-bisphosphatase. *Proc Natl Acad Sci U S A*, 86, 9642-6.
- BECKER, K. J., GEYER, H., EIGENBRODT, E. & SCHONER, W. 1986. Purification of pyruvate kinase isoenzymes type M1 and M2 from dog (*Canis familiaris*) and comparison of their properties with those from chicken and rat. *Comp Biochem Physiol B*, 83, 823-9.
- BEEEMER, F. A., VLUG, A. M., RIJKSEN, G., HAMBURG, A. & STAAL, G. E. 1982. Characterization of some glycolytic enzymes from human retina and retinoblastoma. *Cancer Res*, 42, 4228-32.
- BENNETT, M. J., TIMPERLEY, W. R., TAYLOR, C. B. & SHIRLEY HILL, A. 1975. Fetal forms of pyruvate kinase isoenzymes in tumours of the human nervous system. *Neuropathology and Applied Neurobiology*, 1, 347-356.
- BENSAAD, K., TSURUTA, A., SELAK, M. A., VIDAL, M. N., NAKANO, K., BARTRONS, R., GOTTLIEB, E. & VOUSDEN, K. H. 2006. TIGAR, a p53-inducible regulator of glycolysis and apoptosis. *Cell*, 126, 107-20.

- BLUEMLEIN, K., GRUNING, N. M., FEICHTINGER, R. G., LEHRACH, H., KOFLER, B. & RALSER, M. 2011. No evidence for a shift in pyruvate kinase PKM1 to PKM2 expression during tumorigenesis. *Oncotarget*, 2, 393-400.
- BOADA, J., ROIG, T., PEREZ, X., GAMEZ, A., BARTRONS, R., CASCANTE, M. & BERMUDEZ, J. 2000. Cells overexpressing fructose-2,6-bisphosphatase showed enhanced pentose phosphate pathway flux and resistance to oxidative stress. *FEBS Lett*, 480, 261-4.
- BONNET, S., ARCHER, S. L., ALLALUNIS-TURNER, J., HAROMY, A., BEAULIEU, C., THOMPSON, R., LEE, C. T., LOPASCHUK, G. D., PUTTAGUNTA, L., HARRY, G., HASHIMOTO, K., PORTER, C. J., ANDRADE, M. A., THEBAUD, B. & MICHELAKIS, E. D. 2007. A mitochondria-K⁺ channel axis is suppressed in cancer and its normalization promotes apoptosis and inhibits cancer growth. *Cancer Cell*, 11, 37-51.
- BONNEY, R. J., WALKER, P. R. & POTTER, V. R. 1973. Isoenzyme patterns in parenchymal and non-parenchymal cells isolated from regenerating and regenerated rat liver. *Biochem J*, 136, 947-54.
- BOXER, G. E. & SHONK, C. E. 1960. Low levels of soluble DPN-linked alpha-glycerophosphate dehydrogenase in tumors. *Cancer Res*, 20, 85-91.
- BRADA, M., HOANG-XUAN, K., RAMPLING, R., DIETRICH, P. Y., DIRIX, L. Y., MACDONALD, D., HEIMANS, J. J., ZONNENBERG, B. A., BRAVO-MARQUES, J. M., HENRIKSSON, R., STUPP, R., YUE, N., BRUNER, J., DUGAN, M., RAO, S. & ZAKNOEN, S. 2001. Multicenter phase II trial of temozolomide in patients with glioblastoma multiforme at first relapse. *Ann Oncol*, 12, 259-66.
- BRADA, M., STENNING, S., GABE, R., THOMPSON, L. C., LEVY, D., RAMPLING, R., ERRIDGE, S., SARAN, F., GATTAMANENI, R., HOPKINS, K., BEALL, S., COLLINS, V. P. & LEE, S. M. 2010. Temozolomide versus procarbazine, lomustine, and vincristine in recurrent high-grade glioma. *J Clin Oncol*, 28, 4601-8.
- BRAND, K., AICHINGER, S., FORSTER, S., KUPPER, S., NEUMANN, B., NURNBERG, W. & OHRISCH, G. 1988. Cell-cycle-related metabolic and enzymatic events in proliferating rat thymocytes. *Eur J Biochem*, 172, 695-702.
- BRAT, D. J., PRAYSON, R. A., RYKEN, T. C. & OLSON, J. J. 2008. Diagnosis of malignant glioma: role of neuropathology. *J Neurooncol*, 89, 287-311.
- BURGERING, B. M. & MEDEMA, R. H. 2003. Decisions on life and death: FOXO Forkhead transcription factors are in command when PKB/Akt is off duty. *J Leukoc Biol*, 73, 689-701.
- BURK, D., WOODS, M. & HUNTER, J. 1967. On the significance of glycolysis for cancer growth, with special reference to Morris rat hepatomas. *J Natl Cancer Inst*, 38, 839-63.
- BUZZAI, M., BAUER, D. E., JONES, R. G., DEBERARDINIS, R. J., HATZIVASSILIOU, G., ELSTROM, R. L. & THOMPSON, C. B. 2005. The glucose dependence of Akt-transformed cells can be reversed by pharmacologic activation of fatty acid beta-oxidation. *Oncogene*, 24, 4165-73.
- CASTELLANO, E. & DOWNWARD, J. 2011. RAS Interaction with PI3K: More Than Just Another Effector Pathway. *Genes Cancer*, 2, 261-74.
- CHANCE, B. & HESS, B. 1959. Spectroscopic evidence of metabolic control. *Science*, 129, 700-8.
- CHANETON, B., HILLMANN, P., ZHENG, L., MARTIN, A. C., MADDOCKS, O. D., CHOKKATHUKALAM, A., COYLE, J. E., JANKEVICS, A., HOLDING, F. P., VOUSDEN, K. H., FREZZA, C., O'REILLY, M. & GOTTLIEB, E. 2012. Serine is a natural ligand and allosteric activator of pyruvate kinase M2. *Nature*.
- CHAPMAN, J. D., REUVERS, A. P., BORSA, J. & GREENSTOCK, C. L. 1973. Chemical radioprotection and radiosensitization of mammalian cells growing in vitro. *Radiat Res*, 56, 291-306.
- CHEON, G. J., CHUNG, H. K., CHOI, J. A., LEE, S. J., AHN, S. H., LEE, T. S., CHOI, C. W. & LIM, S. M. 2007. Cellular metabolic responses of PET radiotracers to (188)Re radiation in an MCF7 cell line containing dominant-negative mutant p53. *Nucl Med Biol*, 34, 425-32.
- CHESNEY, J. 2006. 6-phosphofructo-2-kinase/fructose-2,6-bisphosphatase and tumor cell glycolysis. *Curr Opin Clin Nutr Metab Care*, 9, 535-9.
- CHOW, L. M. & BAKER, S. J. 2006. PTEN function in normal and neoplastic growth. *Cancer Lett*, 241, 184-96.
- CHOWDHURY, R., CHATTERJEE, R., GIRI, A. K., MANDAL, C. & CHAUDHURI, K. 2010. Arsenic-induced cell proliferation is associated with enhanced ROS generation, Erk signaling and CyclinA expression. *Toxicol Lett*, 198, 263-71.
- CHRISTOFK, H. R., VANDER HEIDEN, M. G., HARRIS, M. H., RAMANATHAN, A., GERSZTEN, R. E., WEI, R., FLEMING, M. D., SCHREIBER, S. L. & CANTLEY, L. C. 2008a. The M2 splice isoform of pyruvate kinase is important for cancer metabolism and tumour growth. *Nature*, 452, 230-3.
- CHRISTOFK, H. R., VANDER HEIDEN, M. G., WU, N., ASARA, J. M. & CANTLEY, L. C. 2008b. Pyruvate kinase M2 is a phosphotyrosine-binding protein. *Nature*, 452, 181-6.

- CHUNG, H. K., CHEON, G. J., CHOI, C. W., KIM, M. J., LEE, S. J. & LIM, S. M. 2007. Comparison of cellular metabolic responses of (18)F-FDG according to the effect of beta-irradiation in p53 wild and deleted cell lines. *Cancer Biother Radiopharm*, 22, 636-43.
- COHEN, M. H., SHEN, Y. L., KEEGAN, P. & PAZDUR, R. 2009. FDA drug approval summary: bevacizumab (Avastin) as treatment of recurrent glioblastoma multiforme. *Oncologist*, 14, 1131-8.
- CRABTREE, H. G. 1928. The carbohydrate metabolism of certain pathological overgrowths. *Biochem J*, 22, 1289-98.
- CRABTREE, H. G. 1929. Observations on the carbohydrate metabolism of tumours. *Biochem J*, 23, 536-45.
- CRESPO, I., TAO, H., NIETO, A. B., REBELO, O., DOMINGUES, P., VITAL, A. L., PATINO MDEL, C., BARBOSA, M., LOPES, M. C., OLIVEIRA, C. R., ORFAO, A. & TABERNEIRO, M. D. 2012. Amplified and homozygously deleted genes in glioblastoma: impact on gene expression levels. *PLoS One*, 7, e46088.
- CRESPO, I., VITAL, A. L., NIETO, A. B., REBELO, O., TAO, H., LOPES, M. C., OLIVEIRA, C. R., FRENCH, P. J., ORFAO, A. & TABERNEIRO, M. D. 2011. Detailed characterization of alterations of chromosomes 7, 9, and 10 in glioblastomas as assessed by single-nucleotide polymorphism arrays. *J Mol Diagn*, 13, 634-47.
- CROSS, D. A., ALESSI, D. R., COHEN, P., ANDJELKOVICH, M. & HEMMINGS, B. A. 1995. Inhibition of glycogen synthase kinase-3 by insulin mediated by protein kinase B. *Nature*, 378, 785-9.
- DAVID, C. J., CHEN, M., ASSANAH, M., CANOLL, P. & MANLEY, J. L. 2010. HnRNP proteins controlled by c-Myc deregulate pyruvate kinase mRNA splicing in cancer. *Nature*, 463, 364-8.
- DAVIDSON, M., COLLINS, M., BYRNE, J. & VORA, S. 1983. Alterations in phosphofructokinase isoenzymes during early human development. Establishment of adult organ-specific patterns. *Biochem J*, 214, 703-10.
- DAWSON, D. M., GOODFRIEND, T. L. & KAPLAN, N. O. 1964. Lactic Dehydrogenases: Functions of the Two Types Rates of Synthesis of the Two Major Forms Can Be Correlated with Metabolic Differentiation. *Science*, 143, 929-33.
- DEBERARDINIS, R. J., MANCUSO, A., DAIKHIN, E., NISSIM, I., YUDKOFF, M., WEHRLI, S. & THOMPSON, C. B. 2007. Beyond aerobic glycolysis: transformed cells can engage in glutamine metabolism that exceeds the requirement for protein and nucleotide synthesis. *Proc Natl Acad Sci U S A*, 104, 19345-50.
- DEHNE, N., HINTEREDER, G. & BRUNE, B. 2010. High glucose concentrations attenuate hypoxia-inducible factor-1alpha expression and signaling in non-tumor cells. *Exp Cell Res*, 316, 1179-89.
- DEUTSCH, M. B., PANAGEAS, K. S., LASSMAN, A. B. & DEANGELIS, L. M. 2013. Steroid management in newly diagnosed glioblastoma. *J Neurooncol*, 113, 111-6.
- DEYOUNG, M. P., HORAK, P., SOFER, A., SGROI, D. & ELLISEN, L. W. 2008. Hypoxia regulates TSC1/2-mTOR signaling and tumor suppression through REDD1-mediated 14-3-3 shuttling. *Genes Dev*, 22, 239-51.
- DI RENZO, M. F., NARSIMHAN, R. P., OLIVERO, M., BRETTI, S., GIORDANO, S., MEDICO, E., GAGLIA, P., ZARA, P. & COMOGLIO, P. M. 1991. Expression of the Met/HGF receptor in normal and neoplastic human tissues. *Oncogene*, 6, 1997-2003.
- DOMINGO, M., EINIG, C., EIGENBRODT, E. & REINACHER, M. 1992. Immunohistological demonstration of pyruvate kinase isoenzyme type L in rat with monoclonal antibodies. *J Histochem Cytochem*, 40, 665-73.
- DUAN, Y., ZHAO, X., REN, W., WANG, X., YU, K. F., LI, D., ZHANG, X. & ZHANG, Q. 2013. Antitumor activity of dichloroacetate on C6 glioma cell: in vitro and in vivo evaluation. *Onco Targets Ther*, 6, 189-98.
- EGGLESTON, L. V. & KREBS, H. A. 1974. Regulation of the pentose phosphate cycle. *Biochem J*, 138, 425-35.
- EHRISMANN, D., FLASHMAN, E., GENN, D. N., MATHIOUDAKIS, N., HEWITSON, K. S., RATCLIFFE, P. J. & SCHOFIELD, C. J. 2007. Studies on the activity of the hypoxia-inducible-factor hydroxylases using an oxygen consumption assay. *Biochem J*, 401, 227-34.
- EIGENBRODT, E., BASENAU, D., HOLTHUSEN, S., MAZUREK, S. & FISCHER, G. 1997. Quantification of tumor type M2 pyruvate kinase (Tu M2-PK) in human carcinomas. *Anticancer Res*, 17, 3153-6.
- EIGENBRODT, E., LEIB, S., KRAMER, W., FRIIS, R. R. & SCHONER, W. 1983. Structural and kinetic differences between the M2 type pyruvate kinases from lung and various tumors. *Biomed Biochim Acta*, 42, S278-82.
- EIGENBRODT, E., MOSTAFA, M. A. & SCHONER, W. 1977. Inactivation of pyruvate kinase type M2 from chicken liver by phosphorylation, catalyzed by a cAMP-independent protein kinase. *Hoppe Seylers Z Physiol Chem*, 358, 1047-55.
- EKSTRAND, A. J., JAMES, C. D., CAVENEE, W. K., SELIGER, B., PETTERSSON, R. F. & COLLINS, V. P. 1991. Genes for epidermal growth factor receptor, transforming growth factor alpha, and epidermal growth factor and their expression in human gliomas in vivo. *Cancer Res*, 51, 2164-72.

- ELSTROM, R. L., BAUER, D. E., BUZZAI, M., KARNAUSKAS, R., HARRIS, M. H., PLAS, D. R., ZHUANG, H., CINALLI, R. M., ALAVI, A., RUDIN, C. M. & THOMPSON, C. B. 2004. Akt stimulates aerobic glycolysis in cancer cells. *Cancer Res*, 64, 3892-9.
- FELIU, J. E. & SOLS, A. 1976. Interconversion phenomena between two kinetic forms of class a pyruvate kinase from Ehrlich ascites tumor cells. *Mol Cell Biochem*, 13, 31-44.
- FERNANDEZ-MEDARDE, A. & SANTOS, E. 2011. Ras in cancer and developmental diseases. *Genes Cancer*, 2, 344-58.
- FLAVAHAN, W. A., WU, Q., HITOMI, M., RAHIM, N., KIM, Y., SLOAN, A. E., WEIL, R. J., NAKANO, I., SARKARIA, J. N., STRINGER, B. W., DAY, B. W., LI, M., LATHIA, J. D., RICH, J. N. & HJELMELAND, A. B. 2013. Brain tumor initiating cells adapt to restricted nutrition through preferential glucose uptake. *Nat Neurosci*.
- FORRISTAL, C. E., WRIGHT, K. L., HANLEY, N. A., OREFFO, R. O. & HOUGHTON, F. D. 2010. Hypoxia inducible factors regulate pluripotency and proliferation in human embryonic stem cells cultured at reduced oxygen tensions. *Reproduction*, 139, 85-97.
- FORSYTHE, J. A., JIANG, B. H., IYER, N. V., AGANI, F., LEUNG, S. W., KOOS, R. D. & SEMENZA, G. L. 1996. Activation of vascular endothelial growth factor gene transcription by hypoxia-inducible factor 1. *Mol Cell Biol*, 16, 4604-13.
- FRANCHI, A., SILVESTRE, P. & POUYSSEGUR, J. 1981. A genetic approach to the role of energy metabolism in the growth of tumor cells: tumorigenicity of fibroblast mutants deficient either in glycolysis or in respiration. *Int J Cancer*, 27, 819-27.
- FRIEDMAN, H. S., JOHNSON, S. P., DONG, Q., SCHOLD, S. C., RASHEED, B. K., BIGNER, S. H., ALI-OSMAN, F., DOLAN, E., COLVIN, O. M., HOUGHTON, P., GERMAIN, G., DRUMMOND, J. T., KEIR, S., MARCELLI, S., BIGNER, D. D. & MODRICH, P. 1997. Methylator resistance mediated by mismatch repair deficiency in a glioblastoma multiforme xenograft. *Cancer Res*, 57, 2933-6.
- GAN, H. K., KAYE, A. H. & LUWOR, R. B. 2009. The EGFRVIII variant in glioblastoma multiforme. *J Clin Neurosci*, 16, 748-54.
- GERSON, S. L., TREY, J. E., MILLER, K. & BERGER, N. A. 1986. Comparison of O6-alkylguanine-DNA alkyltransferase activity based on cellular DNA content in human, rat and mouse tissues. *Carcinogenesis*, 7, 745-9.
- GNAIGER, E., MENDEZ, G. & HAND, S. C. 2000. High phosphorylation efficiency and depression of uncoupled respiration in mitochondria under hypoxia. *Proc Natl Acad Sci U S A*, 97, 11080-5.
- GOMEZ-PINILLA, F., KNAUER, D. J. & NIETO-SAMPEDRO, M. 1988. Epidermal growth factor receptor immunoreactivity in rat brain. Development and cellular localization. *Brain Res*, 438, 385-90.
- GOSALVEZ, M., LOPEZ-ALARCON, L., GARCIA-SUAREZ, S., MONTALVO, A. & WEINHOUSE, S. 1975. Stimulation of tumor-cell respiration by inhibitors of pyruvate kinase. *Eur J Biochem*, 55, 315-21.
- GOSALVEZ, M., PEREZ-GARCIA, J. & WEINHOUSE, S. 1974. Competition for ADP between pyruvate kinase and mitochondrial oxidative phosphorylation as a control mechanism in glycolysis. *Eur J Biochem*, 46, 133-40.
- GOTTLÖB, K., MAJEWSKI, N., KENNEDY, S., KANDEL, E., ROBEY, R. B. & HAY, N. 2001. Inhibition of early apoptotic events by Akt/PKB is dependent on the first committed step of glycolysis and mitochondrial hexokinase. *Genes Dev*, 15, 1406-18.
- GOULD, G. W. & HOLMAN, G. D. 1993. The glucose transporter family: structure, function and tissue-specific expression. *Biochem J*, 295 (Pt 2), 329-41.
- GRANDAL, M. V., ZANDI, R., PEDERSEN, M. W., WILLUMSEN, B. M., VAN DEURS, B. & POULSEN, H. S. 2007. EGFRVIII escapes down-regulation due to impaired internalization and sorting to lysosomes. *Carcinogenesis*, 28, 1408-17.
- GREIJER, A. E., VAN DER GROEP, P., KEMMING, D., SHVARTS, A., SEMENZA, G. L., MEIJER, G. A., VAN DE WIEL, M. A., BELIEN, J. A., VAN DIEST, P. J. & VAN DER WALL, E. 2005. Up-regulation of gene expression by hypoxia is mediated predominantly by hypoxia-inducible factor 1 (HIF-1). *J Pathol*, 206, 291-304.
- GRUNING, N. M., RINNERHALER, M., BLUEMLEIN, K., MULLEDER, M., WAMELINK, M. M., LEHRACH, H., JAKOBS, C., BREITENBACH, M. & RALSER, M. 2011. Pyruvate kinase triggers a metabolic feedback loop that controls redox metabolism in respiring cells. *Cell Metab*, 14, 415-27.
- GUGUEN-GUILLOUZO, C., SZAJNERT, M. F., MARIE, J., DELAIN, D. & SCHAPIRA, F. 1977. Differentiation in vivo and in vitro of pyruvate kinase isozymes in rat muscle. *Biochimie*, 59, 65-71.
- GUHA, A., FELDKAMP, M. M., LAU, N., BOSS, G. & PAWSON, A. 1997. Proliferation of human malignant astrocytomas is dependent on Ras activation. *Oncogene*, 15, 2755-65.
- GUPPY, M., GREINER, E. & BRAND, K. 1993. The role of the Crabtree effect and an endogenous fuel in the energy metabolism of resting and proliferating thymocytes. *Eur J Biochem*, 212, 95-9.

- GWINN, D. M., SHACKELFORD, D. B., EGAN, D. F., MIHAYLOVA, M. M., MERY, A., VASQUEZ, D. S., TURK, B. E. & SHAW, R. J. 2008. AMPK phosphorylation of raptor mediates a metabolic checkpoint. *Mol Cell*, 30, 214-26.
- HAHN-WINDGASSEN, A., NOGUEIRA, V., CHEN, C. C., SKEEN, J. E., SONENBERG, N. & HAY, N. 2005. Akt activates the mammalian target of rapamycin by regulating cellular ATP level and AMPK activity. *J Biol Chem*, 280, 32081-9.
- HANAHAN, D. & WEINBERG, R. A. 2011. Hallmarks of cancer: the next generation. *Cell*, 144, 646-74.
- HARRIS, A. L. 2002. Hypoxia--a key regulatory factor in tumour growth. *Nat Rev Cancer*, 2, 38-47.
- HARROP, G. A. & BARRON, E. S. 1929. STUDIES ON BLOOD CELL METABOLISM. V. THE METABOLISM OF LEUCOCYTES. *J. Biol. Chem.*, 84, 89-100.
- HAVENS, C. G., HO, A., YOSHIOKA, N. & DOWDY, S. F. 2006. Regulation of late G1/S phase transition and APC Cdh1 by reactive oxygen species. *Mol Cell Biol*, 26, 4701-11.
- HEGI, M. E., DISERENS, A. C., GORLIA, T., HAMOU, M. F., DE TRIBOLET, N., WELLER, M., KROS, J. M., HAINFELLNER, J. A., MASON, W., MARIANI, L., BROMBERG, J. E., HAU, P., MIRIMANOFF, R. O., CAIRNCROSS, J. G., JANZER, R. C. & STUPP, R. 2005. MGMT gene silencing and benefit from temozolomide in glioblastoma. *N Engl J Med*, 352, 997-1003.
- HEIMBERGER, A. B., HLATKY, R., SUKI, D., YANG, D., WEINBERG, J., GILBERT, M., SAWAYA, R. & ALDAPE, K. 2005. Prognostic effect of epidermal growth factor receptor and EGFRvIII in glioblastoma multiforme patients. *Clin Cancer Res*, 11, 1462-6.
- HENNIPMAN, A., VAN OIRSCHOT, B. A., SMITS, J., RIJKSEN, G. & STAAL, G. E. 1988. Glycolytic enzyme activities in breast cancer metastases. *Tumour Biol*, 9, 241-8.
- HIROSE, Y., KATAYAMA, M., MIRZOEVA, O. K., BERGER, M. S. & PIEPER, R. O. 2005. Akt activation suppresses Chk2-mediated, methylating agent-induced G2 arrest and protects from temozolomide-induced mitotic catastrophe and cellular senescence. *Cancer Res*, 65, 4861-9.
- HITOSUGI, T., KANG, S., VANDER HEIDEN, M. G., CHUNG, T. W., ELF, S., LYTHGOE, K., DONG, S., LONIAL, S., WANG, X., CHEN, G. Z., XIE, J., GU, T. L., POLAKIEWICZ, R. D., ROESEL, J. L., BOGGON, T. J., KHURI, F. R., GILLILAND, D. G., CANTLEY, L. C., KAUFMAN, J. & CHEN, J. 2009. Tyrosine phosphorylation inhibits PKM2 to promote the Warburg effect and tumor growth. *Sci Signal*, 2, ra73.
- HOLE, P. S., ZABKIEWICZ, J., MUNJE, C., NEWTON, Z., PEARN, L., WHITE, P., MARQUEZ, N., HILLS, R. K., BURNETT, A. K., TONKS, A. & DARLEY, R. L. 2013. Overproduction of NOX-derived ROS in AML promotes proliferation and is associated with defective oxidative stress signaling. *Blood*, 122, 3322-30.
- HONDA, S., KAGOSHIMA, M., WANAKA, A., TOHYAMA, M., MATSUMOTO, K. & NAKAMURA, T. 1995. Localization and functional coupling of HGF and c-Met/HGF receptor in rat brain: implication as neurotrophic factor. *Brain Res Mol Brain Res*, 32, 197-210.
- HORN, H. F. & VOUSDEN, K. H. 2007. Coping with stress: multiple ways to activate p53. *Oncogene*, 26, 1306-16.
- HUANG, P. H., MUKASA, A., BONAVIA, R., FLYNN, R. A., BREWER, Z. E., CAVENEE, W. K., FURNARI, F. B. & WHITE, F. M. 2007. Quantitative analysis of EGFRvIII cellular signaling networks reveals a combinatorial therapeutic strategy for glioblastoma. *Proc Natl Acad Sci U S A*, 104, 12867-72.
- HUE, L. & RIDER, M. H. 1987. Role of fructose 2,6-bisphosphate in the control of glycolysis in mammalian tissues. *Biochem J*, 245, 313-24.
- IBSEN, K. H., ORLANDO, R. A., GARRATT, K. N., HERNANDEZ, A. M., GIORLANDO, S. & NUNGARAY, G. 1982. Expression of multimolecular forms of pyruvate kinase in normal, benign, and malignant human breast tissue. *Cancer Res*, 42, 888-92.
- IKEDA, Y., TANAKA, T. & NOGUCHI, T. 1997. Conversion of non-allosteric pyruvate kinase isozyme into an allosteric enzyme by a single amino acid substitution. *J Biol Chem*, 272, 20495-501.
- IMAMURA, K. & TANAKA, T. 1982. Pyruvate kinase isozymes from rat. *Methods Enzymol*, 90 Pt E, 150-65.
- INOKI, K., OUYANG, H., ZHU, T., LINDVALL, C., WANG, Y., ZHANG, X., YANG, Q., BENNETT, C., HARADA, Y., STANKUNAS, K., WANG, C. Y., HE, X., MACDOUGALD, O. A., YOU, M., WILLIAMS, B. O. & GUAN, K. L. 2006. TSC2 integrates Wnt and energy signals via a coordinated phosphorylation by AMPK and GSK3 to regulate cell growth. *Cell*, 126, 955-68.
- ISHIBASHI, H. & COTTAM, G. L. 1978. Glucagon-stimulated phosphorylation of pyruvate kinase in hepatocytes. *J Biol Chem*, 253, 8767-71.
- IWAMOTO, F. M., ABREY, L. E., BEAL, K., GUTIN, P. H., ROSENBLUM, M. K., REUTER, V. E., DEANGELIS, L. M. & LASSMAN, A. B. 2009. Patterns of relapse and prognosis after bevacizumab failure in recurrent glioblastoma. *Neurology*, 73, 1200-6.

- IYER, N. V., KOTCH, L. E., AGANI, F., LEUNG, S. W., LAUGHNER, E., WENGER, R. H., GASSMANN, M., GEARHART, J. D., LAWLER, A. M., YU, A. Y. & SEMENZA, G. L. 1998. Cellular and developmental control of O₂ homeostasis by hypoxia-inducible factor 1 alpha. *Genes Dev*, 12, 149-62.
- JAIN, R. K. 2001. Normalizing tumor vasculature with anti-angiogenic therapy: a new paradigm for combination therapy. *Nat Med*, 7, 987-9.
- JEUKEN, J., VAN DEN BROECKE, C., GIJSEN, S., BOOTS-SPRENGER, S. & WESSELING, P. 2007. RAS/RAF pathway activation in gliomas: the result of copy number gains rather than activating mutations. *Acta Neuropathol*, 114, 121-33.
- JOHNSON, D. R., LEEPER, H. E. & UHM, J. H. 2013. Glioblastoma survival in the United States improved after Food and Drug Administration approval of bevacizumab: A population-based analysis. *Cancer*.
- JUNG, W., CASTREN, E., ODENTHAL, M., VANDE WOUDE, G. F., ISHII, T., DIENES, H. P., LINDHOLM, D. & SCHIRMACHER, P. 1994. Expression and functional interaction of hepatocyte growth factor-scatter factor and its receptor c-met in mammalian brain. *J Cell Biol*, 126, 485-94.
- JURICA, M. S., MESECAR, A., HEATH, P. J., SHI, W., NOWAK, T. & STODDARD, B. L. 1998. The allosteric regulation of pyruvate kinase by fructose-1,6-bisphosphate. *Structure*, 6, 195-210.
- KABANOVA, S., KLEINBONGARD, P., VOLKMER, J., ANDREE, B., KELM, M. & JAX, T. W. 2009. Gene expression analysis of human red blood cells. *Int J Med Sci*, 6, 156-9.
- KAHN, A., MEIENHOFER, M. C., COTTREAU, D., LAGRANGE, J. L. & DREYFUS, J. C. 1979. Phosphofructokinase (PFK) isozymes in man. I. Studies of adult human tissues. *Hum Genet*, 48, 93-108.
- KAINA, B., ZIOUTA, A., OCHS, K. & COQUERELLE, T. 1997. Chromosomal instability, reproductive cell death and apoptosis induced by O⁶-methylguanine in Mex⁻, Mex⁺ and methylation-tolerant mismatch repair compromised cells: facts and models. *Mutat Res*, 381, 227-41.
- KAMEL, R. & SCHWARZFISCHER, F. 1975. Hexokinase isozymes in human neoplastic and fetal tissues: the existence of hexokinase II in malignant tumors and in placenta. *Humangenetik*, 30, 181-5.
- KATZEN, H. M. & SCHIMKE, R. T. 1965. Multiple forms of hexokinase in the rat: tissue distribution, age dependency, and properties. *Proc Natl Acad Sci U S A*, 54, 1218-25.
- KAWAUCHI, K., ARAKI, K., TOBIUME, K. & TANAKA, N. 2008. p53 regulates glucose metabolism through an IKK-NF-kappaB pathway and inhibits cell transformation. *Nat Cell Biol*, 10, 611-8.
- KENNEDY, S. G., KANDEL, E. S., CROSS, T. K. & HAY, N. 1999. Akt/Protein kinase B inhibits cell death by preventing the release of cytochrome c from mitochondria. *Mol Cell Biol*, 19, 5800-10.
- KESSLER, R., BLEICHERT, F., WARNKE, J. P. & ESCHRICH, K. 2008. 6-Phosphofructo-2-kinase/fructose-2,6-bisphosphatase (PFKFB3) is up-regulated in high-grade astrocytomas. *J Neurooncol*, 86, 257-64.
- KIM, E., GIESE, A. & DEPPERT, W. 2009. Wild-type p53 in cancer cells: when a guardian turns into a blackguard. *Biochem Pharmacol*, 77, 11-20.
- KIM, J. H., PARK, S. G., SONG, S. Y., KIM, J. K. & SUNG, J. H. 2013. Reactive oxygen species-responsive miR-210 regulates proliferation and migration of adipose-derived stem cells via PTPN2. *Cell Death Dis*, 4, e588.
- KIM, J. W., TCHERNYSHYOV, I., SEMENZA, G. L. & DANG, C. V. 2006. HIF-1-mediated expression of pyruvate dehydrogenase kinase: a metabolic switch required for cellular adaptation to hypoxia. *Cell Metab*, 3, 177-85.
- KING, M. P. & ATTARDI, G. 1989. Human cells lacking mtDNA: repopulation with exogenous mitochondria by complementation. *Science*, 246, 500-3.
- KITANGE, G. J., CARLSON, B. L., SCHROEDER, M. A., GROGAN, P. T., LAMONT, J. D., DECKER, P. A., WU, W., JAMES, C. D. & SARKARIA, J. N. 2009. Induction of MGMT expression is associated with temozolomide resistance in glioblastoma xenografts. *Neuro Oncol*, 11, 281-91.
- KOLE, H. K., RESNICK, R. J., VAN DOREN, M. & RACKER, E. 1991. Regulation of 6-phosphofructo-1-kinase activity in ras-transformed rat-1 fibroblasts. *Arch Biochem Biophys*, 286, 586-90.
- KONDOH, H., LLEONART, M. E., GIL, J., WANG, J., DEGAN, P., PETERS, G., MARTINEZ, D., CARNERO, A. & BEACH, D. 2005. Glycolytic enzymes can modulate cellular life span. *Cancer Res*, 65, 177-85.
- KONG, D. S., SONG, S. Y., KIM, D. H., JOO, K. M., YOO, J. S., KOH, J. S., DONG, S. M., SUH, Y. L., LEE, J. I., PARK, K., KIM, J. H. & NAM, D. H. 2009. Prognostic significance of c-Met expression in glioblastomas. *Cancer*, 115, 140-8.
- KOOCHKPOUR, S., JEFFERS, M., RULONG, S., TAYLOR, G., KLINEBERG, E., HUDSON, E. A., RESAU, J. H. & VANDE WOUDE, G. F. 1997. Met and hepatocyte growth factor/scatter factor expression in human gliomas. *Cancer Res*, 57, 5391-8.
- KORNBLUM, H. I., HUSSAIN, R., WIESEN, J., MIETTINEN, P., ZURCHER, S. D., CHOW, K., DERYNCK, R. & WERB, Z. 1998. Abnormal astrocyte development and neuronal death in mice lacking the epidermal growth factor receptor. *J Neurosci Res*, 53, 697-717.

- KOSS, K., HARRISON, R. F., GREGORY, J., DARNTON, S. J., ANDERSON, M. R. & JANKOWSKI, J. A. 2004. The metabolic marker tumour pyruvate kinase type M2 (tumour M2-PK) shows increased expression along the metaplasia-dysplasia-adenocarcinoma sequence in Barrett's oesophagus. *J Clin Pathol*, 57, 1156-9.
- KRISTIANSEN, K., HAGEN, S., KOLLEVOLD, T., TORVIK, A., HOLME, I., NESBAKKEN, R., HATLEVOLL, R., LINDGREN, M., BRUN, A., LINDGREN, S., NOTTER, G., ANDERSEN, A. P. & ELGEN, K. 1981. Combined modality therapy of operated astrocytomas grade III and IV. Confirmation of the value of postoperative irradiation and lack of potentiation of bleomycin on survival time: a prospective multicenter trial of the Scandinavian Glioblastoma Study Group. *Cancer*, 47, 649-52.
- KUMAR, K., WIGFIELD, S., GEE, H. E., DEVLIN, C. M., SINGLETON, D., LI, J. L., BUFFA, F., HUFFMAN, M., SINN, A. L., SILVER, J., TURLEY, H., LEEK, R., HARRIS, A. L. & IVAN, M. 2013. Dichloroacetate reverses the hypoxic adaptation to bevacizumab and enhances its antitumor effects in mouse xenografts. *J Mol Med (Berl)*, 91, 749-58.
- KUMAR, Y., MAZUREK, S., YANG, S., FAILING, K., WINSLET, M., FULLER, B. & DAVIDSON, B. R. 2010. In vivo factors influencing tumour M2-pyruvate kinase level in human pancreatic cancer cell lines. *Tumour Biol*, 31, 69-77.
- KUNG, C., HIXON, J., CHOE, S., MARKS, K., GROSS, S., MURPHY, E., DELABARRE, B., CIANCHETTA, G., SETHUMADHAVAN, S., WANG, X., YAN, S., GAO, Y., FANG, C., WEI, W., JIANG, F., WANG, S., QIAN, K., SAUNDERS, J., DRIGGERS, E., WOO, H. K., KUNII, K., MURRAY, S., YANG, H., YEN, K., LIU, W., CANTLEY, L. C., VANDER HEIDEN, M. G., SU, S. M., JIN, S., SALITURO, F. G. & DANG, L. 2012. Small Molecule Activation of PKM2 in Cancer Cells Induces Serine Auxotrophy. *Chem Biol*, 19, 1187-98.
- KUROKAWA, M., ODA, S., TSUBOTANI, E., FUJIWARA, H., YOKOYAMA, K. & ISHIBASHI, S. 1982. Characterization of hexokinase isoenzyme types I and II in ascites tumor cells by an interaction with mitochondrial membrane. *Mol Cell Biochem*, 45, 151-7.
- LAMMING, D. W., YE, L., KATAJISTO, P., GONCALVES, M. D., SAITOH, M., STEVENS, D. M., DAVIS, J. G., SALMON, A. B., RICHARDSON, A., AHIMA, R. S., GUERTIN, D. A., SABATINI, D. M. & BAUR, J. A. 2012. Rapamycin-induced insulin resistance is mediated by mTORC2 loss and uncoupled from longevity. *Science*, 335, 1638-43.
- LAND, S. C. & TEE, A. R. 2007. Hypoxia-inducible factor 1alpha is regulated by the mammalian target of rapamycin (mTOR) via an mTOR signaling motif. *J Biol Chem*, 282, 20534-43.
- LANDON, J., FAWCETT, J. K. & WYNN, V. 1962. Blood pyruvate concentration measured by a specific method in control subjects. *J Clin Pathol*, 15, 579-84.
- LE MELLAY, V., HOUBEN, R., TROPPEMAYR, J., HAGEMANN, C., MAZUREK, S., FREY, U., BEIGEL, J., WEBER, C., BENZ, R., EIGENBRODT, E. & RAPP, U. R. 2002. Regulation of glycolysis by Raf protein serine/threonine kinases. *Adv Enzyme Regul*, 42, 317-32.
- LEINO, R. L., GERHART, D. Z., VAN BUEREN, A. M., MCCALL, A. L. & DREWES, L. R. 1997. Ultrastructural localization of GLUT 1 and GLUT 3 glucose transporters in rat brain. *J Neurosci Res*, 49, 617-26.
- LEYBAERT, L. 2005. Neurobarrier coupling in the brain: a partner of neurovascular and neurometabolic coupling? *J Cereb Blood Flow Metab*, 25, 2-16.
- LINKER, W., LOFFLER, M. & SCHNEIDER, F. 1985. Uridine, but not cytidine can sustain growth of Ehrlich ascites tumor cells in glucose-deprived medium with altered proliferation kinetics. *Eur J Cell Biol*, 36, 176-81.
- LISTERNICK, R., LOUIS, D. N., PACKER, R. J. & GUTMANN, D. H. 1997. Optic pathway gliomas in children with neurofibromatosis 1: consensus statement from the NF1 Optic Pathway Glioma Task Force. *Ann Neurol*, 41, 143-9.
- LOPEZ-GINES, C., CERDA-NICOLAS, M., GIL-BENSO, R., PELLIN, A., LOPEZ-GUERRERO, J. A., CALLAGHAN, R., BENITO, R., ROLDAN, P., PIQUER, J., LLACER, J. & BARBERA, J. 2005. Association of chromosome 7, chromosome 10 and EGFR gene amplification in glioblastoma multiforme. *Clin Neuropathol*, 24, 209-18.
- LOPEZ-GINES, C., GIL-BENSO, R., FERRER-LUNA, R., BENITO, R., SERNA, E., GONZALEZ-DARDER, J., QUILIS, V., MONLEON, D., CELDA, B. & CERDA-NICOLAS, M. 2010. New pattern of EGFR amplification in glioblastoma and the relationship of gene copy number with gene expression profile. *Mod Pathol*, 23, 856-65.
- LOUIS, D. N., OHGAKI, H., WIESTLER, O. D., CAVENEE, W. K., BURGER, P. C., JOUVET, A., SCHEITHAUER, B. W. & KLEIHUES, P. 2007. The 2007 WHO classification of tumours of the central nervous system. *Acta Neuropathol*, 114, 97-109.

- LOWRY, O. H., BERGER, S. J., CARTER, J. G., CHI, M. M., MANCHESTER, J. K., KNOR, J. & PUSATERI, M. E. 1983. Diversity of metabolic patterns in human brain tumors: enzymes of energy metabolism and related metabolites and cofactors. *J Neurochem*, 41, 994-1010.
- LU, H., DALGARD, C. L., MOHYELDIN, A., MCFATE, T., TAIT, A. S. & VERMA, A. 2005. Reversible inactivation of HIF-1 prolyl hydroxylases allows cell metabolism to control basal HIF-1. *J Biol Chem*, 280, 41928-39.
- LUNT, S. Y. & VANDER HEIDEN, M. G. 2011. Aerobic glycolysis: meeting the metabolic requirements of cell proliferation. *Annu Rev Cell Dev Biol*, 27, 441-64.
- LV, L., LI, D., ZHAO, D., LIN, R., CHU, Y., ZHANG, H., ZHA, Z., LIU, Y., LI, Z., XU, Y., WANG, G., HUANG, Y., XIONG, Y., GUAN, K. L. & LEI, Q. Y. 2011. Acetylation targets the M2 isoform of pyruvate kinase for degradation through chaperone-mediated autophagy and promotes tumor growth. *Mol Cell*, 42, 719-30.
- MA, L., CHEN, Z., ERDJUMENT-BROMAGE, H., TEMPST, P. & PANDOLFI, P. P. 2005. Phosphorylation and functional inactivation of TSC2 by Erk implications for tuberous sclerosis and cancer pathogenesis. *Cell*, 121, 179-93.
- MA, P. C., MAULIK, G., CHRISTENSEN, J. & SALGIA, R. 2003. c-Met: structure, functions and potential for therapeutic inhibition. *Cancer Metastasis Rev*, 22, 309-25.
- MACDONALD, M. J. & CHANG, C. M. 1985. Pancreatic islets contain the M2 isoenzyme of pyruvate kinase. Its phosphorylation has no effect on enzyme activity. *Mol Cell Biochem*, 68, 115-20.
- MAJEWSKI, N., NOGUEIRA, V., BHASKAR, P., COY, P. E., SKEEN, J. E., GOTTLÖB, K., CHANDEL, N. S., THOMPSON, C. B., ROBEY, R. B. & HAY, N. 2004. Hexokinase-mitochondria interaction mediated by Akt is required to inhibit apoptosis in the presence or absence of Bax and Bak. *Mol Cell*, 16, 819-30.
- MANNERVIK, B. & AXELSSON, K. 1980. Role of cytoplasmic thioltransferase in cellular regulation by thiol-disulphide interchange. *Biochem J*, 190, 125-30.
- MARCUS, H. J., CARPENTER, K. L., PRICE, S. J. & HUTCHINSON, P. J. 2010. In vivo assessment of high-grade glioma biochemistry using microdialysis: a study of energy-related molecules, growth factors and cytokines. *J Neurooncol*, 97, 11-23.
- MATHUPALA, S. P., HEESE, C. & PEDERSEN, P. L. 1997. Glucose catabolism in cancer cells. The type II hexokinase promoter contains functionally active response elements for the tumor suppressor p53. *J Biol Chem*, 272, 22776-80.
- MAWRIN, C., DIETE, S., TREUHEIT, T., KROPF, S., VORWERK, C. K., BOLTZE, C., KIRCHES, E., FIRSCHING, R. & DIETZMANN, K. 2003. Prognostic relevance of MAPK expression in glioblastoma multiforme. *Int J Oncol*, 23, 641-8.
- MAZUREK, S., BOSCHEK, C. B., HUGO, F. & EIGENBRODT, E. 2005. Pyruvate kinase type M2 and its role in tumor growth and spreading. *Semin Cancer Biol*, 15, 300-8.
- MAZUREK, S., DREXLER, H. C., TROPFMAIR, J., EIGENBRODT, E. & RAPP, U. R. 2007. Regulation of pyruvate kinase type M2 by A-Raf: a possible glycolytic stop or go mechanism. *Anticancer Res*, 27, 3963-71.
- MAZUREK, S., GRIMM, H., OEHMKE, M., WEISSE, G., TEIGELKAMP, S. & EIGENBRODT, E. 2000. Tumor M2-PK and glutaminolytic enzymes in the metabolic shift of tumor cells. *Anticancer Res*, 20, 5151-4.
- MAZUREK, S., HUGO, F., FAILING, K. & EIGENBRODT, E. 1996. Studies on associations of glycolytic and glutaminolytic enzymes in MCF-7 cells: role of P36. *J Cell Physiol*, 167, 238-50.
- MCCORD, A. M., JAMAL, M., SHANKAVARAM, U. T., LANG, F. F., CAMPHAUSEN, K. & TOFILON, P. J. 2009. Physiologic oxygen concentration enhances the stem-like properties of CD133+ human glioblastoma cells in vitro. *Mol Cancer Res*, 7, 489-97.
- MCCUBREY, J. A., STEELMAN, L. S., CHAPPELL, W. H., ABRAMS, S. L., WONG, E. W., CHANG, F., LEHMANN, B., TERRIAN, D. M., MILELLA, M., TAFURI, A., STIVALA, F., LIBRA, M., BASECKE, J., EVANGELISTI, C., MARTELLI, A. M. & FRANKLIN, R. A. 2007. Roles of the Raf/MEK/ERK pathway in cell growth, malignant transformation and drug resistance. *Biochim Biophys Acta*, 1773, 1263-84.
- MEBRATU, Y. & TESFAIGZI, Y. 2009. How ERK1/2 activation controls cell proliferation and cell death: Is subcellular localization the answer? *Cell Cycle*, 8, 1168-75.
- MENG, D., LV, D. D. & FANG, J. 2008. Insulin-like growth factor-I induces reactive oxygen species production and cell migration through Nox4 and Rac1 in vascular smooth muscle cells. *Cardiovasc Res*, 80, 299-308.
- MENG, T. C., FUKADA, T. & TONKS, N. K. 2002. Reversible oxidation and inactivation of protein tyrosine phosphatases in vivo. *Mol Cell*, 9, 387-99.
- MICHALOPOULOS, G. K. & DEFRANCES, M. C. 1997. Liver regeneration. *Science*, 276, 60-6.

- MICHELAKIS, E. D., SUTENDRA, G., DROMPARIS, P., WEBSTER, L., HAROMY, A., NIVEN, E., MAGUIRE, C., GAMMER, T. L., MACKEY, J. R., FULTON, D., ABDULKARIM, B., MCMURTRY, M. S. & PETRUK, K. C. 2010. Metabolic modulation of glioblastoma with dichloroacetate. *Sci Transl Med*, 2, 31ra34.
- MINCHENKO, A., LESHCHINSKY, I., OPENTANOVA, I., SANG, N., SRINIVAS, V., ARMSTEAD, V. & CARO, J. 2002. Hypoxia-inducible factor-1-mediated expression of the 6-phosphofructo-2-kinase/fructose-2,6-bisphosphatase-3 (PFKFB3) gene. Its possible role in the Warburg effect. *J Biol Chem*, 277, 6183-7.
- MIRZOEVA, O. K., KAWAGUCHI, T. & PIEPER, R. O. 2006. The Mre11/Rad50/Nbs1 complex interacts with the mismatch repair system and contributes to temozolomide-induced G2 arrest and cytotoxicity. *Mol Cancer Ther*, 5, 2757-66.
- MIYAMOTO, S., MURPHY, A. N. & BROWN, J. H. 2008. Akt mediates mitochondrial protection in cardiomyocytes through phosphorylation of mitochondrial hexokinase-II. *Cell Death Differ*, 15, 521-9.
- MIYANAGA, O., ISHIBASHI, H., KUROKAWA, S., SHIRAHAMA, M. & TSUCHIYA, Y. 1988. Lack of evidence for a pyruvate kinase isozyme shift in hepatocytes of the regenerating rat liver. *Int J Biochem*, 20, 1219-25.
- MONTANO, N., CENCI, T., MARTINI, M., D'ALESSANDRIS, Q. G., PELACCHI, F., RICCI-VITIANI, L., MAIRA, G., DE MARIA, R., LAROCCA, L. M. & PALLINI, R. 2011. Expression of EGFRvIII in glioblastoma: prognostic significance revisited. *Neoplasia*, 13, 1113-21.
- MORAIS, R., ZINKEWICH-PEOTTI, K., PARENT, M., WANG, H., BABAI, F. & ZOLLINGER, M. 1994. Tumor-forming ability in athymic nude mice of human cell lines devoid of mitochondrial DNA. *Cancer Res*, 54, 3889-96.
- MUIRHEAD, H. 1990. Isoenzymes of pyruvate kinase. *Biochem Soc Trans*, 18, 193-6.
- MUKHERJEE, J., PHILLIPS, J. J., ZHENG, S., WIENCKE, J., RONEN, S. M. & PIEPER, R. O. 2013. Pyruvate kinase M2 expression, but not pyruvate kinase activity, is up-regulated in a grade-specific manner in human glioma. *PLoS One*, 8, e57610.
- MURPHY, M. P. 2009. How mitochondria produce reactive oxygen species. *Biochem J*, 417, 1-13.
- NAGAYAMA, T., NAGAYAMA, M., KOHARA, S., KAMIGUCHI, H., SHIBUYA, M., KATOH, Y., ITOH, J. & SHINOHARA, Y. 2004. Post-ischemic delayed expression of hepatocyte growth factor and c-Met in mouse brain following focal cerebral ischemia. *Brain Res*, 999, 155-66.
- NAGPAL, S., HARSH, G. & RECHT, L. 2011. Bevacizumab improves quality of life in patients with recurrent glioblastoma. *Chemother Res Pract*, 2011, 602812.
- NARAYANA, A., GRUBER, D., KUNNAKAT, S., GOLFINOS, J. G., PARKER, E., RAZA, S., ZAGZAG, D., EAGAN, P. & GRUBER, M. L. 2012. A clinical trial of bevacizumab, temozolomide, and radiation for newly diagnosed glioblastoma. *J Neurosurg*, 116, 341-5.
- NASCIMENTO, E. B., SNEL, M., GUIGAS, B., VAN DER ZON, G. C., KRIEK, J., MAASSEN, J. A., JAZET, I. M., DIAMANT, M. & OUWENS, D. M. 2010. Phosphorylation of PRAS40 on Thr246 by PKB/AKT facilitates efficient phosphorylation of Ser183 by mTORC1. *Cell Signal*, 22, 961-7.
- NETZKER, R., GREINER, E., EIGENBRODT, E., NOGUCHI, T., TANAKA, T. & BRAND, K. 1992. Cell cycle-associated expression of M2-type isozyme of pyruvate kinase in proliferating rat thymocytes. *J Biol Chem*, 267, 6421-4.
- NEWLANDS, E. S., STEVENS, M. F., WEDGE, S. R., WHEELHOUSE, R. T. & BROCK, C. 1997. Temozolomide: a review of its discovery, chemical properties, pre-clinical development and clinical trials. *Cancer Treat Rev*, 23, 35-61.
- NORDEN, A. D., YOUNG, G. S., SETAYESH, K., MUZIKANSKY, A., KLUFAS, R., ROSS, G. L., CIAMPA, A. S., EBBELING, L. G., LEVY, B., DRAPPATZ, J., KESARI, S. & WEN, P. Y. 2008. Bevacizumab for recurrent malignant gliomas: efficacy, toxicity, and patterns of recurrence. *Neurology*, 70, 779-87.
- OGAWARA, Y., KISHISHITA, S., OBATA, T., ISAZAWA, Y., SUZUKI, T., TANAKA, K., MASUYAMA, N. & GOTOH, Y. 2002. Akt enhances Mdm2-mediated ubiquitination and degradation of p53. *J Biol Chem*, 277, 21843-50.
- OHGAKI, H. & KLEIHUES, P. 2005. Epidemiology and etiology of gliomas. *Acta Neuropathol*, 109, 93-108.
- ORR, J. W. & STICKLAND, L. H. 1938. The metabolism of bone marrow. *Biochem J*, 32, 567-71.
- PAPANDREOU, I., CAIRNS, R. A., FONTANA, L., LIM, A. L. & DENKO, N. C. 2006. HIF-1 mediates adaptation to hypoxia by actively downregulating mitochondrial oxygen consumption. *Cell Metab*, 3, 187-97.
- PAPANDREOU, I., KRISHNA, C., KAPER, F., CAI, D., GIACCIA, A. J. & DENKO, N. C. 2005. Anoxia is necessary for tumor cell toxicity caused by a low-oxygen environment. *Cancer Res*, 65, 3171-8.
- PASTEUR, L. 1858. Production constante de glycérine dans la fermentation alcoolique. *C R Acad Sci*, 1858;46:857.
- PENA-RICO, M. A., CALVO-VIDAL, M. N., VILLALONGA-PLANELLAS, R., MARTINEZ-SOLER, F., GIMENEZ-BONAFE, P., NAVARRO-SABATE, A., TORTOSA, A., BARTRONS, R. & MANZANO, A. 2011. TP53 induced glycolysis

- and apoptosis regulator (TIGAR) knockdown results in radiosensitization of glioma cells. *Radiother Oncol*, 101, 132-9.
- PIAO, Y., LIANG, J., HOLMES, L., HENRY, V., SULMAN, E. & DE GROOT, J. F. 2013. Acquired Resistance to Anti-VEGF Therapy in Glioblastoma Is Associated with a Mesenchymal Transition. *Clin Cancer Res*, 19, 4392-403.
- PILLAY, V., ALLAF, L., WILDING, A. L., DONOGHUE, J. F., COURT, N. W., GREENALL, S. A., SCOTT, A. M. & JOHNS, T. G. 2009. The plasticity of oncogene addiction: implications for targeted therapies directed to receptor tyrosine kinases. *Neoplasia*, 11, 448-58, 2 p following 458.
- PISTOLLATO, F., ABBADI, S., RAMPAZZO, E., PERSANO, L., DELLA PUPPA, A., FRASSON, C., SARTO, E., SCIENZA, R., D'AVELLA, D. & BASSO, G. 2010. Intratumoral hypoxic gradient drives stem cells distribution and MGMT expression in glioblastoma. *Stem Cells*, 28, 851-62.
- PISTOLLATO, F., CHEN, H. L., ROOD, B. R., ZHANG, H. Z., D'AVELLA, D., DENARO, L., GARDIMAN, M., TE KRONNIE, G., SCHWARTZ, P. H., FAVARO, E., INDRACCOLO, S., BASSO, G. & PANCHISION, D. M. 2009. Hypoxia and HIF1alpha repress the differentiative effects of BMPs in high-grade glioma. *Stem Cells*, 27, 7-17.
- PLANAS, A. M., JUSTICIA, C., SORIANO, M. A. & FERRER, I. 1998. Epidermal growth factor receptor in proliferating reactive glia following transient focal ischemia in the rat brain. *Glia*, 23, 120-9.
- POUYSSÉGUR, J., FRANCHI, A., SALOMON, J. C. & SILVESTRE, P. 1980. Isolation of a Chinese hamster fibroblast mutant defective in hexose transport and aerobic glycolysis: its use to dissect the malignant phenotype. *Proc Natl Acad Sci U S A*, 77, 2698-701.
- PRESEK, P., GLOSSMANN, H., EIGENBRODT, E., SCHONER, W., RUBSAMEN, H., FRIIS, R. R. & BAUER, H. 1980. Similarities between a phosphoprotein (pp60src)-associated protein kinase of Rous sarcoma virus and a cyclic adenosine 3':5'-monophosphate-independent protein kinase that phosphorylates pyruvate kinase type M2. *Cancer Res*, 40, 1733-41.
- PRESEK, P., REINACHER, M. & EIGENBRODT, E. 1988. Pyruvate kinase type M2 is phosphorylated at tyrosine residues in cells transformed by Rous sarcoma virus. *FEBS Lett*, 242, 194-8.
- PRINTZ, R. L., KOCH, S., POTTER, L. R., O'DOHERTY, R. M., TIESINGA, J. J., MORITZ, S. & GRANNER, D. K. 1993. Hexokinase II mRNA and gene structure, regulation by insulin, and evolution. *J Biol Chem*, 268, 5209-19.
- PRISE, K. M., GILLIES, N. E. & MICHAEL, B. D. 1998. Evidence for a hypoxic fixation reaction leading to the induction of ssb and dsb in irradiated DNA. *Int J Radiat Biol*, 74, 53-9.
- QUASTEL, J. H. & BICKIS, I. J. 1959. Metabolism of normal tissues and neoplasms in vitro. *Nature*, 183, 281-6.
- RAPISARDA, A., HOLLINGSHEAD, M., URANCHIMEG, B., BONOMI, C. A., BORGEL, S. D., CARTER, J. P., GEHR, B., RAFFELD, M., KINDERS, R. J., PARCHMENT, R., ANVER, M. R., SHOEMAKER, R. H. & MELILLO, G. 2009. Increased antitumor activity of bevacizumab in combination with hypoxia inducible factor-1 inhibition. *Mol Cancer Ther*, 8, 1867-77.
- RATHMELL, J. C., FOX, C. J., PLAS, D. R., HAMMERMAN, P. S., CINALLI, R. M. & THOMPSON, C. B. 2003. Akt-directed glucose metabolism can prevent Bax conformation change and promote growth factor-independent survival. *Mol Cell Biol*, 23, 7315-28.
- REINACHER, M. & EIGENBRODT, E. 1981. Immunohistological demonstration of the same type of pyruvate kinase isoenzyme (M2-Pk) in tumors of chicken and rat. *Virchows Arch B Cell Pathol Incl Mol Pathol*, 37, 79-88.
- REINACHER, M., EIGENBRODT, E., GERBRACHT, U., ZENK, G., TIMMERMANN-TROSIENER, I., BENTLEY, P., WAECHTER, F. & SCHULTE-HERMANN, R. 1986. Pyruvate kinase isoenzymes in altered foci and carcinoma of rat liver. *Carcinogenesis*, 7, 1351-7.
- REITZER, L. J., WICE, B. M. & KENNEL, D. 1979. Evidence that glutamine, not sugar, is the major energy source for cultured HeLa cells. *J Biol Chem*, 254, 2669-76.
- RIJKSEN, G., VAN DER HEIJDEN, M. C., OSKAM, R. & STAAL, G. E. 1988. Subunit-specific phosphorylation of pyruvate kinase in medullary thyroid carcinomas of the rat. *FEBS Lett*, 233, 69-73.
- ROBEY, R. B. & HAY, N. 2006. Mitochondrial hexokinases, novel mediators of the antiapoptotic effects of growth factors and Akt. *Oncogene*, 25, 4683-96.
- ROBIN, E. D., MURPHY, B. J. & THEODORE, J. 1984. Coordinate regulation of glycolysis by hypoxia in mammalian cells. *J Cell Physiol*, 118, 287-90.
- ROJIANI, A. M. & DOROVINI-ZIS, K. 1996. Glomeruloid vascular structures in glioblastoma multiforme: an immunohistochemical and ultrastructural study. *J Neurosurg*, 85, 1078-84.

- RONG, Y., DURDEN, D. L., VAN MEIR, E. G. & BRAT, D. J. 2006. 'Pseudopalisading' necrosis in glioblastoma: a familiar morphologic feature that links vascular pathology, hypoxia, and angiogenesis. *J Neuropathol Exp Neurol*, 65, 529-39.
- RUSSELL, R. C., FANG, C. & GUAN, K. L. 2011. An emerging role for TOR signaling in mammalian tissue and stem cell physiology. *Development*, 138, 3343-56.
- RUVINSKY, I. & MEYUHAS, O. 2006. Ribosomal protein S6 phosphorylation: from protein synthesis to cell size. *Trends Biochem Sci*, 31, 342-8.
- SARBASSOV, D. D., GUERTIN, D. A., ALI, S. M. & SABATINI, D. M. 2005. Phosphorylation and regulation of Akt/PKB by the rictor-mTOR complex. *Science*, 307, 1098-101.
- SAUER, H., KLIMM, B., HESCHELER, J. & WARTENBERG, M. 2001. Activation of p90RSK and growth stimulation of multicellular tumor spheroids are dependent on reactive oxygen species generated after purinergic receptor stimulation by ATP. *FASEB J*, 15, 2539-41.
- SCHEFFZEK, K., AHMADIAN, M. R., KABSCH, W., WIESMULLER, L., LAUTWEIN, A., SCHMITZ, F. & WITTINGHOFER, A. 1997. The Ras-RasGAP complex: structural basis for GTPase activation and its loss in oncogenic Ras mutants. *Science*, 277, 333-8.
- SCHWARTZENBERG-BAR-YOSEPH, F., ARMONI, M. & KARNIELI, E. 2004. The tumor suppressor p53 down-regulates glucose transporters GLUT1 and GLUT4 gene expression. *Cancer Res*, 64, 2627-33.
- SHERWIN, A. L., LEBLANC, F. E. & MCCANN, W. P. 1968. Altered LDH isoenzymes in brain tumors. *Arch Neurol*, 18, 311-5.
- SHINOJIMA, N., TADA, K., SHIRAIISHI, S., KAMIRYO, T., KOCHI, M., NAKAMURA, H., MAKINO, K., SAYA, H., HIRANO, H., KURATSU, J., OKA, K., ISHIMARU, Y. & USHIO, Y. 2003. Prognostic value of epidermal growth factor receptor in patients with glioblastoma multiforme. *Cancer Res*, 63, 6962-70.
- SHOSHANI, T., FAERMAN, A., METT, I., ZELIN, E., TENNE, T., GORODIN, S., MOSHEL, Y., ELBAZ, S., BUDANOV, A., CHAJUT, A., KALINSKI, H., KAMER, I., ROZEN, A., MOR, O., KESHET, E., LESHKOWITZ, D., EINAT, P., SKALITER, R. & FEINSTEIN, E. 2002. Identification of a novel hypoxia-inducible factor 1-responsive gene, RTP801, involved in apoptosis. *Mol Cell Biol*, 22, 2283-93.
- SIBILIA, M., STEINBACH, J. P., STINGL, L., AGUZZI, A. & WAGNER, E. F. 1998. A strain-independent postnatal neurodegeneration in mice lacking the EGF receptor. *EMBO J*, 17, 719-31.
- SILBER, J. R., BLANK, A., BOBOLA, M. S., MUELLER, B. A., KOLSTOE, D. D., OJEMANN, G. A. & BERGER, M. S. 1996. Lack of the DNA repair protein O6-methylguanine-DNA methyltransferase in histologically normal brain adjacent to primary human brain tumors. *Proc Natl Acad Sci U S A*, 93, 6941-6.
- SILBERGELD, D. L., ROSTOMILY, R. C. & ALVORD, E. C., JR. 1991. The cause of death in patients with glioblastoma is multifactorial: clinical factors and autopsy findings in 117 cases of supratentorial glioblastoma in adults. *J Neurooncol*, 10, 179-85.
- SMITH, J. S., TACHIBANA, I., PASSE, S. M., HUNTLEY, B. K., BORELL, T. J., ITURRIA, N., O'FALLON, J. R., SCHAEFER, P. L., SCHEITHAUER, B. W., JAMES, C. D., BUCKNER, J. C. & JENKINS, R. B. 2001. PTEN mutation, EGFR amplification, and outcome in patients with anaplastic astrocytoma and glioblastoma multiforme. *J Natl Cancer Inst*, 93, 1246-56.
- SMITH, T. A., SHARMA, R. I., THOMPSON, A. M. & PAULIN, F. E. 2006. Tumor 18F-FDG incorporation is enhanced by attenuation of P53 function in breast cancer cells in vitro. *J Nucl Med*, 47, 1525-30.
- SOEDA, A., PARK, M., LEE, D., MINTZ, A., ANDROUTSELLIS-THEOTOKIS, A., MCKAY, R. D., ENGH, J., IWAMA, T., KUNISADA, T., KASSAM, A. B., POLLACK, I. F. & PARK, D. M. 2009. Hypoxia promotes expansion of the CD133-positive glioma stem cells through activation of HIF-1alpha. *Oncogene*, 28, 3949-59.
- SPELLMAN, C. M. & FOTTRELL, P. F. 1973. Similarities between pyruvate kinase from human placenta and tumours. *FEBS Lett*, 37, 281-4.
- STEINBERG, P., KLINGELHOFFER, A., SCHAFFER, A., WUST, G., WEISSE, G., OESCH, F. & EIGENBRODT, E. 1999. Expression of pyruvate kinase M2 in preneoplastic hepatic foci of N-nitrosomorpholine-treated rats. *Virchows Arch*, 434, 213-20.
- STUPP, R., MASON, W. P., VAN DEN BENT, M. J., WELLER, M., FISHER, B., TAPHOORN, M. J., BELANGER, K., BRANDES, A. A., MAROSI, C., BOGDAHN, U., CURSCHMANN, J., JANZER, R. C., LUDWIN, S. K., GORLIA, T., ALLGEIER, A., LACOMBE, D., CAIRNCROSS, J. G., EISENHAEUER, E. & MIRIMANOFF, R. O. 2005. Radiotherapy plus concomitant and adjuvant temozolomide for glioblastoma. *N Engl J Med*, 352, 987-96.
- TAKEGAWA, S., FUJII, H. & MIWA, S. 1983. Change of pyruvate kinase isozymes from M2- to L-type during development of the red cell. *Br J Haematol*, 54, 467-74.

- TAKEUCHI, H., NATSUME, A., WAKABAYASHI, T., AOSHIMA, C., SHIMATO, S., ITO, M., ISHII, J., MAEDA, Y., HARA, M., KIM, S. U. & YOSHIDA, J. 2007. Intravenously transplanted human neural stem cells migrate to the injured spinal cord in adult mice in an SDF-1- and HGF-dependent manner. *Neurosci Lett*, 426, 69-74.
- TCGA-CONSORTIUM 2008. Comprehensive genomic characterization defines human glioblastoma genes and core pathways. *Nature*, 455, 1061-8.
- TEJWANI, G. A. 1978. The role of phosphofructokinase in the Pasteur effect. *Trends in biochemical sciences*, 3, 30-33.
- TREMP, G. L., BOQUET, D., RIPOCHE, M. A., COGNET, M., LONE, Y. C., JAMI, J., KAHN, A. & DAEGELEN, D. 1989. Expression of the rat L-type pyruvate kinase gene from its dual erythroid- and liver-specific promoter in transgenic mice. *J Biol Chem*, 264, 19904-10.
- VAN ERP, H. E., VAN UNNIK, J. A., RIJKSEN, G., SMITS, J. G. & STAAL, G. E. 1991. Cellular expression of K-type pyruvate kinase in normal and neoplastic human tissues. *Cancer*, 68, 2595-601.
- VAN VEELLEN, C. W., VERBIEST, H., VLUG, A. M., RIJKSEN, G. & STAAL, G. E. 1978. Isozymes of pyruvate kinase from human brain, meningiomas, and malignant gliomas. *Cancer Res*, 38, 4681-7.
- VAUPEL, P., KALLINOWSKI, F. & OKUNIEFF, P. 1989. Blood flow, oxygen and nutrient supply, and metabolic microenvironment of human tumors: a review. *Cancer Res*, 49, 6449-65.
- VENKATESAN, A., UZASCI, L., CHEN, Z., RAJBHANDARI, L., ANDERSON, C., LEE, M. H., BIANCHET, M. A., COTTER, R., SONG, H. & NATH, A. 2011. Impairment of adult hippocampal neural progenitor proliferation by methamphetamine: role for nitrotyrosination. *Mol Brain*, 4, 28.
- VERHAGEN, J. N., VAN DER HEIJDEN, M. C., DE JONG-VAN DIJKEN, J., RIJKSEN, G., DER KINDEREN, P. J., VAN UNNIK, J. A. & STAAL, G. E. 1985. Pyruvate kinase in normal human thyroid tissue and thyroid neoplasms. *Cancer*, 55, 142-8.
- WAHA, A., BAUMANN, A., WOLF, H. K., FIMMERS, R., NEUMANN, J., KINDERMANN, D., ASTRAHANTSEFF, K., BLUMCKE, I., VON DEIMLING, A. & SCHLEGEL, U. 1996. Lack of prognostic relevance of alterations in the epidermal growth factor receptor-transforming growth factor-alpha pathway in human astrocytic gliomas. *J Neurosurg*, 85, 634-41.
- WANG, T., MARQUARDT, C. & FOKER, J. 1976. Aerobic glycolysis during lymphocyte proliferation. *Nature*, 261, 702-5.
- WANG, Z., CHATTERJEE, D., JEON, H. Y., AKERMAN, M., VANDER HEIDEN, M. G., CANTLEY, L. C. & KRAINER, A. R. 2012. Exon-centric regulation of pyruvate kinase M alternative splicing via mutually exclusive exons. *J Mol Cell Biol*, 4, 79-87.
- WANKA, C., STEINBACH, J. P. & RIEGER, J. 2012. Tp53-induced glycolysis and apoptosis regulator (TIGAR) protects glioma cells from starvation-induced cell death by upregulating respiration and improving cellular redox homeostasis. *J Biol Chem*.
- WARBURG, O. 1956. On the origin of cancer cells. *Science*, 123, 309-14.
- WARBURG, O., WIND, F. & NEGELEIN, E. 1927. The Metabolism of Tumors in the Body. *J Gen Physiol*, 8, 519-30.
- WEERNINK, P. A., RIJKSEN, G., MASCINI, E. M. & STAAL, G. E. 1992. Phosphorylation of pyruvate kinase type K is restricted to the dimeric form. *Biochim Biophys Acta*, 1121, 61-8.
- WEERNINK, P. A., RIJKSEN, G., VAN DER HEIJDEN, M. C. & STAAL, G. E. 1990. Phosphorylation of pyruvate kinase type K in human gliomas by a cyclic adenosine 5'-monophosphate-independent protein kinase. *Cancer Res*, 50, 4604-10.
- WEINBERG, F., HAMANAKA, R., WHEATON, W. W., WEINBERG, S., JOSEPH, J., LOPEZ, M., KALYANARAMAN, B., MUTLU, G. M., BUDINGER, G. R. & CHANDEL, N. S. 2010. Mitochondrial metabolism and ROS generation are essential for Kras-mediated tumorigenicity. *Proc Natl Acad Sci U S A*, 107, 8788-93.
- WEINSTEIN, I. B. & JOE, A. 2008. Oncogene addiction. *Cancer Res*, 68, 3077-80; discussion 3080.
- WICE, B. M., REITZER, L. J. & KENNELL, D. 1981. The continuous growth of vertebrate cells in the absence of sugar. *J Biol Chem*, 256, 7812-9.
- WILSON, J. E. 1995. Hexokinases. *Rev Physiol Biochem Pharmacol*, 126, 65-198.
- WILSON, J. E. 2003. Isozymes of mammalian hexokinase: structure, subcellular localization and metabolic function. *J Exp Biol*, 206, 2049-57.
- WOLF, A., AGNIHOTRI, S., MICALLEF, J., MUKHERJEE, J., SABHA, N., CAIRNS, R., HAWKINS, C. & GUHA, A. 2011. Hexokinase 2 is a key mediator of aerobic glycolysis and promotes tumor growth in human glioblastoma multiforme. *J Exp Med*, 208, 313-26.
- YAMASHITA, K., DISCHER, D. J., HU, J., BISHOPRIC, N. H. & WEBSTER, K. A. 2001. Molecular regulation of the endothelin-1 gene by hypoxia. Contributions of hypoxia-inducible factor-1, activator protein-1, GATA-2, AND p300/CBP. *J Biol Chem*, 276, 12645-53.

- YANO, S., KONDO, K., YAMAGUCHI, M., RICHMOND, G., HUTCHISON, M., WAKELING, A., AVERBUCH, S. & WADSWORTH, P. 2003. Distribution and function of EGFR in human tissue and the effect of EGFR tyrosine kinase inhibition. *Anticancer Res*, 23, 3639-50.
- YEH, W. L., LIN, C. J. & FU, W. M. 2008. Enhancement of glucose transporter expression of brain endothelial cells by vascular endothelial growth factor derived from glioma exposed to hypoxia. *Mol Pharmacol*, 73, 170-7.
- YIP, S., MIAO, J., CAHILL, D. P., IAFRATE, A. J., ALDAPE, K., NUTT, C. L. & LOUIS, D. N. 2009. MSH6 mutations arise in glioblastomas during temozolomide therapy and mediate temozolomide resistance. *Clin Cancer Res*, 15, 4622-9.
- YUN, K. 1980. LDH isozyme analyses of ethylnitrosourea-induced central nervous system tumors in rats. *Acta Pathol Jpn*, 30, 397-406.
- YUNG, W. K., PRADOS, M. D., YAYA-TUR, R., ROSENFELD, S. S., BRADA, M., FRIEDMAN, H. S., ALBRIGHT, R., OLSON, J., CHANG, S. M., O'NEILL, A. M., FRIEDMAN, A. H., BRUNER, J., YUE, N., DUGAN, M., ZAKNOEN, S. & LEVIN, V. A. 1999. Multicenter phase II trial of temozolomide in patients with anaplastic astrocytoma or anaplastic oligoastrocytoma at first relapse. Temodal Brain Tumor Group. *J Clin Oncol*, 17, 2762-71.
- ZHONG, H., CHILES, K., FELDSER, D., LAUGHNER, E., HANRAHAN, C., GEORGESCU, M. M., SIMONS, J. W. & SEMENZA, G. L. 2000. Modulation of hypoxia-inducible factor 1alpha expression by the epidermal growth factor/phosphatidylinositol 3-kinase/PTEN/AKT/FRAP pathway in human prostate cancer cells: implications for tumor angiogenesis and therapeutics. *Cancer Res*, 60, 1541-5.
- ZIEGLER, D. M. 1985. Role of reversible oxidation-reduction of enzyme thiols-disulfides in metabolic regulation. *Annu Rev Biochem*, 54, 305-29.
- ZUNDEL, W., SCHINDLER, C., HAAS-KOGAN, D., KOONG, A., KAPER, F., CHEN, E., GOTTSCHALK, A. R., RYAN, H. E., JOHNSON, R. S., JEFFERSON, A. B., STOKOE, D. & GIACCIA, A. J. 2000. Loss of PTEN facilitates HIF-1-mediated gene expression. *Genes Dev*, 14, 391-6.
- ZWERSCHKE, W., MAZUREK, S., MASSIMI, P., BANKS, L., EIGENBRODT, E. & JANSEN-DURR, P. 1999. Modulation of type M2 pyruvate kinase activity by the human papillomavirus type 16 E7 oncoprotein. *Proc Natl Acad Sci U S A*, 96, 1291-6.

Chapter 2 - Materials and Methods

Buffers.....	89
Cell culture.....	89
FCS based cell lines.....	89
Serum free cell lines.....	90
Protein methods.....	90
Whole cell lysate preparation.....	90
Pull-down of cysteine oxidised proteins.....	91
SDS-PAGE.....	92
Blue native PAGE.....	92
Immunoblotting.....	93
Luminex bead based ELISA.....	93
Protein quantification – BCA assay.....	94
Flow cytometry.....	94
Mitochondrial membrane potential.....	94
Cell cycle analysis.....	94
Measurement of NADPH/NADP ⁺	95
Measurement of ATP.....	96
Measurement of PEP.....	96
Luciferase coupled pyruvate kinase assay.....	97

Hexokinase assay	97
pH indicator based extracellular acidification assay.....	98
Seahorse XF Bioanalyser	98
Oroboros Oxygraph	99
Respiration of intact cells.....	99
Respiration of digitonin permeabilised cells.....	100
Micro-plate based real-time cell death assay.....	101
Statistical analysis	101
References	101

Unless stated otherwise, all chemicals were sourced from Sigma, MO USA. WAY677099 was obtained from Pfizer, NY USA.

Buffers

Phosphate Buffered Saline (PBS): 120 mM NaCl, 16 mM Na₂HPO₄, 3.47 mM NaH₂PO₄ (VWR International, England)

Cell culture

FCS based cell lines

The human glioblastoma cell lines U87MG and SF767 were sourced from American Type Culture Collection (ATCC, VA, USA) and the Brain Tissue Tumour Bank at University of California, San Francisco (CA, USA) respectively. For routine cell culture, cells were grown as adherent monolayers in T175 culture flasks with DMEM/F12 1:1 (Life Technologies, NY USA) supplemented with 5% Australian fetal bovine serum (FCS) (Lonza, MD USA), 1x Glutamax (Life Technologies, NY USA), 100 units/ml penicillin and 100 µg/ml streptomycin (Pen Strep, Life Technologies, NY USA).

For routine passaging, before reaching confluency cells were lifted using trypsin/EDTA (PBS, 0.25% Trypsin (Life Technologies, NY USA), 0.05% EDTA (Sigma, MO USA)). Once lifted, trypsin was inactivated by dilution in media. Cells were pelleted by centrifugation then resuspended in fresh media. To determine cell density and viability, a small aliquot of cell suspension was combined with a volume of 0.4% trypan blue and cells counted using a haemocytometer (Germany). Cells were replated for continued maintenance or for use in experimental procedures. All cell culture plasticware including flasks and multi-well plates were vacuum gas plasma treated polystyrene (Becton Dickinson, NJ USA)

Serum free cell lines

Human glioblastoma cell lines GBM-L1, GBM-L2 and GBM-L3 were provided by Angus Harding, University of Queensland, Brisbane, Australia. GBM4 was created in-house by Dr. Hui Gan. CSC#014 and CSC#020 were provided by Giovanna Dabaco, Royal Melbourne Hospital, Melbourne, Australia. These cell lines were cultured in StemPro® NSC SFM - Serum-Free Human Neural Stem Cell Culture Medium (Life Technologies, NY USA) supplemented with 1x Glutamax, 100 units/ml penicillin and 100 µg/ml streptomycin (Life Technologies, NY USA). Under these conditions, GBM-L1, GBM-L2, GBM-L3 and CSC#014 grew as floating spheroids. For routine passaging of these cell lines, spheroids were pelleted by centrifugation, media removed and cells dissociated with trypsin/EDTA and gentle agitation. In all other respects these cells were treated the same way as FCS based cell lines.

Protein methods

Whole cell lysate preparation

Unless otherwise specified, protein samples were prepared using RIPA lysis buffer, consisting of 50 mM Tris base, pH 7.5, 150 mM NaCl, 5 mM EDTA, 0.5% Sodium Deoxycholate, 0.05% Sodium Dodecyl Sulfate (SDS), 10 mM NaF and Protease Inhibitor Cocktail Set I (EMD Millipore Corporation, MA USA, final concentration of 500 µM AEBSF Hydrochloride, 150 nM Aprotinin, 1 µM E-64 Protease Inhibitor, 0.5 mM Sodium EDTA, 1 µM Leupeptin Hemisulfate) stored at -80°C.

50x stock of pervanadate was prepared fresh by combining 5 µl of 100 mM Sodium Orthovanadate, 35.5 µl of water and 9.5 µl 30% H₂O₂ (Ajax Finechem, Australia). As H₂O₂ interferes with subsequent BCA protein quantification (Baker, 1991), ~300 U of Catalase from bovine liver was added to degrade remaining H₂O₂ before addition to RIPA lysis buffer.

For adherent cell lysates, cells were rinsed once with ice cold PBS. Lysis buffer was added directly to cells. Cell scrapers were used to aid in recovery of samples, which were driven through 28G syringe needles to ensure efficient lysis. For non-adherent cell lysates, cells were pelleted by

centrifugation, rinsed with ice cold PBS and then lysed with the addition of lysis buffer, and driven through 28G syringe needles.

To clarify the sample by removal precipitated material, samples were spun at 21,000 g for 20 minutes. Protein concentration was determined using a BCA assay and concentration normalised with additional lysis buffer.

Pull-down of cysteine oxidised proteins

Sub-confluent cells from T75 flasks were lifted with trypsin/EDTA and pelleted by centrifugation. Cells were then washed with ice cold PBS and pelleted into 1.7 ml tubes. Cells were lysed for 15 minutes in 500 µl of biotin labelling lysis buffer (BLLB, 50 mM Tris-HCl pH 7.0, 5 mM EDTA, 0.5% NP-40, Protease Inhibitor Cocktail Set I) plus 100 mM maleimide. Under these conditions, maleimide will covalently bind to reduced cysteines, blocking their involvement in the subsequent biotin-maleimide labelling reaction. Precipitated material was removed by centrifugation at 21,000 g for 10 minutes, and the supernatant transferred to clean tubes. Protein concentration was quantified by BCA assay and adjusted with the addition of BLLB to 1 µg/ml for a final volume of 450 µl. Fifty µl of 10% SDS was added to each sample, which were then incubated rotating for 2 hours at room temperature. To remove unreacted maleimide, samples were transferred to 15 ml tubes, and proteins precipitated with the addition of 2.5 ml pre-cooled acetone and incubation at -20°C for 20 minutes. Samples were transferred back to 1.7 ml tubes (2 per sample) and precipitated proteins pelleted by centrifugation at 21,000 g for 10 minutes. Supernatant was removed and the pellets air-dried. Pellets were resuspended and recombined in 200 µl BLLB plus 1% SDS, 10 mM DTT and 100 µM biotin-maleimide. DTT, a potent reducing agent, reduces the previously oxidised cysteine residues, allowing their reaction with biotin-maleimide. To remove unreacted biotin-maleimide, proteins were precipitated with 1 ml pre-cooled methanol and incubated at -20°C for 20 minutes. Precipitated proteins were pelleted by centrifugation at 21,000 g for 10 minutes. Supernatant was removed and the pellets air-dried. Pellets were resuspended in 500 µl BLLB. Twenty µl of samples were reserved for loading

controls, while the remainder was transferred to tubes containing 10 μ l 50% streptavidin-sepharose beads (Cell Signalling Technology, MA USA) and incubated rotating at 4°C for 2 hours. Beads were washed four times with 500 μ l BLLB. Beads were resuspended in 40 μ l 2x LDS and heated to 95°C for 5 minutes. Samples were then analysed by SDS-PAGE and immuno-blotting.

SDS-PAGE

Samples were combined 1:1 with 2x LDS loading buffer (prepared with 5 parts NuPAGE LDS Sample Buffer, 1 part NuPAGE Sample Reducing Agent (Life Technologies, NY USA) and 4 parts water) and heated to 95°C for 5 minutes to reduce disulphide linkages and linearise proteins. After cooling to room temperature, samples were loaded onto wells of a NuPAGE® 4-12% Bis-Tris Gel 1.0 mm, 10 well precast gel and subjected to electrophoresis at 150 V for 75-90 minutes using NuPAGE MES SDS Running Buffer, with 500 μ l of NuPAGE Antioxidant added to the cathode chamber. Following electrophoresis, the gel was removed from the cast and incubated in equilibration buffer (2x NuPAGE MES SDS Running Buffer, 10% methanol) for 10 minutes.

Blue native PAGE

PKM2 complex formation was assessed by separation by Blue Native PAGE (BN-PAGE), using the NativePAGE Gel System (Life Technologies, NY USA) followed by immuno-blotting for PKM2. To prepare lysates, cells cultured in 6 well plates were washed with ice cold PBS, and 80 μ l of 1x NativePAGE Sample Buffer containing no detergents. Cell scrapers were used to aid in recovery of samples, which were driven through 28G syringe needles to ensure efficient lysis. Samples were clarified, and protein content quantified as previously described. Protein concentration was adjusted to 0.3 μ g/ μ l with the addition of sample buffer. For BN-PAGE, 20 μ l (6 μ g) of sample was combined with 1 μ l of 1% G250 sample additive immediately prior to loading onto a NativePAGE Novex 4-16% Bis-Tris Gel. Ten μ l of a molecular weight standards mix (0.25 μ g/ μ l each of rabbit muscle pyruvate kinase (~240 kDa), D-Lactate Dehydrogenase (~146 kDa) bovine serum albumin (~66 kDa), 0.12%

G250 sample additive and 10% glycerol) was added for estimation of complex size. 10 μ l (3 μ g) of sample was also separated by SDS-PAGE as described above.

Proteins were separated by electrophoresis at 150 V for 90 minutes. The anode buffer consisted of 1x NativePAGE Running Buffer, while the cathode buffer additionally consisted of 1x NativePAGE Cathode Buffer Additive (dark blue) for the first 15 minutes, and 0.1x NativePAGE Cathode Buffer Additive (light blue) for the remaining 75 minutes. Following electrophoresis, the gel was removed from its casting, trimmed along the dark blue/light blue dye front and incubated in 2x NuPAGE Transfer Buffer for 10 minutes.

Immunoblotting

Transfer of proteins from polyacrylamide gels to PVDF membranes was achieved using the iBlot 7-Minute Blotting System. Following transfer, PVDF membranes were blocked in Odyssey Blocking Buffer (LI-COR Biosciences, NE USA) for 1 hour. Primary antibodies were added at indicated concentration and incubated overnight at 4°C. PVDF membranes were washed 3x 15 minutes in TBS-T (50 mM Tris.HCl, pH 7.4, 154 mM NaCl, 0.1% Tween-20). Appropriate fluorescently labelled secondary antibodies were added with Odyssey Blocking Buffer to the PVDF membrane and incubated at room temperature for 1 hour, protected from light. PVDF membrane was washed 3x 15 minutes in TBS-T and imaged using the Odyssey Infrared Imaging System. Where performed, densitometry was conducted using Odyssey Application Software version 3.0.

Luminex bead based ELISA

Levels of c-Met (total and panTyr) and p70-S6K (total and Thr412) in cell lysates was determined using Milliplex MAP Multiplex Assay Kits (EMD Millipore Corporation, MA USA) following manufacturer's instructions. Total and phosphorylated Akt (total and Ser473) was determined using Bioplex Assay Kits (Bio-Rad, Hercules CA) following manufacturer's instructions.

Protein quantification – BCA assay

Protein concentration was quantitated using the bicinchoninic acid (BCA) assay method. Typically, 10 μ l of protein sample was added to replicate wells of a 96 well plate. Wells containing known quantities of BSA were used as standards. $\text{CuSO}_4 \cdot 5\text{H}_2\text{O}$, final concentration 0.08% w/v was added to bicinchoninic acid solution immediately prior to use. 200 μ l of this mix was added to each well, and the plate incubated at 60°C for 15 minutes. Absorbance was measured at 560 nm using the FLUOstar Optima.

Flow cytometry

Mitochondrial membrane potential

Mitochondrial membrane potential ($\Delta\Psi_m$) was measured using the fluorescent and positively charged dye rhodamine 123. Rhodamine 123 accumulation, and therefore fluorescence is dependent on the membrane potential of the mitochondria. To measure $\Delta\Psi_m$, rhodamine 123 was added to the culture media of adherent cells to a final concentration of 100 ng/ml for two hours. Cells were rinsed once with PBS, lifted using trypsin/EDTA. Cells were pelleted by centrifugation and washed with ice cold PBS. Cells were again pelleted and resuspended in ice cold PBS and maintained on ice until analysis by flow cytometry. Flow cytometry was performed on a FACS Canto II (BD Biosciences (San Jose, CA). Data was analysed using FloJo version 7.5.5 (Tree Star, Ashland, OR)

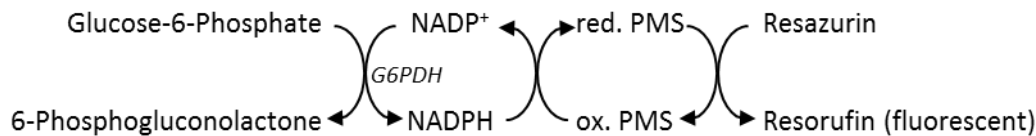
Cell cycle analysis

Cell cycle analysis was based on DNA dependent fluorescence of 4',6-diamidino-2-phenylindole (DAPI). Cells were harvested with trypsin/EDTA, resuspended in PBS and counted using a haemocytometer. Cells were pelleted by centrifugation and resuspended in DAPI staining solution (1 μ g/ml DAPI, 0.1% Tween-20 in PBS) at a density of 10^6 cells/ml and incubated rotating at 4°C for 30 minutes. Cells were pelleted and washed with PBS twice before a final resuspension in PBS. Flow cytometry was performed using the FACS Canto II. To calculate the fraction of cells at different

stages of the cell cycle, data was fitted using the Watson (Pragmatic) model within the FloJo software.

Measurement of NADPH/NADP⁺

Quantitation of intracellular NADP levels was based on the cycling reaction described below:



Cells cultured and treated in 6 well plates were rinsed with ice cold PBS, which was then thoroughly removed. Cells were lysed with the addition of 100 μ l of Extraction Buffer (20 mM NaHCO₃, 100 mM Na₂CO₃, 10 mM nicotinamide, 0.05% Triton-X-100). The use of cell scrapers and 28G syringes ensured efficient sample recovery and homogenisation of samples. Samples were divided in two, with one aliquot heated to 95°C for 5 minutes while the other remained on ice. Incubation of extracts at 95°C under highly basic conditions results in selective decomposition of NADP⁺ allowing for subsequent quantitation of NADPH, while unheated samples containing both NADPH and NADP⁺ allowed for quantitation of total levels (NADPt).

Twenty μ l of heated and unheated samples were transferred to wells of a black wall, clear bottom, 96 well plate. Wells containing known quantities of NADPH were used for generating standard curves. Freshly prepared Cycling Buffer (180 μ l (100 mM Tris HCl pH 8.0, 5 mM EDTA, 200 μ M phenazine methosulfate, 3 μ l/ml AlamarBlue Cell Viability Reagent (Life Technologies, NY USA) and 5 μ g/ml yeast glucose-6-phosphate dehydrogenase (Roche, Switzerland))) was added to each well and the plate incubated at room temperature for 5 minutes protected from light. To initiate the reaction, 50 μ l of 10 mM glucose-6-phosphate was added to each well and fluorescence (Em: 560 nm, Ex: 590 nm) was monitored every five minutes for 2 hours. Under these conditions, the concentration of NADP⁺ and NADPH is rate limiting, such that the rate of fluorescence increase over time is proportional to the concentration of NADP⁺ and NADPH.

Measurement of ATP

Concentration of ATP was determined using the ViaLight HS Kit (Lonza, MD USA) following manufacturer's instructions with modifications. 96 well cell culture plates with wells containing cells and 100 µl culture media were removed from incubation at 37°C and allowed to cool to room temperature, and all subsequent steps were performed at room temperature. Fifty µl of nucleotide releasing agent (NLR) was added to each well. Plates were shaken at 900 rpm for 5 minutes to achieve efficient lysis and homogenisation. 10 µl of ATP monitoring reagent (AMR, reconstituted in tris-acetate buffer as per manufacturer's instructions) was added to the required wells of a white walled 96 well plate. 80 µl of cell lysate was transferred to wells and luminescence was measured using the FLUOstar Optima.

Measurement of PEP

Cells cultured in T175 flasks were lifted with trypsin/EDTA, washed with PBS pelleted by centrifugation in 1.7 ml tubes by centrifugation. Lysis and enzyme inactivation was achieved with the addition of 1 ml of 0.05% triton-x 100 and heating to 100°C for 10 minutes. A tube containing 1 ml of 20 µM PEP was treated under identical conditions throughout the procedure. Tubes were cooled on ice then spun at 21,000 g to pellet precipitated material. To remove endogenous adenine nucleotides, supernatant was transferred to 1.7 ml tubes containing 10 µg activated carbon (AC) and incubated on ice with regular mixing. Samples were spun at 21,000 g to pellet AC and supernatants transferred to new tubes. 100 µl of 5% AC, 100 mM KH₂PO₄ was added and samples incubated on ice for 5 minutes. Samples were subject to two rounds of centrifugation at 21,000 g and supernatant transfer to remove all trace of AC. To ensure total enzyme inactivation, 5 µl of 100 mg/ml Proteinase K was added to each sample and incubated at 56°C for 20 minutes. To inactivate Proteinase K, 2.5 µl of 250 mM PMSF in 100% isopropanol was added to each sample. Serial dilutions of the PEP standard in 0.05% Triton-X 100, 10 mM KH₂PO₄ were prepared.

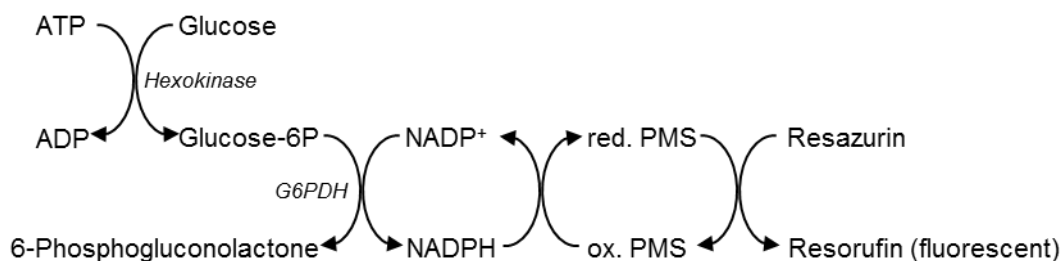
One hundred μl of samples and standards were transferred to wells of a 96 well plate. Twenty five μl of 5x PEP assay buffer (1.2 mM MgCl_2 , 3.6 μM ADP, ± 17.7 U rabbit muscle pyruvate kinase) was added to each well and the plate incubated for 15 minutes to allow the PEP dependent phosphorylation of ADP to ATP. The reaction was terminated with the addition of 13.9 μl of 600 mM NaF. 95 μl of reaction mixture was transferred to wells of a 96 well plate containing 5 μl of AMR and luminescence measured using the FLUOstar Optima.

Luciferase coupled pyruvate kinase assay

Pyruvate kinase activity in cell lysates prepared for BN-PAGE was determined using a luciferase coupled assay. One μl of cell lysate (300 ng protein) was added to replicate wells of a white walled 96 well plate. Added fresh was 5.4 μl of 1 mM ADP, 7.5 μl of 1 mM PEP or water and 60 μl of Vialight ATP monitoring reagent to 1 ml of pyruvate kinase assay buffer (10% glycerol, 240 μM MgCl_2 , 10 mM KH_2PO_4 , pH 7.4). To initiate the reaction, 50 μl of buffer was added to each well and luminescence was monitored for up to 15 minutes. The slope of a linear portion (typically 0-5 minutes) of each luminescence vs. time curve was calculated. The slope in wells without exogenous PEP was deemed due to non-PK dependent ATP production and was subtracted from the slope of PEP containing wells.

Hexokinase assay

Hexokinase activity in cell lysates was determined using a G6PDH coupled assay based on the coupled reaction outlined below:



Cell lysates were prepared as described for BN-PAGE except centrifugation was omitted. Twenty μl of lysate (equivalent of $\sim 50,000$ cells) was combined with 80 μl of hexokinase assay buffer (75 mM

Tris-HCl pH 8.0, 15 mM MgCl₂, 30 mM glucose, 0.5 mM ATP, 1 mM NADP, 200 µM PMS, 5 µg/ml G6PDH, and 3 µl/ml alamar blue (resazurin)) in black wall, clear bottom 96 well plates and incubated at room temperature for 30 minutes. Fluorescence (Em: 560 nm, Ex: 590 nm) was measured using the Fluostar Optima microplate reader.

pH indicator based extracellular acidification assay

Extracellular acidification was measured based on the pH dependent absorbance spectra of phenol red. Cells were seeded into up to 40 wells of a 96 well plate, typically 80,000 cells per well and allowed to attach for 3 hours. The outer perimeter of wells was filled with PBS to minimise evaporation edge effects. To 10 ml of Seahorse XF Assay Media, was added 500 µl FCS (dialysed if using low glucose), 100 µl of 100 mM sodium pyruvate, 100 µl of 200 mM glutamax, up to 100 µl of 17.5 M glucose and 16.5 µl of 1 M NaOH, raising the pH to 7.8. To generate a standard curve, HCl was added typically up to a final concentration of 3.5 mM in 0.5 mM increments, and NaOH to a final concentration of 0.5 and 1 mM. 100 µl of each standard was added in duplicate to the remaining wells of the 96 well plate. Wells containing cells were rinsed once with 50 µl of assay media and 100 µl of assay media containing the appropriate drugs and glucose was added. The plate was placed in the FLUOstar Optima maintained at 37°C with the lid removed. Absorbance at 560 nm and 450 nm was monitored every 5 minutes for 10 hours. The 560 nm/450 nm absorbance ratio vs. H⁺ change (mM) was fitted using least squares, to the equation below.

$$y = \frac{a - b}{1 + e^{kx+d}} + b$$

This equation was then used to calculate the amount of H⁺ produced in cell containing wells.

Seahorse XF Bioanalyser

The Seahorse XF Bioanalyser (Seahorse Bioscience, MA USA) utilises pH sensitive and O₂ sensitive fluorescent probes embedded in a matrix to simultaneously measure the oxygen consumption rate (OCR) and extracellular acidification rate (ECAR) of a cell monolayer. During

measurement phases, sensor probes are lowered, forming a temporary closed chamber with a volume of 7 μ l. Cellular respiration causes a drop in O₂ and glycolytic fermentation lowers pH. To correct for diffusion of O₂ from the surroundings, cellular OCR was calculated using the 'Akos method', described in (Gerencser et al., 2009). Following the measurement phase, the mix phase consisted of the sensor probes being raised and lowered repetitively to mix the assay media, and the wait phase consisted of the sensor probes remaining in the raised position. The XF Bioanalyser allows for up-to four separate automated injection events through pneumatic injection ports. During a typical experiment, three cycles consisting of 3 minutes mix, 3 minutes wait and 4 minutes measure were run before and after each injection event.

Cells were seeded into XF24 cell culture microplates at a density of 80,000 cells per well in standard culture media. After 1 hour incubation at 37°C for U87MG cells or overnight for SF767 cells, media was replaced with 600 μ l XF assay media (a modified DMEM formulation with no glucose, pyruvate or buffers) supplemented with 1 mM pyruvate, 2 mM glutamax, 5% dialysed FCS, and glucose as indicated in main body, and incubated at 37°C without added CO₂.

Oroboros Oxygraph

Respiration measurements were performed using an Oroboros Oxygraph-2k. This device features two temperature controlled chambers each containing a magnetic stir bar and a Clark-type polarographic for determination of oxygen tension. Upon closure with PVDF stoppers, each chamber is sealed from the atmosphere, with an effective volume of 2 ml. Cells, substrates, and inhibitors can be added by means of Hamilton syringes through a long and narrow opening through the stopper. Oxygen consumption rate is determined from the slope of oxygen tension over time.

Respiration of intact cells

Approximately 2.4 ml of glucose free DMEM was added to both chambers of the Oxygraph. Excess volume was added to minimise the likelihood of foam or air bubbles becoming trapped after closure. Chambers remained open for 30 minutes to allow equilibration with atmospheric O₂.

Chambers were closed (reducing the enclosed volume to 2 ml) and inspected to ensure no trapped air bubbles and allowed to stabilise for ~15 minutes.

SF767 or U87MG cells (1.5×10^6) resuspended in 50 μ l of glucose free DMEM, maintained on ice until injection, and were added to each chamber. Substrates, drugs and inhibitors were added as indicated in the results chapters. All substrates were dissolved in water to achieve a 20 μ l injection volume, while drugs and inhibitors dissolved in DMSO were further diluted 5-10 fold in water to achieve a 10 μ l injection volume.

Respiration of digitonin permeabilised cells

Detailed analysis of mitochondrial function was conducted by measuring respiration of cells permeabilised with digitonin. Permeabilisation facilitates free diffusion of mitochondrial substrates across the plasma membrane, allowing substrates for specific complexes to be supplied.

Approximately 2.2 ml of freshly prepared respiration buffer (250 mM Sucrose, 2 mM KH_2PO_4 , 5 mM MgCl_2 , 1 mM EDTA, 20 mM 3-(N-morpholino)propanesulfonic acid (MOPS, pH 7.4)) was added to both chambers of the Oxygraph. Chambers remained open for 30 minutes to allow saturation of with O_2 . Chambers were closed and inspected to ensure no trapped air bubbles and allowed to stabilise for ~15 minutes. 1.5×10^6 SF767 cells resuspended in 50 μ l of respiration buffer was added to each chamber. After obtaining a stable respiration rate, 9 μ g of digitonin in 9 μ l of water was added.

Substrates, inhibitors and uncouplers were sequentially added as indicated in the results chapters.

Micro-plate based real-time cell death assay

Propidium Iodide (PI) is a nucleic acid intercalating agent that increases in fluorescence dramatically upon binding to DNA or RNA. Because PI is membrane impermeable, only cells with compromised plasma membranes will accumulate PI to become fluorescent. This allows PI staining to be used as a marker of dead cells in techniques such as flow cytometry. Here, PI included in cell media allowed for monitoring of cell death in real time.

Cells were plated in black wall, clear bottom 96 well plates at a density of 50,000 cells per well in standard media. Once attached, media was replaced with media containing treatments and 20 µg/ml propidium iodide. During monitoring of cell death, cells were incubated at 37°C in the FLUOstar Optima plate reader, and fluorescence (Ex 500-10 nm/Em 590-10 nm) was measured every 5 minutes.

Statistical analysis

The results displayed in this thesis are from single experiments that are representative of experiments that have been repeated in triplicate. Where statistical analysis has been performed, at least three replicate wells were used within each experiment, except for synergy drug screen experiments, where two replicate wells were used. Unless otherwise stated, error bars represent standard error of the mean, and statistical significance was determined using the Student's t-Test, where '*' indicates $p < 0.05$, '**' indicates $p < 0.01$ and '***' indicates $p > 0.001$.

References

- BAKER, W. L. 1991. Potential interference of hydrogen peroxide in the 2,2'-bichinonic acid protein assay. *Anal Biochem*, 192, 212-4.
- GERENCSEK, A. A., NEILSON, A., CHOI, S. W., EDMAN, U., YADAVA, N., OH, R. J., FERRICK, D. A., NICHOLLS, D. G. & BRAND, M. D. 2009. Quantitative microplate-based respirometry with correction for oxygen diffusion. *Anal Chem*, 81, 6868-78.

Chapter 3 - Development of a Synergy Drug Screen

Table of Figures	104
Introduction.....	105
Hill model/ Median effects equation.....	106
Loewe Additivity/ Isobologram method	107
Combination index.....	108
Bliss independence model	109
Study outline.....	109
Results	111
Docetaxel and vinblastine.....	120
Salinomycin and ABT-737	134
Axitinib and docetaxel	135
ABT-737 and bisindolylmaleimide VIII	135
Bortezomib and salinomycin	135
Remaining combinations	136
Discussion.....	136
References.....	140

Table of Figures

Table 3.1 Reported mechanism of action of agents used in this study.....	113
Figure 3.1. 10 μ M drug screen on GBM cell lines.....	117
Figure 3.2. Dose response curves of selected agents on GBM cell line proliferation.	118
Table 3.2. IC ₅₀ values of selected agents on GBM cell line proliferation.....	119
Figure 3.3. Combination of docetaxel and vinblastine on GBM-L2 cells.....	121
Figure 3.4. Combination of ABT-737 and salinomycin on GBM-L2 cells.....	122
Figure 3.5. Combination of ABT-737 and salinomycin on CSC#020 cells.....	123
Figure 3.6. Combination of ABT-737 and salinomycin on GBM4 cells.....	124
Figure 3.7. Combination of axitinib and docetaxel on GBM-L2 cells.....	125
Figure 3.8. Combination of ABT-737 and bisindolylmaleimide on CSC#020 cells.	126
Figure 3.9. Combination of bortezomib and salinomycin on CSC#020 cells.	127
Figure 3.10. Combination of salinomycin and docetaxel on CSC#020 cells.	128
Figure 3.11. Combination of bortezomib and docetaxel on CSC#020 cells.....	129
Figure 3.12. Combination of docetaxel and bisindolylmaleimide on CSC#020 cells.	130
Figure 3.13. Combination of bortezomib and docetaxel on GBM-L2 cells.....	131
Figure 3.14. Combination of dasatinib and docetaxel on GBM-L2 cells.....	132
Figure 3.15. Combination of bortezomib and axitinib on GBM-L2 cells.....	133
Table 3.3 Summary of Drug Interactions.....	137

Introduction

One of the major goals for the development of novel treatment strategies, whether it be for treatment of cancer, infection or any other disease, is to identify combinations of therapies that produce a so called 'synergistic' response. In the clinical setting, achieving synergy can be viewed as a strategy to maximise therapeutic effect, while minimising off target side effects by using a combination of therapeutic modalities.

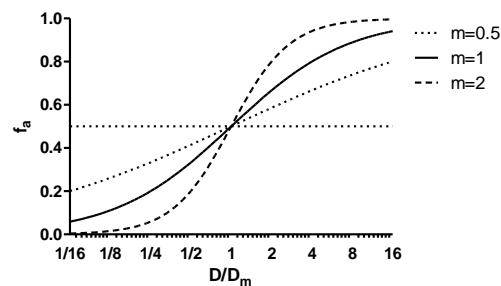
In the *in vitro* setting, 'synergy' can be more precisely defined as an effect of two or more agents that is *more than additive*. Likewise, 'antagonism' can be defined as an effect that is less than additive. By mathematically predicting the effect of two agents/drugs used in combination that are assumed to be 'additive', experimentally observing a deviation from the predicted effect can lead to rejection of the null hypothesis, and a conclusion that a particular combination is synergistic or antagonistic. Similarly, mathematical predictions can be made about the dosage of two agents used in combination required to achieve a particular effect level. If the actual concentration of those two agents required to achieve a particular effect is less than that predicted by the mathematical model, a synergistic effect can be concluded.

While defining synergy and antagonism as deviations from additivity appears relatively simple, mathematically defining what is an additive effect is not a straight forward task. Predicting the effect of two additive cytotoxic agents used to kill cancer cells is not simply a matter of adding their effect levels. To demonstrate this, consider two cytotoxic agents that when used at a particular concentration each result in 60% cell death. Used in combination, the combined effect obviously cannot be $60\%+60\%=120\%$. The three most widely used mathematical models used to predict additive effects, and therefore to test synergy and antagonism are the Bliss Independence model, Loewe Additivity (Isobologram method) and the Combination Index.

Hill model/ Median effects equation

Before introducing models for drugs used in combination, it is pertinent to introduce the 'Hill model', or 'median effects equation'. This equation was originally developed to describe the dose response effect of inhibitors on enzyme activity, and can also be used to describe the response of more complicated systems such as cells or even whole organisms. The Hill model, also known as the 'median effects equation' states that;

$$\frac{f_a}{f_u} = \frac{f_a}{1-f_a} = \left(\frac{D}{D_m}\right)^m \quad (1)$$



Where D is the dose, D_m is the dose required to achieve half maximal response (similar to IC_{50}), f_a and f_u is the fraction of the system affected and unaffected respectively. m is termed the Hill coefficient and describes the shape of a dose-response curve. A dose response curve is considered to be hyperbolic when $m=1$, sigmoidal when $m>1$, and flat sigmoidal when $m<1$. The plot above is the hypothetical response curve for an agent with a D_m of 50, and a hill slope of either 0.5, 1 or 2.

Because $f_a + f_u = 1$, equation can be rearranged to its more familiar form such that:

$$f_a = \frac{\left(\frac{D}{D_m}\right)^m}{1 + \left(\frac{D}{D_m}\right)^m} \quad (2)$$

The median effects equation can be linearised by applying a logarithmic transformation to both sides of equation 1 to produce equation 3.

$$\log\left(\frac{f_a}{1-f_a}\right) = m(\log(D) - \log(D_m)) \quad (3)$$

In a plot of $\log(D)$ vs. $\log\left(\frac{f_a}{1-f_a}\right)$, known as a 'median effects plot' where the anti-log of the horizontal intercept is equal to D_m while the slope is equal to m .

Loewe Additivity/ Isobologram method

Loewe additivity is a concept which is based on the 'sham experiment', where a single agent will by definition, always be additive with itself. If two uncharacterised agents tested in combination are identical, then the sum amount of each agent used at different ratios, required to produce a particular effect level will always sum to the same value. If one were to plot the concentrations of these two agents (with one agent on each axis on a two dimensional plot) required to produce a particular effect (for example 50% inhibition), each point would lie in a straight line. For example, if 10 units of agent A or 10 units of agent B are required to produce an effect of 50%, then a 1 to 1 mixture will require 5 units of each etc. A plot containing data points of drug combinations yielding the same effect is called an isobologram.

Consider different two agents that act in the same manner and behave additively when used in combination. Drug 2 is r times more potent than drug 1, i.e. $D_{m1}=rD_{m2}$ where D_{m1} and D_{m2} are the doses of drug 1 and drug 2 respectively required to produce the median effect. In other word the relative potency of drug 2 vs drug 1 is equal to r . The amount of each drug used in combination to produce the median effect is such that $D_1+D_2=D_{m1}$, where D_1 and D_2 are the doses of drug 1 and drug 2. An isobologram of D_1 and D_2 at the median effect will produce a straight line intersecting at D_{m1} and D_{m2} .

The isobologram method predicts the amount of two drugs used in combination required to produce a given effect based on the individual potency of each drug. If an experiment is conducted and the isobologram deviates below the straight line intersecting D_{m1} and D_{m2} , the amount of each agent was less than was predicted to produce an effect. Therefore the drugs can

be said to be synergistic. Conversely if the isobologram deviates above the line then more of each agent was required than predicted, meaning the interaction is antagonistic.

While the isobologram method provides a visual representation of the synergistic or antagonistic interaction of two agents, it does not quantitatively define the degree of synergy or antagonism.

One issue with the isobologram method is that it assumes that two drugs behave with similar kinetics, i.e. $m_1=m_2$ where m_1 and m_2 are the hill coefficient of drug 1 and drug 2 respectively. If $m_1 \neq m_2$ then the relative potency will not be constant across different effect levels, resulting in a failure of the model.

Combination index

The combination index (CI) method was developed by (Chou and Talalay, 1984) using the principles of mass action, which have principally been used to describe enzyme kinetics. The theoretical basis and methodology for applying the CI method has been extensively described (Chou and Talalay, 1984) and will only be briefly introduced here. When applying the combination index method, each of two drugs are used individually and in combination at a fixed ratio. The dose response profile of each individual drug, as well as the fixed ratio combination, is described using the median effects equation to obtain value of D_m and m for each drug and their combination. In brief, these equations are used to describe how much of an observed effect can be accounted for by the predicted combined action of each of the two drugs. This measure is termed the combination index (CI). A CI value of 1 indicates that the effect observed at a particular effect level is fully accounted for by the fractional effects of each of the drugs. A CI of less than 1 indicates that the fractional effects of each drug account for less than the effect observed, i.e. there is a synergistic interaction, while a CI greater than 1 indicates that the fractional effects of each drug is more than the effect observed, i.e. there is an antagonistic interaction. The CI for a fixed ratio is calculated across the full spectrum of effects levels i.e. $0 < f_a < 1$.

For meaningful application of the CI method, it is essential that the dose-response relationship of each drug and the fixed ratio combination is accurately represented by the median effects equation, i.e. median effects plots have regression lines with correlation coefficients >0.9 .

Bliss independence model

Conceptually, the simplest mathematical model of additivity is that of Bliss Independence. This model assumes that two drugs act independently (i.e. have distinct cellular targets) such that the fraction of cells surviving exposure to the first agent are as sensitive to a second agent as cells that were not exposed to the first agent.

For example, if drug 1 and drug 2 each produce an effect of 50% when used alone, drug 2 can be thought of as acting on the 50% of cells that remain after treatment with drug 1. An effect of 50% on the remaining 50% will result in loss of a further 25% of the original population, meaning a combined effect of 75% predicted by the model. If an observed effect is greater than that predicted by the model, a synergistic interaction of the drugs is inferred.

One criticism of the Bliss independence model is that it is incompatible with the idea of a sham experiment as introduced earlier. If two drugs used in combination are the same, combining two doses that each individually produce a 50% effect would not necessarily be predicted to produce a combined effect of 75% based on the median effects equation. For example for a drug that followed hyperbolic kinetics (i.e. $m=1$), the predicted effect of such a combination would be 66.7%. However unlike Loewe additivity which assumes a similar mode of action, Bliss independence assumes a distinct mechanism of action of each agent, an assumption that is obviously false the case of a sham experiment.

Study outline

In this chapter, a work flow for the identification and evaluation of potential synergistic drug combinations for the treatment of glioblastoma was developed. The effect of inhibition of

proliferation was assessed by using the MTS proliferation assay, which utilises a substrate that becomes optically dense when metabolised by living cells, thus allowing relative quantification of cell number based on absorbance.

Six GBM cell lines were used in this study. Unlike 'traditional' GBM cell lines such as U87MG and SF767 which are cultured in the presence of foetal calf serum, these cell lines were maintained in serum free defined media containing EGF and bFGF. Gene expression studies have shown that GBM cells cultured under such serum free conditions maintain an expression profile more closely resembling that of the parent tumour. Therefore the response of these cell lines to novel drugs is more likely to be reflective of the way they would respond *in vivo* than if they were cultured in the presence of FCS.

This study was divided into three phases. In the first phase, each proliferation/survival of cell line was screened against a panel of therapeutic agents at a fixed concentration, typically 10 μ M. In the second phase, compounds selected based on single agent efficacy in the first phase were titrated in order to determine the IC_{50} in each of the cell lines. This was a prerequisite for the third phase, in which selected combinations of agents were evaluated to identify potentially synergistic interactions.

To summarise, the aims of this chapter are to:

- Identify compounds that effectively inhibit proliferation of glioma cells as single agents
- Develop a workflow that can identify the interaction of two compounds used in combination
- Employ this workflow in order to identify potential synergistic interaction of pairs of compounds.

Results

The first phase in selecting potential drugs for use in combination was to identify drugs with potent effects when used as a single agent. Six GBM cell lines were used to screen an array of compounds that included rationally designed 'targeted therapies', inhibitors of a number of cell signalling pathways as well as a number of cytotoxic chemotherapeutic compounds. The majority of the agents evaluated are already approved for use in humans to treat other malignancies or have had at least some clinical testing. **Table 3.1** lists the compounds used together with their reported mechanism of action.

GBM cells were cultured in 96 well plates for 5 days in the presence of each compound at a concentration of 10 μ M unless otherwise specified, and the effect on cell survival/proliferation was evaluated using the MTS assay (**Figure 3.1**). For each cell line, absorbance values were normalised against vehicle only (DMSO) treated controls such that a value of 1 indicates no effect.

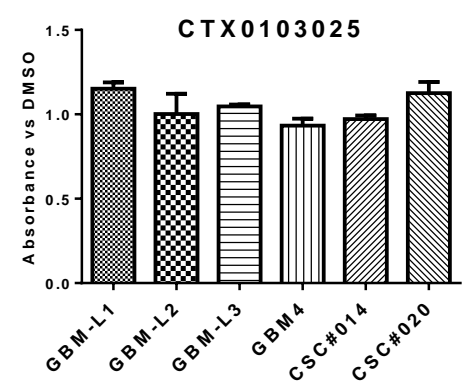
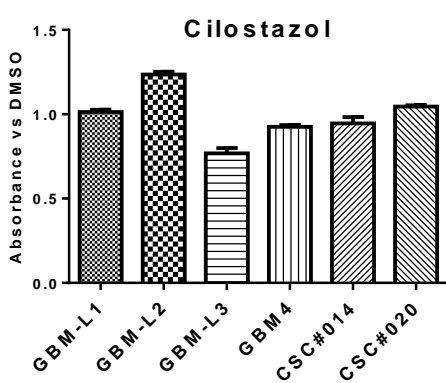
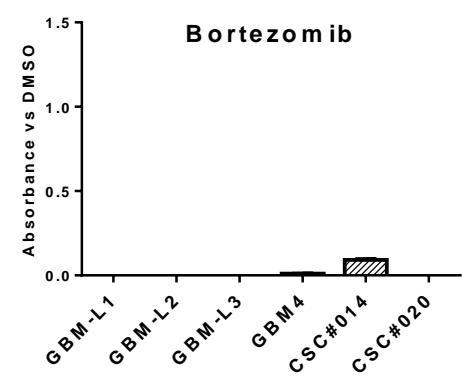
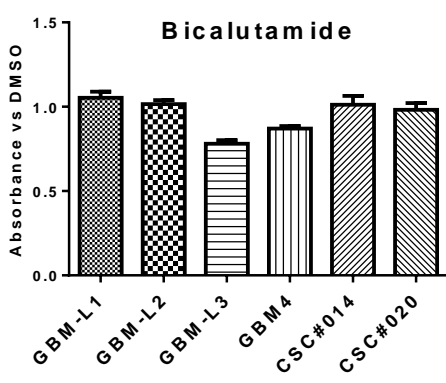
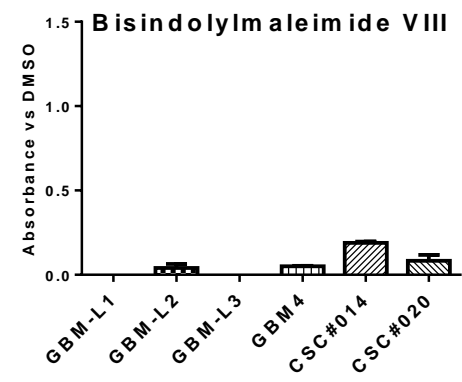
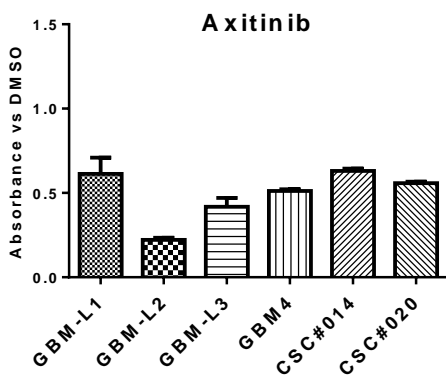
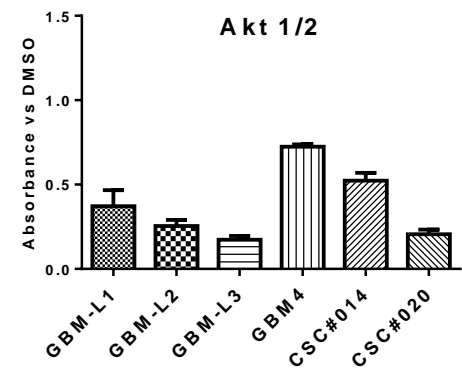
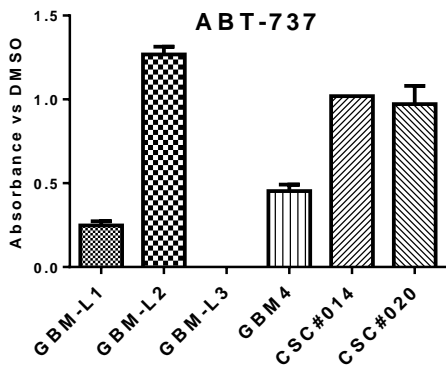
A substantial proportion of the agents tested caused robust inhibition of proliferation of at least 50% across the six cell lines used, including the anti-mitotic agents docetaxel and vinblastine, as well as bisindolylmaleimide VIII, bortezomib and salinomycin.

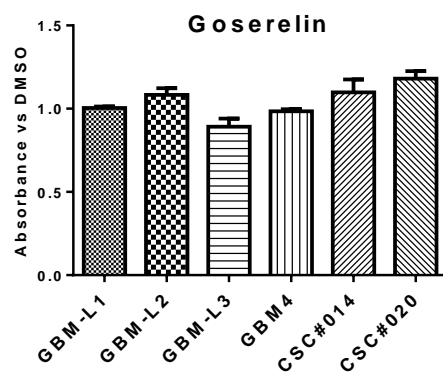
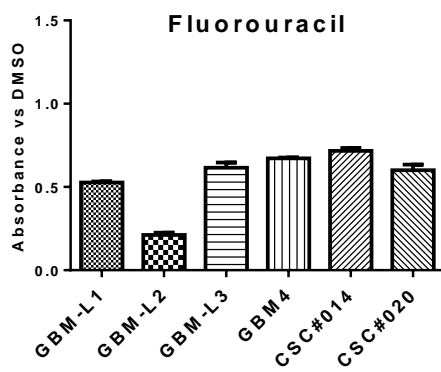
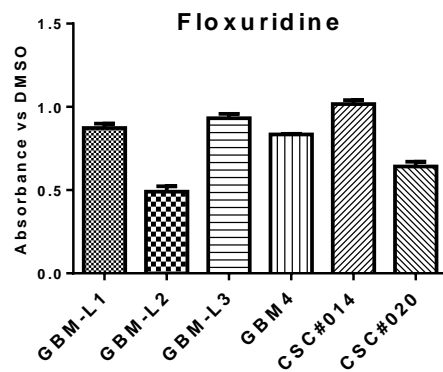
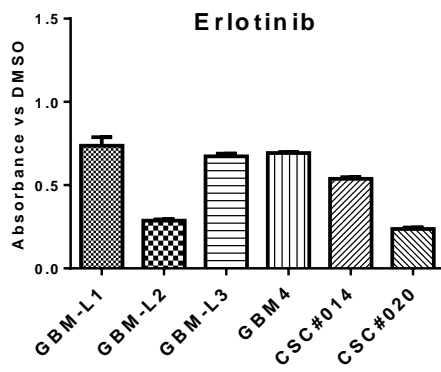
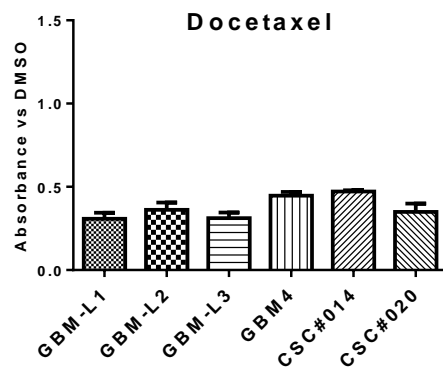
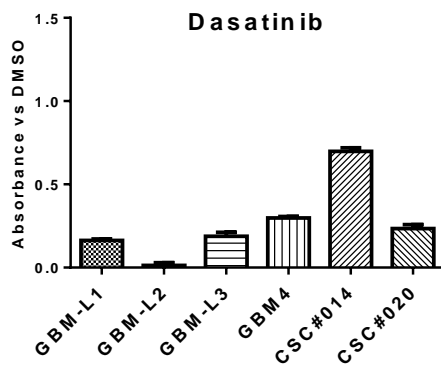
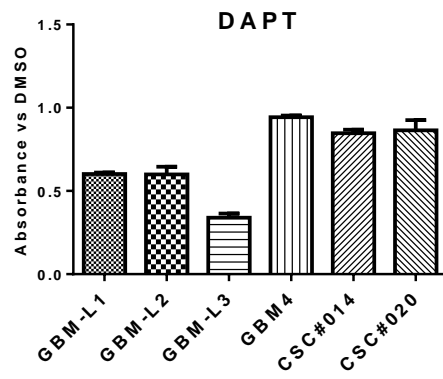
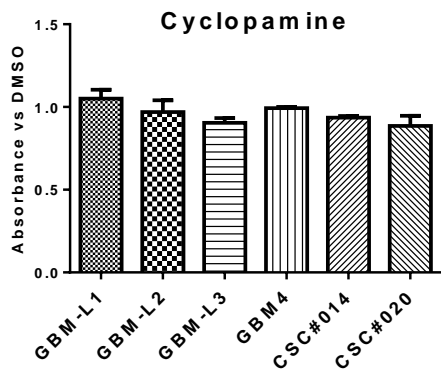
A number of the so called 'targeted therapies' resulted in highly variable responses. Notably ABT-737 was highly effective in GBM-L1, GBM-L3 and to a lesser extent in GBM4, while GBM-L2 and CSC#014 and CSC#020 were resistant to the compound.

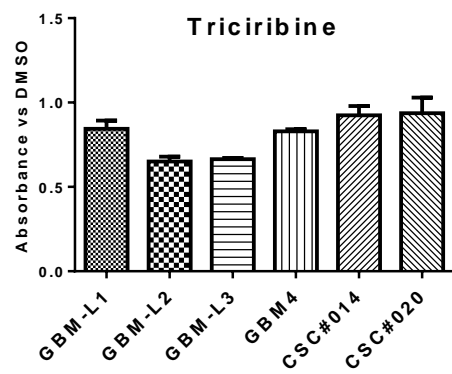
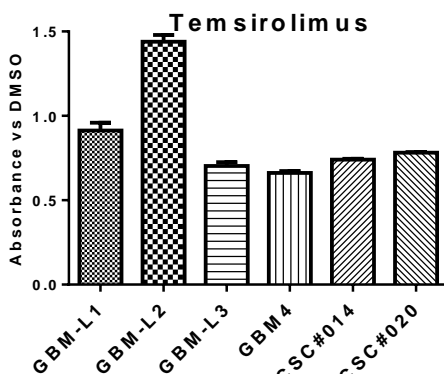
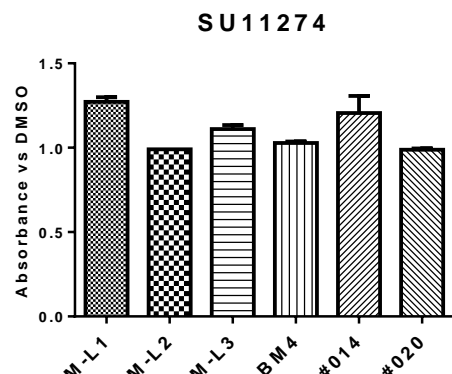
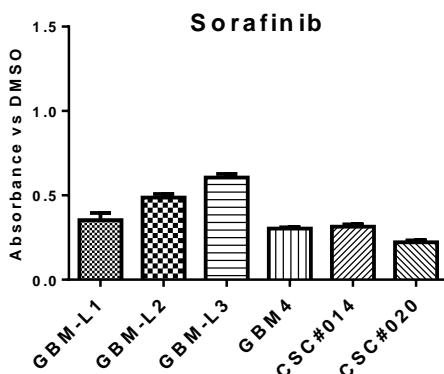
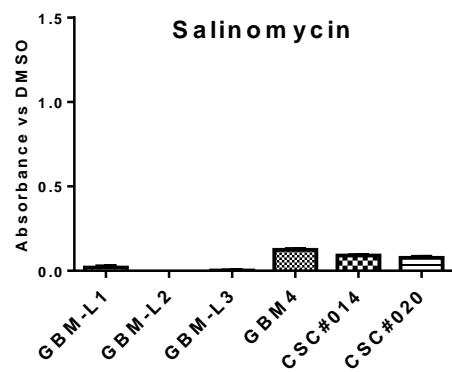
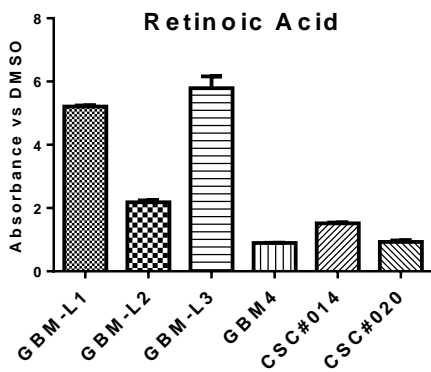
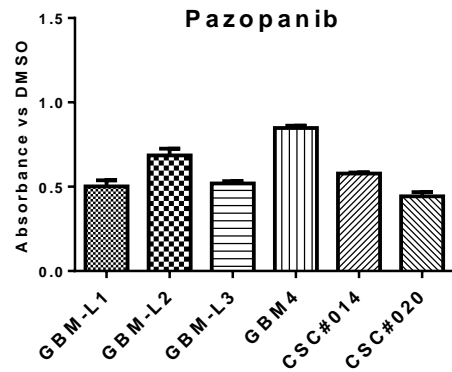
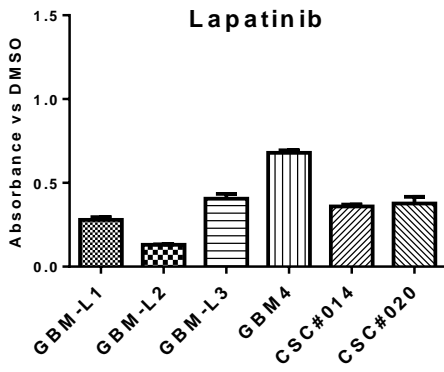
Compound	Mechanism of action	Stage of development	Reference
ABT-737	BH3 mimetic, antagonises anti-apoptotic Bcl-2 family proteins	Clinical trials for a range of malignancies.	(Gandhi et al., 2011)
Akt Inhibitor VIII	Selective inhibitor of Akt1 and Akt2	Preclinical.	
Axitinib	Multikinase inhibitor, targets include VEGFRs, PDGFRs and c-Kit	Approved for treatment of RCC.	
Bisindolylmaleimide VIII	Protein kinase C inhibitor	Preclinical.	
Bicalutamide	Androgen receptor antagonist	Approved for treatment of prostate cancer.	(Schellhammer, 2002)
Bortezomib	26S proteasome inhibitor	Approved for treatment of multiple myeloma.	(San Miguel et al., 2008)
Cilostazol	Phosphodiesterase type III inhibitor, intended to elevate intracellular cAMP levels	Approved as an anti-clotting agent. Preclinical for cancer treatment.	(Murata et al., 1999)
CTX0103025	Fak inhibitor	Preclinical.	
Cyclopamine	Inhibitor of hedgehog pathway signalling, known to be important in maintaining a stem cell phenotype in medulloblastoma	Derivative compound in clinical trials for pancreatic cancer and medulloblastoma.	(Berman et al., 2002) (Rudin et al., 2009)
DAPT	γ -secretase inhibitor, prevents Notch signalling to promote neural differentiation	Preclinical.	(Crawford and Roelink, 2007)
Dasatinib	Inhibitor of BCR-Abl and Src family kinases	Approved for treatment of acute lymphoblastic leukemia.	(Ottmann et al., 2007)
Docetaxel	Prevents depolymerisation by stabilising microtubules resulting in inhibition of mitotic cell division	Approved for treatment of a range of solid tumours.	(Montero et al., 2005)
Erlotinib	Epidermal Growth Factor Receptor (EGFR) inhibitor	Approved for treatment of NSCLC.	(Shepherd et al., 2005)

Floxuridine	Pyrimidine antimetabolite. Disrupts S-phase of the cell cycle by disrupting DNA and RNA synthesis	Approved for treatment of metastatic colorectal cancer.	(Rougier et al., 1992)
Fluorouracil	Pyrimidine analogue and irreversible inhibitor of thymidylate synthase.	Approved for treatment of a range of solid tumours.	(Longley et al., 2003)
Goserelin	GnRH agonist. Used to suppress synthesis of testosterone.	Approved for treatment of prostate cancer.	(Seidenfeld et al., 2000)
Lapatinib	Inhibitor of EGFR and ErbB2 tyrosine kinases	Approved for treatment of ErbB2 positive breast cancer.	(Geyer et al., 2006)
Pazopanib	Multikinase inhibitor, targets include VEGFRs, PDGFRs and c-Kit	Approved for treatment of advanced renal cell carcinoma.	(Sternberg et al., 2010)
Retinoic acid	Binds to retinoic acid receptors in the nucleus leading to transcriptional activity	Approved for treatment of acute promyelocytic leukemia.	(Warrell et al., 1991)
Salinomycin	Antibiotic and K ⁺ ionophore. Displays activity against drug resistant cancer cells. Inhibits gp170 drug transporters.	Preclinical.	(Gupta et al., 2009) (Riccioni et al., 2010)
Sorafenib	Multikinase inhibitor, targets include VEGFRs, PDGFRs and Raf family kinases	Approved for treatment of renal cell carcinoma and hepatocellular carcinoma. Undergoing trials for treatment of GBM.	(Escudier et al., 2007) (Llovet et al., 2008)
SU11274	Selective inhibitor of c-Met tyrosine kinase	Preclinical. Other c-Met inhibitors in early clinical testing	(Sattler et al., 2003)
Temsirolimus	Specific inhibitor of TORC1 through binding of FKBP12	Approved for treatment of renal cell carcinoma. Undergoing trials for treatment of GBM	(Sarkaria et al., 2010)
Triciribine	Inhibitor of Akt1 Akt2 and Akt3 and purine analogue. Inhibits DNA and protein synthesis	Clinical trials for treatment of breast cancer.	
Vinblastine	Binds tubulin to prevent assembly of microtubules resulting in M-phase cell cycle arrest	Approved for treatment of numerous malignancies including Hodgkin's and other lymphomas.	(Jordan et al., 1998)

Table 3.1 Reported mechanism of action of agents used in this study.







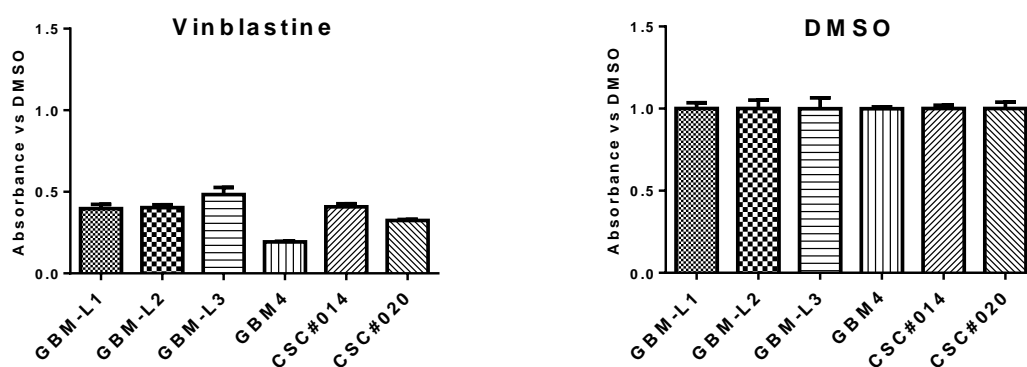


Figure 3.1. 10 μ M drug screen on GBM cell lines. Glioma cell lines were treated with various agents at a final concentration of 10 μ M and cultured for 5 days before performing an MTS cell proliferation assay. Background subtracted absorbance values were normalised against vehicle only (0.1% DMSO) treated controls.

After identifying a number of compounds with single agent efficacy a work flow was established for efficiently evaluating the effect of pairs of compounds used in combination.

As combinations of agents would be evaluated by using a ‘checkerboard’ configuration with a limited dose range, it was necessary to first determine IC_{50} values of each agent for each cell line. GBM cells were cultured for 5 days in the presence of varying amounts of each agent and the effect on cell survival/proliferation was evaluated using the MTS assay (**Figure 3.2**). These data were used to calculate IC_{50} values as shown in **Table 3.2**.

Determination of IC_{50} values for each agent allowed for combination plates to be prepared with pairs of agents arranged on each 96 well plate as a duplicate 6x6 matrix, with each agent at a concentration of $4 \times IC_{50}$, $2 \times IC_{50}$, $1 \times IC_{50}$, $\frac{1}{2} \times IC_{50}$, $\frac{1}{4} \times IC_{50}$ and $0 \times IC_{50}$. This arrangement allowed the same data set to be interpreted using Bliss independence, Loewe additivity and the combination index approaches.

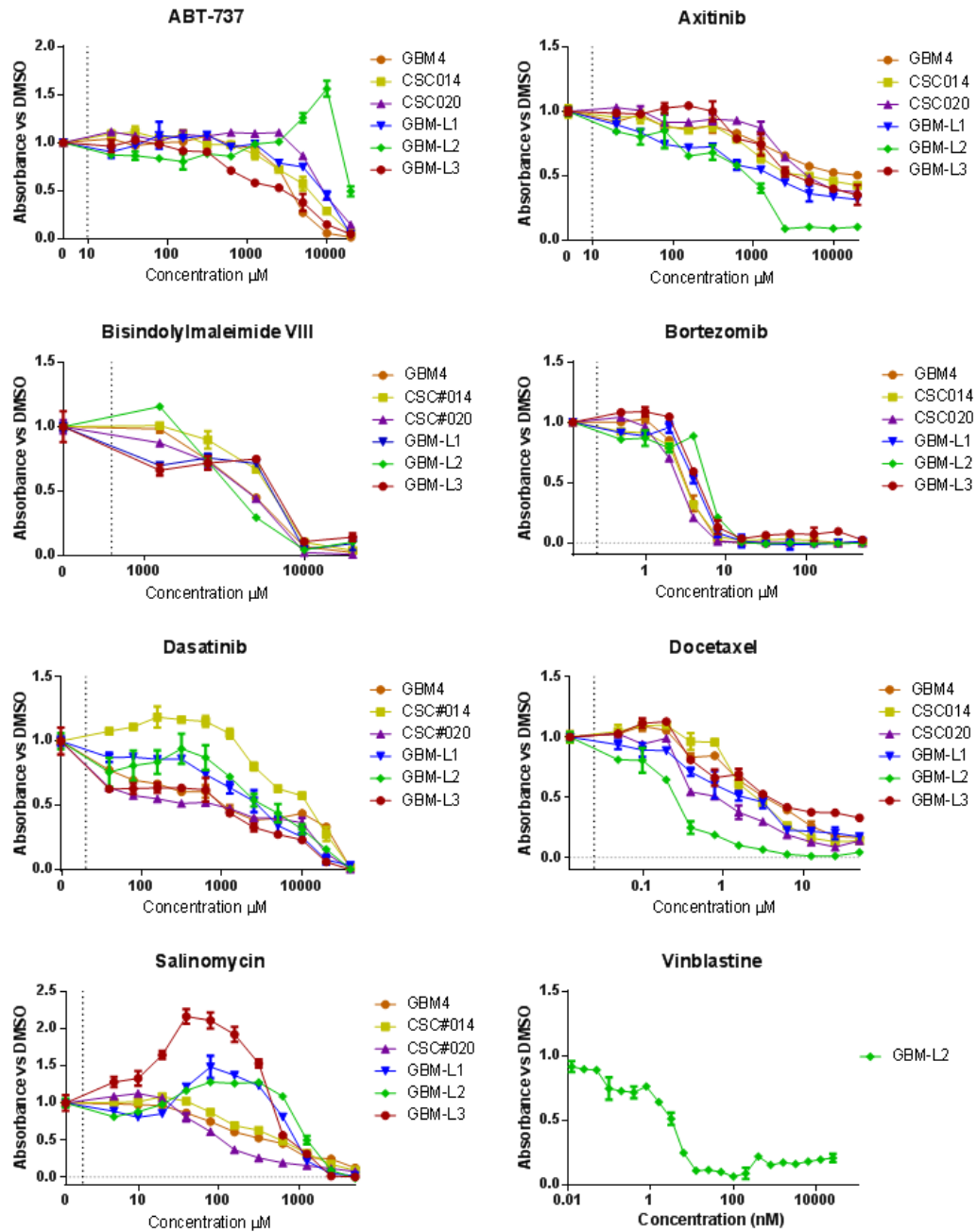


Figure 3.2. Dose response curves of selected agents on GBM cell line proliferation. Glioma cell lines were treated with a range of doses of various compounds and cultured for 5 days before performing an MTS cell proliferation assay.

Compound	IC50 (nM)					
	GBM4	CSC#014	CSC#020	GBM-L1	GBM-L2	GBM-L3
ABT-737	3700	6200	9200	9200	20000	3000
Axitinib	>20,000	4700	4800	1800	910	3500
Bisindolylmaleimide VIII	4600	6500	4500	6600	3800	6900
Bortezomib	3.30	3.20	2.80	4.20	6.10	4.70
Dasatinib	4600	6500	4500	6600	3800	6900
Docetaxel	3.40	2.70	0.80	2.00	0.30	3.90
Salinomycin	420	600	110	950	1300	780
Vinblastine	N.D.	N.D.	N.D.	N.D.	3.26	N.D.

Table 3.2. IC₅₀ values of selected agents on GBM cell line proliferation. Dose response curves from Figure 3.1 were used to calculate IC₅₀ values for each of the tested compounds in each cell line.

Each of the figures from **(Figure 3.3)** to **(Figure 3.15)** are arranged in a similar fashion;

Absorbance data (background subtracted and normalised against vehicle only treated controls) is shown in part A of each figure. Concentrations of the first drug are plotted along the horizontal axis, while each coloured line represents each concentration of the second drug, as shown in the legend in nM.

Plots in part B are isobolograms, plotting the doses of combined drugs that result in 50% inhibition of GBM cells. The ‘additivity line’ is a straight line drawn between the IC₅₀ values of each agent in isolation on their respective axis. Data points of drug combinations are expected to fall on this line assuming an additive interaction. Deviation above and below the additivity line indicate antagonism and synergy respectively.

Part D displays dose-response data as median effects plots as described by (Chou and Talalay, 1984). Blue and red data points are derived from the first and second agents respectively used alone, while the purple data points are derived from wells where the two agents were used in combination at a fixed ratio, i.e. along the diagonal of the 6x6 array. These data points are expected to lie in a straight line assuming the cells respond to each of the agents as described by the hill model. Linear regression curves fitted to these data points are used to calculate the combination index in part C.

For the combination index to be considered reliable output, the correlation coefficients of these regression curves should be greater than 0.9 ($r > 0.9$, $r^2 > 0.81$).

Part E is a graphical representation of the dose response of cells to each drug combination compared to the predicted response based on Bliss independence. Each pixel in the 6x6 grid represents one dose combination, with concentrations of the first drug increasing from top to bottom, and the second drug increasing from left to right. A white pixel represents minimum effect (i.e. maximum absorbance), while a black pixel represents maximum effect (i.e. minimum absorbance). Observed effect data determined the brightness on green and blue channels (of the red-green-blue image), and Bliss independence predicted effect determined brightness on the red channels. Where Bliss independence is the same as the observed effect, pixels are grey, while observed effects greater than predicted (synergy) is indicated by red pixels, and effects less than predicted (antagonism) is indicated by cyan pixels.

Docetaxel and vinblastine

GBM-L2 cells were treated with a combination of docetaxel and vinblastine (**Figure 3.3**). Isobologram, combination index and Bliss independence methods all indicated robust synergy of these two drugs. The dose response to each drug separately and in combination was well represented by the median effects equation as indicated by the high r^2 values for each. This makes the combination of docetaxel and vinblastine one of the most convincing example of synergy amongst the combinations tested.

A number of studies have previously demonstrated a synergistic response of taxanes and vinca alkaloids in other cancer types. Paclitaxel and vinorelbine were shown to induce a synergistic inhibition of proliferation of melanoma cells *in vitro* (Photiou et al., 1997). In a leukaemia mouse model paclitaxel and vinorelbine produced synergistic anti-cancer effects *in vivo*. Paclitaxel also appeared to reduce the toxicity of vinorelbine, allowing higher dosages to be administered

Docetaxel and Vinblastine in GBM-L2

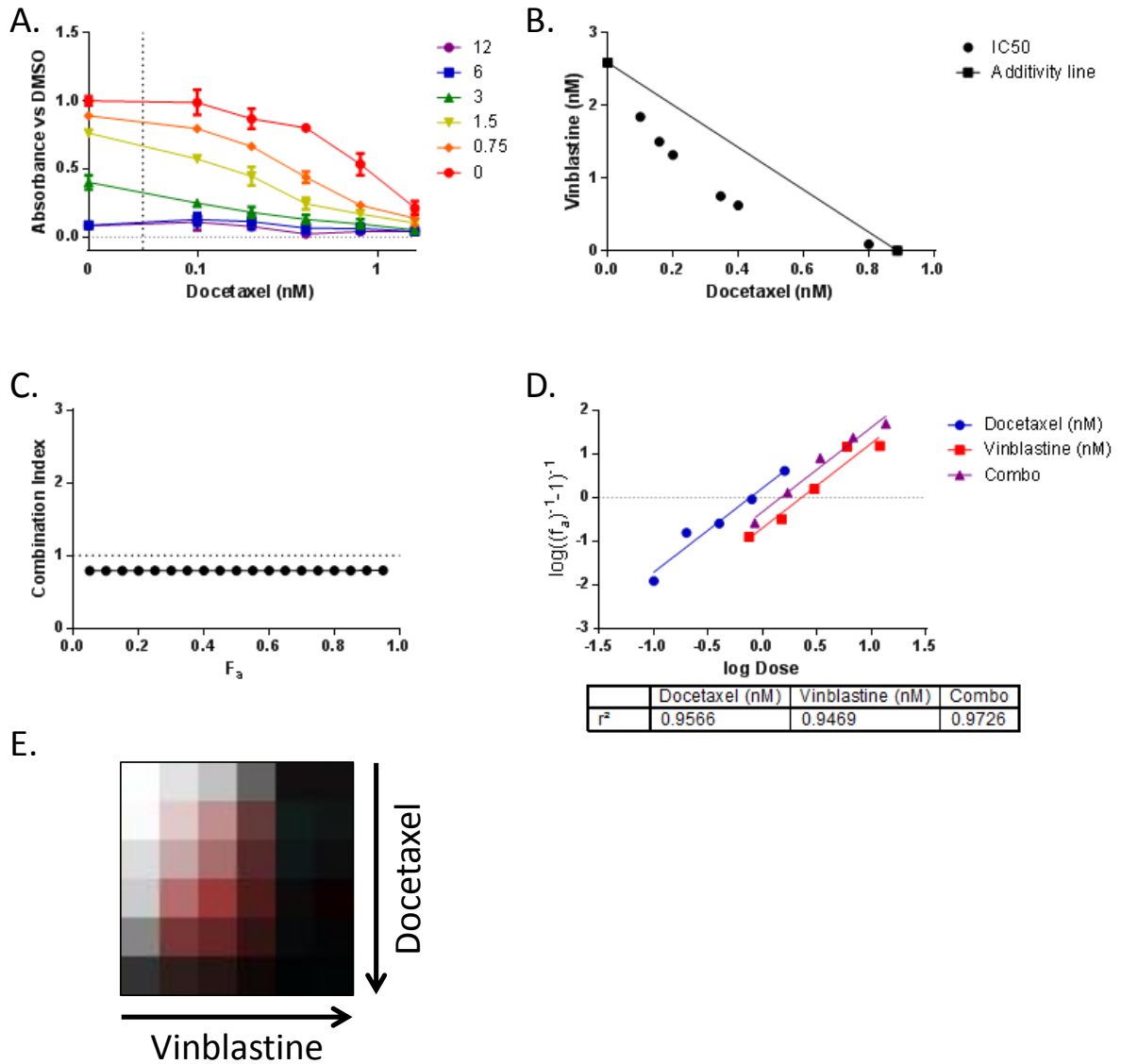


Figure 3.3. Combination of docetaxel and vinblastine on GBM-L2 cells. GBM-L2 cells were treated with 1 in 2 dilutions of docetaxel and vinblastine with starting concentrations of 1.6 nM and 12 nM respectively. Cells were treated with the indicated concentrations and cultured for 5 days before performing an MTS cell proliferation assay. Explanation for each sub-figure can be found in the main text.

ABT-737 and Salinomycin in GBM-L2

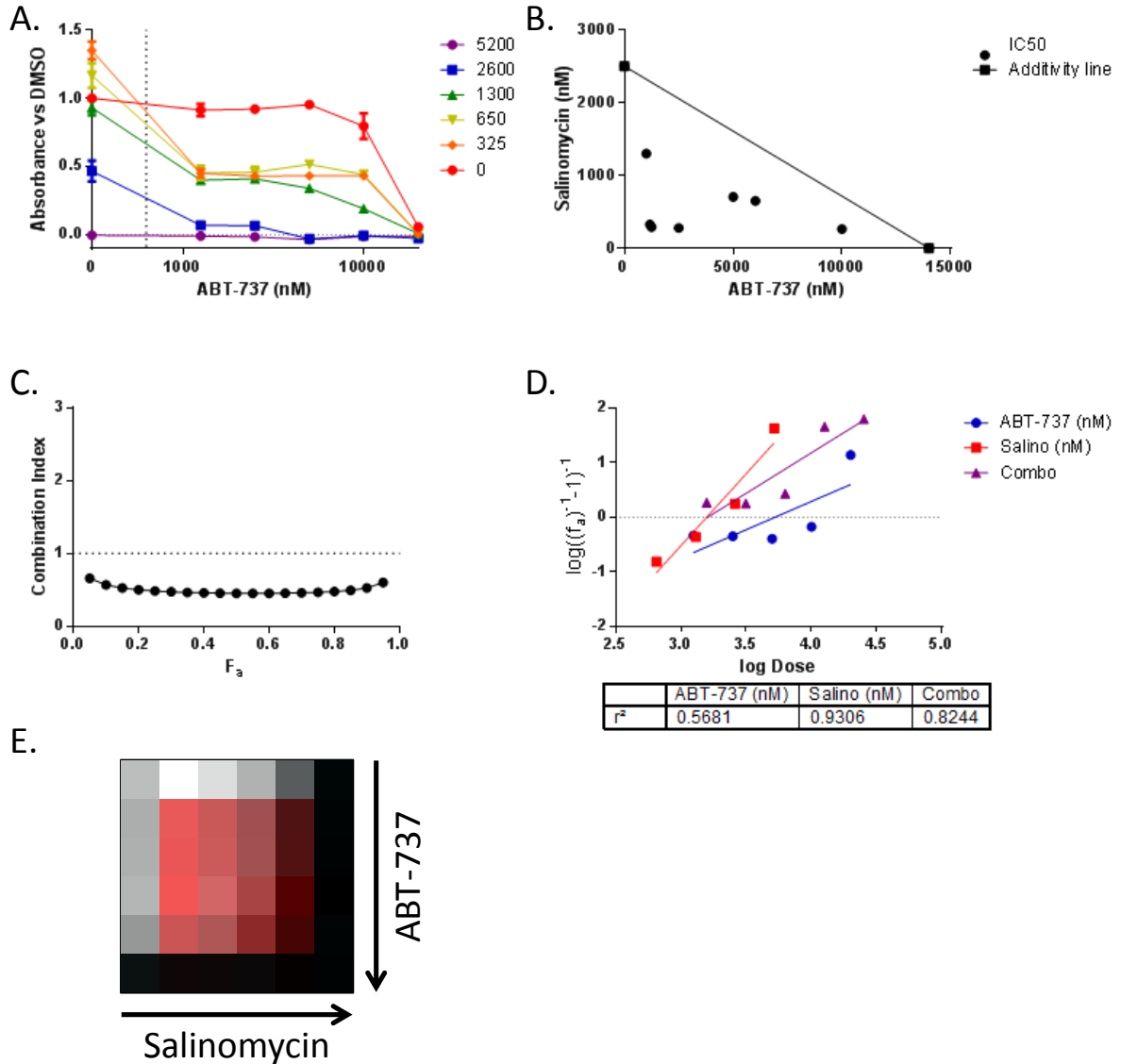


Figure 3.4. Combination of ABT-737 and salinomycin on GBM-L2 cells. GBM-L2 cells were treated with 1 in 2 dilutions of ABT-737 and salinomycin with starting concentrations of 20 μ M and 5.2 μ M respectively. Cells were treated with the indicated concentrations and cultured for 5 days before performing an MTS cell proliferation assay. Explanation for each sub-figure can be found in the main text.

ABT-737 and Salinomycin in CSC#020

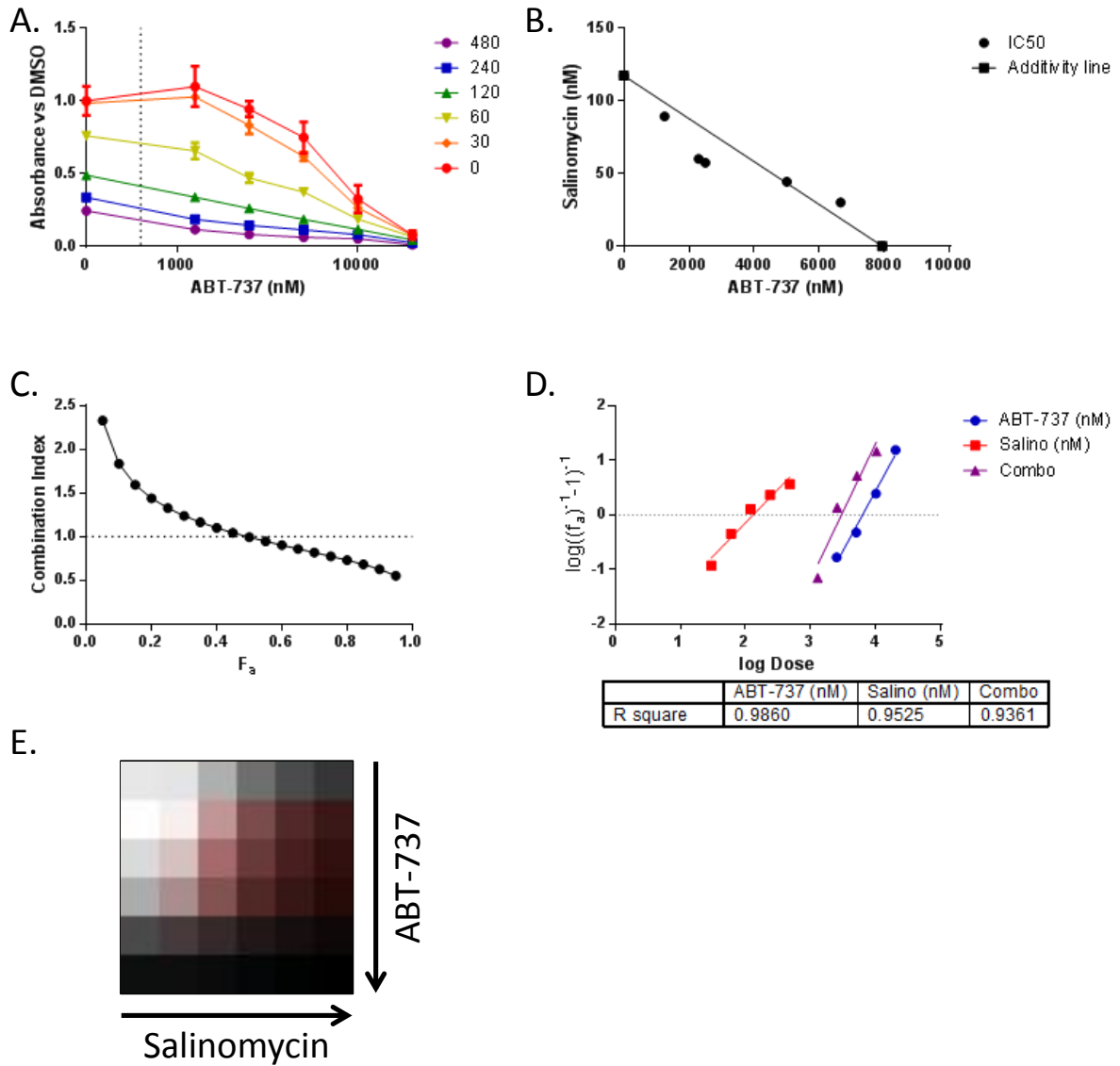


Figure 3.5. Combination of ABT-737 and salinomycin on CSC#020 cells. CSC#020 cells were treated with 1 in 2 dilutions of ABT-737 and Salinomycin with starting concentrations of 20 μ M and 480 nM respectively. Cells were treated with the indicated concentrations and cultured for 5 days before performing an MTS cell proliferation assay. Explanation for each sub-figure can be found in the main text.

ABT-737 and Salinomycin in GBM4

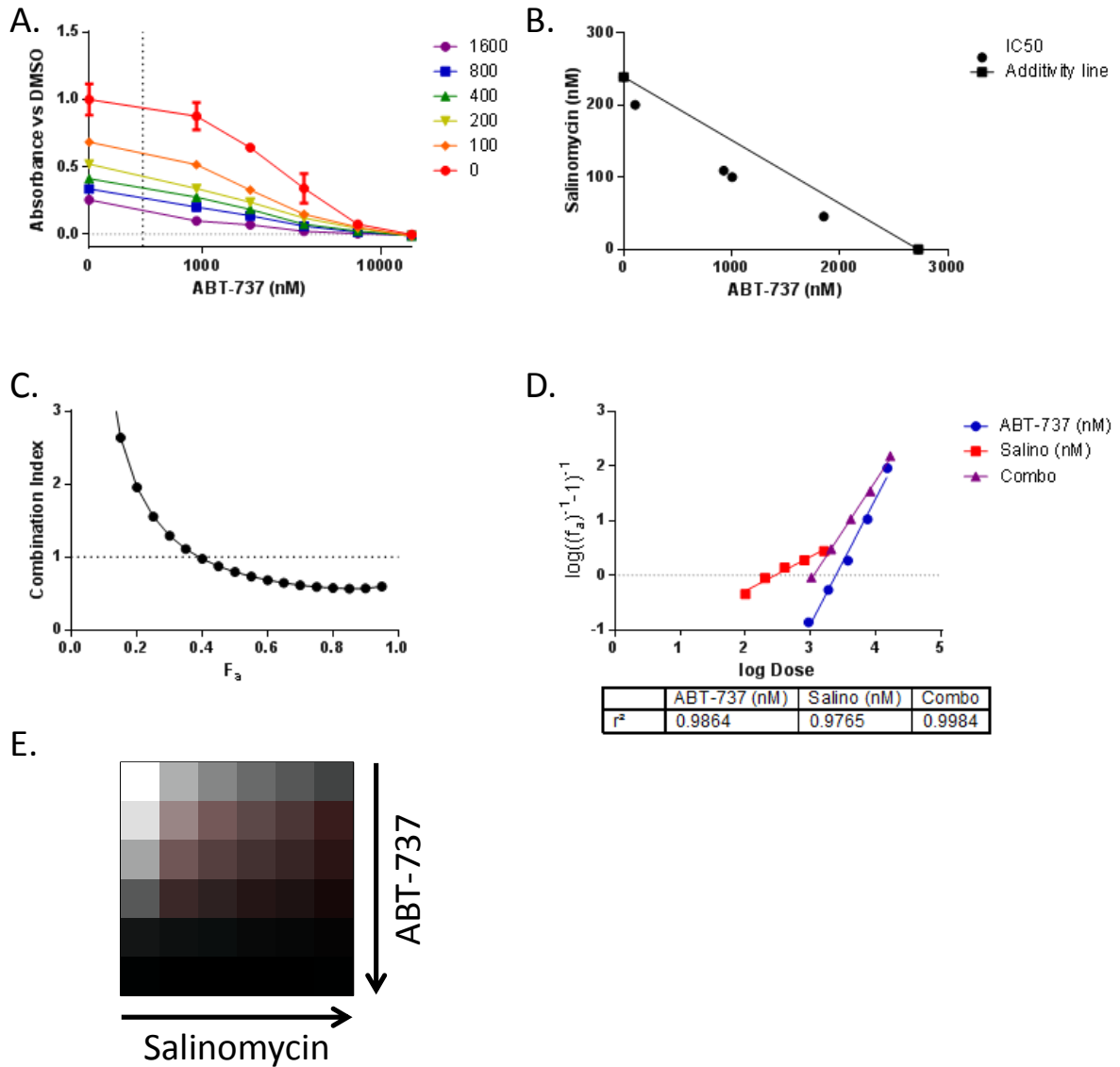


Figure 3.6. Combination of ABT-737 and salinomycin on GBM4 cells. GBM4 cells were treated with 1 in 2 dilutions of ABT-737 and salinomycin with starting concentrations of 14.8 μ M and 1.6 μ M respectively. Cells were treated with the indicated concentrations and cultured for 5 days before performing an MTS cell proliferation assay. Explanation for each sub-figure can be found in the main text.

Axitinib and Docetaxel in GBM-L2

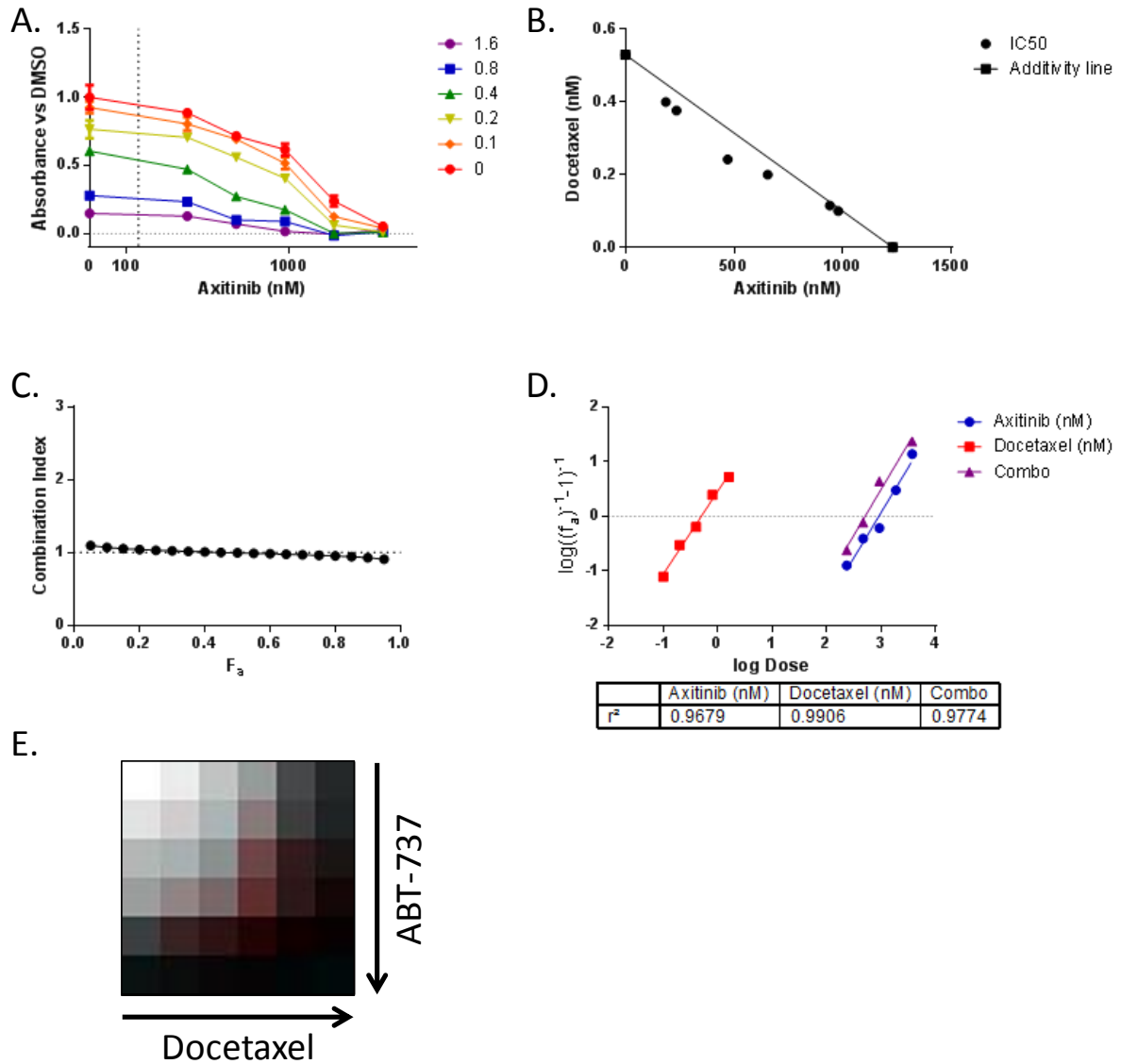


Figure 3.7. Combination of axitinib and docetaxel on GBM-L2 cells. GBM-L2 cells were treated with 1 in 2 dilutions of axitinib and docetaxel with starting concentrations of 3.76 μ M and 1.6 nM respectively. Cells were treated with the indicated concentrations and cultured for 5 days before performing an MTS cell proliferation assay. Explanation for each sub-figure can be found in the main text.

ABT-737 and Bisindolylmaleimide VIII in CSC#020

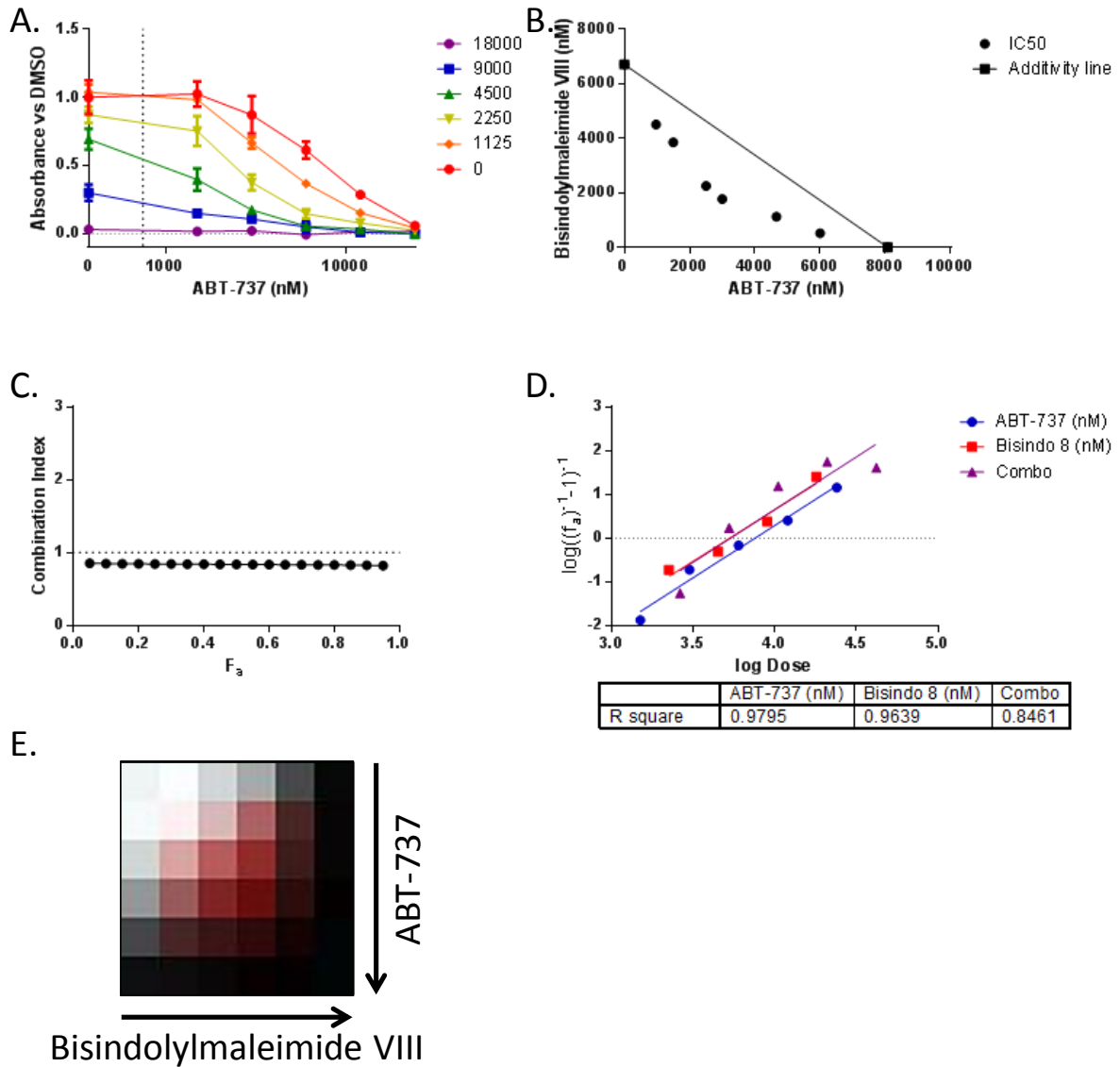


Figure 3.8. Combination of ABT-737 and bisindolylmaleimide on CSC#020 cells. CSC#020 cells were treated with 1 in 2 dilutions of ABT-737 and bisindolylmaleimide with starting concentrations of 24 μM and 18 μM respectively. Cells were treated with the indicated concentrations and cultured for 5 days before performing an MTS cell proliferation assay. Explanation for each sub-figure can be found in the main text.

Bortezomib and Salinomycin in CSC#020

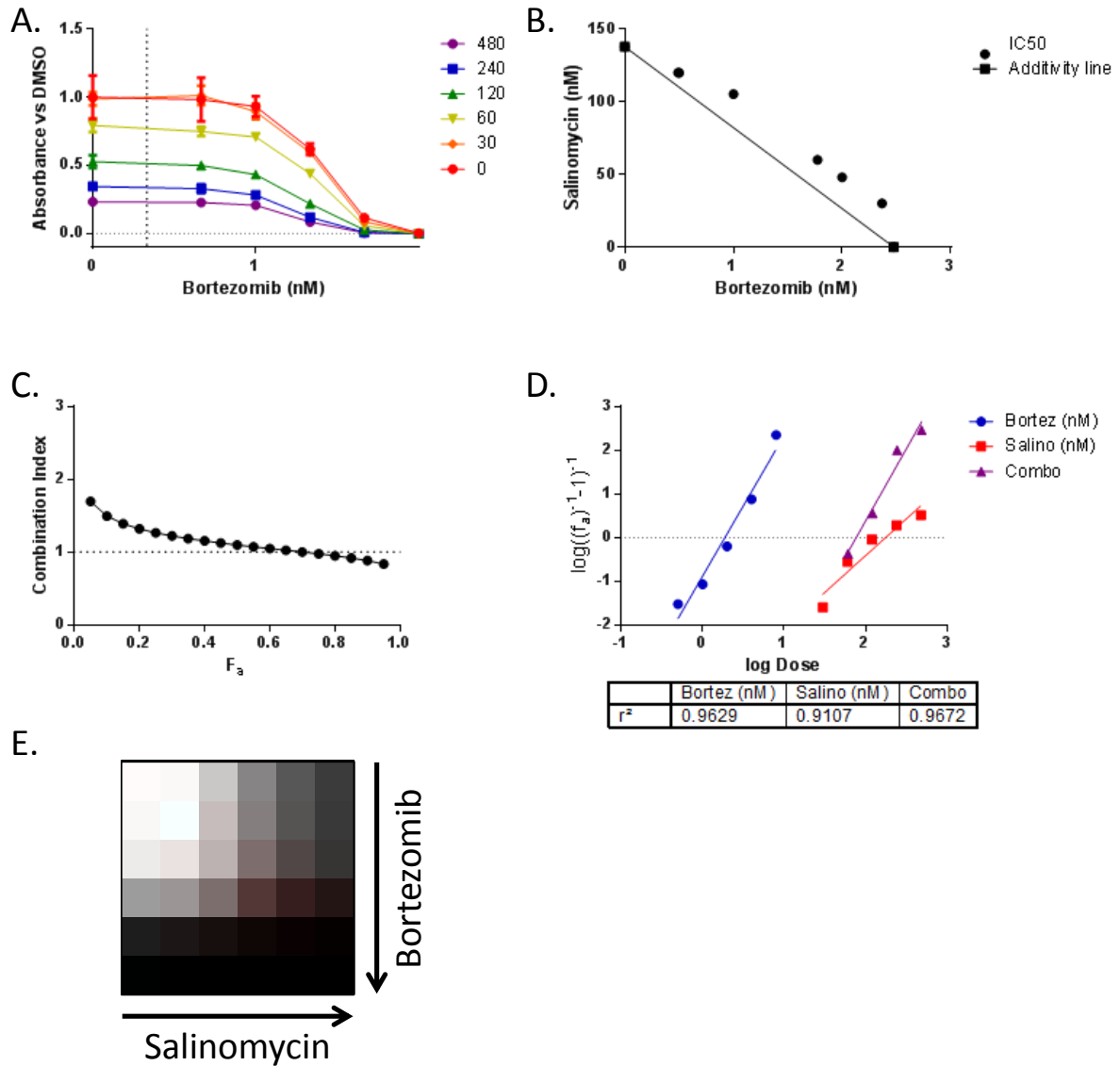


Figure 3.9. Combination of bortezomib and salinomycin on CSC#020 cells. CSC#020 cells were treated with 1 in 2 dilutions of bortezomib and salinomycin with starting concentrations of 8 nM and 480 nM respectively. Cells were treated with the indicated concentrations and cultured for 5 days before performing an MTS cell proliferation assay. Explanation for each sub-figure can be found in the main text.

Salinomycin and Docetaxel in CSC#020

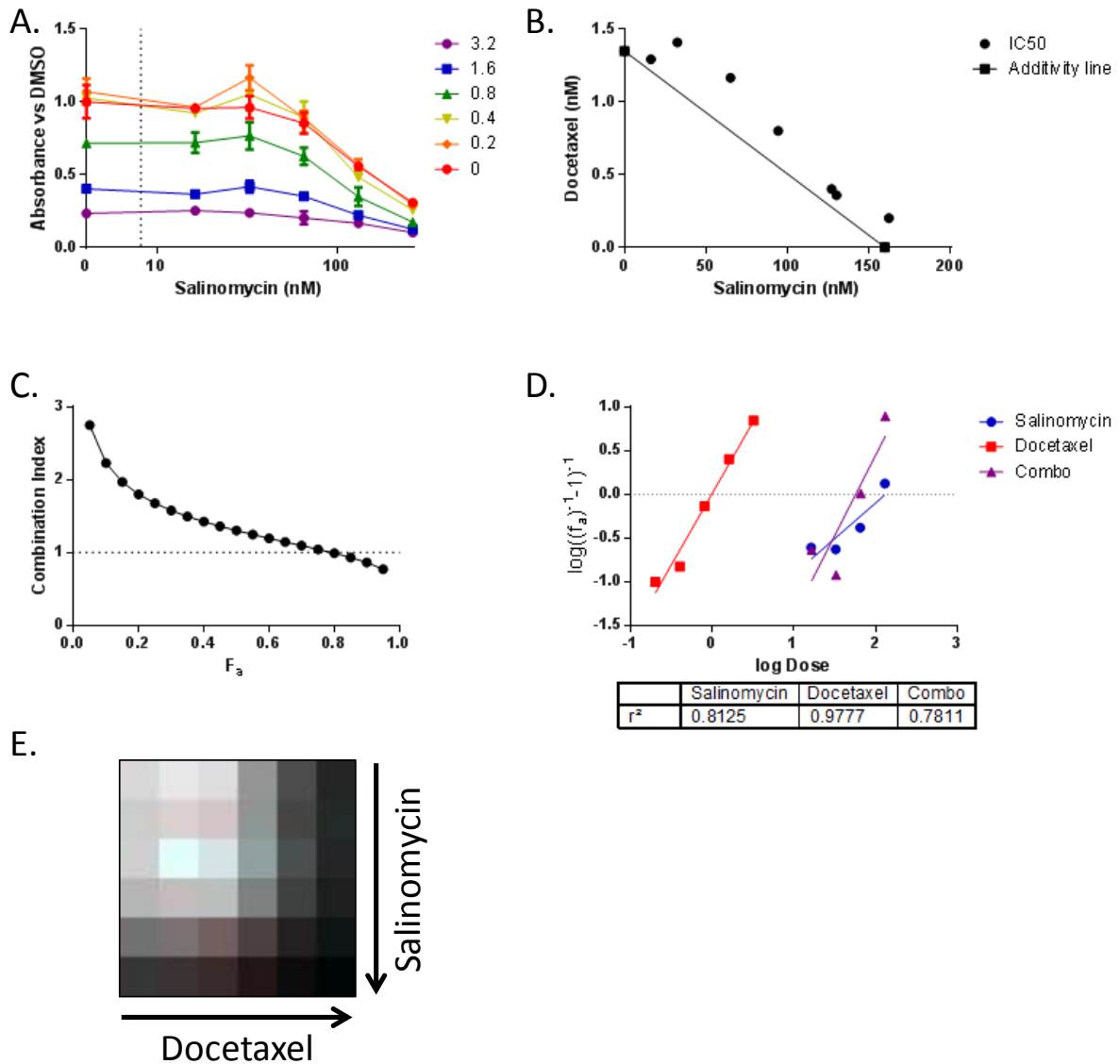


Figure 3.10. Combination of salinomycin and docetaxel on CSC#020 cells. CSC#020 cells were treated with 1 in 2 dilutions of salinomycin and docetaxel with starting concentrations of 260 nM and 3.2 nM respectively. Cells were treated with the indicated concentrations and cultured for 5 days before performing an MTS cell proliferation assay. Explanation for each sub-figure can be found in the main text.

Bortezomib and Docetaxel in CSC#020

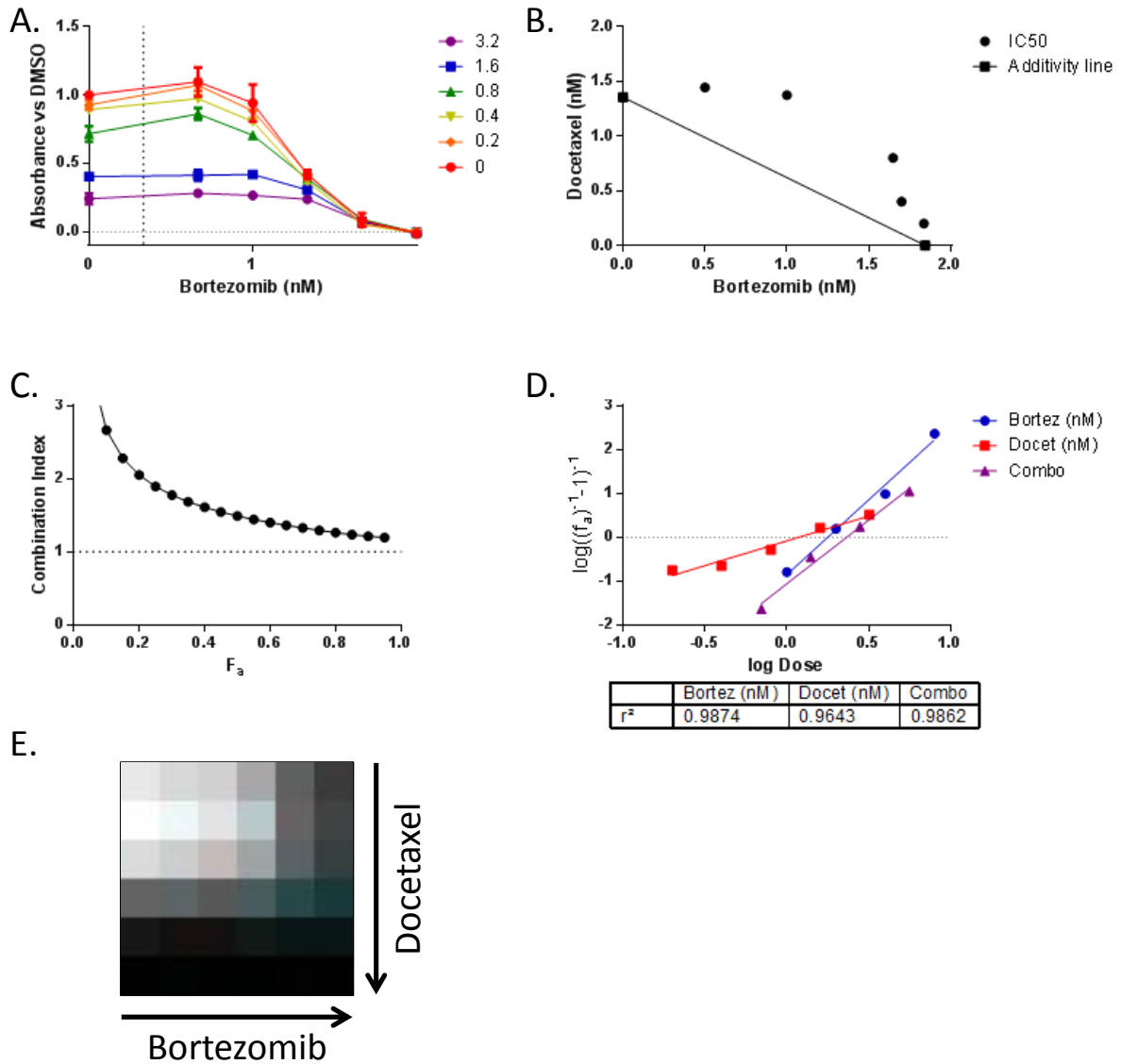


Figure 3.11. Combination of bortezomib and docetaxel on CSC#020 cells. CSC#020 cells were treated with 1 in 2 dilutions of bortezomib and docetaxel with starting concentrations of 8 nM and 3.2 nM respectively. Cells were treated with the indicated concentrations and cultured for 5 days before performing an MTS cell proliferation assay. Explanation for each sub-figure can be found in the main text.

Docetaxel and Bisindolylmaleimide VIII in CSC#020

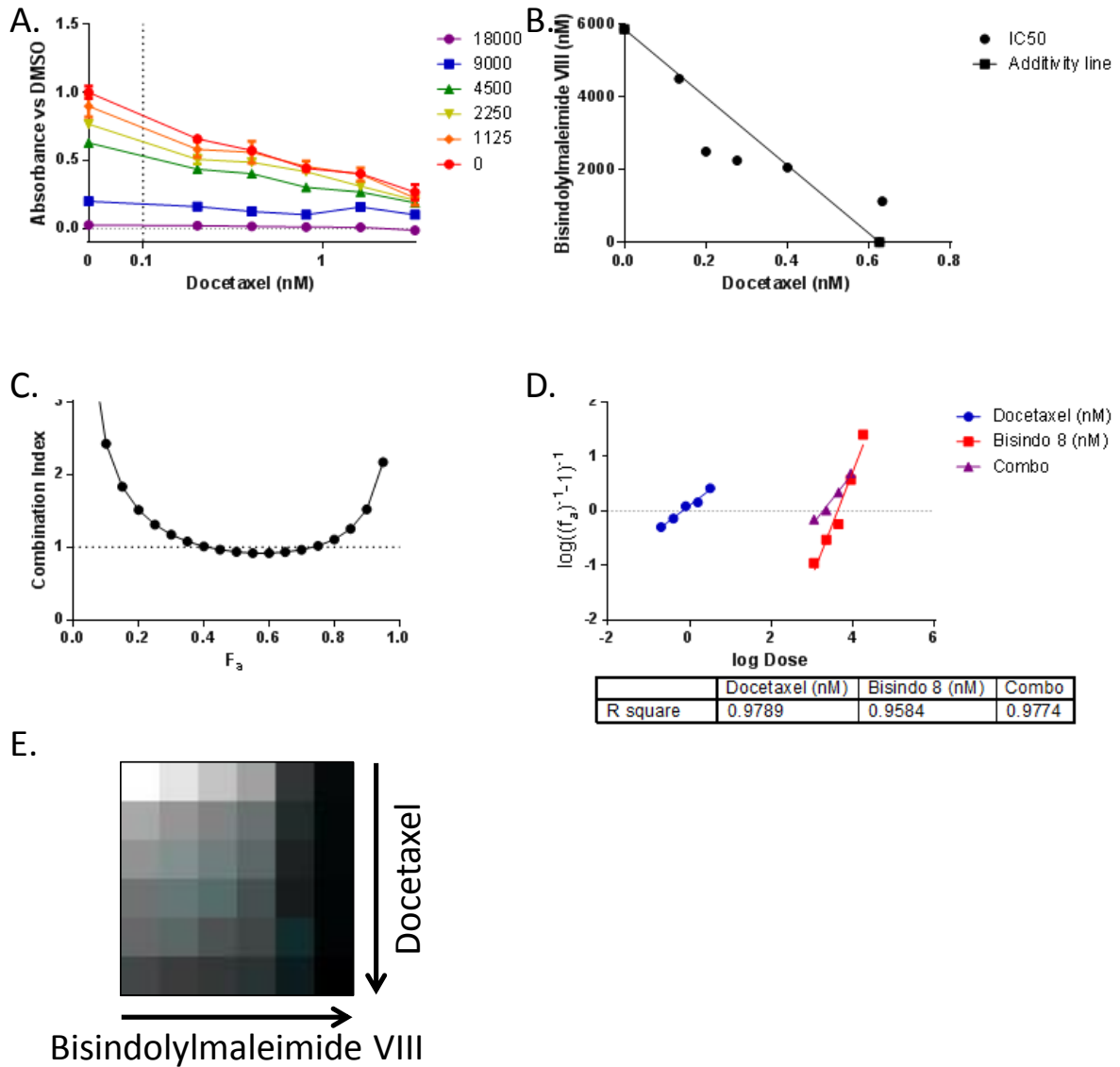


Figure 3.12. Combination of docetaxel and bisindolylmaleimide on CSC#020 cells. CSC#020 cells were treated with 1 in 2 dilutions of docetaxel and bisindolylmaleimide with starting concentrations of 3.2 nM and 18 μ M respectively. Cells were treated with the indicated concentrations and cultured for 5 days before performing an MTS cell proliferation assay. Explanation for each sub-figure can be found in the main text.

Bortezomib and Docetaxel in GBM-L2

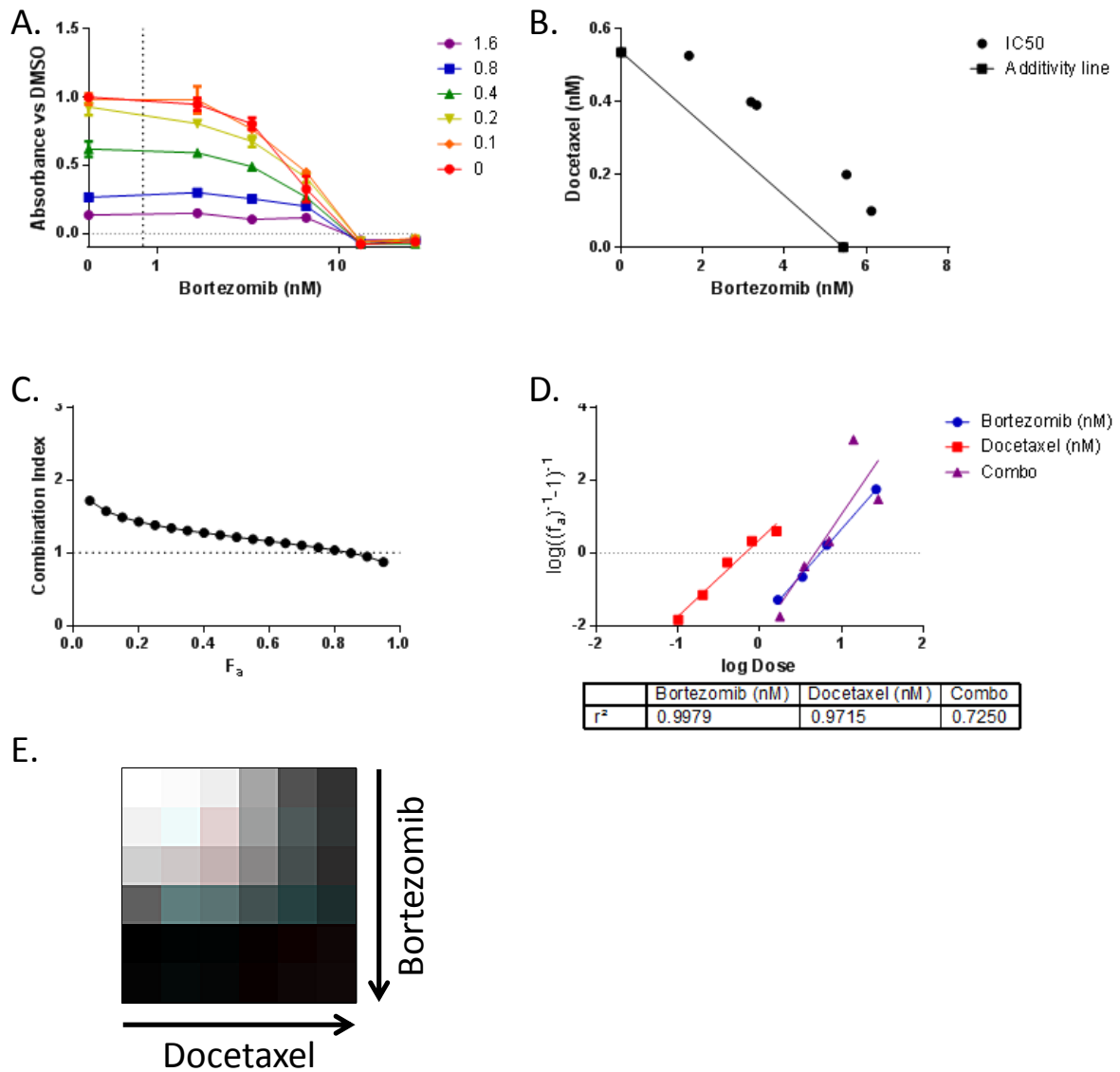


Figure 3.13. Combination of bortezomib and docetaxel on GBM-L2 cells. GBM-L2 cells were treated with 1 in 2 dilutions of bortezomib and docetaxel with starting concentrations of 26.6 nM and 1.6 nM respectively. Cells were treated with the indicated concentrations and cultured for 5 days before performing an MTS cell proliferation assay. Explanation for each sub-figure can be found in the main text.

Dasatinib and Docetaxel in GBM-L2

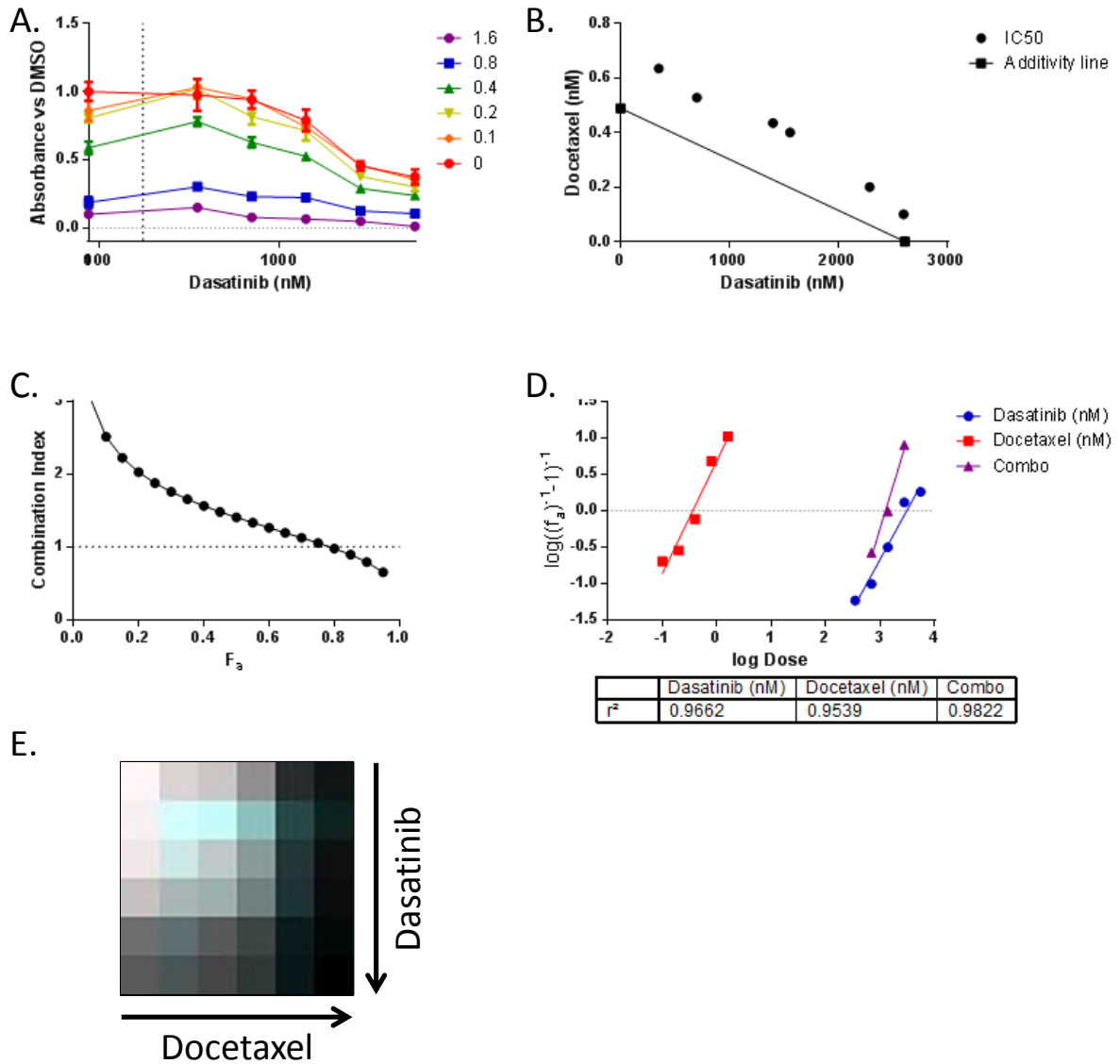


Figure 3.14. Combination of dasatinib and docetaxel on GBM-L2 cells. GBM-L2 cells were treated with 1 in 2 dilutions of dasatinib and docetaxel with starting concentrations of 5.6 μ M and 1.6 nM respectively. Cells were treated with the indicated concentrations and cultured for 5 days before performing an MTS cell proliferation assay. Explanation for each sub-figure can be found in the main text.

Bortezomib and Axitinib in GBM-L2

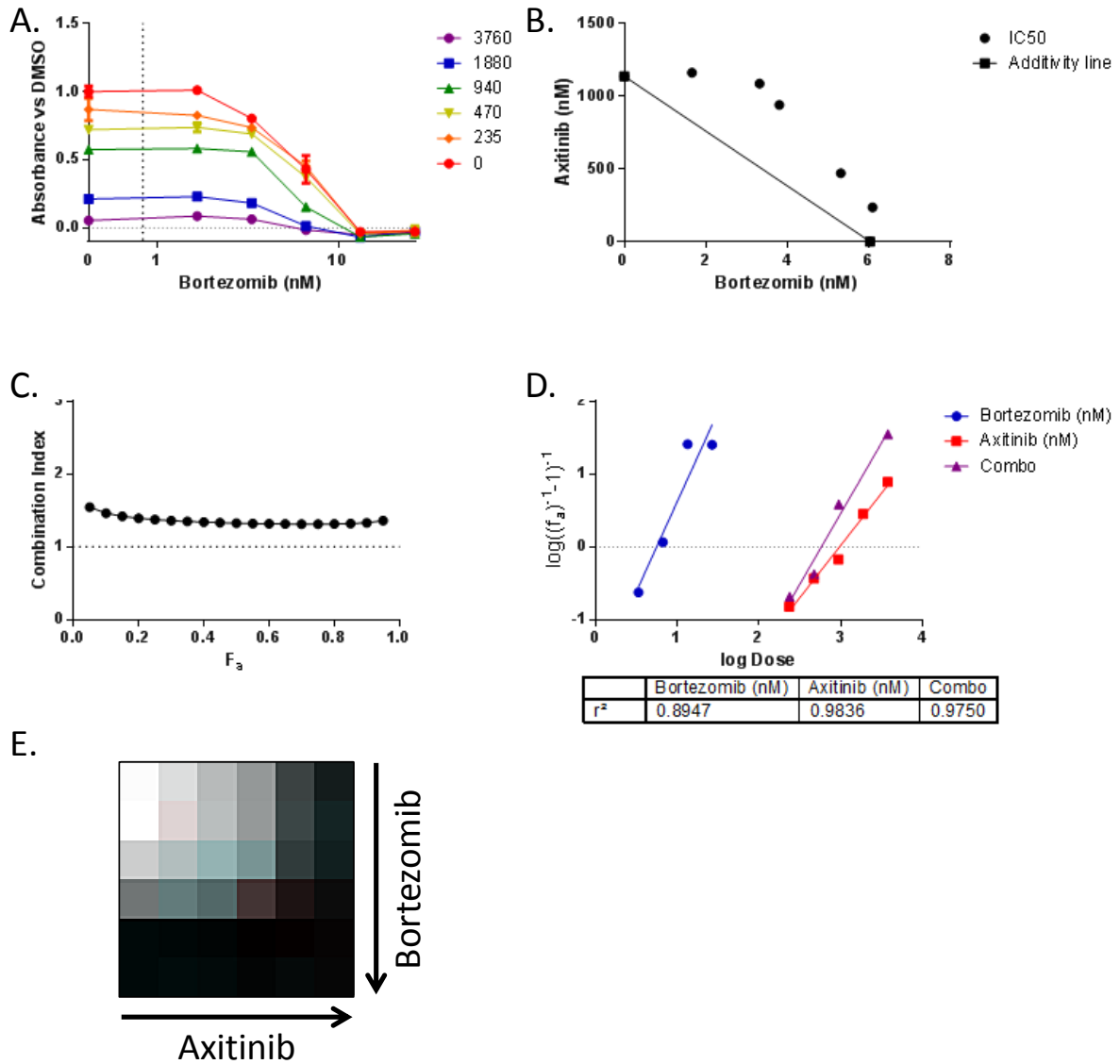


Figure 3.15. Combination of bortezomib and axitinib on GBM-L2 cells. GBM-L2 cells were treated with 1 in 2 dilutions of bortezomib and axitinib with starting concentrations of 26.6 nM and 3.76 μ M respectively. Cells were treated with the indicated concentrations and cultured for 5 days before performing an MTS cell proliferation assay. Explanation for each sub-figure can be found in the main text.

(Knick et al., 1995). The combination of taxanes and vinca alkaloids has also yielded favourable outcomes in the clinical setting for a range of cancers (Limentani et al., 2006, Pectasides et al., 2009, Miller, 1997).

Salinomycin and ABT-737

GBM-L2 cells were treated with a combination of salinomycin and ABT-737 (**Figure 3.4**). Note that while GBM-L2 cells were highly sensitive to salinomycin in the initial drug screen, these cells were insensitive to ABT-737 at 10 μ M.

As a single agent, ABT-737 caused near complete inhibition of cell survival/proliferation at 20 μ M while having little effect at 10 μ M. ABT-737 binds to the anti-apoptotic BCL-2 family members BCL-2, BCL-XL and BCL-W at high affinity ($K_i < 1$ nM) and in sensitive cancer cell lines *in vitro*, ABT-737 frequently displays IC_{50} s in the nanomolar range (Konopleva et al., 2006, Oltersdorf et al., 2005). Therefore it is reasonable to assume that the response observed at 20 μ M ABT-737 is due to off target effects.

In contrast, in the presence of each concentration of salinomycin used, GBM-L2 cells became highly sensitive to ABT-737, which caused a greater than 50% inhibition of proliferation/survival at even the lowest dose tested (1.25 μ M). The effect of ABT-737 on salinomycin treated GBM-L2 cells was biphasic, reaching a plateau below 1.25 μ M which remained relatively flat until >10 μ M. The sensitisation of GBM-L2 cells to ABT-737 by salinomycin was reflected by the isobologram, in which points deviated well below the additivity line to suggest strong synergy between the two agents. The median effects equation was a poor fit for the response of GBM-L2 to ABT-737 and the combination, not surprising considering the biphasic response that was evident in part A. Nevertheless the combination index returned an indication of synergistic response.

Because of the strong synergy of salinomycin and ABT-737 observed in GBM-L2 cells, the combination of these two agents was evaluated in two additional glioma cell lines CSC#020 (**Figure**

3.5) and GBM4 (**Figure 3.6**). Unlike the response observed in GBM-L2 cells, the combination of salinomycin and ABT-737 had only additive or weak synergistic effects as indicated by the isobolograms. The median effects equation produced a good fit of the data, and CI plots indicated synergy at higher effect levels.

Axitinib and docetaxel

GBM-L2 cells were treated with a combination of axitinib and docetaxel (**Figure 3.7**). All points of on the isobologram lay very close to the additivity line suggesting that these agents behave in an additive manner in these cells. The combination index plot also suggested an interaction very close to additivity, with CI values close to 1 for all effect levels. Dose response curves were very well represented by the median effects equation for each drug separately and in combination, suggesting a high degree of reliability of the combination index method. Bliss independence suggested that axitinib and docetaxel tended to produce a slight synergistic response at higher dosages, as indicated by the red pixels towards the bottom right, while producing a very slight antagonistic response at some lower doses, as indicated by the cyan pixels towards the top left.

ABT-737 and bisindolylmaleimide VIII

CSC#020 cells were treated with a combination of ABT-737 and bisindolylmaleimide VIII (**Figure 3.8**). A synergistic response was clearly evident by both isobologram and bliss independence based analysis. The CI plot also suggested a modest synergistic effect however the median effects equation produced a poor fit for the combination dose response as indicated by the low r^2 value. This suggests that the combination index is not a reliable indicator of synergy in this particular combination.

Bortezomib and salinomycin

CSC#020 cells were treated with a combination of bortezomib and salinomycin (**Figure 3.9**). Both the isobologram and combination index plot suggested slight antagonism of this combination in these cells. Conversely Bliss independence suggested very slight synergy.

Remaining combinations

The results of the remaining combinations are shown in **figures 3.10 through 3.15**. These combinations produced predominantly antagonistic responses as demonstrated by IC₅₀ points lying above the additivity line on isobologram plots, CI values greater than 1 on combination index plots and cyan pixels in the Bliss independence analysis.

The data from **figures 3.3 to 3.15** are summarised in (**Table 3.3**). Using each of the three analysis methods, the interaction of each combination was evaluated as synergistic, additive or antagonistic. Where the nature of the combination was ambiguous, the interaction was described as 'mixed'.

Discussion

For the initial drug screen, an array of 24 drugs was screened against a panel of six glioma cell lines. With such a small number of drugs screened, this study was not designed to identify potentially novel therapeutic agents for the treatment of glioblastoma, but to explore the applicability of various combination approaches for the identification of synergistic interactions.

For a small number of compounds, a highly variable response rate was observed across the six cell lines. For example GBM-L1, GBM-L3 and GBM4 were responsive to ABT-737 while GBM-L2, CSC#014 and CSC#020 were not. Resistance to ABT-737 is known to be heavily influenced by expression of the pro-survival Bcl2 family members Mcl1 and A1. Therefore one could reasonably expect that expression levels of these two proteins would be elevated in GBM-L2, CSC#014 and CSC#020. Similarly erlotinib more potently inhibited proliferation in GBM-L2 and CSC#020 than the other cell lines. One could anticipate that these two cell lines may have higher expression or activation of EGFR resulting in their dependence on this receptor. Alternatively, EGFR levels could be similar, with resistance to erlotinib mediated through any number of mechanisms.. With only six cell lines used in this study, an analysis of protein levels as biomarkers of sensitivity would be severely underpowered to come to any meaningful conclusions.

Cell line	Drug A	Drug B	Isobologram	Combination Index	Bliss independence
GBM-L2	Docetaxel	Vinblastine	Synergistic	Synergistic	Synergistic
	Docetaxel	Axitinib	Additive	Additive	Mixed
	Docetaxel	Bortezomib	Antagonistic	Antagonistic	Mixed
	Docetaxel	Dasatinib	Antagonistic	Antagonistic	Antagonistic
	Axitinib	Bortezomib	Antagonistic	Antagonistic	Antagonistic
	Salinomycin	ABT-737	Synergistic	Synergistic	Synergistic
CSC#020	Docetaxel	Bisindolylmaleimide	Additive	Mixed	Antagonistic
	Docetaxel	Bortezomib	Antagonistic	Antagonistic	Antagonistic
	Docetaxel	Salinomycin	Antagonistic	Antagonistic	Antagonistic
	Salinomycin	Bortezomib	Antagonistic	Antagonistic	Synergistic
	Bisindolylmaleimide	ABT-737	Synergistic	Synergistic	Synergistic
	Salinomycin	ABT-737	Additive	Mixed	Synergistic
GBM4	Salinomycin	ABT-737	Synergistic	Mixed	Synergistic

Table 3.3 Summary of Drug Interactions. The interaction of each drug combination shown in figures 3.3 to 3.15 was evaluated using the isobologram, combination index and Bliss independence approaches. Interactions were determined to be synergistic, antagonistic or additive. Where the conclusion is ambiguous, the interaction was reported as mixed.

Compounds such as bisindolylmaleimide VIII, bortezomib and salinomycin potently eliminated survival and proliferation in all six cell lines, highlighting their potential as therapeutic agents in GBM. However a major drawback of this study was the absence of a control 'normal' cell line such as human astrocytes with which a comparison can be made. Without such a control, one could reasonably assert that these compounds are likely cytotoxic to normal and glioma cells alike and therefore have not applicability as therapeutic agents in glioma.

In order to perform combination studies, it was first necessary to determine the IC_{50} values of each compound to be tested. Few of the compounds produced a dose response curve that could have been accurately represented by the median effects equation. For this reason, curve fitting methods were not used for determination of IC_{50} . Rather IC_{50} was calculated as a weighted average of the two drug concentrations that lay on either side of a 50% effect level. This technique was also used in subsequent analyses of drug combinations when applying the isobologram method.

Combinations of treatments were set up in a checkerboard configuration with each drug concentration ranging from $4 \times IC_{50}$ to $\frac{1}{4} \times IC_{50}$. This format allowed the same set of data to be analysed using three distinct methods; the isobologram (Loewe additivity), combination index and Bliss independence. In most instances, there was generally agreement between each of the three methods as to whether an interaction was synergistic or antagonistic. Only one case (bortezomib and salinomycin in CSC#020 cells) resulted in conflicting conclusions, with isobologram and combination index methods demonstrating antagonism while Bliss independence demonstrating synergy. However the degree of synergy or antagonism was modest and very close to additive.

The identification of highly synergistic interactions is of high interest in the field of cancer biology. It is well recognised that single agent therapy is unlikely to be effective, particularly in genetically and biologically complex cancers such as glioblastoma. The combination index method is

the most widely used approach for demonstrating synergistic interactions of two agents, and many of these synergistic interactions have been far more profound than the synergistic interactions identified here. A strongly synergistic (or antagonistic) interaction would most likely be recognisable as synergistic (or antagonistic) regardless of the approach used. A comparison of the methods is only of significance when approaching the boundary condition, i.e. when the interaction is very close to additive.

Two agents can be said to behave in an additive manner when their effect in combination is the same as that predicted by the reference model. How far does the observed effect need to deviate from the predicted effect in order for the null hypothesis (an additive interaction) to be rejected? Values on CI plots greater or less than 1 indicate antagonism or synergy respectively. However the combination index method described by (Chou and Talalay, 1984) lacks any statistical measure of the uncertainty of the CI plot, precluding one from testing for statistical significance. The isobologram also suffers from a similar shortfall as there is no defined measure of uncertainty, precluding statistical evaluation.

Statistical methods can be used when using the Bliss independence approach. When the mean and standard deviation of effects of individual drugs is known, the standard deviation of the predicted combined effect can also be determined. From there, a confidence interval (such as 95%) of the predicted effect can be determined. If the observed combination effect falls outside these bounds, the null hypothesis is rejected and a conclusion of synergy or antagonism can be made. While this statistical testing was not performed in this chapter, such an approach was used in Chapter 5, Figure 5.5.

Each of the three approaches used here reached largely the same conclusion for each combination tested. With perhaps only the exception of ABT-737 and salinomycin in GBM-L2, no combination produced a synergistic effect that was particularly striking, and would not warrant further investigation.

The finding that most combinations only results in predominantly antagonistic or additive effects weighs in favour of evaluating combinations in this fashion. If we assume that only a small fraction of treatment modalities that work *in vitro* will also work *in vivo*, only combinations that produce remarkably potent synergy *in vitro* should be pursued further. Such potent synergy will be clearly evident regardless of the method used to assess synergy. Ultimately, it is a matter of personal choice as to which method is used.

References

- BERMAN, D. M., KARHADKAR, S. S., HALLAHAN, A. R., PRITCHARD, J. I., EBERHART, C. G., WATKINS, D. N., CHEN, J. K., COOPER, M. K., TAIPALE, J., OLSON, J. M. & BEACHY, P. A. 2002. Medulloblastoma growth inhibition by hedgehog pathway blockade. *Science*, 297, 1559-61.
- CHOU, T. C. & TALALAY, P. 1984. Quantitative analysis of dose-effect relationships: the combined effects of multiple drugs or enzyme inhibitors. *Adv Enzyme Regul*, 22, 27-55.
- CRAWFORD, T. Q. & ROELINK, H. 2007. The notch response inhibitor DAPT enhances neuronal differentiation in embryonic stem cell-derived embryoid bodies independently of sonic hedgehog signaling. *Dev Dyn*, 236, 886-92.
- ESCUDIER, B., EISEN, T., STADLER, W. M., SZCZYLIK, C., OUDARD, S., SIEBELS, M., NEGRIER, S., CHEVREAU, C., SOLSKA, E., DESAI, A. A., ROLLAND, F., DEMKOW, T., HUTSON, T. E., GORE, M., FREEMAN, S., SCHWARTZ, B., SHAN, M., SIMANTOV, R. & BUKOWSKI, R. M. 2007. Sorafenib in advanced clear-cell renal-cell carcinoma. *N Engl J Med*, 356, 125-34.
- GANDHI, L., CAMIDGE, D. R., RIBEIRO DE OLIVEIRA, M., BONOMI, P., GANDARA, D., KHAIRA, D., HANN, C. L., MCKEEGAN, E. M., LITVINOVICH, E., HEMKEN, P. M., DIVE, C., ENSCHEDE, S. H., NOLAN, C., CHIU, Y. L., BUSMAN, T., XIONG, H., KRIVOSHIK, A. P., HUMERICKHOUSE, R., SHAPIRO, G. I. & RUDIN, C. M. 2011. Phase I study of Navitoclax (ABT-263), a novel Bcl-2 family inhibitor, in patients with small-cell lung cancer and other solid tumors. *J Clin Oncol*, 29, 909-16.
- GEYER, C. E., FORSTER, J., LINDQUIST, D., CHAN, S., ROMIEU, C. G., PIENKOWSKI, T., JAGIELLO-GRUSZFELD, A., CROWN, J., CHAN, A., KAUFMAN, B., SKARLOS, D., CAMPONE, M., DAVIDSON, N., BERGER, M., OLIVA, C., RUBIN, S. D., STEIN, S. & CAMERON, D. 2006. Lapatinib plus capecitabine for HER2-positive advanced breast cancer. *N Engl J Med*, 355, 2733-43.
- GUPTA, P. B., ONDER, T. T., JIANG, G., TAO, K., KUPERWASSER, C., WEINBERG, R. A. & LANDER, E. S. 2009. Identification of selective inhibitors of cancer stem cells by high-throughput screening. *Cell*, 138, 645-59.
- JORDAN, A., HADFIELD, J. A., LAWRENCE, N. J. & MCGOWN, A. T. 1998. Tubulin as a target for anticancer drugs: agents which interact with the mitotic spindle. *Med Res Rev*, 18, 259-96.
- KNICK, V. C., EBERWEIN, D. J. & MILLER, C. G. 1995. Vinorelbine tartrate and paclitaxel combinations: enhanced activity against *in vivo* P388 murine leukemia cells. *J Natl Cancer Inst*, 87, 1072-7.
- KONOPLEVA, M., CONTRACTOR, R., TSAO, T., SAMUDIO, I., RUVOLO, P. P., KITADA, S., DENG, X., ZHAI, D., SHI, Y. X., SNEED, T., VERHAEGEN, M., SOENGAS, M., RUVOLO, V. R., MCQUEEN, T., SCHOBER, W. D., WATT, J. C., JIFFAR, T., LING, X., MARINI, F. C., HARRIS, D., DIETRICH, M., ESTROV, Z., MCCUBREY, J., MAY, W. S., REED, J. C. & ANDREEFF, M. 2006. Mechanisms of apoptosis sensitivity and resistance to the BH3 mimetic ABT-737 in acute myeloid leukemia. *Cancer Cell*, 10, 375-88.

- LIMENTANI, S. A., BRUFISKY, A. M., ERBAN, J. K., JAHANZEB, M. & LEWIS, D. 2006. Phase II study of neoadjuvant docetaxel/ vinorelbine followed by surgery and adjuvant doxorubicin/cyclophosphamide in women with stage II/III breast cancer. *Clin Breast Cancer*, 6, 511-7.
- LLOVET, J. M., RICCI, S., MAZZAFERRO, V., HILGARD, P., GANE, E., BLANC, J. F., DE OLIVEIRA, A. C., SANTORO, A., RAOUL, J. L., FORNER, A., SCHWARTZ, M., PORTA, C., ZEUZEM, S., BOLONDI, L., GRETEN, T. F., GALLE, P. R., SEITZ, J. F., BORBATH, I., HAUSSINGER, D., GIANNARIS, T., SHAN, M., MOSCOVICI, M., VOLIOTIS, D. & BRUIX, J. 2008. Sorafenib in advanced hepatocellular carcinoma. *N Engl J Med*, 359, 378-90.
- LONGLEY, D. B., HARKIN, D. P. & JOHNSTON, P. G. 2003. 5-fluorouracil: mechanisms of action and clinical strategies. *Nat Rev Cancer*, 3, 330-8.
- MILLER, V. A. 1997. Docetaxel (Taxotere) and vinorelbine in the treatment of advanced non-small cell lung cancer: preliminary results of a phase I/II trial. *Semin Oncol*, 24, S14-15-S14-17.
- MONTERO, A., FOSSELLA, F., HORTOBAGYI, G. & VALERO, V. 2005. Docetaxel for treatment of solid tumours: a systematic review of clinical data. *Lancet Oncol*, 6, 229-39.
- MURATA, K., KAMEYAMA, M., FUKUI, F., OHIGASHI, H., HIRATSUKA, M., SASAKI, Y., KABUTO, T., MUKAI, M., MAMMOTO, T., AKEDO, H., ISHIKAWA, O. & IMAOKA, S. 1999. Phosphodiesterase type III inhibitor, cilostazol, inhibits colon cancer cell motility. *Clin Exp Metastasis*, 17, 525-30.
- OLTERSODORF, T., ELMORE, S. W., SHOEMAKER, A. R., ARMSTRONG, R. C., AUGERI, D. J., BELLI, B. A., BRUNCKO, M., DECKWERTH, T. L., DINGES, J., HAJDUK, P. J., JOSEPH, M. K., KITADA, S., KORSMEYER, S. J., KUNZER, A. R., LETAI, A., LI, C., MITTEN, M. J., NETTESHEIM, D. G., NG, S., NIMMER, P. M., O'CONNOR, J. M., OLEKSIJEV, A., PETROS, A. M., REED, J. C., SHEN, W., TAHIR, S. K., THOMPSON, C. B., TOMASELLI, K. J., WANG, B., WENDT, M. D., ZHANG, H., FESIK, S. W. & ROSENBERG, S. H. 2005. An inhibitor of Bcl-2 family proteins induces regression of solid tumours. *Nature*, 435, 677-81.
- OTTMANN, O., DOMBRET, H., MARTINELLI, G., SIMONSSON, B., GUILHOT, F., LARSON, R. A., REGE-CAMBRIN, G., RADICH, J., HOCHHAUS, A., APANOVITCH, A. M., GOLLERKERI, A. & COUTRE, S. 2007. Dasatinib induces rapid hematologic and cytogenetic responses in adult patients with Philadelphia chromosome positive acute lymphoblastic leukemia with resistance or intolerance to imatinib: interim results of a phase 2 study. *Blood*, 110, 2309-15.
- PECTASIDES, D., PECTASIDES, E., PAPAXOINIS, G., KOUMARIANOU, A., PSYRRI, A., XIROS, N., TOUNTAS, N., KAMPOSIORAS, K., PAPATSIBAS, G., FLOROS, T., GOUVERIS, P., KARAGEORGOPOULOU, S. & ECONOMOPOULOS, T. 2009. Combination chemotherapy with docetaxel, vinorelbine and estramustine phosphate in metastatic androgen-resistant prostate cancer: a single institution experience. *Anticancer Res*, 29, 769-75.
- PHOTIOU, A., SHAH, P., LEONG, L. K., MOSS, J. & RETSAS, S. 1997. In vitro synergy of paclitaxel (Taxol) and vinorelbine (navelbine) against human melanoma cell lines. *Eur J Cancer*, 33, 463-70.
- RICCIONI, R., DUPUIS, M. L., BERNABELI, M., PETRUCCI, E., PASQUINI, L., MARIANI, G., CIANFRIGLIA, M. & TESTA, U. 2010. The cancer stem cell selective inhibitor salinomycin is a p-glycoprotein inhibitor. *Blood Cells Mol Dis*, 45, 86-92.
- ROUGIER, P., LAPLANCHE, A., HUGUIER, M., HAY, J. M., OLLIVIER, J. M., ESCAT, J., SALMON, R., JULIEN, M., ROULLET AUDY, J. C., GALLOT, D. & ET AL. 1992. Hepatic arterial infusion of floxuridine in patients with liver metastases from colorectal carcinoma: long-term results of a prospective randomized trial. *J Clin Oncol*, 10, 1112-8.
- RUDIN, C. M., HANN, C. L., LATERRA, J., YAUCH, R. L., CALLAHAN, C. A., FU, L., HOLCOMB, T., STINSON, J., GOULD, S. E., COLEMAN, B., LORUSSO, P. M., VON HOFF, D. D., DE SAUVAGE, F. J. & LOW, J. A. 2009. Treatment of medulloblastoma with hedgehog pathway inhibitor GDC-0449. *N Engl J Med*, 361, 1173-8.
- SAN MIGUEL, J. F., SCHLAG, R., KHUAGEVA, N. K., DIMOPOULOS, M. A., SHPILBERG, O., KROPFF, M., SPICKA, I., PETRUCCI, M. T., PALUMBO, A., SAMOILOVA, O. S., DMOSZYNSKA, A.,

- ABDULKADYROV, K. M., SCHOTS, R., JIANG, B., MATEOS, M. V., ANDERSON, K. C., ESSELTINE, D. L., LIU, K., CAKANA, A., VAN DE VELDE, H. & RICHARDSON, P. G. 2008. Bortezomib plus melphalan and prednisone for initial treatment of multiple myeloma. *N Engl J Med*, 359, 906-17.
- SARKARIA, J. N., GALANIS, E., WU, W., DIETZ, A. B., KAUFMANN, T. J., GUSTAFSON, M. P., BROWN, P. D., UHM, J. H., RAO, R. D., DOYLE, L., GIANNINI, C., JAECKLE, K. A. & BUCKNER, J. C. 2010. Combination of temsirolimus (CCI-779) with chemoradiation in newly diagnosed glioblastoma multiforme (GBM) (NCCTG trial N027D) is associated with increased infectious risks. *Clin Cancer Res*, 16, 5573-80.
- SATTLER, M., PRIDE, Y. B., MA, P., GRAMLICH, J. L., CHU, S. C., QUINNAN, L. A., SHIRAZIAN, S., LIANG, C., PODAR, K., CHRISTENSEN, J. G. & SALGIA, R. 2003. A novel small molecule met inhibitor induces apoptosis in cells transformed by the oncogenic TPR-MET tyrosine kinase. *Cancer Res*, 63, 5462-9.
- SCHELLHAMMER, P. F. 2002. An evaluation of bicalutamide in the treatment of prostate cancer. *Expert Opin Pharmacother*, 3, 1313-28.
- SEIDENFELD, J., SAMSON, D. J., HASSELBLAD, V., ARONSON, N., ALBERTSEN, P. C., BENNETT, C. L. & WILT, T. J. 2000. Single-therapy androgen suppression in men with advanced prostate cancer: a systematic review and meta-analysis. *Ann Intern Med*, 132, 566-77.
- SHEPHERD, F. A., RODRIGUES PEREIRA, J., CIULEANU, T., TAN, E. H., HIRSH, V., THONGPRASERT, S., CAMPOS, D., MAOLEEKOONPIROJ, S., SMYLLIE, M., MARTINS, R., VAN KOOTEN, M., DEDIU, M., FINDLAY, B., TU, D., JOHNSTON, D., BEZJAK, A., CLARK, G., SANTABARBARA, P. & SEYMOUR, L. 2005. Erlotinib in previously treated non-small-cell lung cancer. *N Engl J Med*, 353, 123-32.
- STERNBERG, C. N., DAVIS, I. D., MARDIAK, J., SZCZYLIK, C., LEE, E., WAGSTAFF, J., BARRIOS, C. H., SALMAN, P., GLADKOV, O. A., KAVINA, A., ZARBA, J. J., CHEN, M., MCCANN, L., PANDITE, L., ROYCHOWDHURY, D. F. & HAWKINS, R. E. 2010. Pazopanib in locally advanced or metastatic renal cell carcinoma: results of a randomized phase III trial. *J Clin Oncol*, 28, 1061-8.
- WARRELL, R. P., JR., FRANKEL, S. R., MILLER, W. H., JR., SCHEINBERG, D. A., ITRI, L. M., HITTELMAN, W. N., VYAS, R., ANDREEFF, M., TAFURI, A., JAKUBOWSKI, A. & ET AL. 1991. Differentiation therapy of acute promyelocytic leukemia with tretinoin (all-trans-retinoic acid). *N Engl J Med*, 324, 1385-93.

Chapter 4 - Regulation of Pyruvate Kinase in Glioma

Table of Figures	144
Introduction.....	145
Results	148
PKM2 tetramer formation and activity is influenced by glucose concentration.....	150
Effect of 2-deoxyglucose and WAY677099 on PEP concentration.....	151
PKM2 tetramer formation is regulated during the cell cycle	153
Effect of glucose concentration and WAY677099 on the glycolytic rate	157
Effects of glucose concentration and WAY677099 on respiration	159
Glioma cells exhibit the Crabtree effect	161
Uncoupled mitochondrial respiration promotes oxidation, dimerisation and inhibition of PKM2	165
Effect of WAY677099 on NADPH levels	168
Resistance to oxidative stress.....	170
Discussion	172
References.....	177

Table of Figures

Figure 4.1. Hypothesis for sensitisation of cancer cells to oxidative using a PKM2 activator.....	149
Figure 4.2. Dependence of glucose concentration on PKM2 tetramer formation and pyruvate kinase activity.	150
Figure 4.3. Effect of WAY677099 on PKM2 tetramer formation and PK activity.	152
Figure 4.4. Effect of 2-deoxyglucose and WAY677099 on intracellular phosphoenolpyruvate.	153
Figure 4.5. Effect of cell density on PKM2 tetramer formation and pyruvate kinase activity.	154
Figure 4.6. PKM2 tetramer formation in cell synchronised U87MG cells.	156
Figure 4.7. WAY677099 does not affect cell cycle or proliferation of glioma cells.	157
Figure 4.8. PKM2 activation increases glycolytic rate in some HCC cell lines.	158
Figure 4.9. Effect of WAY677099 on the glycolytic rate of glioma cells.	159
Figure 4.10. PKM2 activation suppresses oxygen consumption rate in HCC cell lines.....	160
Figure 4.11. 'Crabtree effect' hypothesis for suppression of respiration by WAY677099.	161
Figure 4.12. Effect of WAY677099 on mitochondrial function in glioma cells.	162
Figure 4.13. Effect of glucose on coupled and uncoupled respiration.	163
Figure 4.14. Suppression of respiration induced by WAY677099.	164
Figure 4.15. Redox feedback loop hypothesis for suppression of respiration by WAY677099.....	166
Figure 4.16. Oxidation and inhibition of PKM2 in FCCP treated U87MG cells.	167
Figure 4.17. Diamide disrupts NADPH/NADPt levels under reduced glucose conditions.	169
Figure 4.18. WAY677099 does not affect NADPH/NADPt levels in response to diamide.	170
Figure 4.19. WAY677099 does not increase sensitivity to diamide induced cell death.	171
Table 4.1. Factors promoting PKM2 dimer or tetramer formation in U87MG cells.....	176

Introduction

The metabolism of tumours is dramatically different to that of normal tissue. The field of cancer metabolism began in the early 20th century with the pioneering work of Otto Warburg who showed that cancer cells preferentially derive energy from glycolysis rather than respiration even in the presence of oxygen (a phenomenon termed 'aerobic glycolysis' or the 'Warburg effect'). The field of cancer metabolism has experienced a resurgence of interest in recent years. More recently, the glycolytic enzyme pyruvate kinase M2 has received an increasing amount of attention in the cancer metabolism field.

Glucose is a nutrient essential for proliferation of mammalian cells and as such, proliferating cells have high rates of glucose consumption. Many anabolic processes rely on glucose derived precursors as a source of carbon (such as serine, folate and ribose sugar synthesis) and as a source of reducing power (i.e. NADPH regeneration via the pentose phosphate pathway) required for a range of anabolic processes. Despite these important functions, the vast majority of glucose consumed by proliferating cells, including cancer cells is metabolised via glycolysis to pyruvate, supplying neither anabolic carbon nor NADPH, providing only a source energy for regeneration of ATP. Rather than being oxidised via mitochondrial respiration, this pyruvate is then reduced to lactate and excreted from the cell. As such, proliferating cells derive most of their energy from glycolysis rather than respiration (Lunt and Vander Heiden, 2011).

As discussed in depth in Chapter 1, no theory has yet convincingly described why proliferating cells engage in aerobic glycolysis; however its ubiquity amongst proliferating cells and particularly cancer cells implies its importance.

Pyruvate kinase catalyses the final reaction of the glycolytic pathway, transferring the high energy phosphate group of phosphoenolpyruvate (PEP) to ADP, yielding ATP and pyruvate. Activity of the M2 isoform of pyruvate kinase, unlike that of the constitutively active M1, is dynamically

regulated and the isozyme is able to associate and dissociate into high PEP affinity tetramers to the low PEP affinity dimers in response to a range of cellular cues (Yang and Lu, 2013).

Most adult cells express PKM2, except for muscle fibres and neurons (which express the PKM1) and erythrocytes (which express PK-R). Gluconeogenic cells such as the parenchymal cells of the liver express predominantly PK-L which is subject to distinct mechanisms of regulation from PKM2 (Trempe et al., 1989). It is frequently claimed that PKM2 expression is largely restricted to embryonic tissue and highly proliferating cells, while most adult tissues express PKM1 and that carcinogenesis frequently involves a reversion back to expression of PKM2 in tumour cells (Lv et al., 2011, Christofk et al., 2008). However these claims are counter to almost all historical and modern experimental evidence demonstrating that PKM2 is the predominant isoform expressed in most adult tissues and that cells do not switch pyruvate kinase isoforms during carcinogenesis (Desai et al., 2013, Bluemlein et al., 2011, Ibsen et al., 1982, Reinacher et al., 1986).

Nevertheless, tumour cells and other cell types entering the cell cycle have dramatically increased expression of PKM2 and other glycolytic enzymes. This suggests a requirement for high enzyme activity of glycolytic enzymes, including pyruvate kinase. However the capacity to down-regulate pyruvate kinase activity is also critical. Cancer cells engineered to express the constitutively active PKM1 rather than PKM2 that are unable to grow *in vivo* or resist environmental stressors such as hypoxia or oxidative stress (Christofk et al., 2008). Similarly, expression of engineered PKM2 mutants that are resistant to environmental cues that would normally inhibit PKM2 activity produces a similar outcome (Anastasiou et al., 2011). Paradoxically, expression of PKM2 with low catalytic activity (relative to PKM1) appears to be involved in directing pyruvate away from mitochondrial respiration and thus promoting the Warburg effect (Christofk et al., 2008).

Observation of high PKM2 expression in proliferating and cancer cells, and the loss of tumourigenicity imparted by PKM1 expression suggest that proliferating cells require the capacity for high pyruvate kinase activity, but also the capacity for down-regulation. Following from this, both

small molecule PKM2 activators and inhibitors have the potential to perturb cancer cell metabolism to produce a therapeutic effect. Even while the function of aerobic glycolysis in cancer cells remains enigmatic, it is plausible that its paradoxical reversal by a PKM2 activator (as proposed by some (Lv et al., 2011)) could lead to an anti-tumour response.

Chronic metabolic stresses encountered by tumour cells *in vivo* including hypoxia and nutrient insufficiency, high levels of oxidative stress as well as hyper-activation of receptor tyrosine kinase signalling have all been shown to inhibit PKM2 activity (Anastasiou et al., 2011, Hitosugi et al., 2009). While expression of PKM2 *per se* is absolutely not cancer specific, predominantly dimeric PKM2 is a feature of tumour cells. This suggests that PKM2 activators may be selectively disrupt the biology of PKM2 expressing tumour cells rather than all PKM2 expressing cells.

WAY677099 is a small molecule developed by Pfizer Inc. as a proprietary and prototypical activator of PKM2. This small molecule was identified from a screen to identify activators of PKM2. The author is not aware of any other prior work involving this compound. The overall objective of this study was to explore the utility of a PKM2 activator as an anti-tumour agent using the glioma cell line U87MG as a model system.

Because PKM2 activity is dynamically regulated, we reasoned that a PKM2 activator such as WAY677099 would most likely exert meaningful biological effects under conditions in which PKM2 is otherwise inactive. Therefore the first aim was to identify conditions in which PKM2 is predominantly dimeric and inactive. To achieve this aim, a novel method for detecting PKM2 complex formation was employed utilising PKM2 immunoblotting following blue native polyacrylamide gel electrophoresis (BN-PAGE). The outcome of this first aim was used to guide experimental conditions for the second aim, to evaluate the biological effect and therapeutic potential of WAY677099 on glioma cells.

In particular, regulation of PKM2 activity is believed to influence flux through the oxidative arm of the pentose phosphate pathway (oxPPP), enabling an adaptive response to oxidative stress. Therefore we sought to explore the effect of pharmacologic PKM2 activation on redox control and cell survival following oxidative stress. This hypothesis is graphically depicted in **(Figure 4.1)**

Modulation of pyruvate kinase activity is believed to influence flux through the oxPPP, thus enabling an adaptive response to oxidative stress by promoting NADPH regeneration. Therefore we specifically sought to explore the relationship of PKM2, PKM2 activators and oxidative stress. We hypothesised that an externally applied source of oxidative stress would induce inhibition of PKM2 facilitating increased flux through the oxPPP and maintenance of NADPH levels. Further, we hypothesised that the PKM2 activator WAY677099 could block this inhibition, leading to reduced oxPPP flux, decreased levels of NADPH and impaired cell survival in response to oxidative stress.

It has been suggested that low activity PKM2 somehow promotes aerobic glycolysis and suppresses respiration. Because of the apparent importance of aerobic glycolysis to cancer cell biology, the third aim was to explore the paradoxical relationship between PKM2 inactivity and aerobic glycolysis.

Results

The proposed therapeutic potential of a PKM2 activator is in its ability to force tetramerisation and activation of PKM2 in cancer cells, under conditions where dimerisation and inactivation would normally occur because of the growth/survival advantage dimerisation confers. Therefore, we first sought to identify the factors that contribute to regulation of PKM2 tetramer/dimer formation of glioblastoma cells *in vitro*.

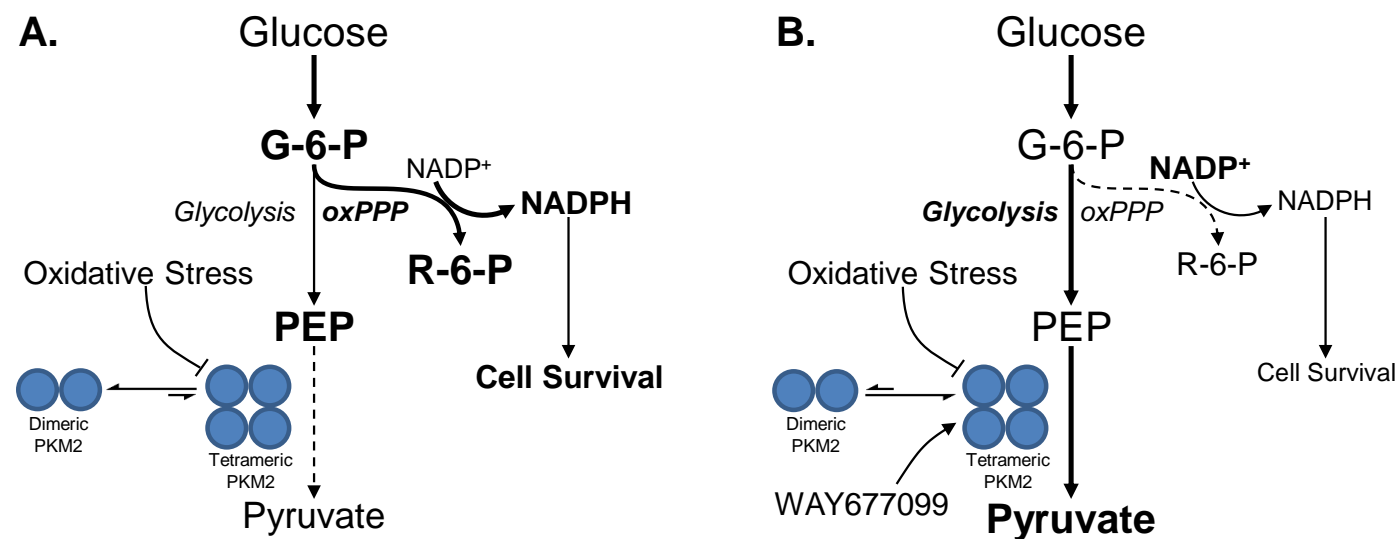


Figure 4.1. Hypothesis for sensitisation of cancer cells to oxidative using a PKM2 activator. **A.** Cellular response to oxidative stress under normal conditions. Oxidative stress inhibits PKM2 activity, shifting the enzyme to the dimeric form. Reduced PKM2 activity results in reduced flux through glycolysis and an increase in upstream metabolites including glucose-6-phosphate (G-6-P) which can be channelled into the oxidative arm of the pentose phosphate pathway (oxPPP) which regenerates NADPH enabling resistance to oxidative stress and cell survival. **B. Cellular response to oxidative stress in the presence of WAY677099.** WAY677099 promotes the active tetrameric form of PKM2 even in the presence of oxidative stress curtailing the adaptive response resulting in reduced flux through the oxPPP, low levels of NADPH and impaired cell survival.

PKM2 tetramer formation and activity is influenced by glucose concentration

Within the heterogeneous tumour environment, cells are exposed to a range of environmental stressors including nutrient restriction. The effect of glucose concentration on PKM2 activation was examined. U87MG cells were cultured overnight in media containing 17.5 mM glucose, or 1 in 2 dilutions (8.8 mM, 4.4 mM, 2.2 mM, and 1.1 mM) and no glucose. Standard DMEM formulations typically contain 17.5 mM glucose, while 4.4 mM glucose is very similar to normal short term fasting (i.e. hours without feeding) blood glucose concentration (Daly et al., 1998). A substantial fraction of PKM2 was found to be tetrameric in lysates from cells cultured in 17.5 mM glucose. This fraction declined rapidly with a reduction in glucose concentration, such that at physiologically relevant concentrations, PKM2 tetramer formation was minimal (**Figure 4.2 A**). The decline in PKM2 tetramer at reduced glucose concentration was closely mirrored by a decline in pyruvate kinase activity (**Figure 4.2 B**).

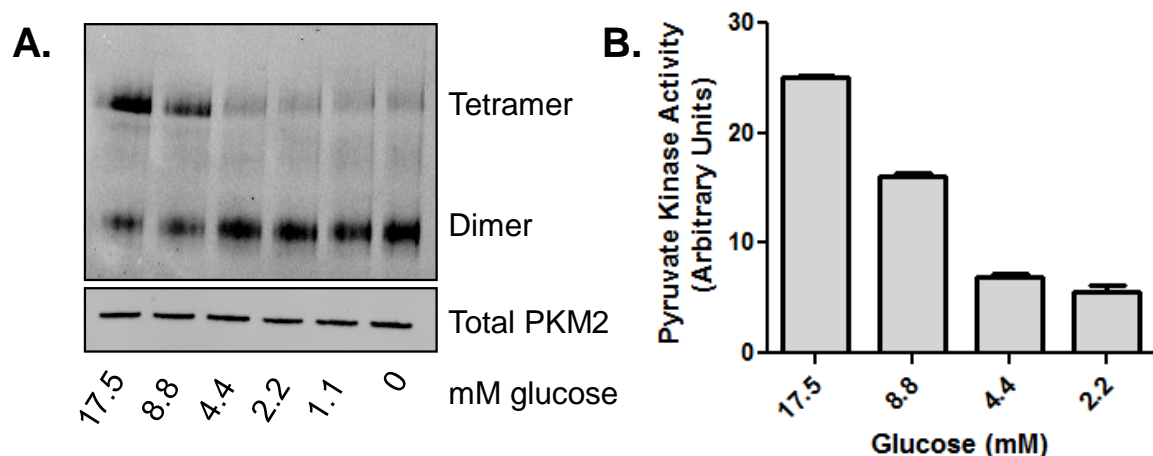


Figure 4.2. Dependence of glucose concentration on PKM2 tetramer formation and pyruvate kinase activity. U87MG cells were cultured overnight in DMEM +5% FCS supplemented with a range of glucose concentrations **A**. PKM2 tetramer formation in cell lysates. **B**. Pyruvate kinase activity in cell lysates.

To test the ability of the PKM2 activator WAY677099 to activate PKM2 under glucose starvation conditions, U87MG cells were incubated overnight in media containing 17.5 mM, 4.4 mM, 0 mM glucose, or 17.5 mM glucose and 25 mM of the glycolysis inhibitor 2-deoxyglucose (2-DG) in the presence or absence of 5 μ M of WAY677099 (**Figure 4.3**).

As with glucose withdrawal, inhibition of glycolysis with 2-DG caused a loss of PKM2 tetramer and pyruvate kinase activity. WAY677099 was able to induce robust PKM2 tetramer formation, resulting in increased catalytic activity, reversing the inhibitory effect of low glucose or 2-DG. However, in the complete absence of glucose, WAY677099 was not able to promote tetramer formation and pyruvate kinase activity remained low.

Effect of 2-deoxyglucose and WAY677099 on PEP concentration

PKM2, along with PKL and PKR is allosterically regulated by the upstream glycolysis intermediate fructose-1,6-BP (FBP). This allows for inhibition of pyruvate kinase activity when upstream glycolysis is limited, and may function to maintain elevated levels of glycolysis phospho-metabolites during glucose restriction (Ashizawa et al., 1991). Indeed glucose starvation in yeast (which expresses a pyruvate kinase with similar characteristics to PKM2) leads to a rapid drop in FBP and an increase in PEP (Brauer et al., 2006).

We investigated the effects of glycolysis inhibition on levels of PEP, which were expected to be maintained at elevated levels due to down-regulation of pyruvate kinase activity, and the effect of PKM2 activation by WAY677099. U87MG cells cultured overnight in DMEM/F12 +5% FCS were treated with 25 mM 2-DG and/or WAY677099 for 1 hour before collecting the cells for determination of PEP.

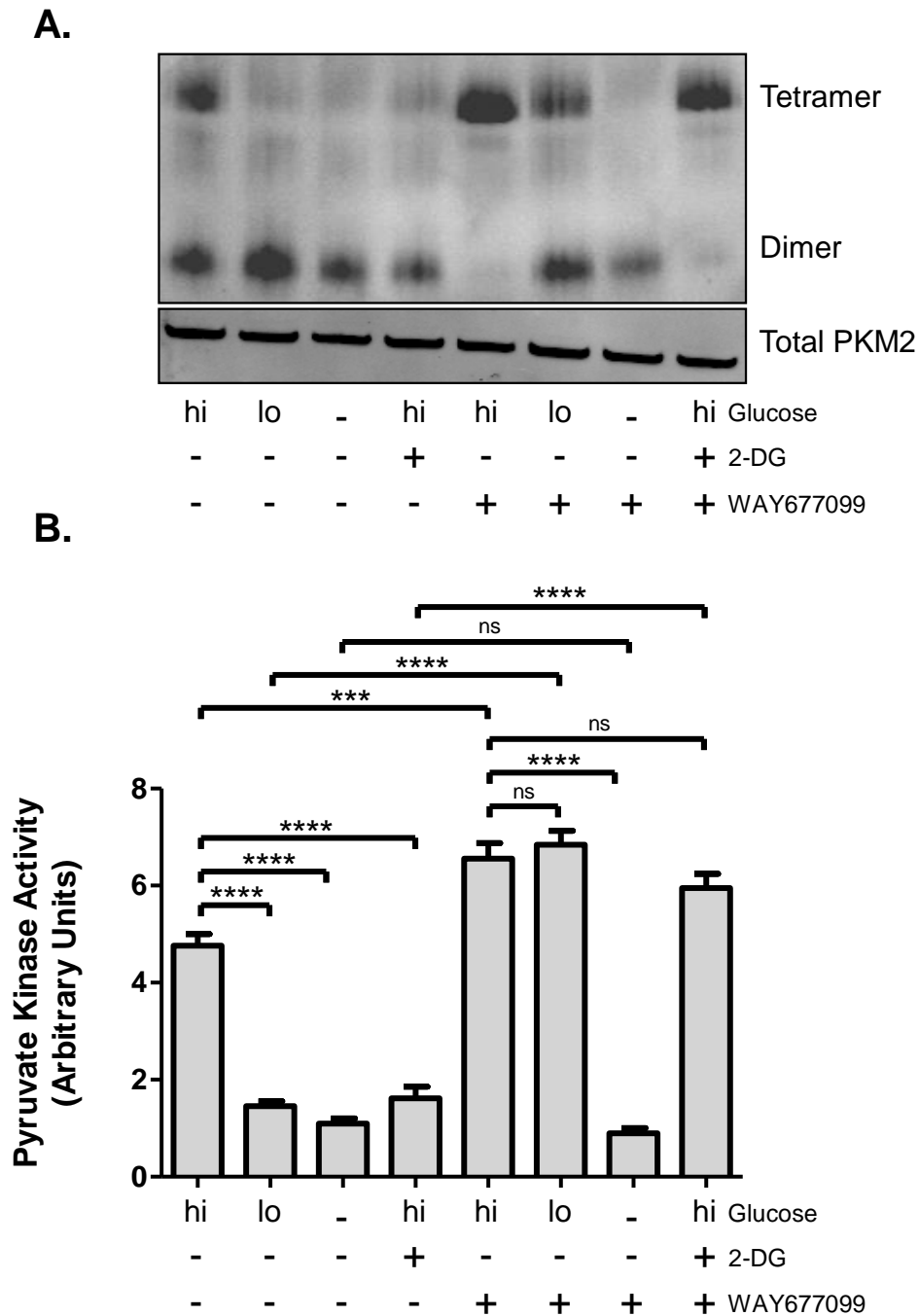


Figure 4.3. Effect of WAY677099 on PKM2 tetramer formation and PK activity. U87MG cells were cultured overnight in DMEM +5%FCS supplemented with 17.5 mM (hi), 4.4 mM (lo) or 0 mM (-) glucose, with or without 25 mM 2-deoxyglucose or 5 μ M WAY677099. **A.** PKM2 tetramer formation in cell lysates. **B.** Pyruvate kinase activity in cell lysates.

Glycolysis inhibition by the glucose analogue 2-DG resulted in an increase in intracellular levels of the downstream glycolysis intermediate phosphoenolpyruvate (**Figure 4.4 A**). Treatment of U87MG cells with WAY677099 lowered the intracellular level of PEP, both in glycolysing, and glycolysis inhibited cells (**Figure 4.4 A**). A schematic of how 2-DG and WAY677099 affect PEP levels is shown in (**Figure 4.4 B**)

These experiments demonstrate that regulation of PKM2 can serve to maintain intracellular concentrations of glycolysis intermediates in glioma cells, and that this function can be abrogated by WAY677099.

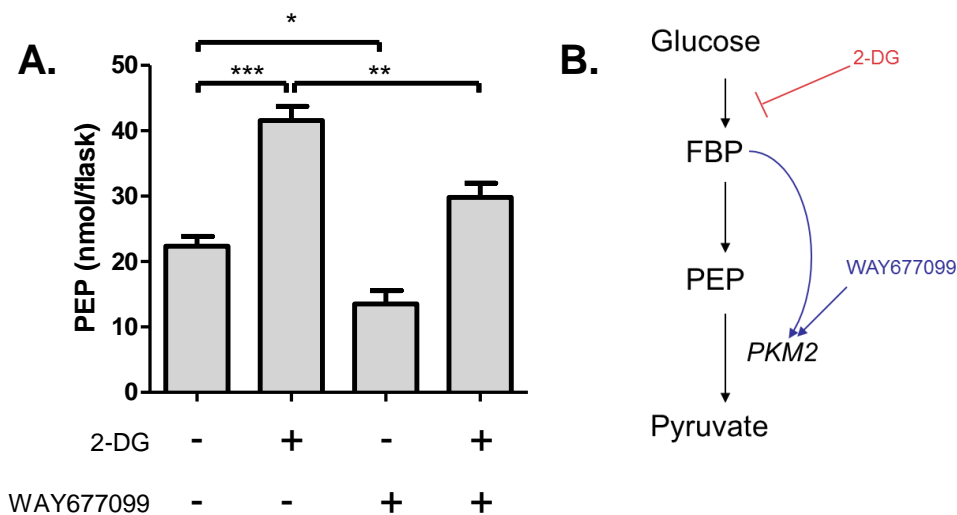


Figure 4.4. Effect of 2-deoxyglucose and WAY677099 on intracellular phosphoenolpyruvate. **A.** U87MG cells were cultured overnight in DMEM/F12 in the presence of 2-deoxyglucose and/or WAY677099 and intracellular PEP determined enzymatically. **B.** Proposed model for regulation of intracellular PEP concentration via regulation of PKM2 activity.

PKM2 tetramer formation is regulated during the cell cycle

Increasing cell density has previously been shown to promote a reduction in dimeric PKM2 in pancreatic cancer cell lines (Kumar et al., 2010). Therefore we tested whether the same was also true for U87MG. U87MG cells were seeded at different cell densities and cultured overnight. After normalising for protein concentration, cell lysates were analysed for pyruvate kinase activity and PKM2 tetramer formation (**Figure 4.5 A**). Both activity and tetramer formation were highly

influenced by seeding density. Pyruvate kinase activity of cells seeded at 330 cells/mm² was over three times that of cells seeded at 82.5 cells/mm².

U87MG cells are subject to contact inhibition at high cell density (Sinn et al., 2010). We reasoned that the effect of plating density on PKM2 activation may be mediated by regulation of proliferation

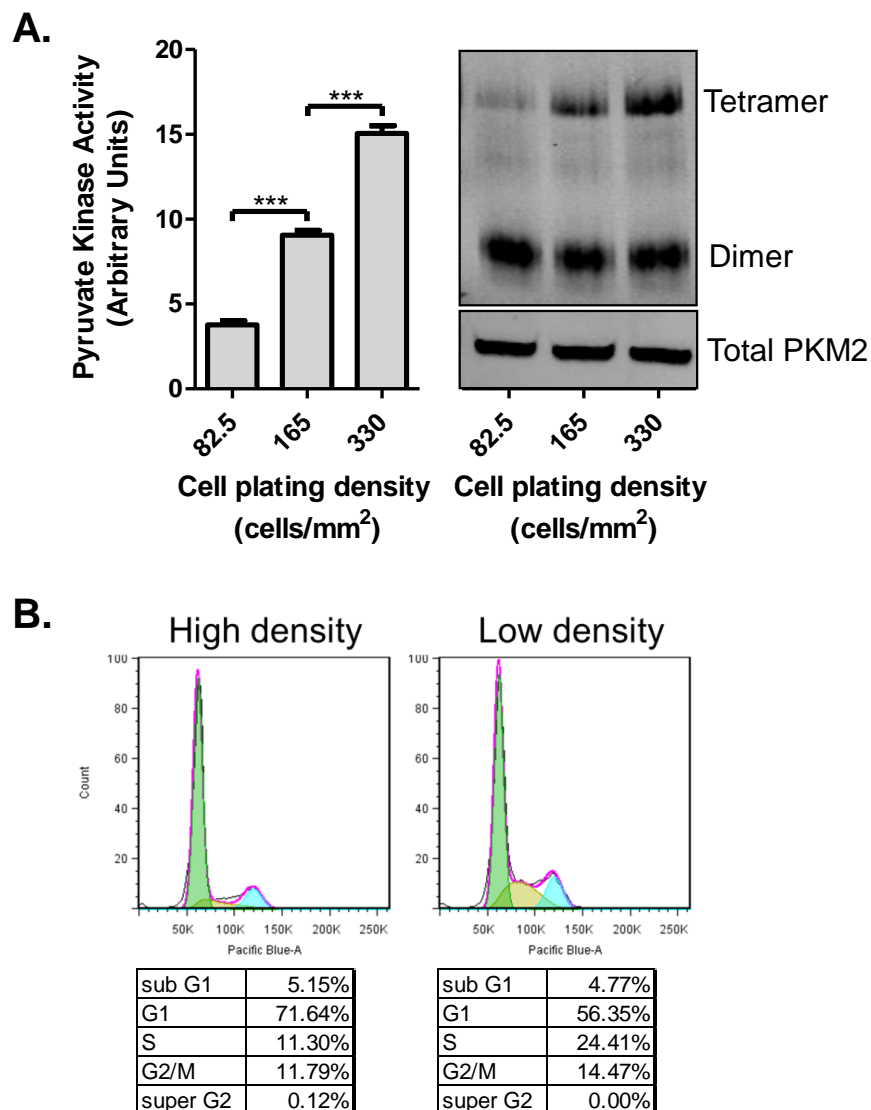


Figure 4.5. Effect of cell density on PKM2 tetramer formation and pyruvate kinase activity. U87MG cells were plated at various seeding densities and cultured overnight **A.** Pyruvate kinase activity and PKM2 tetramer formation in cell lysates of cells plated at different seeding densities **B.** Cell cycle analysis of cells seeded at 300 (high density) and 82.5 (low density) cells/mm²

and the cell cycle. Cell cycle analysis of cells seeded at 330 cells/mm² and 82.5 cells/mm² confirmed that high density reduced the fraction of cells in S and G2/M phase of the cell cycle (**Figure 4.5 B**). This suggested that PKM2 activity may be suppressed during these phases of the cell cycle.

In order to show that cell density was affecting PKM2 tetramer formation via its effects on proliferation, PKM2 tetramer formation was measured in U87MG cells at different stages of the cell cycle. Serum starvation for 24 hours, which prevents progression through G1 phase, was used to synchronise cells. Serum was then re-introduced for varying lengths of time to allow resumption of the cell cycle. To minimise variation in cell density as a result of different lengths of time in the presence of serum, cells grown for shorter periods post starvation were subject to a longer period of growth before serum starvation, as indicated in (**Figure 4.6 E**).

Following serum starvation, the fraction of cells in S and G2/M phase remained low until 12 hours post starvation when the S phase fraction began to increase. The fraction of S and G2/M phase cells reached a peak at 18 hours, and subsided reaching a minimum at 30 hours (**Figure 4.6 A and B**). PKM2 tetramer formation was determined in these populations by BN-PAGE (**Figure 4.6 C**). Densitometry analysis was used to quantify the tetramerisation of PKM2, expressed as either tetramer vs. dimer, or tetramer vs. total PKM2 (**Figure 4.6 D**). PKM2 tetramer formation was low at 0 and 30 minutes following addition of serum. Following these time points, the temporal expression of PKM2 tetramer followed a broadly similar pattern as the cell cycle analysis, with high tetramer levels at 2 and 6 hours, followed by a trough from 12-30 hours (when the S/G2/M fraction was high).

As PKM2 was shown to be dynamically regulated through the cell cycle, we hypothesised that constitutively activating PKM2 with WAY677099 would disrupt the cell cycle and reduce proliferation in these cells. U87MG cells synchronised by serum starvation were cultured in the presence of 5% FCS for 18, 24 or 30 hours with either 5 μ M WAY677099 or vehicle control. Cell cycle analysis showed no effect of treatment with the PKM2 activator (**Figure 4.7 A**). The proliferation rate of

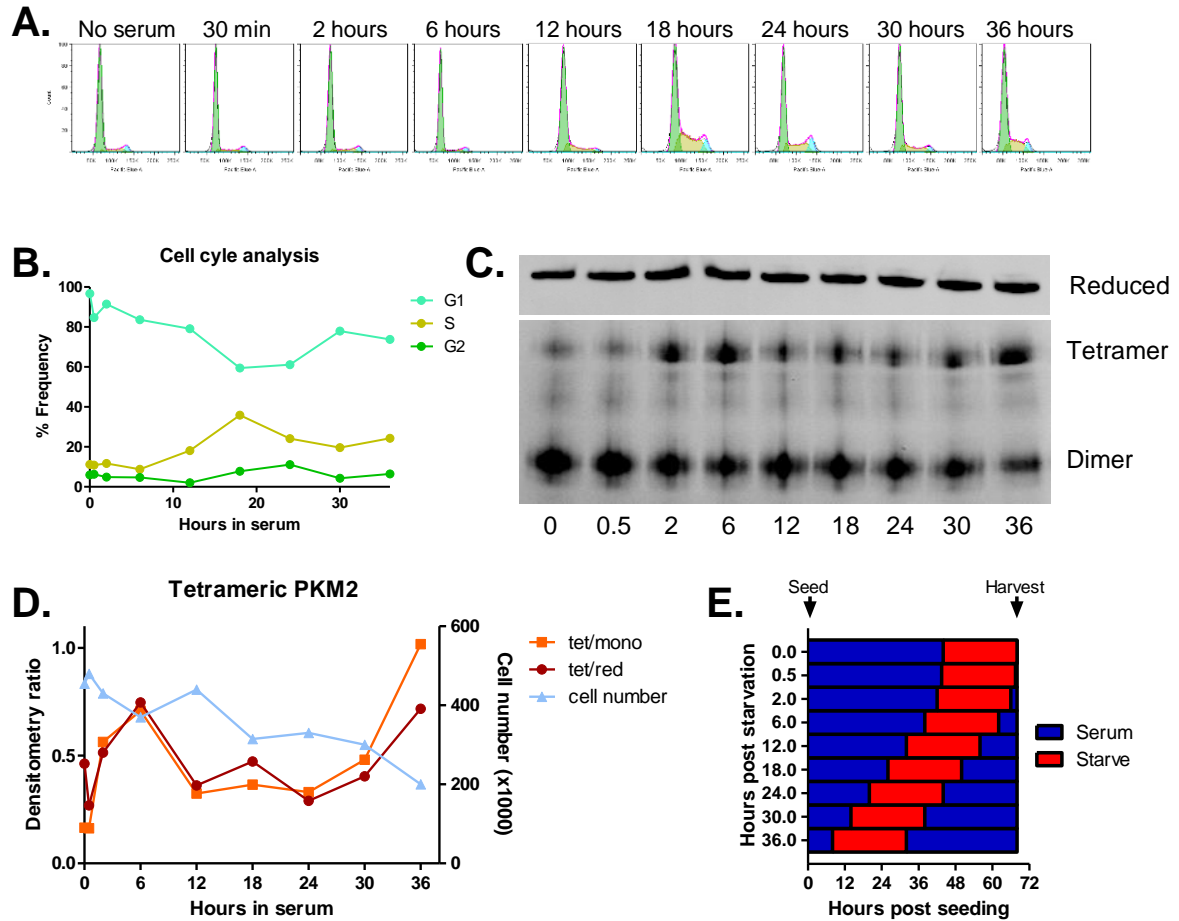


Figure 4.6. PKM2 tetramer formation in cell synchronised U87MG cells. U87MG cells were serum starved for 24 hours to synchronise cells in G1, and re-exposed to 5% serum for varied lengths of time. **A.** Determination of DNA content by flow cytometric analysis of DAPI stained cells. **B.** Fraction of cells at each stage of the cell cycle. **C.** Native western blot of PKM2. **D.** Densitometric analysis of tetrameric PKM2 vs. total PKM2 (orange) and tetrameric vs. dimeric PKM2 (brown). Cell number per flask as determined using a haemocytometer (blue). **E.** Experimental design indicating the timing of cell seeding, serum starvation, serum reintroduction and cell harvesting.

U87MG cells and SF767 cells was not affected by the presence of WAY677099 as determined by MTS cell proliferation assay (**Figure 4.7 B**).

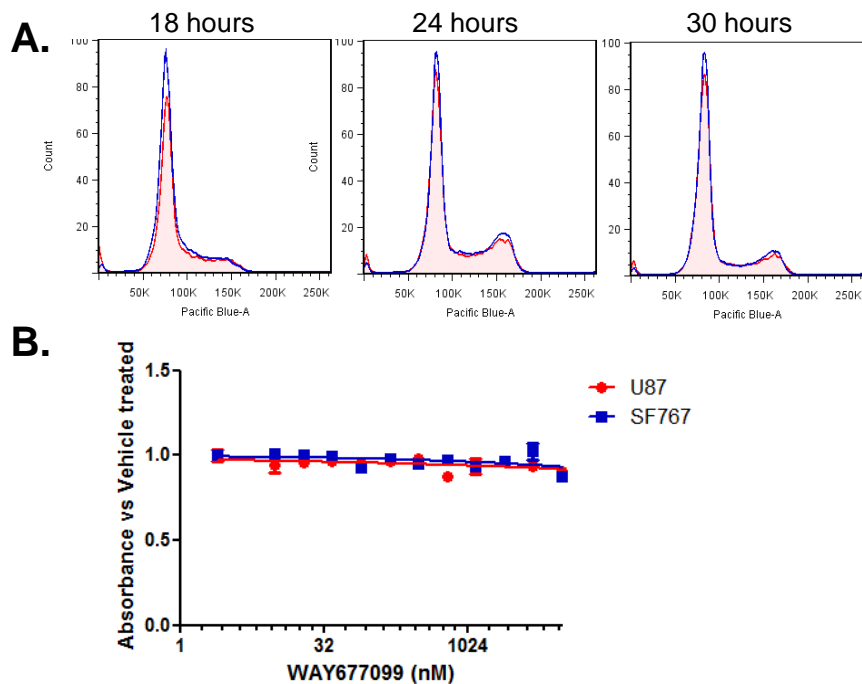


Figure 4.7. WAY677099 does not affect cell cycle or proliferation of glioma cells. **A.** U87MG cells were serum starved for 24 hours to synchronise cells in G1, and re-exposed to 5% serum for 18, 24 or 30 hours with vehicle control (blue) or WAY677099 (red). DNA content determined by flow cytometric analysis of DAPI stained cells. **B.** U87MG and SF767 cells were cultured for 4 days at a range of concentrations of WAY677099 and cell viability/proliferation assessed by MTS assay

Effect of glucose concentration and WAY677099 on the glycolytic rate

While pharmacologic activation of PKM2 had no apparent effect on glioma cell proliferation *in vitro*, we were interested in what effect WAY677099 would have on energy production from glycolysis and respiration. Some cell types with a high glycolytic capacity including proliferating cells and cancer cells exhibit the Crabtree effect, where the addition of glucose suppresses respiration. Intuitively, increasing the activity of pyruvate kinase would be expected to lead to an increase in glycolysis and a concomitant reduction in respiration. Indeed a number of past experiments have shown a positive correlation between pyruvate kinase activity and glycolytic rate, and a negative correlation with oxygen consumption (Gosalvez et al., 1975). However recent studies have shown a

negative correlation between pyruvate kinase activity and glycolytic rate, suggesting that a PKM2 activator should reverse the Warburg effect (Christofk et al., 2008, Hitosugi et al., 2009, Anastasiou et al., 2012).

The effect of the PKM2 activator on glycolytic rate was initially described in a number of hepatocellular carcinoma (HCC) cell lines using the Seahorse XF Analyser (**Figure 4.8**). In these cells, the addition of WAY677099 had an immediate but variable stimulatory effect on glycolysis, suggesting that pyruvate kinase is a rate limiting glycolytic enzyme in these cells.

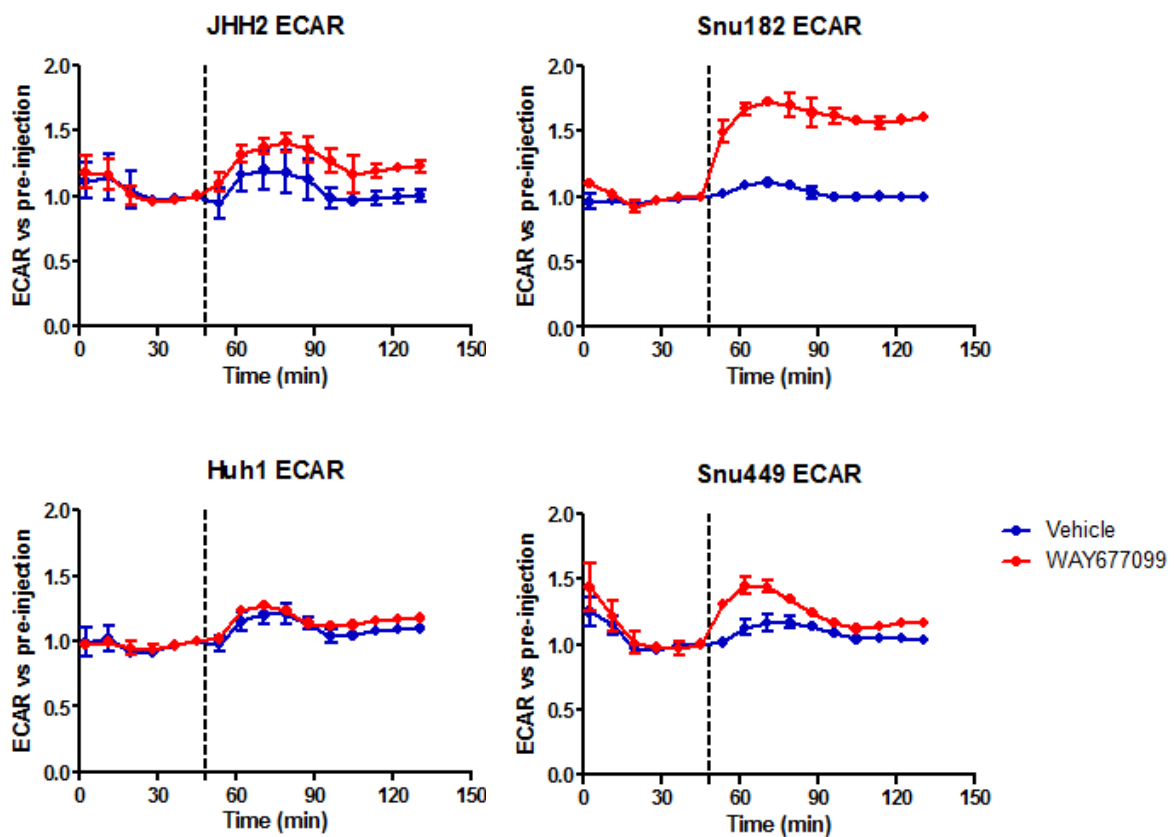


Figure 4.8. PKM2 activation increases glycolytic rate in some HCC cell lines. Glycolytic rate was monitored in a range of HCC cell lines in XF assay media supplemented with 17.5 mM glucose using the Seahorse XF Analyser. At the time indicated by the dashed line, 5 μM WAY677099 or vehicle control was added to the cells.

Glycolysis in glioma cell lines was assessed using the phenol red based H^+ production assay (Figure 4.9). The glycolytic rate in U87MG cells was completely unaffected by the presence of WAY677099. A statistically significant increase in glycolysis was observed in SF767 cells however the effect was very moderate. Therefore PKM2 activity does not appear to be rate limiting for glycolysis in these cells.

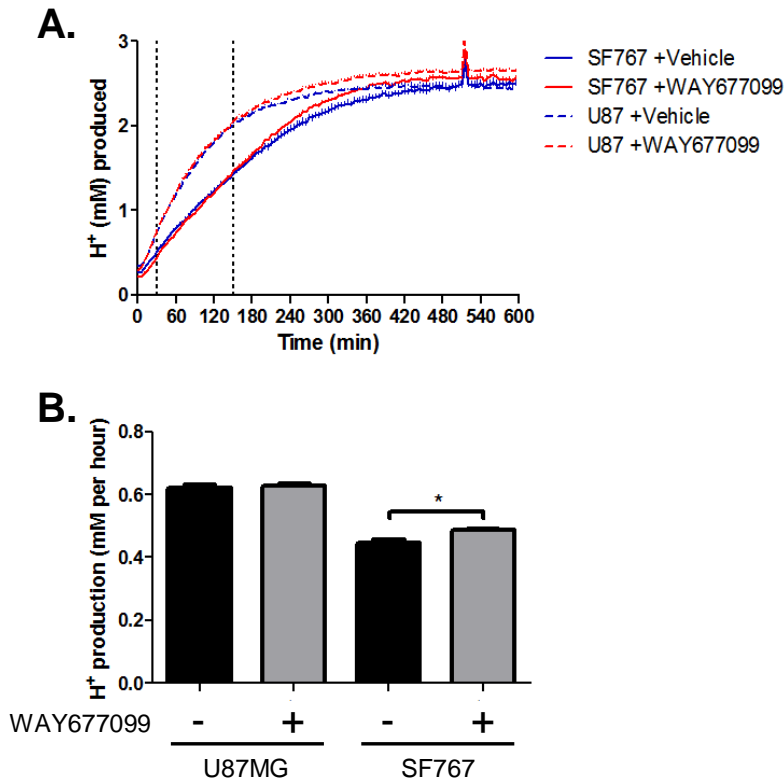


Figure 4.9. Effect of WAY677099 on the glycolytic rate of glioma cells. U87MG and SF767 cells plated at 80,000 cells per well were incubated in XF assay media containing 17.5 mM glucose and either vehicle control or 5 μ M WAY677099. **A.** Increase in extracellular H^+ over time. **B.** H^+ production rate between 30 minutes and 150 minutes.

Effects of glucose concentration and WAY677099 on respiration

A characteristic feature of cancer cells is elevated glycolysis and suppressed respiration, believed to be mediated by expression of primarily inactive, dimeric PKM2. A number of small molecule activators of PKM2 have been designed in an effort to counter abnormal cancer metabolism (Yacovan et al., 2012). We examined the relationship between glucose metabolism and mitochondrial respiration, and the effect of PKM2 activation on this relationship.

Earlier work in HCC cell lines showed that the addition of WAY677099 caused a rapid decline in mitochondrial respiration (**Figure 4.10**). We hypothesised that this effect was a manifestation of the Crabtree effect, where increased ATP/ADP ratio as a result of increase pyruvate kinase activity was suppressing mitochondrial respiration. If this were the case, addition of FCCP to uncouple mitochondrial respiration from oxidative phosphorylation should relieve this suppression. This hypothesis is graphically depicted in (**Figure 4.11**).

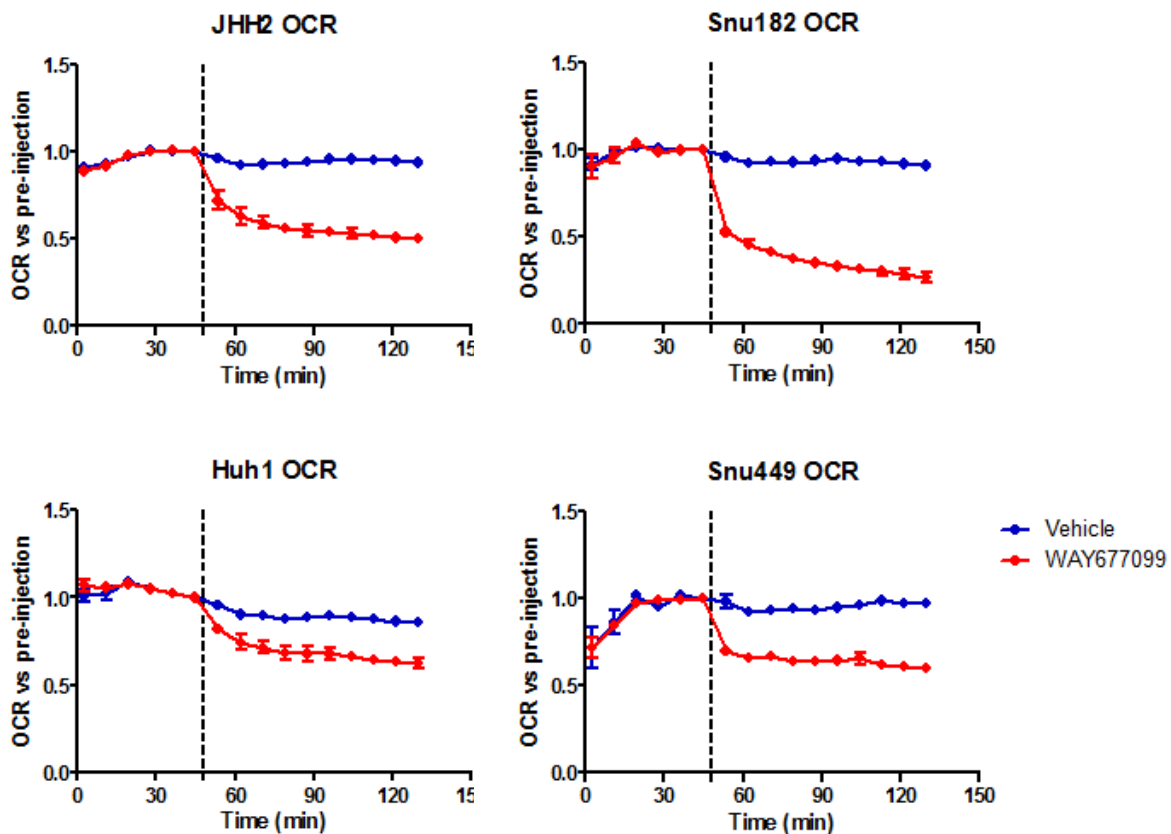


Figure 4.10. PKM2 activation suppresses oxygen consumption rate in HCC cell lines. Oxygen consumption rate was monitored in a range of HCC cell lines in XF assay media supplemented with 17.5 mM glucose using the Seahorse XF Analyser. At the time indicated by the dashed line, 5 μ M WAY677099 or vehicle control was added to the cells.

Respiration was measured in glioma cell lines in XF DMEM supplemented with 17.5 mM glucose using the XF Analyser. Respiration was measured at basal conditions and following the sequential addition of WAY677099 or vehicle control, followed by oligomycin, FCCP and Antimycin A + Rotenone (**Figure 4.12**). In SF767 cells, the addition of the PKM2 activator had a small inhibitory

effect on respiration (t-test, $p < 0.001$), while no effect was observed in U87MG cells (t-test, $p = 0.08$) Oligomycin was added to inhibit ATP synthase, followed by FCCP to stimulate uncoupled, ATP synthase independent respiration. Rather than relieving the PKM2 activator induced inhibition of respiration, uncoupling maintained (SF767) or increased (U87MG) the inhibitory effects of WAY677099. Respiration in uncoupled U87MG cells was significantly lower in WAY677099 cells compared to controls (t-test, $p = 0.014$). These results demonstrate that a Crabtree like effect does not explain PKM2 activator induced suppression of respiration.

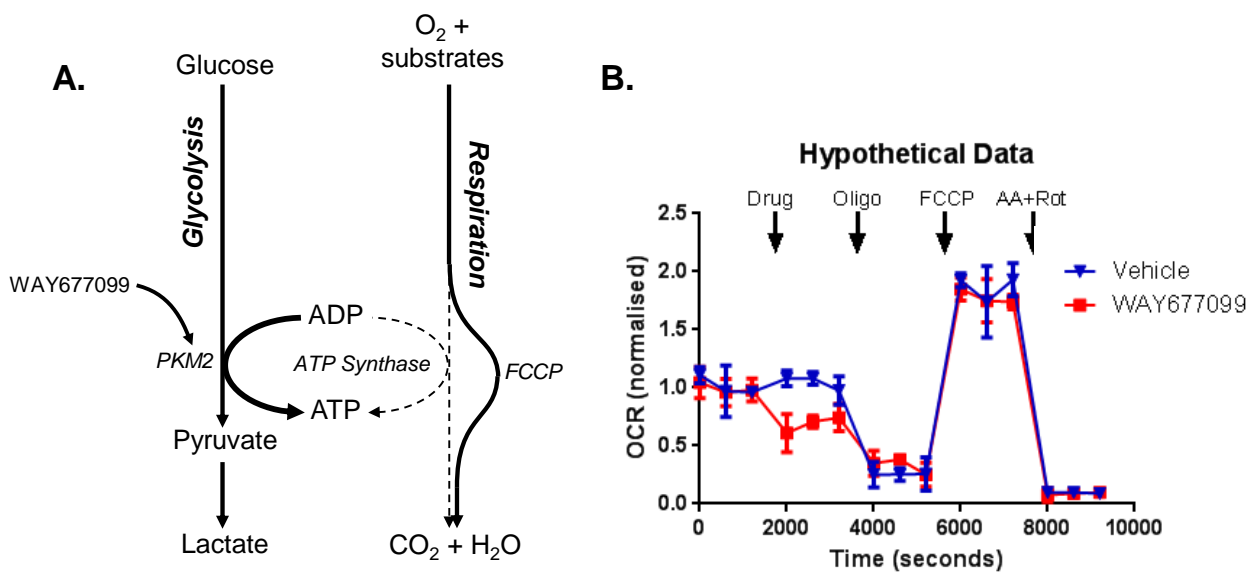


Figure 4.11. 'Crabtree effect' hypothesis for suppression of respiration by WAY677099. **A.** Glycolysis and respiration both phosphorylate ADP to ATP and are thus rate limited by the availability of ADP. Increasing PKM2 activity resulting in increased glycolytic ATP production causes a block in respiration at Complex V due to a shortage of ADP resulting in reduced O_2 consumption. The addition of the proton ionophore FCCP uncouples respiration from ADP phosphorylation facilitating increased respiration despite the shortage of ADP. **B.** Anticipated results of oxygen consumption data based on the Crabtree effect hypothesis. The addition of WAY677099 suppresses oxygen consumption. The addition of oligomycin to inhibit ATP synthase and FCCP to facilitate maximal uncoupled (ATP synthase independent) respiration results in reversal of respiration suppression by WAY677099.

Glioma cells exhibit the Crabtree effect

To demonstrate that glioma cells do indeed exhibit the Crabtree effect, respiration was measured in the presence and absence of glucose. Respiration and glycolysis was measured in U87MG cells using the XF Analyser in the presence of varying amounts of glucose (**Figure 4.13 A**).

Not surprisingly, the glycolytic rate (ECAR) was highly dependent on the presence of glucose. Similarly, respiration (OCR) was inhibited by the presence of glucose in a dose dependent manner. Uncoupling mitochondria with the addition of FCCP relieved this inhibition. Further, uncoupled respiration was actually higher when in the presence of glucose. This effect was examined in more detail using the Oroboros Oxygraph (**Figure 4.13 B**). SF767 cells were injected into the oxygraph chambers filled with glucose free DMEM and basal respiration was recorded. The addition of glucose to 8.8 mM caused an immediate drop in respiration rate compared to addition of water only. FCCP added to a final concentration of 500 nM relieved this inhibition, increasing respiration in the presence and absence of glucose to a similar level. In the presence of glucose, increasing the concentration of FCCP to 1 μ M further stimulated respiration. However in the absence of glucose, additional FCCP caused a decline in respiration.

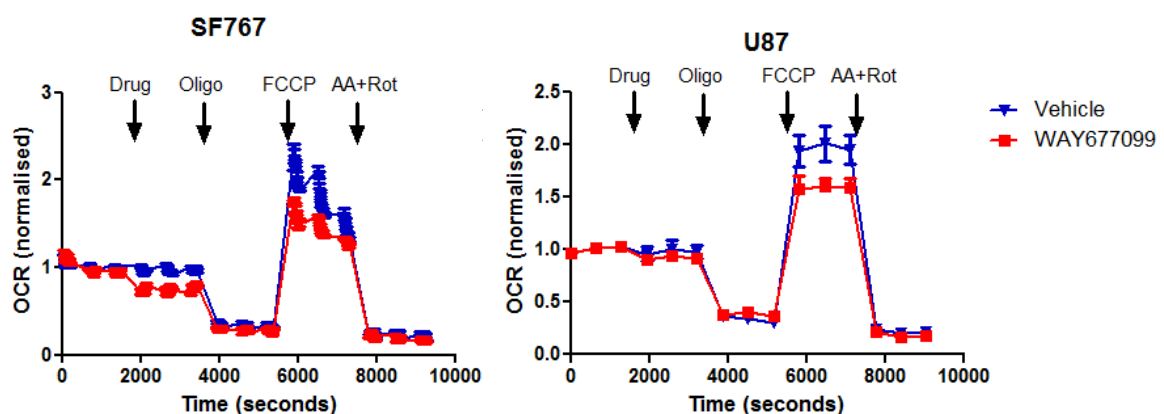


Figure 4.12. Effect of WAY677099 on mitochondrial function in glioma cells. Oxygen consumption rate (OCR) measured in U87MG and SF767 cells using the Seahorse XF Analyser. OCR was measured for three cycles prior to the addition of any compounds, then for three cycles following by the injection of 5 μ M WAY677099 or vehicle control (DMSO), 2.5 μ M oligomycin, 500 nM FCCP, and 2.5 μ M antimycin A plus 2.5 μ M rotenone.

The earlier observation that uncoupling enhanced the suppression of respiration by PKM2 activation (**Figure 4.12**), demonstrated that competition for ADP between glycolysis and respiration was not the cause for suppressed respiration. An alternative explanation is that increased pyruvate kinase activity redirects glycolysis intermediates away from the pentose phosphate pathway which generates NADPH required to counter ROS production and support mitochondrial respiration.

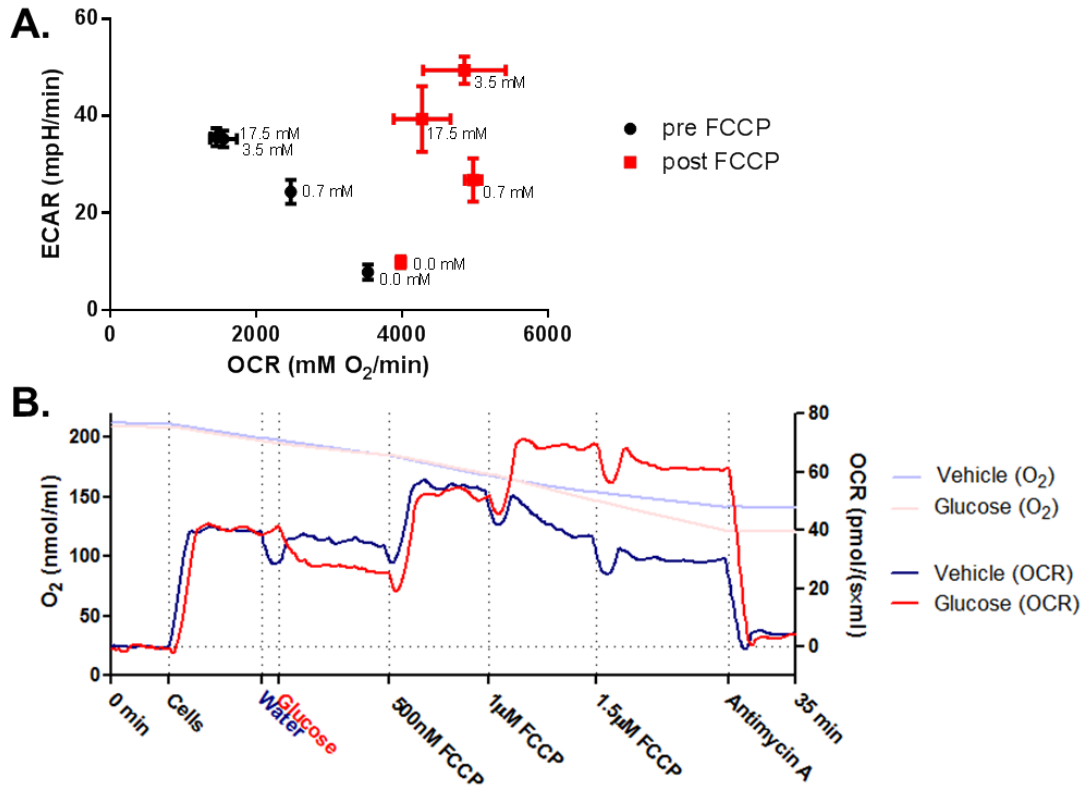


Figure 4.13. Effect of glucose on coupled and uncoupled respiration. A. Oxygen consumption rate (OCR) and extracellular acidification rate (ECAR) of U87MG cells at various concentrations of glucose using the XF Analyser prior to (black) and following (red) the addition of 500 nM FCCP. **B.** Respiration of SF767 cells in glucose free DMEM assessed using Oxygraph. Water or 8.8 mM glucose was added to induce the Crabtree effect. The mitochondrial uncoupler FCCP was added sequentially to a final concentration of 500 nM, 1 µM and 1.5 µM.

We reasoned that if redirection of glycolysis intermediates was the cause of limited mitochondrial respiration, this effect may be enhanced by restricting the supply of glucose. By limiting the supply of glucose to these cells, pharmacologic activation of PKM2 would have a more substantial effect on redirecting flux away from the pentose phosphate pathway and hence reveal a more substantial effect on mitochondrial respiration.

To test this, oxygen consumption of glioma cells in the presence of WAY677099 or vehicle control was measured at a range of glucose concentrations (**Figure 4.14**). U87MG and SF767 cells were added to the oxygraph chambers filled with glucose free DMEM. WAY677099, to a final concentration of 5 µM or vehicle control was added to each chamber. Under glucose free conditions, PKM2 activation lead to a dramatic reduction in OCR of both cell lines. In the SF767 cell line, with

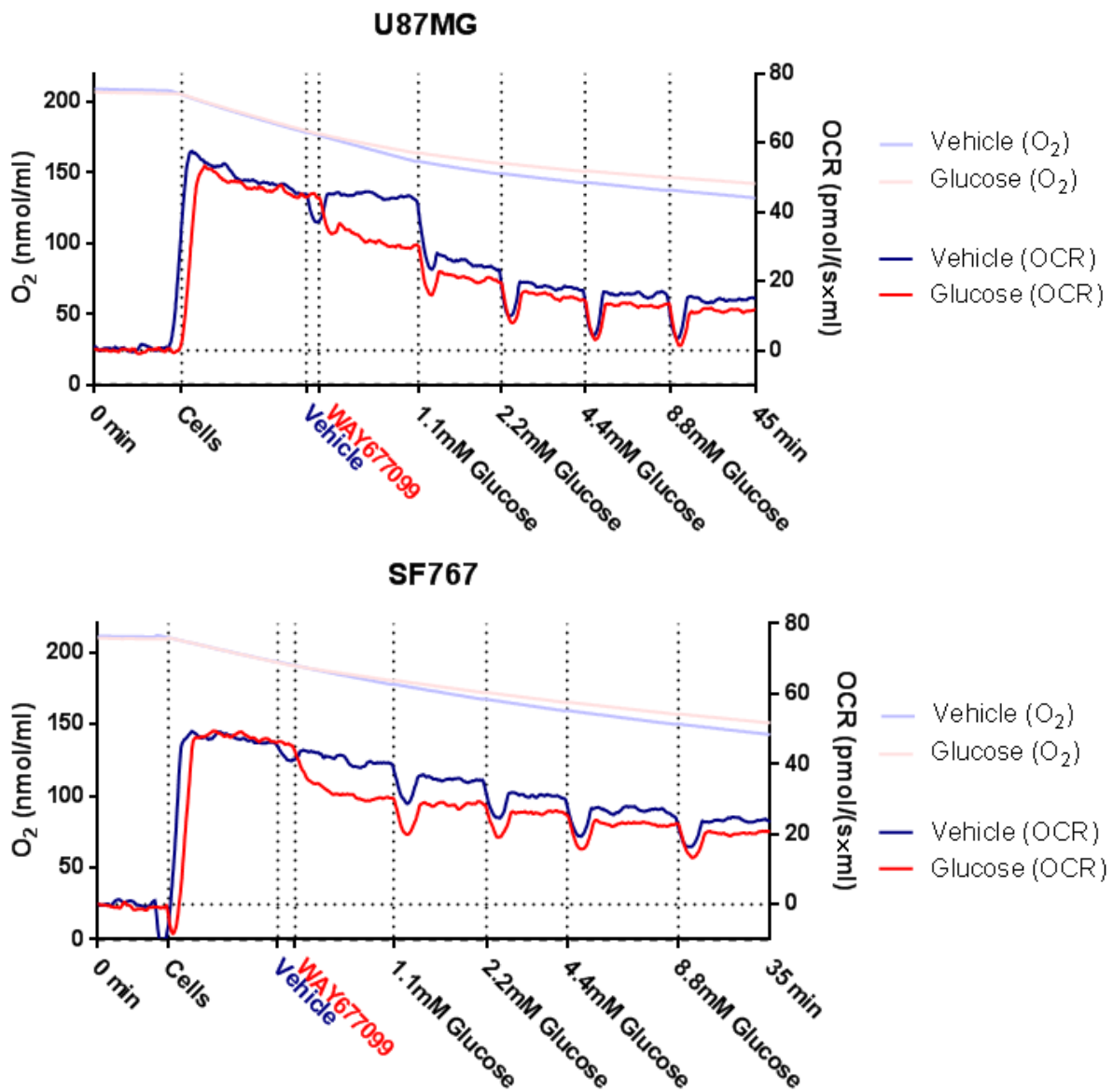


Figure 4.14. Suppression of respiration induced by WAY677099. Respiration of U87MG and SF767 cells in glucose free DMEM measured using the oxygraph. Vehicle control or WAY677099 to a final concentration of 5 μ M was added to each chamber, followed by increasing concentrations of glucose as indicated.

each sequential addition of glucose, respiration was suppressed such that the OCR of WAY677099 and vehicle treated cells converged gradually as the concentration of glucose increased. The U87MG cell line responded more dramatically to the addition of glucose. The addition of just 1.1 mM glucose was sufficient to cause a dramatic reduction in respiration such that any difference in OCR of WAY677099 and vehicle control treated cells was minimised.

To summarise, the addition of glucose to glioma cells suppresses oxygen consumption, an effect which can be reversed by the addition of FCCP, i.e. glioma cells exhibit the Crabtree effect. Suppression of respiration as a consequence of PKM2 activation by WAY677099 is not a Crabtree-like effect. Respiration can be stimulated by FCCP to a greater extent and at higher concentrations when cells are in the presence of glucose, suggesting glycolytic intermediates support respiration. PKM2 activation by WAY677099 produced the most dramatic inhibitory effect on respiration when glucose supply was restricted, conditions in which PKM2 activation should be of greater consequence in terms of maintenance of glycolytic intermediates.

Uncoupled mitochondrial respiration promotes oxidation, dimerisation and inhibition of PKM2

Rejecting the Crabtree effect explanation for respiration suppression by WAY677099, an alternative hypothesis was formulated based on that described by Gruning et al., 2011. In this hypothesis outlined in **(Figure 4.15)**, PKM2 modulates mitochondrial respiration by regulating the supply of intermediates into the oxPPP for the production of NADPH. NADPH suppresses the accumulation of ROS, which are a by-product of respiration and can damage the mitochondria leading to impaired respiration. It was recently shown that oxidation of PKM2 inhibits catalytic activity in response to ROS (Anastasiou et al., 2011). This observation provides a feedback mechanism through which PKM2 activity can be suppressed in response to and in order to support increased mitochondrial respiration.

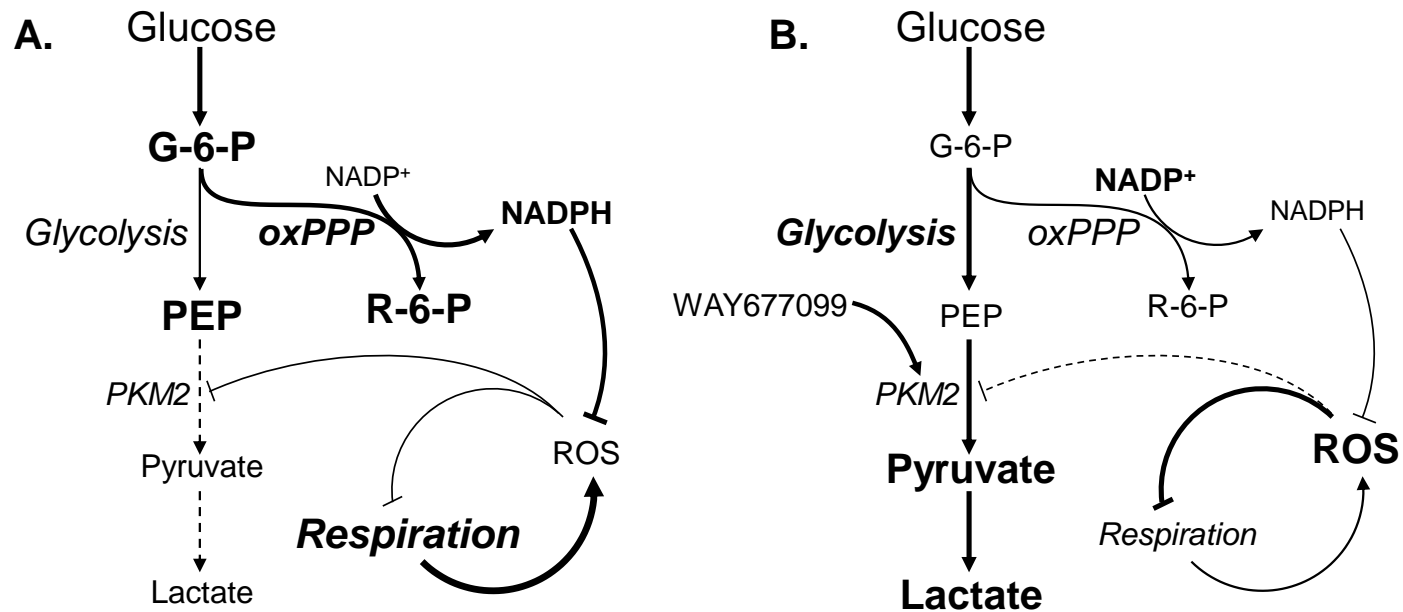


Figure 4.15. Redox feedback loop hypothesis for suppression of respiration by WAY677099. **A.** Normal cellular respiration generates reactive oxygen species (ROS) which lead to a suppression of respiration. ROS also leads to inhibition of PKM2, suppressing glycolysis and redirecting flux through the oxidative arm of the pentose phosphate pathway (oxPPP) to regenerate NADPH. NADPH can serve to counter ROS production enabling continued respiration. **B.** In the presence of the PKM2 activator WAY677099, ROS no longer suppresses PKM2 and glycolytic intermediates are no longer redirected into the oxPPP for NADPH regeneration. This allows ROS to accumulate and inhibit mitochondrial respiration.

We aimed to demonstrate that stimulating increased respiration using FCCP, or applying oxidative stress directly using diamide could lead to oxidation of PKM2 leading to tetramer dissociation and loss of enzyme activity. U87MG cells were treated with 1 μ M FCCP or 250 μ M diamide for 15 minutes before assaying for PKM2 complex formation and catalytic activity. Both treatments resulted in a dramatic reduction in PKM2 tetramer formation (**Figure 4.16 A**) and pyruvate kinase activity (**Figure 4.16 C**). These effects could be completely blocked with the WAY677099, added 15 minutes prior to treatment.

Inactivation of PKM2 by ROS is dependent on oxidation of a specific cysteine at residue 358 (Anastasiou et al., 2011). To detect cysteine oxidation of PKM2, oxidised cysteine residues were specifically labelled with biotin for precipitation with streptavidin conjugated beads, and presence of PKM2 in the precipitate was detected by western blot. Both FCCP and diamide treatment resulted in an increase in cysteine oxidised PKM2. Oxidation was completely prevented by prior addition of WAY677099 (**Figure 4.16 B**).

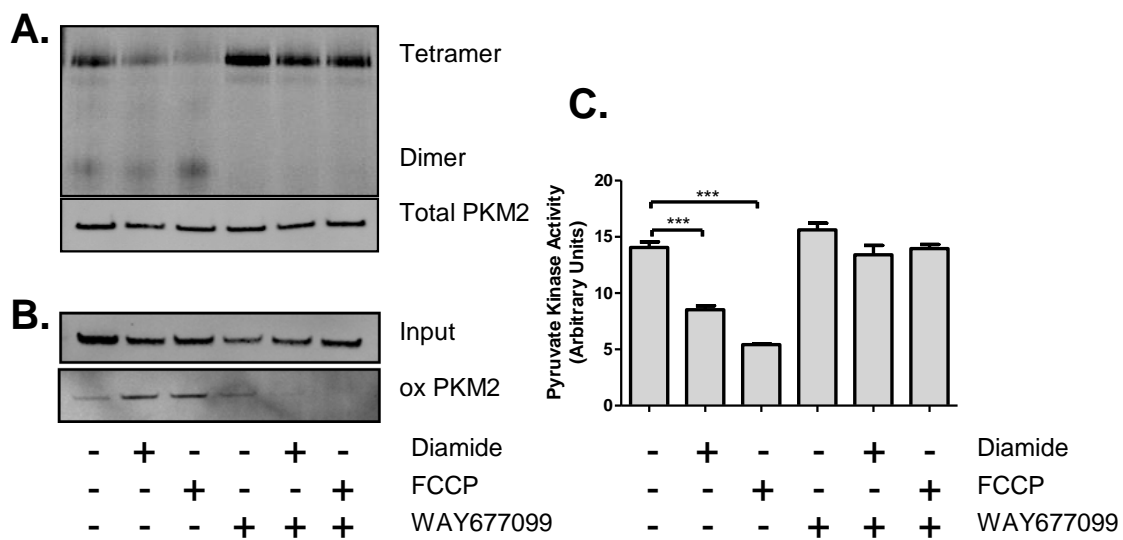


Figure 4.16. Oxidation and inhibition of PKM2 in FCCP treated U87MG cells. U87MG cells were treated with 5 μ M of WAY677099 or vehicle control for 15 minutes. Subsequently, 250 μ M Diamide or 1 μ M FCCP was added for a further 15 minutes. **A.** Native western blots of PKM2 **B.** Detection of oxidised PKM2 by biotin labelling and streptavidin pulldown of oxidised cystines followed by western blotting. **C.** Pyruvate kinase activity in lysates of cells treated under identical conditions.

Stimulation of respiration by FCCP results in cysteine oxidation, dimerisation and loss of catalytic activity of PKM2, as does oxidative stress by diamide. These effects can be completely blocked by the prior addition of WAY677099. This suggests that PKM2 activity is dynamically regulated in order to respond to oxidative stress and to maintain mitochondrial respiration, and that WAY677099 can potentially disrupt this response.

Effect of WAY677099 on NADPH levels

Next, we evaluated the effect of WAY677099 on levels of NADPH which we hypothesised would be diminished in response to PKM2 activation and oxidative stress. This observation would serve as a component of both hypotheses of **(Figure 4.1)** and **(Figure 4.15)**.

Glucose is essential to NADPH homeostasis during oxidative stress as shown in **(Figure 4.17)**. U87MG cells were cultured overnight at various glucose concentrations and then treated with 250 μ M diamide for 15 minutes before cell lysates were collected for determination of NADPH/NADP⁺.

Limiting the supply of glucose from 8.8 mM to 1.1 mM glucose in control cells slightly decreased the amount of total (NADPt) and reduced (NADPH), without affecting the ratio. Diamide affected NADPH/NADPt in a manner highly dependent on glucose concentration. In the presence of glucose, NADPt levels increased following diamide exposure. NADPH levels increased following diamide exposure at glucose concentrations 4.4 mM and above, remained steady at 2.2 mM glucose and were dramatically lower at 1.1 mM glucose and below **(Figure 4.17)**.

The NADPH/NADPt ratio following diamide exposure was similarly highly dependent on glucose concentration. This effect was most apparent between the concentrations of 4.4 mM and 1.1 mM glucose. Therefore a glucose concentration of 2.2 mM was used to evaluate the compounding effect of PKM2 activation on NADPH/NADPt levels following diamide exposure.

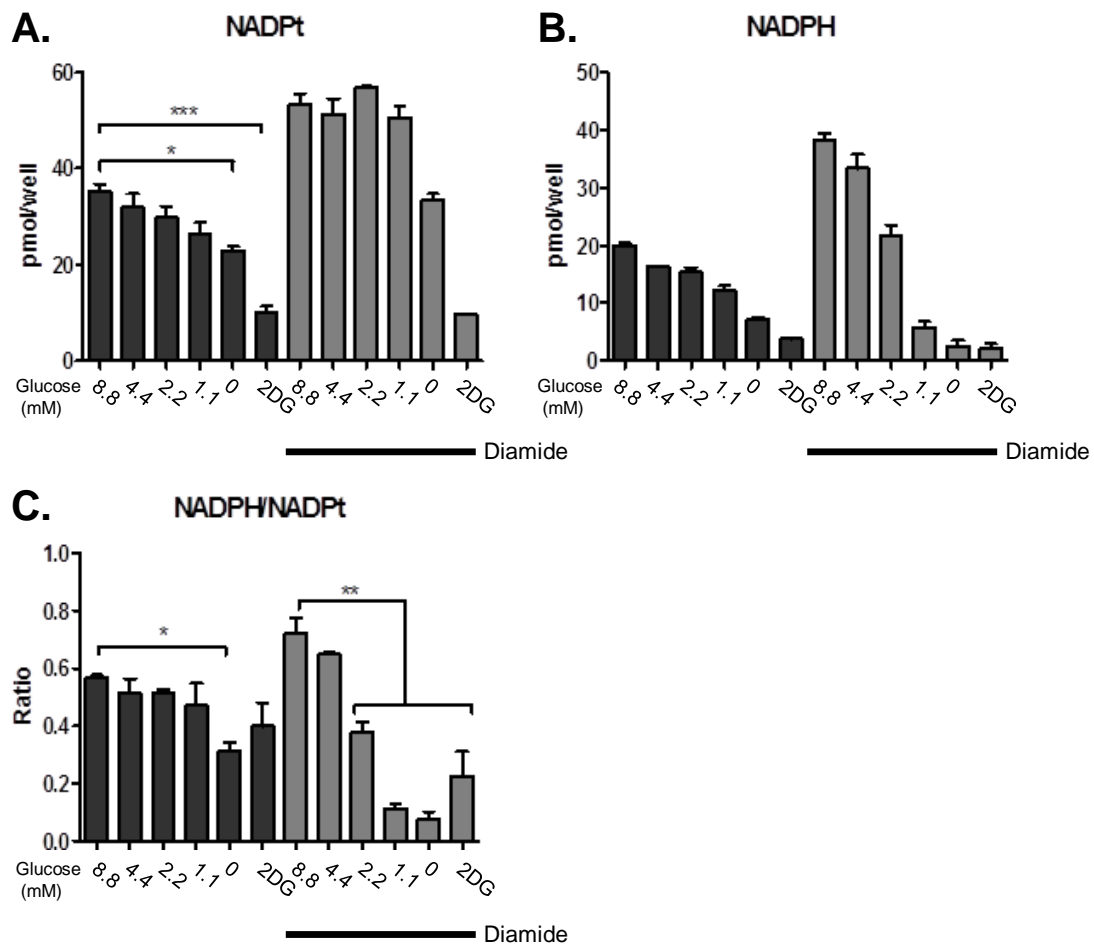


Figure 4.17. Diamide disrupts NADPH/NADPt levels under reduced glucose conditions. U87MG cells were cultured overnight in DMEM +5% FCS supplemented with glucose at the indicated concentrations or 25 mM 2-DG. Cells were then treated with 250 μ M diamide for 15 minutes. Cell lysates were assayed for **A.** total, and **B.** reduced NADPH in order to determine their **C.** ratio.

To evaluate the effect of pharmacologic PKM2 activation on NADPH levels, U87MG cells cultured overnight in the presence of 2.2 mM glucose were treated with WAY677099 or vehicle control for 15 minutes before diamide was added for a further 15 minutes (**Figure 4.18 A-C**). As expected, diamide treatment significantly increased NADPt and decreased NADPH levels, and hence the NADPH/NADPt ratio. Pre-treatment with WAY677099 had no effect on NADPt or NADPH. In a similar experiment, cells were treated with diamide for different lengths of time in order to measure the recovery of NADPH/NADPt following diamide exposure (**Figure 4.18 D**). The drop in NADPH/NADPt induced by diamide exposure persisted for 30 minutes, before recovering to baseline levels at 45 minutes. The

presence of WAY677099 had no inhibitory effect on NADPH/NADPt recovery. In our hands, activation of PKM2 had no effect of NADPH/NADPt in U87MG cells.

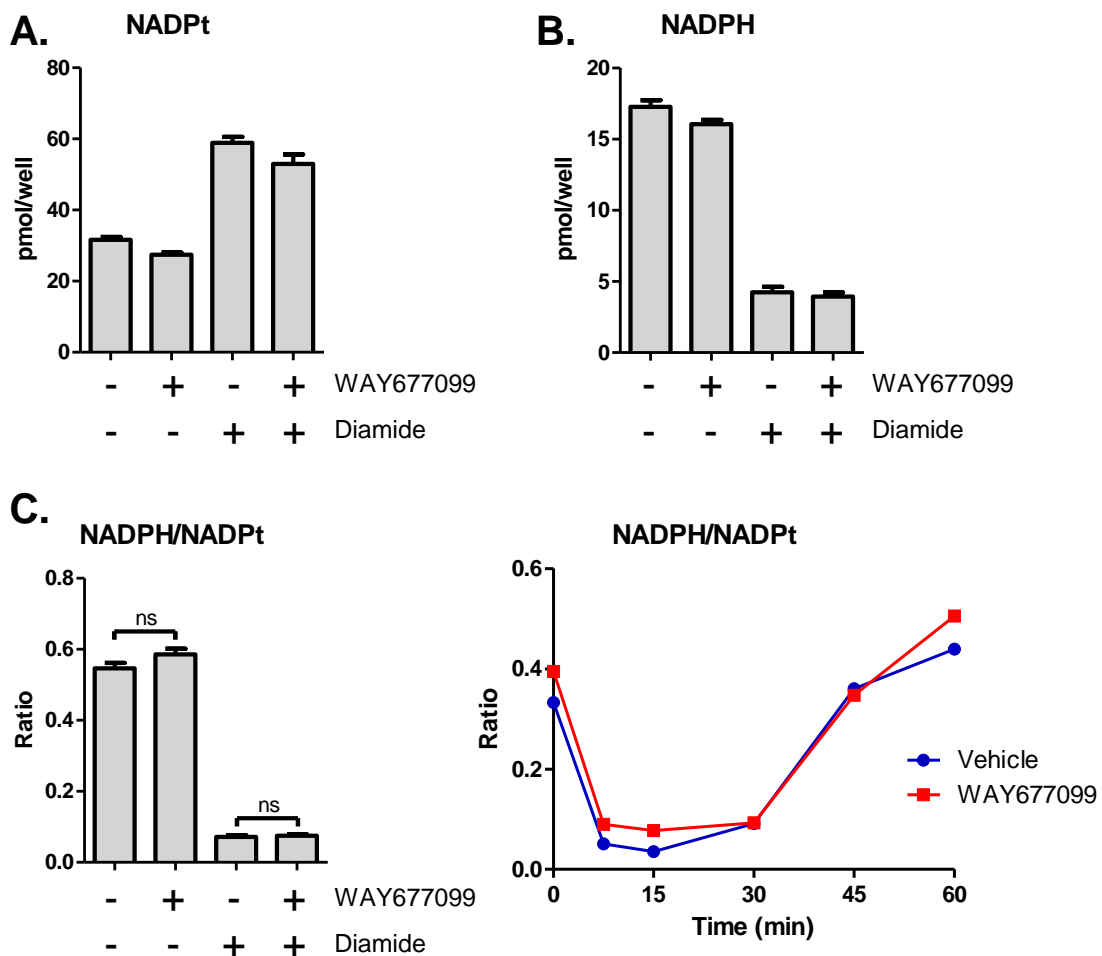


Figure 4.18. WAY677099 does not affect NADPH/NADPt levels in response to diamide.

U87MG cells were cultured overnight in DMEM +5% FCS supplemented with 2.2 mM glucose. **A-C.** WAY677099 was added 15 minutes prior to the addition of diamide. Following 15 minutes exposure to diamide, cell lysates were assayed to determine **A.** total and **B.** reduced NADPH and their **C.** ratio. **D.** The NADPH/NADPt ratio was determined in lysates of U87MG cells exposed to diamide over time in the presence/absence of WAY677099.

Resistance to oxidative stress

PKM2 inactivation is believed to promote cell survival by conferring resistance to oxidative stress.

The PKM2 activator DASA-10 was shown to promote sensitivity to diamide induced oxidative stress and cell death in H1299 cells (Anastasiou et al., 2011).

The present study investigated whether this was also the case for glioma cells treated with WAY677099. Loss of cell viability was assessed in real time in U87MG and SF767 cells treated with WAY677099 or vehicle control with various concentrations of glucose. To induce oxidative stress, 250 μ M diamide was added to the culture media and cells were incubated at 37°C. The culture media also contained 20 μ g/ml propidium iodide (PI), allowing loss of cell viability to be monitored in real time as an increase in PI fluorescence.

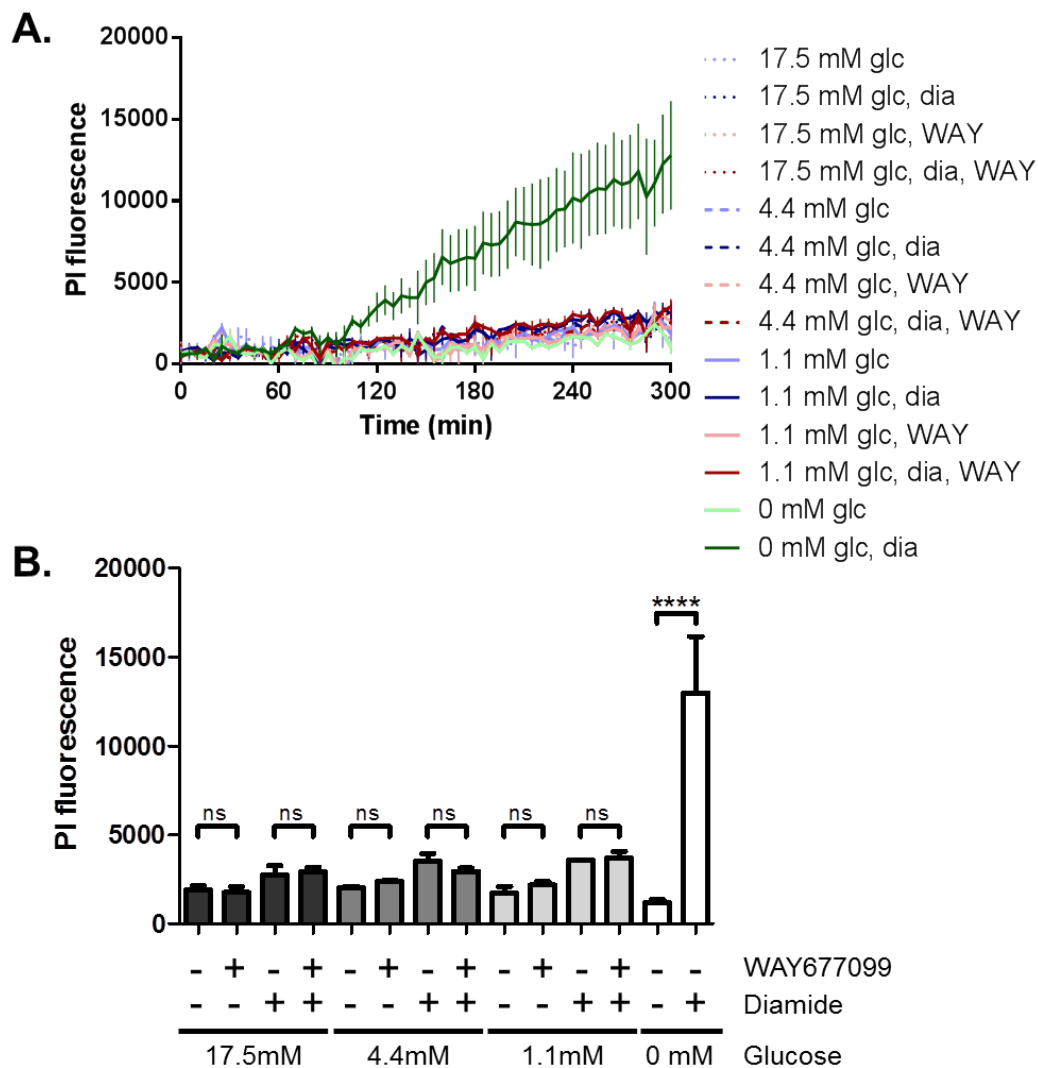


Figure 4.19. WAY677099 does not increase sensitivity to diamide induced cell death. A. U87MG cells were plated at 50,000 cells per well (96 well plate) and treated with 5 μ M WAY677099 (WAY) or vehicle control for 15 minutes in DMEM supplemented with 5% FCS, 20 μ g/ml propidium iodide (PI) and differing concentrations of glucose (glc). 250 μ M of diamide (dia) was added or omitted cells incubated at 37°C for 5 hours while monitoring PI fluorescence. **B.** PI fluorescence at 300 minutes post diamide treatment.

Sensitivity to diamide was highly dependent on glucose availability. In the absence of glucose, loss of viability was detectable in both U87MG and SF767 cells 90 minutes following diamide exposure (**Figure 4.19**). The presence of only 1.1 mM glucose substantially limited the diamide induced loss of viability compared to glucose starved cells. WAY677099 had no detectable effect on the viability of cells following exposure to diamide (**Figure 4.19**). Thus despite the essential requirement of glucose for resistance to oxidative stress, activation of PKM2 has no sensitising effect in glioma cells.

Discussion

Predominant expression of the embryonic pyruvate kinase isoform, PKM2, is a prominent feature of many cancers including high grade gliomas. This isoform has regulatory controls absent in the other PK isoforms, and it has been proposed that these regulatory controls are what allow PKM2 to promote tumour growth by reducing glycolysis flux when necessary. Following on from this, we reasoned that pharmacological activation of PKM2 would abrogate the pro-tumorigenic effects of PKM2 expression.

To test this hypothesis *in vitro*, it was first necessary to identify conditions which favoured dimerisation and inactivation of the enzyme, as it would most likely be these conditions under which a PKM2 activator would exert anti-proliferative effects. Under standard culture conditions, PKM2 in U87MG cells was predominantly tetrameric. Standard culture media glucose concentration is supra-physiological. Lowering glucose concentration to physiologically relevant levels and lower causes the disappearance of tetrameric PKM2, as did inhibition of glycolysis with 2-DG. Overall, this results in increased levels of the upstream glycolysis intermediate phosphoenolpyruvate, and presumably other glycolysis intermediates also, even though glycolytic flux is restricted. This phenomenon has been observed in yeast and *E.coli* cells (Brauer et al., 2006) and may allow cells to maintain levels of

glycolysis intermediates despite glucose restriction, sparing these metabolites for alternate pathways such as the pentose phosphate pathway.

The novel PKM2 activator WAY677099 was capable of promoting tetramer formation under all conditions, except during prolonged (overnight) glucose withdrawal. PKM2 activation resulted in reduced PEP concentration under both normal and glycolysis inhibited conditions.

PKM2 tetramer formation and catalytic activity was lower in proliferating glioma cells compared to cells growth arrested due to contact inhibition. We therefore sought to examine PKM2 tetramer formation at specific stages of the cell cycle. Enrichment of cells at different stages of the cell cycle was achieved through cell cycle synchronisation by serum starvation. This method proved to be quite inefficient, with G_0/G_1 cells out-numbering $S/G_2/M$ cells in every fraction. Nevertheless, fractions with elevated levels of $S/G_2/M$ cells had reduced levels of tetrameric PKM2, suggesting that activity is suppressed during at least some of these stages of the cell cycle. Rather than synchronisation, separation of cells at different stages from a mixed population by techniques such as centrifugal elutriation should yield fractions of much higher purity and give a much clearer picture of PKM2 regulation during the cell cycle.

The current data suggests that PKM2 tetramer formation is suppressed as cells progress through the cell cycle. Others have hypothesised that reducing pyruvate kinase activity favours proliferation by redirection of glycolysis intermediates down alternative biosynthetic pathways, although work in proliferating lymphocytes has shown dramatically increased pyruvate kinase activity during cell cycle progression (Netzker et al., 1992).

Dynamic regulation of PKM2 activity during the cell cycle suggests that this regulation is important for proliferation and that disrupting this regulation by promoting high activity pharmacologically would disrupt cell cycle progression and cell proliferation. U87MG cells were synchronised by serum starvation as before, then cultured in the presence of serum and either

vehicle control or WAY677099 for 18, 24 or 30 hours as these time points exhibit the highest fraction of S/G₂/M cells. The PKM2 activator had no effect on progression through the cell cycle of synchronised cells as shown by flow cytometry. Similarly, WAY677099 had no effect on cell proliferation as determined by MTS assay.

Aerobic glycolysis is a ubiquitous phenomenon of proliferating cells including cancer cells. While the function of aerobic glycolysis remains elusive, it is believed that its reversal may have anti-proliferative effects, providing a novel therapeutic avenue for the treatment of cancer. It has been suggested that low activity PKM2 is a key driver of aerobic glycolysis and that increasing pyruvate kinase activity would suppress aerobic glycolysis and increase respiration, shifting cells away from a metabolic phenotype that favours proliferation.

Pharmacologic activation of PKM2 with WAY677099 led to suppression of respiration in both glioma cell lines and HCC cell lines. WAY677099 also increased glycolytic rates in HCC cell lines, however this effect was not observed in glioma cell lines. This is consistent with the recent observation that HK2 and not PKM2 is a major driver of aerobic glycolysis in glioma cells (Wolf et al., 2011). Nevertheless, the overall effect of PKM2 activation was to increase the fraction of ATP generated via glycolysis rather than respiration. PKM2 activation enhances, rather than suppresses the Warburg effect.

We initially hypothesised that the decrease in mitochondrial respiration was a manifestation of the Crabtree effect, where the presence of glucose promotes increased glycolysis and in turn decreases respiration in proliferating cells. While different theories exist to explain this phenomenon, it is known that uncouplers such as DNP and FCCP release mitochondria from this effect. If the Crabtree effect was responsible for suppression of respiration by WAY677099, this suppression should be relieved by uncoupling mitochondria with FCCP. This was not the case. FCCP actually maintained or exacerbated the inhibitory effects WAY677099 on respiration. Therefore an alternative explanation was required.

It was recently shown in yeast that low pyruvate kinase activity supports respiration by redirecting glycolytic intermediates into the oxidative arm of the pentose phosphate pathway (oxPPP), allowing for the maintenance of NADPH levels necessary to counteract the effects of mitochondrially derived reactive oxygen species that can inhibit mitochondrial respiration. Thus while glucose can suppress respiration via the Crabtree effect, supply of glucose for production of glycolytic intermediates is necessary for maximal mitochondrial respiration due to its role in suppressing oxidative stress.

Here, we show that glucose supports higher respiration rates in uncoupled mitochondria. Compared to glucose fed cells, where respiration continued to increase with up-to 1 mM FCCP, the same concentration of FCCP led to a reduction in respiration in the absence of glucose. Supply of glucose is a limiting factor in determining maximal mitochondrial respiration. It is unlikely that this effect is due to a limitation of substrates for the TCA cycle, as cells were supplied with glutamine and/or pyruvate in respiration experiments. Therefore withdrawal of glucose likely led to depletion of glycolytic intermediates that support respiration via activity of the oxPPP.

If this were the case, PKM2 activation with WAY677099 and glucose withdrawal should be expected to cooperate to suppress mitochondrial respiratory capacity. Indeed WAY677099 was far more potent at inhibiting respiration when glucose supply was restricted.

One obvious question raised is how a glycolytic enzyme activator can have metabolic effects in the absence of glucose. Astrocytes maintain glycogen stores to support neuronal activity during hypoglycaemia or periods of intense activity (Brown and Ransom, 2007, Wender et al., 2000). The glycogen content of human gliomas is extremely variable, ranging from 0.05% to 6% of dry weight (Lowry et al., 1977). Glycogen, if present in the cells used here may provide an alternate, limited source of glycolysis intermediates during glucose withdrawal.

We sought to demonstrate that activation of PKM2 with WAY677099 could disrupt NADPH homeostasis. This is a key aspect of the redox feedback hypothesis of how PKM2 activation suppresses respiration, as well as the hypothesis that PKM2 activators are of therapeutic significance due to their ability to sensitise cells to oxidative stress. Increasing pyruvate kinase activity has previously been shown to increase susceptibility to oxidative stress in both mammalian and yeast cells. Further, in yeast at least, this effect appears to be responsible for decreased capacity for mitochondrial respiration.

PKM2 was shown to undergo oxidation of cysteine residues in response to diamide induced oxidative stress as well as FCCP induced respiratory stimulation, each leading to dissociation of PKM2 tetramers and loss of enzyme activity. All these effects could be blocked by WAY677099. These observations support the notion that PKM2 can respond to oxidative stress, becoming inactive in order to redirect flux into the oxPPP in order to maintain NADPH levels. However, although glucose was essential for maintenance of NADPH during diamide induced oxidative stress, PKM2 activation with WAY677099 had no impact on the capacity of glioma cells to maintain NADPH levels. PKM2 activation with WAY677099 also had no effect on cell viability following diamide exposure.

Factors that influence PKM2 dimer and tetramer formation are summarised in (**Table4.1.**)

Promotes dimer formation	Promotes tetramer formation
Glucose restriction/glycolysis inhibition	Glucose availability
Serum starvation	Serum stimulation
S/G2/M phase of cell cycle	G1 phase of cell cycle
Oxidative stress	
Mitochondrial uncoupling	

Table 4.1. Factors promoting PKM2 dimer or tetramer formation in U87MG cells

In conclusion, despite evidence for dynamic regulation of PKM2 activity and tetramer formation in glioma cells, no evidence for therapeutic value of pharmacologic activation of PKM2 could be identified. It remains to be seen whether glioma cells are sensitive to PKM2 activation during other stress conditions such as hypoxia or serine withdrawal as has been reported in other cell systems.

Activation of PKM2 with WAY677099 resulted in suppression of mitochondrial respiration. The Crabtree effect hypothesis was ruled out as a possible mechanism for this effect. While some experimental results were consistent with the 'redox feedback loop' hypothesis, others were inconsistent with the model. In particular the lack of effect of WAY677099 on NADPH levels, means that a description of how PKM2 activation causes suppression of respiration remains unknown.

References

- ANASTASIOU, D., POULOGIANNIS, G., ASARA, J. M., BOXER, M. B., JIANG, J. K., SHEN, M., BELLINGER, G., SASAKI, A. T., LOCASALE, J. W., AULD, D. S., THOMAS, C. J., VANDER HEIDEN, M. G. & CANTLEY, L. C. 2011. Inhibition of pyruvate kinase M2 by reactive oxygen species contributes to cellular antioxidant responses. *Science*, 334, 1278-83.
- ANASTASIOU, D., YU, Y., ISRAELSEN, W. J., JIANG, J. K., BOXER, M. B., HONG, B. S., TEMPEL, W., DIMOV, S., SHEN, M., JHA, A., YANG, H., MATTAINI, K. R., METALLO, C. M., FISKE, B. P., COURTNEY, K. D., MALSTROM, S., KHAN, T. M., KUNG, C., SKOUMBOURDIS, A. P., VEITH, H., SOUTHALL, N., WALSH, M. J., BRIMACOMBE, K. R., LEISTER, W., LUNT, S. Y., JOHNSON, Z. R., YEN, K. E., KUNII, K., DAVIDSON, S. M., CHRISTOFK, H. R., AUSTIN, C. P., INGLESE, J., HARRIS, M. H., ASARA, J. M., STEPHANOPOULOS, G., SALITURO, F. G., JIN, S., DANG, L., AULD, D. S., PARK, H. W., CANTLEY, L. C., THOMAS, C. J. & VANDER HEIDEN, M. G. 2012. Pyruvate kinase M2 activators promote tetramer formation and suppress tumorigenesis. *Nat Chem Biol*.
- ASHIZAWA, K., WILLINGHAM, M. C., LIANG, C. M. & CHENG, S. Y. 1991. In vivo regulation of monomer-tetramer conversion of pyruvate kinase subtype M2 by glucose is mediated via fructose 1,6-bisphosphate. *J Biol Chem*, 266, 16842-6.
- BLUEMLEIN, K., GRUNING, N. M., FEICHTINGER, R. G., LEHRACH, H., KOFLER, B. & RALSER, M. 2011. No evidence for a shift in pyruvate kinase PKM1 to PKM2 expression during tumorigenesis. *Oncotarget*, 2, 393-400.
- BRAUER, M. J., YUAN, J., BENNETT, B. D., LU, W., KIMBALL, E., BOTSTEIN, D. & RABINOWITZ, J. D. 2006. Conservation of the metabolomic response to starvation across two divergent microbes. *Proc Natl Acad Sci U S A*, 103, 19302-7.
- BROWN, A. M. & RANSOM, B. R. 2007. Astrocyte glycogen and brain energy metabolism. *Glia*, 55, 1263-71.
- CHRISTOFK, H. R., VANDER HEIDEN, M. G., HARRIS, M. H., RAMANATHAN, A., GERSZTEN, R. E., WEI, R., FLEMING, M. D., SCHREIBER, S. L. & CANTLEY, L. C. 2008. The M2 splice isoform of pyruvate kinase is important for cancer metabolism and tumour growth. *Nature*, 452, 230-3.
- DALY, M. E., VALE, C., WALKER, M., LITTLEFIELD, A., ALBERTI, K. G. & MATHERS, J. C. 1998. Acute effects on insulin sensitivity and diurnal metabolic profiles of a high-sucrose compared with a high-starch diet. *Am J Clin Nutr*, 67, 1186-96.
- DESAI, S., DING, M., WANG, B., LU, Z., ZHAO, Q., SHAW, K., YUNG, W. K., WEINSTEIN, J. N., TAN, M. & YAO, J. 2013. Tissue-specific isoform switch and DNA hypomethylation of the pyruvate kinase PKM gene in human cancers. *Oncotarget*.
- GOSALVEZ, M., LOPEZ-ALARCON, L., GARCIA-SUAREZ, S., MONTALVO, A. & WEINHOUSE, S. 1975. Stimulation of tumor-cell respiration by inhibitors of pyruvate kinase. *Eur J Biochem*, 55, 315-21.

- GRUNING, N. M., RINNERHALER, M., BLUEMLEIN, K., MULLEDER, M., WAMELINK, M. M., LEHRACH, H., JAKOBS, C., BREITENBACH, M. & RALSER, M. 2011. Pyruvate kinase triggers a metabolic feedback loop that controls redox metabolism in respiring cells. *Cell Metab*, 14, 415-27.
- HITOSUGI, T., KANG, S., VANDER HEIDEN, M. G., CHUNG, T. W., ELF, S., LYTHGOE, K., DONG, S., LONIAL, S., WANG, X., CHEN, G. Z., XIE, J., GU, T. L., POLAKIEWICZ, R. D., ROESEL, J. L., BOGGON, T. J., KHURI, F. R., GILLILAND, D. G., CANTLEY, L. C., KAUFMAN, J. & CHEN, J. 2009. Tyrosine phosphorylation inhibits PKM2 to promote the Warburg effect and tumor growth. *Sci Signal*, 2, ra73.
- IBSEN, K. H., ORLANDO, R. A., GARRATT, K. N., HERNANDEZ, A. M., GIORLANDO, S. & NUNGARAY, G. 1982. Expression of multimolecular forms of pyruvate kinase in normal, benign, and malignant human breast tissue. *Cancer Res*, 42, 888-92.
- KUMAR, Y., MAZUREK, S., YANG, S., FAILING, K., WINSLET, M., FULLER, B. & DAVIDSON, B. R. 2010. In vivo factors influencing tumour M2-pyruvate kinase level in human pancreatic cancer cell lines. *Tumour Biol*, 31, 69-77.
- LOWRY, O. H., BERGER, S. J., CHI, M. M., CARTER, J. G., BLACKSHAW, A. & OUTLAW, W. 1977. Diversity of metabolic patterns in human brain tumors--I. High energy phosphate compounds and basic composition. *J Neurochem*, 29, 959-77.
- LUNT, S. Y. & VANDER HEIDEN, M. G. 2011. Aerobic glycolysis: meeting the metabolic requirements of cell proliferation. *Annu Rev Cell Dev Biol*, 27, 441-64.
- LV, L., LI, D., ZHAO, D., LIN, R., CHU, Y., ZHANG, H., ZHA, Z., LIU, Y., LI, Z., XU, Y., WANG, G., HUANG, Y., XIONG, Y., GUAN, K. L. & LEI, Q. Y. 2011. Acetylation targets the M2 isoform of pyruvate kinase for degradation through chaperone-mediated autophagy and promotes tumor growth. *Mol Cell*, 42, 719-30.
- NETZKER, R., GREINER, E., EIGENBRODT, E., NOGUCHI, T., TANAKA, T. & BRAND, K. 1992. Cell cycle-associated expression of M2-type isozyme of pyruvate kinase in proliferating rat thymocytes. *J Biol Chem*, 267, 6421-4.
- REINACHER, M., EIGENBRODT, E., GERBRACHT, U., ZENK, G., TIMMERMANN-TROSIENER, I., BENTLEY, P., WAECHTER, F. & SCHULTE-HERMANN, R. 1986. Pyruvate kinase isoenzymes in altered foci and carcinoma of rat liver. *Carcinogenesis*, 7, 1351-7.
- SINN, B., TALLEN, G., SCHROEDER, G., GRASSL, B., SCHULZE, J., BUDACH, V. & TINHOFER, I. 2010. Caffeine confers radiosensitisation of PTEN-deficient malignant glioma cells by enhancing ionizing radiation-induced G1 arrest and negatively regulating Akt phosphorylation. *Mol Cancer Ther*, 9, 480-8.
- TREMP, G. L., BOQUET, D., RIPOCHE, M. A., COGNET, M., LONE, Y. C., JAMI, J., KAHN, A. & DAEGELEN, D. 1989. Expression of the rat L-type pyruvate kinase gene from its dual erythroid- and liver-specific promoter in transgenic mice. *J Biol Chem*, 264, 19904-10.
- WENDER, R., BROWN, A. M., FERN, R., SWANSON, R. A., FARRELL, K. & RANSOM, B. R. 2000. Astrocytic glycogen influences axon function and survival during glucose deprivation in central white matter. *J Neurosci*, 20, 6804-10.
- WOLF, A., AGNIHOTRI, S., MICALLEF, J., MUKHERJEE, J., SABHA, N., CAIRNS, R., HAWKINS, C. & GUHA, A. 2011. Hexokinase 2 is a key mediator of aerobic glycolysis and promotes tumor growth in human glioblastoma multiforme. *J Exp Med*, 208, 313-26.
- YACOVAN, A., OZERI, R., KEHAT, T., MIRILASHVILI, S., SHERMAN, D., AIZIKOVICH, A., SHITRIT, A., BEN-ZEEV, E., SCHUTZ, N., BOHANA-KASHTAN, O., KONSON, A., BEHAR, V. & BECKER, O. M. 2012. 1-(sulfonyl)-5-(arylsulfonyl)indoline as activators of the tumor cell specific M2 isoform of pyruvate kinase. *Bioorg Med Chem Lett*.
- YANG, W. & LU, Z. 2013. Regulation and function of pyruvate kinase M2 in cancer. *Cancer Lett*.

Chapter 5 - Inhibition of Glucose Metabolism by Temsirolimus

Table of Figures	180
Introduction.....	181
Results	182
PKM2 tetramer formation is promoted by c-Met signalling	182
PKM2 tetramer formation is promoted by mTOR independent of c-Met.....	182
Temsirolimus inhibits glycolysis to reverse the Warburg effect.....	183
Activation of PKM2 fails to restore glycolysis inhibited by Temsirolimus	187
Inhibition of mTOR increases sensitivity to oxidative stress	188
Temsirolimus does not acutely affect hexokinase activity	190
Temsirolimus mimics the effects of glucose restriction on coupled and uncoupled respiration	191
Discussion	192
References.....	195

Table of Figures

Figure 5.1. Effect of c-Met and mTOR inhibition on PKM2 tetramer and PK activity.	183
Figure 5.2. Effect of c-Met and mTOR inhibition on activation of the c-Met/Akt/mTOR signalling axis.	184
Figure 5.3. Temsirolimus inhibits glycolysis to reverse the Warburg effect.....	186
Figure 5.4. Temsirolimus inhibition of PKM2 activity, but not inhibition of glycolysis reversed by WAY677099.	187
Figure 5.5. Glucose dependent effects of diamide and temsirolimus on cellular NADPH.	188
Figure 5.6. Glucose concentration dependent sensitisation to diamide induced cell death by temsirolimus.	189
Figure 5.7. Temsirolimus does not acutely inhibit hexokinase activity.	190
Figure 5.8. Effect of Temsirolimus on coupled and uncoupled respiration.	191

Introduction

The rapamycin sensitive mTOR complex TORC1 is a major node of intracellular signalling, integrating inputs originating from a diverse range of stimuli including growth factor signalling via PI3K/Akt and Raf/MAPK, along with sensors of the metabolic state of the cell, including energy state, nutrient and amino-acid availability, as well as redox balance and cellular stress (Russell et al., 2011). Mutation, overexpression or activation of cell surface receptor tyrosine kinases (RTKs) is a frequently observed feature of many cancers, particularly GBMs and leads to increased activation of TORC1 (TCGA-Consortium, 2008). This activation has profound effects on the cell including increased protein translation and ribosome biogenesis, increased cell size and suppression of autophagy. By integrating inputs from mitogenic signalling and metabolic sensors, TORC1 signalling allows cells to grow and proliferate only in the context of a favourable metabolic state (Gwinn et al., 2008).

When active, TORC1 functions as a serine/threonine kinase. Two of the best described targets of TORC1 phosphorylation are p70-S6K and 4E-BP1. TORC1 phosphorylation of p70-S6K initiates a cascade of events leading to phosphorylation and activation of the S6 ribosomal protein. Although the function of the S6 ribosomal protein is only poorly understood, phosphorylation is believed to enhance protein translation by the ribosomes (Ruvinsky and Meyuhas, 2006). Phosphorylation of 4EBP1 by TORC1 promotes its dissociation from the eukaryotic translation initiation factor eIF4E allowing assembly of the eukaryotic translation apparatus and cap dependent protein translation.

Despite some reports to the contrary (Ramanathan and Schreiber, 2009), signalling through TORC1 is generally considered to promote increased glycolysis (Wei et al., 2008, Buller et al., 2008). These effects have been primarily ascribed to TORC1 up-regulation of HIF1 α even in normoxic conditions, leading to increased expression of glycolytic enzymes (Duvel et al., 2010).

While investigating factors that regulate PKM2, we found that inhibition of TORC1 by the rapalog temsirolimus resulted in inhibition of PKM2. This effect was secondary to a rapid and profound inhibition of glycolysis in glioma cells. Using lessons learned from the previous chapter about the

requirement of glucose for resistance to oxidative stress, we attempted to exploit this glycolysis inhibiting effect to sensitise glioma cells to oxidative induced cell death.

Here, we show that TORC1 inhibition results in rapid reversal of the Warburg effect in glioma cells. By suppressing glucose metabolism, temsirolimus also hinders the ability of glioma cells to maintain redox control, sensitising these cells to oxidant induced cell death.

Results

PKM2 tetramer formation is promoted by c-Met signalling

Phosphorylation, mediated by a number of tyrosine kinases has previously been shown to promote dissociation of PKM2 tetramers and a reduction in activity. The role of c-Met signalling in the regulation of PKM2 signalling has not been examined previously. Production of HGF by the U87MG cell line maintains low level c-Met activation in this cell line, which can be inhibited by the c-Met inhibitor su11274. Exposure of U87MG cells to su11274 resulted in a reduction in both PKM2 tetramer formation and PK activity (**Figure 5.1**), suggesting that c-Met signalling promotes, rather than suppresses PKM2 activation. Similar effects of PKM2 inactivation have been observed in the HCC cell line Huh1 using the c-Met inhibitor PF2341066 (not shown).

PKM2 tetramer formation is promoted by mTOR independent of c-Met

A major effector pathway of c-Met signalling is the PI3K/Akt/mTOR signalling pathway. We anticipated that if down-regulation of PKM2 tetramer by c-Met inhibition was due to suppression of PI3K/Akt/mTOR signalling, inhibition of mTOR with rapalogs should produce a similar effect. Indeed exposure of U87MG cells to temsirolimus also resulted in loss of PKM2 tetramer and PK activity (**Figure 5.1**).

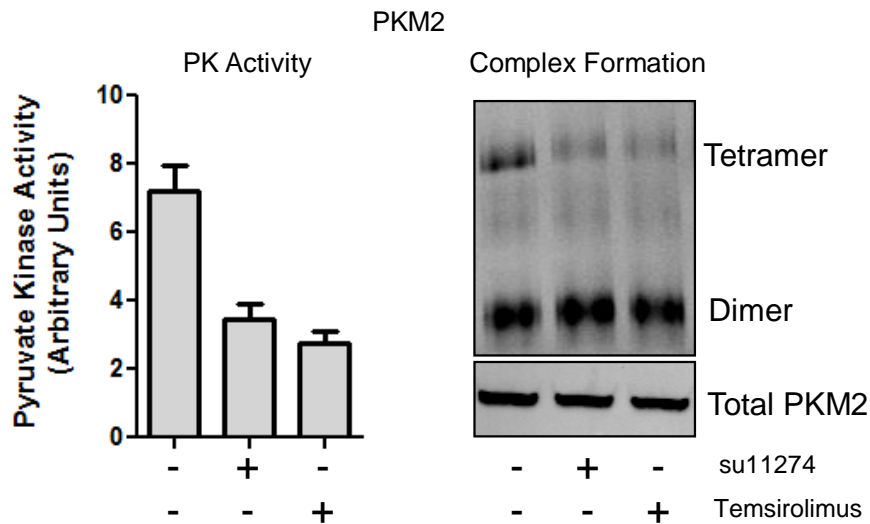


Figure 5.1. Effect of c-Met and mTOR inhibition on PKM2 tetramer and PK activity. U87MG cells were treated with the c-Met inhibitor, su11274 2 μ M or the mTOR inhibitor, temsirolimus 5 μ M overnight. Cell lysates were assayed for pyruvate kinase activity and PKM2 tetramer formation.

To confirm that the c-Met inhibitor su11274 and the rapalog temsirolimus were both acting via inhibition of TORC1 inhibition, the effect of each inhibitor on components of the c-Met/mTOR signalling axis was measured. Activation of c-Met was assessed by tyrosine phosphorylation (**Figure 5.2 A**), Akt activation by serine phosphorylation (**Figure 5.2 B**), and TORC1 activity was determined by measuring p70-S6K threonine phosphorylation (**Figure 5.2 C**).

As expected, treatment of U87MG cells with su11274 dramatically inhibited c-Met, leading to reduced pAkt. However surprisingly, p70-S6K phosphorylation was maintained in c-Met inhibited cells, demonstrating that reduced TORC1 signalling does not mediate the effects of c-Met on PKM2. As expected, temsirolimus did lead to robust inhibition of p70-S6K phosphorylation, indicating a reduction in TORC1 activity. Together, these results show that while inhibition of c-Met and TORC1 lead to loss of PKM2 tetramers, they are not acting via a similar pathway.

Temsirolimus inhibits glycolysis to reverse the Warburg effect

Because su11274 and temsirolimus both resulted in reduced PKM2 activity, their effects on glycolytic rate were evaluated using the pH indicator based H^+ production assay. temsirolimus, but not su11274 resulted in a dramatic inhibition of glycolysis in U87MG cells (**Figure 5.3 B**). By

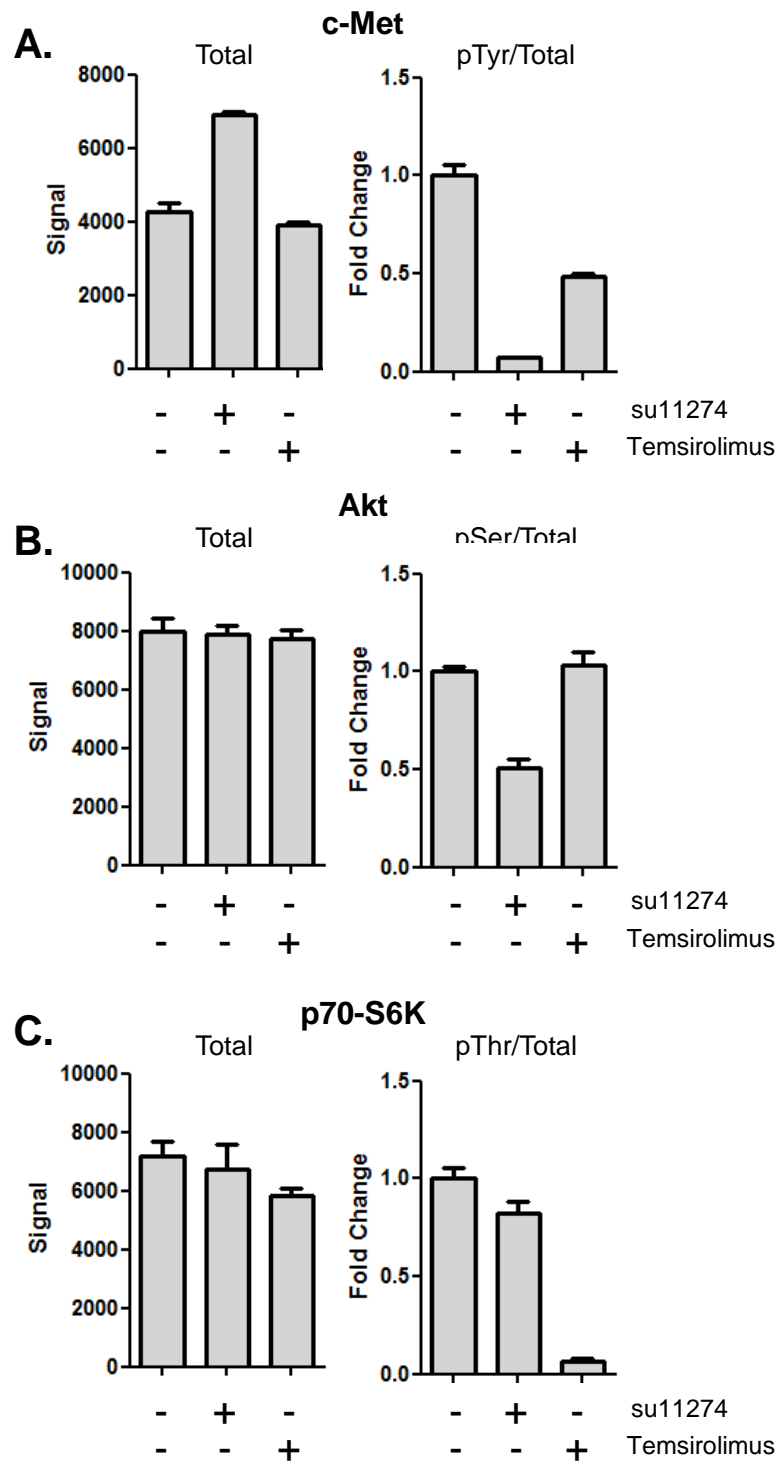


Figure 5.2. Effect of c-Met and mTOR inhibition on activation of the c-Met/Akt/mTOR signalling axis. U87MG cells were treated with the c-Met inhibitor, su11274 2 μ M or the mTOR inhibitor 5 μ M, temsirolimus overnight and cell lysates were analysed by Luminex bead based ELISA. **A.** Expression of total c-Met and the ratio of phospho/total c-Met. **B.** Expression of total Akt and the ratio of phospho/total Akt in cell lysates **C.** Expression of total p70S6K and the ratio of phospho/total p70S6K.

inhibiting glycolysis, temsirolimus was also able to block the Crabtree effect (described in Chapter 1), resulting in increased oxygen consumption in glioma cells in the presence of glucose (**Figure 5.3 A**). Using the Oroboros Oxygraph, respiration was measured in U87MG and SF767 cells in glucose free DMEM. Under these conditions, temsirolimus had no effect on respiration, suggesting the compound has no acute effect on mitochondrial function. In vehicle control treated cells, addition of 1.1 mM glucose caused an immediate drop in respiration in vehicle control treated U87MG cells. The addition of temsirolimus just a few minutes prior severely blunted the inhibitory effect of glucose on respiration. Additional glucose did promote further suppression of respiration in temsirolimus treated U87MG cells.

SF767 cells exhibited a much weaker Crabtree effect, with higher glucose concentrations required before inhibition of respiration became apparent. As with U87MG, treatment of SF767 cells with temsirolimus had no effect on respiration in the absence of glucose, but prevented glucose induced suppression of respiration.

Just as glucose is able to suppress respiration through the Crabtree effect, aerobic respiration can also suppress glycolysis, known as the Pasteur effect. Another potential explanation for suppression of glycolysis by temsirolimus is that the drug promotes increased mitochondrial function and energy production via OXPHOS leading to a suppression of glycolysis i.e. the Pasteur effect.

To evaluate this possibility, the glycolytic rate was measured in the presence of FCCP to uncouple respiration from ATP production (**Figure 5.3 C**). If glycolysis suppression is due to a favouring of energy production via OXPHOS, FCCP would be expected to restore the glycolytic rate in the presence of temsirolimus. As expected, the addition of FCCP to control treated cells resulted in increased H⁺ production, as the cells become dependent on glycolysis for ATP regeneration. Temsirolimus was able to suppress glycolysis in FCCP treated cells to the same extent as vehicle control treated cells. Therefore suppressed glycolysis is not a consequence of increased

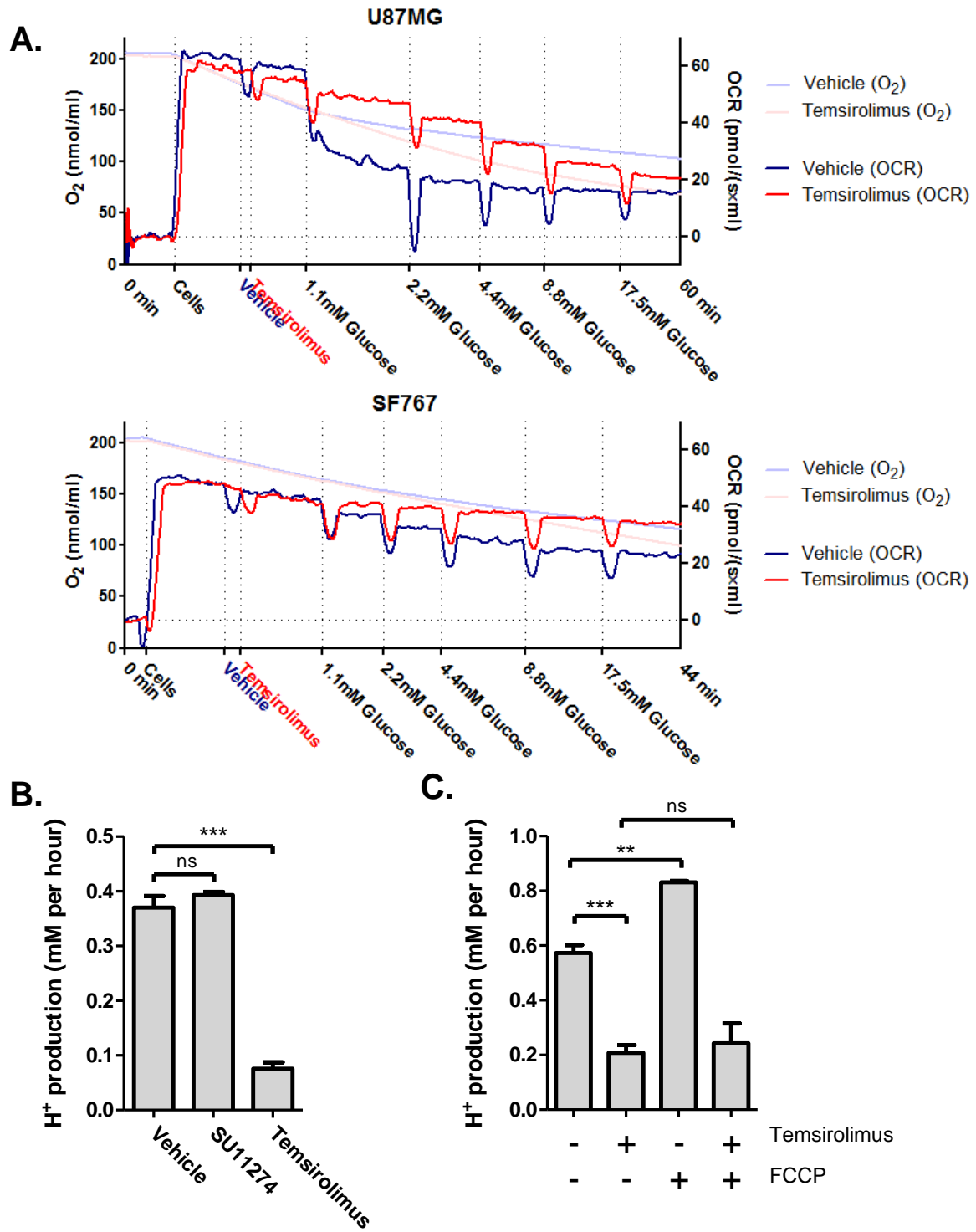


Figure 5.3. Temsirolimus inhibits glycolysis to reverse the Warburg effect. **A.** Respiration of U87MG and SF767 cells in glucose free DMEM measured using the oxygraph. Vehicle control or temsirolimus to a final concentration of 5 μ M was added to each chamber, followed by increasing concentrations of glucose as indicated. **B.** Glycolytic rate of U87MG cells in assay media containing 4 mM glucose and either vehicle control, 2 μ M SU11274, or 5 μ M temsirolimus. **C.** Glycolytic rate of SF767 cells in assay media containing 17.5 mM glucose and vehicle control, 5 μ M temsirolimus or 1 μ M FCCP.

mitochondrial respiration, but rather respiration is maintained to compensate for reduced glycolytic flux.

Activation of PKM2 fails to restore glycolysis inhibited by Temsirolimus

Treating glioma cells with temsirolimus led to inhibition of glycolysis, and the glycolytic enzyme PKM2. Inhibition of pyruvate kinase would be expected to result in inhibition of glycolysis. Similarly, as was seen in Chapter 4, inhibition of glycolysis can also result in inhibition of PKM2. To determine whether PKM2 inhibition was the cause or a consequence of inhibition of glycolysis, PKM2 activity was restored using WAY677099 and the effect on glycolysis was assessed. WAY677099 was able to completely restore pyruvate kinase activity in cells treated with temsirolimus (**Figure 5.4 A**) however this did not lead to a recovery in the glycolytic rate (**Figure 5.4 B**). Therefore it was concluded that PKM2 inhibition was a consequence of inhibition of glycolysis at a different point in the pathway.

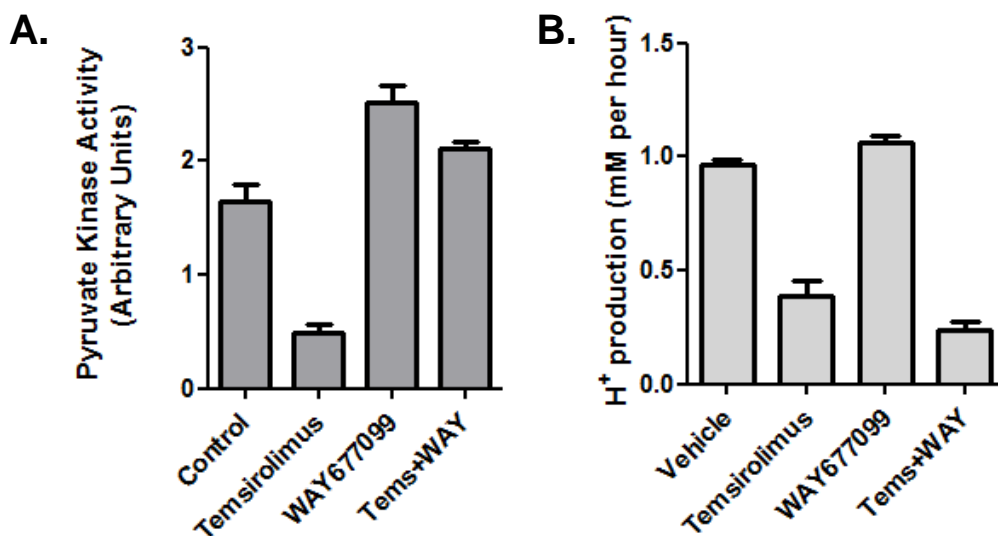


Figure 5.4. Temsirolimus inhibition of PKM2 activity, but not inhibition of glycolysis reversed by WAY677099. **A.** U87MG cells were treated with vehicle control, temsirolimus or WAY677099 for 1 hour and assayed for PK activity. **B.** U87MG cells plated at 80,000 cells per well. H⁺ production monitored in assay media containing 17.5 mM glucose with vehicle control or 5 μ M temsirolimus in the absence or presence of WAY677099. Calculated glycolytic rates from 30-150 minutes post treatment.

Inhibition of mTOR increases sensitivity to oxidative stress

In Chapter 4, it was shown that resistance of U87MG and SF767 cells to oxidative stress induced by diamide was highly dependent on the availability of glucose, and this was associated with the ability of cells to maintain a high NADPH/NADPt ratio, presumably via oxidative PPP activity, following diamide exposure.

Temsirolimus inhibits glycolysis through an unknown mechanism. If the target site of temsirolimus lies upstream of the branching of glycolysis and the oxidative pentose phosphate pathway, i.e. at hexokinase or the glucose transporters, then treatment with temsirolimus should mimic the effects of glucose restriction on redox control and sensitivity to oxidative stress.

U87MG cells cultured short term (90 minutes) in different concentrations of glucose in the presence of temsirolimus or vehicle control were treated with diamide for 15 minutes and the levels of NADPH/NADPt in cell lysates was measured (**Figure 5.5**). Temsirolimus alone had no effect on the NADPH/NADPt ratio. However, cells treated with temsirolimus were less capable of maintaining a high NADPH/NADPt ratio when challenged with diamide induced oxidative stress.

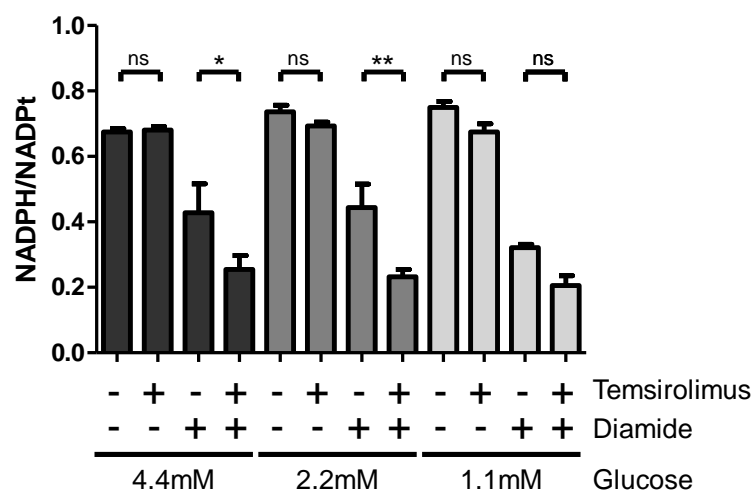


Figure 5.5. Glucose dependent effects of diamide and temsirolimus on cellular NADPH. U87MG cells plated at 80,000 cells/well (96 well plate) were treated with 5 μ M temsirolimus or vehicle control for 90 minutes in DMEM supplemented with 5% FCS and differing concentrations of glucose. 250 μ M of diamide was added or omitted and cells incubated for a further 15 minutes. NADPH/NADPt ratio was determined.

oxidative stress and cell death. The onset of diamide induced cell death in temsirolimus-treated cells became apparent approximately 90 minutes following diamide exposure. The magnitude of this effect was influenced by glucose concentration, with cell death significantly higher in the presence of 1.1 mM glucose compared to 4.4 mM glucose.

Temsirolimus does not acutely affect hexokinase activity

The inability of temsirolimus-treated glioma cells to maintain NADPH levels following diamide exposure is indicative of inhibition of flux through the PPP. Inhibition of both glycolysis and the PPP by temsirolimus suggests that the metabolic target lies upstream of the branching of these two pathways, i.e. at the level of glucose transport or hexokinase.

Inhibition of TORC1 in U87MG cells by rapamycin has been shown previously to have no effect on the activity or localisation of glucose transporters, however a reduction in hexokinase activity was apparent 24 hours following treatment (Wei et al., 2008). To evaluate whether hexokinase activity could account for the rapid effects observed, hexokinase activity in lysates from U87MG cells was measured after treatment with temsirolimus for 1 and 3 hours. At these time points, temsirolimus had no effect on hexokinase activity (**Figure 5.7**).

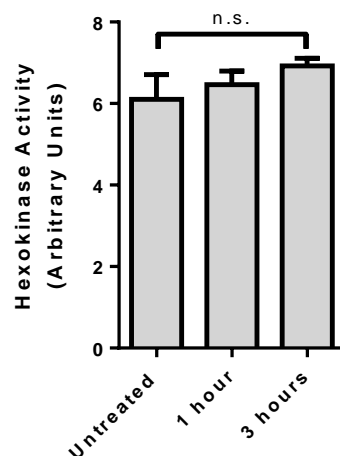


Figure 5.7. Temsirolimus does not acutely inhibit hexokinase activity. U87MG cells were untreated or treated with 5 μ M temsirolimus for 1 or 3 hours and lysates assayed for hexokinase activity.

Temsirolimus mimics the effects of glucose restriction on coupled and uncoupled respiration

In Chapter 4, it was shown that while glucose can suppress coupled respiration, while supporting FCCP uncoupled respiration. We suspected, but did not demonstrate, that this effect was a due to glucose feeding into the pentose phosphate pathway for production of NADPH.

We tested whether temsirolimus could also block this second effect of glucose on respiration. Respiration was measured in SF767 cells in glucose free DMEM using the Oxygraph (**Figure 5.8**). As seen in (**Figure 5.3**), temsirolimus addition had no effect on respiration but compared to vehicle control treatment, prevented the suppressive effects of glucose. With the addition of 500 nM FCCP, respiration increased to a similar level in both chambers. With additional FCCP, respiration in vehicle control treated cells continued to increase, while respiration failed to increase, eventually decreasing in cells treated with temsirolimus. Thus temsirolimus produces a similar effect on coupled and uncoupled respiration to glucose withdrawal.

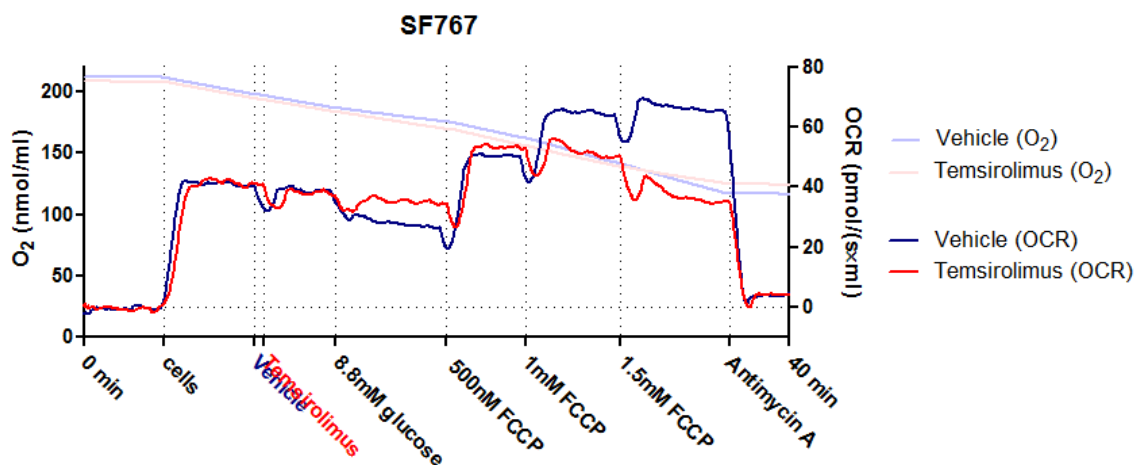


Figure 5.8. Effect of Temsirolimus on coupled and uncoupled respiration. Respiration of SF767 cells using oxygraph. 1.5×10^6 SF767 cells were injected into each chamber containing glucose free DMEM followed by injections of 5 μ M temsirolimus or vehicle control, glucose and increasing amounts of FCCP. Respiration was terminated with the addition of 1.25 μ M Antimycin A.

Discussion

Reports of the effect of TORC1 signalling and its inhibition on glycolysis and respiration have been mixed, with some publications showing TORC1 signalling favours glycolysis, while others show increased respiration. In Jurkat cells, increased $\Delta\Psi_m$ and respiration correlated positively with p70S6K phosphorylation, and rapamycin treatment resulted in reduced oxygen consumption in these cells (Schieke et al., 2006). This was also associated with increased glycolysis and sensitivity to glycolysis inhibition by 2-DG (Ramanathan and Schreiber, 2009). Treatment with rapamycin has also been shown to reduce respiration in C2C12 myotubes (Ye et al., 2012).

Conversely, stimulating TORC1 signalling through inhibition of GSK3 β results in rapid (within 30 minutes) stimulation of glucose uptake (Buller et al., 2008). Treatment with rapamycin reduces glucose uptake in U87MG cells *in vitro* and *in vivo* while having no effect in the rapamycin resistant glioma cell line LN-229 (Wei et al., 2008). In L6 myotubes, rapamycin inhibited basal and insulin stimulated glucose uptake, and resulted in increased fatty acid oxidation (Sipula et al., 2006) and rapamycin increases $\Delta\Psi_m$ in MCF-7 cells (Paglin et al., 2005).

The results presented here support the notion that TORC1 signalling promotes glycolysis and suppression of respiration, in glioma cells at least. Inhibition of TORC1 promotes increased respiration by preventing suppression of respiration induced by glucose, i.e. temsirolimus inhibits the Crabtree effect. In the absence of glucose, temsirolimus has no effect on respiration.

How TORC1 regulates glucose metabolism is currently unknown. TORC1 increases expression of glycolysis genes by increasing HIF-1 α expression, and promotes PPP flux and lipid biosynthesis through SREBP1/2 (Duvet et al., 2010), however these mechanisms, based on enhancing transcription and translation, are far too slow to account for the rapid effects on metabolism observed here and elsewhere. Stimulating TORC1 through GSK3 β inhibition promoted a gradual increase in Glut-1 expression over 48 hours, however the maximal effect on glucose uptake was

already evident at the earliest measured time point, 30 minutes following treatment (Buller et al., 2008).

Rapamycin was found to not affect expression or localisation of Glut-1 or Glut-3 in U87MG cells. Further, uptake of 3-OMeG, a glucose analogue that cannot be phosphorylated by hexokinase is not affected by rapamycin treatment, ruling out involvement of glucose transporters in mediating reduced glucose uptake. Hexokinase activity was found to be reduced by more than 60% when measured 24 hours after treatment (Wei et al., 2008).

We found no effect on hexokinase activity at 1 or 3 hours following treatment with temsirolimus despite suppression of glycolysis being achieved well before this time. Therefore the reduced hexokinase activity observed by (Wei et al., 2008) cannot account for the rapid inhibition of glycolysis shown here. It is possible that standard assays of hexokinase activity in cell lysates is a poor reflection of activity in the intact cell. Cell lysis and release of hexokinase into the assay buffer is likely to eliminate allosteric and other regulatory influences (such as intracellular localisation, mitochondrial binding etc.) on hexokinase such that measured activity is proportional only to the amount of enzyme present in the lysate rather than its activity in the intact cell. Therefore acute regulation of hexokinase activity by TORC1 cannot be ruled out.

Our data suggests that temsirolimus also inhibits glucose flux through the oxidative arm of the pentose phosphate pathway. The most direct method for determining flux through this pathway is determined by measuring the release of $^{14}\text{CO}_2$ from 1- ^{14}C -glucose compared to 6- ^{14}C -glucose. Here, activity of the pentose phosphate pathway was inferred from the ability of cells to maintain a high NADPH/NADP^t ratio following a redox insult induced by diamide. While multiple pathways exist for the reduction of NADP⁺ to NADPH, the dependence on glucose to maintain the reduced form suggests heavy reliance on the pentose phosphate pathway in these cells.

Like glucose starvation, treatment with temsirolimus restricted the ability of cells to maintain a high NADPH/NADP^t ratio following treatment with diamide. Branching of glycolysis and the PPP occurs at glucose-6-phosphate. Inhibition of flux through both of these pathways is most simply explained by inhibition upstream of this point, i.e. at glucose transporters or hexokinase, although inhibition at distinct points within each of these pathways cannot be ruled out.

By disrupting redox control, temsirolimus sensitised glioma cells to diamide induced cell death in a manner dependent on glucose concentration. Thiol specific oxidants such as diamide are a research tool only, and not considered to be a viable tool for inducing oxidative stress in tumours. However radiation therapy, which exerts cytotoxic effects beyond direct DNA damage by driving free radical formation and oxidative stress, has been a cornerstone of glioma management for decades.

Rapamycin has been shown to sensitise U87MG cells to fractionated radiation therapy *in vitro*, but only when cells were grown as non-adherent spheroids but not as an adherent monolayer. This synergy of TORC1 inhibition and fractionated radiation also had a powerful growth delaying effect on U87MG xenograft tumours (Eshleman et al., 2002). The authors suggested that restricted diffusion of nutrients into the spheroids, as is the case for tumours *in vivo*, was a key determinant of this synergy. Radiation therapy, like diamide is a major inducer of oxidative stress. The work presented here suggests that inhibition of TORC1 using rapalogs may achieve its synergistic effect with radiation therapy due to its effects on glucose metabolism and redox control.

There has been a great deal of interest in the use of rapalogs for the treatment of glioblastoma. However phase I and II clinical trials have been largely disappointing (Chang et al., 2005, Galanis et al., 2005, Sarkaria et al., 2010). A phase I trial of rapamycin in PTEN deficient tumours showed that while inhibitory drug concentrations can be consistently achieved, partial response is only observed in half (7 of 14) of patients and is strongly associated with reduced TORC1 activity (Cloughesy et al., 2008). Surprisingly, tumour derived cells of resistant tumours regained sensitivity to rapamycin *in vitro* suggesting a non-cell autonomous resistance mechanism. Driving efficient knockdown of

TORC1 activity in patients is therefore a major objective yet to be achieved with mTOR targeting drugs.

Partial response in gliomas treated with the rapalog everolimus can be detected as a reduction in FDG uptake following treatment (Sarkaria et al., 2011), indicating that the effects of TORC1 inhibition on glucose metabolism are recapitulated in the clinical setting. Because TORC1 inhibition is not itself cytotoxic to glioma cells, a proper understanding of the effects of TORC1 inhibitors will be key to designing effective therapeutic strategies using these compounds.

Here we show that inhibition of TORC1 with temsirolimus greatly enhances sensitivity of glioma cells to oxidative stress. This effect is enhanced substantially by reducing glucose availability and explains the observed conditional synergy of fractionated radiation therapy and rapamycin in U87MG cells observed by (Eshleman et al., 2002). Such observations highlight the potential use of TORC1 targeting drugs as neoadjuvants, to be used prior to and during radiation therapy. Evidence presented here suggests that TORC1 inhibition sensitises glioma cells by inhibiting their ability to metabolise glucose. Lowering of blood glucose levels using a ketogenic diet regimen, which has been shown to improve survival in radiation treated glioma mouse models (Abdelwahab et al., 2012), may further enhance this effect. Because of the difficulty of achieving effective inhibition of TORC1 activity in glioma patients, elucidating the downstream metabolic targets of TORC1 is likely to highlight alternative therapeutic avenues of glycolysis inhibition which could be used for adjuvant and neoadjuvant therapy.

References

- ABDELWAHAB, M. G., FENTON, K. E., PREUL, M. C., RHO, J. M., LYNCH, A., STAFFORD, P. & SCHECK, A. C. 2012. The ketogenic diet is an effective adjuvant to radiation therapy for the treatment of malignant glioma. *PLoS One*, 7, e36197.
- BULLER, C. L., LOBERG, R. D., FAN, M. H., ZHU, Q., PARK, J. L., VESELY, E., INOKI, K., GUAN, K. L. & BROSIUS, F. C., 3RD 2008. A GSK-3/TSC2/mTOR pathway regulates glucose uptake and GLUT1 glucose transporter expression. *Am J Physiol Cell Physiol*, 295, C836-43.
- CHANG, S. M., WEN, P., CLOUGHESY, T., GREENBERG, H., SCHIFF, D., CONRAD, C., FINK, K., ROBINS, H. I., DE ANGELIS, L., RAIZER, J., HESS, K., ALDAPE, K., LAMBORN, K. R., KUHN, J., DANCEY, J. & PRADOS, M. D.

2005. Phase II study of CCI-779 in patients with recurrent glioblastoma multiforme. *Invest New Drugs*, 23, 357-61.
- CLOUGHESY, T. F., YOSHIMOTO, K., NGHIEMPHU, P., BROWN, K., DANG, J., ZHU, S., HSUEH, T., CHEN, Y., WANG, W., YOUNGKIN, D., LIAU, L., MARTIN, N., BECKER, D., BERGSNEIDER, M., LAI, A., GREEN, R., OGLESBY, T., KOLETO, M., TRENT, J., HORVATH, S., MISCHER, P. S., MELLINGHOFF, I. K. & SAWYERS, C. L. 2008. Antitumor activity of rapamycin in a Phase I trial for patients with recurrent PTEN-deficient glioblastoma. *PLoS Med*, 5, e8.
- DUVEL, K., YECIES, J. L., MENON, S., RAMAN, P., LIPOVSKY, A. I., SOUZA, A. L., TRIANTAFELLOW, E., MA, Q., GORSKI, R., CLEAVER, S., VANDER HEIDEN, M. G., MACKEIGAN, J. P., FINAN, P. M., CLISH, C. B., MURPHY, L. O. & MANNING, B. D. 2010. Activation of a metabolic gene regulatory network downstream of mTOR complex 1. *Mol Cell*, 39, 171-83.
- ESHLEMAN, J. S., CARLSON, B. L., MLADEK, A. C., KASTNER, B. D., SHIDE, K. L. & SARKARIA, J. N. 2002. Inhibition of the mammalian target of rapamycin sensitizes U87 xenografts to fractionated radiation therapy. *Cancer Res*, 62, 7291-7.
- GALANIS, E., BUCKNER, J. C., MAURER, M. J., KREISBERG, J. I., BALLMAN, K., BONI, J., PERALBA, J. M., JENKINS, R. B., DAKHIL, S. R., MORTON, R. F., JAECKLE, K. A., SCHEITHAUER, B. W., DANCEY, J., HIDALGO, M. & WALSH, D. J. 2005. Phase II trial of temsirolimus (CCI-779) in recurrent glioblastoma multiforme: a North Central Cancer Treatment Group Study. *J Clin Oncol*, 23, 5294-304.
- GWINN, D. M., SHACKELFORD, D. B., EGAN, D. F., MIHAYLOVA, M. M., MERY, A., VASQUEZ, D. S., TURK, B. E. & SHAW, R. J. 2008. AMPK phosphorylation of raptor mediates a metabolic checkpoint. *Mol Cell*, 30, 214-26.
- PAGLIN, S., LEE, N. Y., NAKAR, C., FITZGERALD, M., PLOTKIN, J., DEUEL, B., HACKETT, N., MCMAHILL, M., SPHICAS, E., LAMPEN, N. & YAHALOM, J. 2005. Rapamycin-sensitive pathway regulates mitochondrial membrane potential, autophagy, and survival in irradiated MCF-7 cells. *Cancer Res*, 65, 11061-70.
- RAMANATHAN, A. & SCHREIBER, S. L. 2009. Direct control of mitochondrial function by mTOR. *Proc Natl Acad Sci U S A*, 106, 22229-32.
- RUSSELL, R. C., FANG, C. & GUAN, K. L. 2011. An emerging role for TOR signaling in mammalian tissue and stem cell physiology. *Development*, 138, 3343-56.
- RUVINSKY, I. & MEYUHAS, O. 2006. Ribosomal protein S6 phosphorylation: from protein synthesis to cell size. *Trends Biochem Sci*, 31, 342-8.
- SARKARIA, J. N., GALANIS, E., WU, W., DIETZ, A. B., KAUFMANN, T. J., GUSTAFSON, M. P., BROWN, P. D., UHM, J. H., RAO, R. D., DOYLE, L., GIANNINI, C., JAECKLE, K. A. & BUCKNER, J. C. 2010. Combination of temsirolimus (CCI-779) with chemoradiation in newly diagnosed glioblastoma multiforme (GBM) (NCCTG trial N027D) is associated with increased infectious risks. *Clin Cancer Res*, 16, 5573-80.
- SARKARIA, J. N., GALANIS, E., WU, W., PELLER, P. J., GIANNINI, C., BROWN, P. D., UHM, J. H., MCGRAW, S., JAECKLE, K. A. & BUCKNER, J. C. 2011. North Central Cancer Treatment Group Phase I trial N057K of everolimus (RAD001) and temozolomide in combination with radiation therapy in patients with newly diagnosed glioblastoma multiforme. *Int J Radiat Oncol Biol Phys*, 81, 468-75.
- SCHIEKE, S. M., PHILLIPS, D., MCCOY, J. P., JR., APONTE, A. M., SHEN, R. F., BALABAN, R. S. & FINKEL, T. 2006. The mammalian target of rapamycin (mTOR) pathway regulates mitochondrial oxygen consumption and oxidative capacity. *J Biol Chem*, 281, 27643-52.
- SIPULA, I. J., BROWN, N. F. & PERDOMO, G. 2006. Rapamycin-mediated inhibition of mammalian target of rapamycin in skeletal muscle cells reduces glucose utilization and increases fatty acid oxidation. *Metabolism*, 55, 1637-44.
- TCGA-CONSORTIUM 2008. Comprehensive genomic characterization defines human glioblastoma genes and core pathways. *Nature*, 455, 1061-8.
- WEI, L. H., SU, H., HILDEBRANDT, I. J., PHELPS, M. E., CZERNIN, J. & WEBER, W. A. 2008. Changes in tumor metabolism as readout for Mammalian target of rapamycin kinase inhibition by rapamycin in glioblastoma. *Clin Cancer Res*, 14, 3416-26.
- YE, L., VARAMINI, B., LAMMING, D. W., SABATINI, D. M. & BAUR, J. A. 2012. Rapamycin has a biphasic effect on insulin sensitivity in C2C12 myotubes due to sequential disruption of mTORC1 and mTORC2. *Front Genet*, 3, 177.

Chapter 6 - Inhibition of Respiration with Sorafenib

Table of Figures	198
Introduction.....	199
Results	203
Sorafenib disrupts mitochondrial function in glioma cells	203
High resolution respirometry.....	205
Canonical targets of sorafenib cannot account for effects on mitochondria.....	208
Sorafenib promotes dependence on glycolysis for ATP production	209
Sorafenib synergises with 2-DG to inhibit proliferation in vitro.....	213
Combined Sorafenib and 2-DG treatment of U87MG xenograft tumours.....	217
Discussion	218
References.....	222

Table of Figures

Figure 6.1. Disruption of mitochondrial function in whole cells treated with sorafenib.	204
Figure 6.2. Detailed analysis of mitochondrial function in SF767 cells treated with sorafenib. ...	206
Figure 6.3. Respiration of SF767 cells treated with sorafenib and other tyrosine kinase inhibitors on routine and uncoupled respiration.....	210
Figure 6.4. Sorafenib induced increase in glycolysis blocked by 2-DG	211
Figure 6.5. Synergistic Effect of Sorafenib and 2-Deoxyglucose on Intracellular ATP.....	212
Figure 6.6. Promotion of an autophagic phenotype in U87MG cells with combination treatment.	212
Figure 6.7. Effect of Sorafenib and 2-Deoxyglucose on cell proliferation in U87MG and SF767. .	214
Figure 6.8. Interaction of sorafenib and 2-deoxyglucose on U87MG cell proliferation.....	215
Figure 6.9. Interaction of sorafenib and 2-deoxyglucose on SF767 cell proliferation.....	216
Figure 6.10. U87MG xenograft growth curves with sorafenib and 2-DG treatment.	217

Introduction

Activation of the MAPK signalling cascade is frequently observed in many cancers, often as a result of activating mutations of Ras or Raf family kinases. For instance, virtually all melanomas feature elevated MAPK signalling, frequently driven by B-Raf or N-Ras mutations (Fecher et al., 2008).

The therapeutic potential of targeting this pathway was demonstrated when RNAi suppression of B-Raf resulted in potent growth arrest and apoptosis in mutant B-Raf expressing melanoma cells (Hingorani et al., 2003). MEK inhibition using small molecules similarly resulted in caspase activation and cell death due to de-repression of the pro-apoptotic Bcl-2 member Bad (Eisenmann et al., 2003).

A high throughput screening effort to identify inhibitors of Ras/Raf/MEK/Erk signalling by Bayer and Onyx ultimately lead to the development of Sorafenib, a potent inhibitor of Raf-1 and B-Raf (Lyons et al., 2001). Sorafenib, like the MEK inhibitors PD98059 and U0126 inhibited phosphorylation of Erk leading to repression of Bad in melanoma cells. However unlike MEK inhibitors, sorafenib also promoted polymerisation of Bak and Bax, loss of $\Delta\Psi_m$, nuclear translocation of AIF and caspase independent cell death (Panka et al., 2006). In the lymphoma cell line U937, expression of a constitutively active MEK was unable to prevent the pro-apoptotic effects of sorafenib (Rahmani et al., 2007). These observations demonstrated that sorafenib could induce cell death in cancer cells independent of its effects on MAPK signalling, its rationally designed target, and that sorafenib must be acting through alternative, off target effects.

Several years after its discovery, results were published showing that sorafenib is also a potent inhibitor of a broad range of tyrosine kinases including VEGFR 2 and 3, PDGFR β , c-kit and FLT-3 (Wilhelm et al., 2004). Despite the failure of sorafenib as a therapy for melanoma (Eisen et al., 2006), this broad target specificity suggested that sorafenib may be useful in treating a range of other tumour types.

Initial evaluations of the drug in a mixed patient population with several types of cancer identified renal cell carcinoma (RCC) as responsive to sorafenib (Wilhelm et al., 2006), and the drug was approved by the FDA for treatment of RCC in December 2005 and HCC in November 2007. In both of these tumour types, the therapeutic effectiveness of sorafenib have been attributed to its inhibition of PDGF and VEGF receptors to block tumour angiogenesis, and specifically in HCC, inhibition of Raf to block tumour cell survival and proliferation (Liu et al., 2006, Escudier et al., 2007, Llovet et al., 2008).

A significant side effect experienced by RCC patients treated with sorafenib is cardiac toxicity (Schmidinger et al., 2008). When compared to a number of other tyrosine kinase inhibitors, sorafenib was shown to have a number of distinct effects on mitochondrial function in isolated rat heart mitochondria not seen with other tyrosine kinase inhibitors. At low doses, sorafenib increased basal (state IV) respiration and inhibited state IV and ADP stimulated (state III) respiration at higher concentrations, suggesting that the drug both enhanced proton leak (evident at low concentration) and interfered with electron transport chain (ETC) function (Will et al., 2008).

Enzyme assays for activity of individual immuno-captured ETC complexes revealed IC_{50} values of 31 μ M for complex I NADH oxidase activity, 3 μ M for complex II+III cytochrome c reductase activity, >75 μ M for complex IV cytochrome c oxidase activity and 5.1 μ M for complex V ATPase activity, suggesting that complex II or III as well as complex V were direct targets of sorafenib (Will et al., 2008).

Mounting evidence suggests that effects of mitochondrial function may be relevant to the therapeutic effectiveness of sorafenib in cancer treatment. Sorafenib completely abolished respiration in the HCC cell line PLC/PRF/5 while partially inhibiting respiration in Snu-449 cells. Both of these cell lines became entirely dependent on glycolysis for ATP production, resulting in severe ATP depletion of sorafenib treated cells cultured on galactose instead of glucose, or in the presence of the LDH inhibitor oxamate (Fiume et al., 2011).

Sorafenib was shown to induce a rapid increase in reactive oxygen species (ROS) which plateaued 30 minutes after treatment, depletion of intracellular glutathione, mitochondrial calcium overload and cell death in the radio- and chemo- resistant HCC cell line HepG2 (Chiou et al., 2009). The mechanism of action was not explored, however these observations are consistent with ROS production as a consequence of ETC disruption.

There is some evidence that these mitochondrial effects are also relevant to its therapeutic effectiveness *in vivo*. Elevated serum levels of advanced oxidation protein products (AOPP) in HCC patients treated with sorafenib is predictive of prolonged progression free survival and overall survival. The anti-tumour effects of sorafenib in mouse xenografts can be suppressed with co-administration of the super-oxide dismutase mimetic MnTBAP suggesting ROS generation is an important effector of sorafenib treatment (Coriat et al., 2012).

The mitochondrial effects of sorafenib also appear relevant to other tumour cell types. Sorafenib induced caspase activation and cell death in the neuroblastoma cell line SH-SY5Y. Proteomics analysis of these cells at 0, 12 and 24 hours following sorafenib treatment revealed that a large fraction of proteins down-regulated in response to sorafenib were associated with mitochondrial function, including members of the ETC, mitochondrial ribosomes and proteins involved in mitochondrial translocation. When measured at 12 and 24 hours, sorafenib treatment led to a complete loss of complex I NADH oxidase activity. The authors attributed these effects to a reduction in protein stability of complex I components (Bull et al., 2012).

Sorafenib has been shown to exert anti-proliferative effects on glioma cells *in vitro* and in mouse models (Siegelin et al., 2010). However, as with every other targeted therapy evaluated for high grade glioma, results in the clinic for sorafenib have been disappointing (Hainsworth et al., 2010).

The anti-proliferative effects of sorafenib on glioma cells has been attributed to inhibition of STAT3 signalling, which is frequently up-regulated in glioblastoma (Siegelin et al., 2010). In U87MG

cells, sorafenib did not affect phosphorylation of MAPK and activation of Akt was only partially reduced and only following prolonged exposure to the drug. On the other hand, phosphorylation of STAT3 Tyr705 was robustly inhibited by sorafenib, although the mechanistic pathway was not elucidated (Yang et al., 2010).

Tyrosine phosphorylation of STAT3 is critical for dimerisation and transcription factor activation. Expression of a constitutively dimerised STAT3 mutant was only capable of blocking the anti-proliferative effects of sorafenib by ~20% in glioma cell lines indicating that inhibition of STAT3 transcriptional activity cannot account for the observed anti-proliferative effects of sorafenib (Yang et al., 2010).

STAT3 has another phosphorylation site at Ser727. The phosphorylation state of this site is rarely reported. While serine phosphorylation has only modulatory effects on STAT3 transcriptional activity, this site has been shown to be critical for effects of STAT3 on mitochondrial function. Along with cytoplasm and nucleus, STAT3 is also localised to the mitochondria. In isolated mouse heart cells deficient in STAT3, ETC complex I and II activity are significantly impaired. The phenotype can be rescued with expression of STAT3 mutants lacking the Tyr705 phosphorylation site but not the Ser727 phosphorylation site (Wegrzyn et al., 2009) suggesting serine phosphorylated STAT3 is required for normal mitochondrial function. Mitochondrial STAT3, and the Ser727 site are also required for Ras dependent transformation of fibroblasts. In Ras transformed fibroblasts, loss of STAT3 expression resulted in a dramatic reduction in complex II and complex V activity (Gough et al., 2009).

Limited evidence suggests that sorafenib may be inhibiting STAT3 tyrosine phosphorylation via its effects on PI3K signalling, while affecting serine phosphorylation via its effects on MAPK. In a number of HCC cell lines, sorafenib inhibited phosphorylation of STAT3 at both sites along with Erk1/2 and Akt. MEK inhibition with U0126 specifically inhibited phosphorylation of STAT3 at Ser727, while the PI3K inhibitor LY294002 specifically inhibited phosphorylation of STAT3 at Tyr705 (Gu et al.,

2011). Note that these results are inconsistent with those of (Yang et al., 2010) which indicate a lack of involvement of Akt and particularly MAPK signalling, in glioma cells at least.

In this chapter, we show that mitochondrial function in glioma cells as a target of sorafenib and perform detailed analysis of the electron transport chain to identify which components are ultimately affected by exposure to this drug. Inhibition of the canonical targets of sorafenib do not account for the observed effects. In attempt to achieve a synergistic response, targeting of mitochondrial function with sorafenib is used in conjunction with the glycolysis inhibitor 2-DG.

Results

Sorafenib disrupts mitochondrial function in glioma cells

To characterise the effect of sorafenib on mitochondrial function in glioma cells, respiration of the cell lines U87MG and SF767 was measured using the Seahorse XF Analyser. The XF Analyser measures respiration as the 'oxygen consumption rate' (OCR). Because the XF Analyser allows for up-to four independent injection events, respiration in these cell lines was measured prior to and following injection of sorafenib or vehicle control, followed by oligomycin, FCCP and antimycin A + rotenone. This configuration allowed for the determination of multiple parameters of mitochondrial function as outlined in the schematic in **(Figure 6.1 A)**. Oligomycin blocks the flow of protons through Complex V (ATP synthase), preventing flux through the ETC and oxygen consumption at complex IV. Residual oxygen consumption is a consequence of proton flow through other means such as uncoupling proteins, transhydrogenase, membrane potential dependent transporters and compromised membrane integrity, collectively known as 'proton leak'. Oxygen utilised for production of ATP via the electron transport chain (oxidative phosphorylation, OXPHOS) is indicated as the difference between basal respiration and proton leak. The proton ionophore FCCP allows protons to flow across the inner membrane space (IMM), bypassing ATP synthase and stimulating so

called uncoupled respiration and indicates the maximum flux capacity of the ETC. Finally antimycin and rotenone efficiently inhibit Complex III and Complex I respectively, inhibiting all mitochondrial

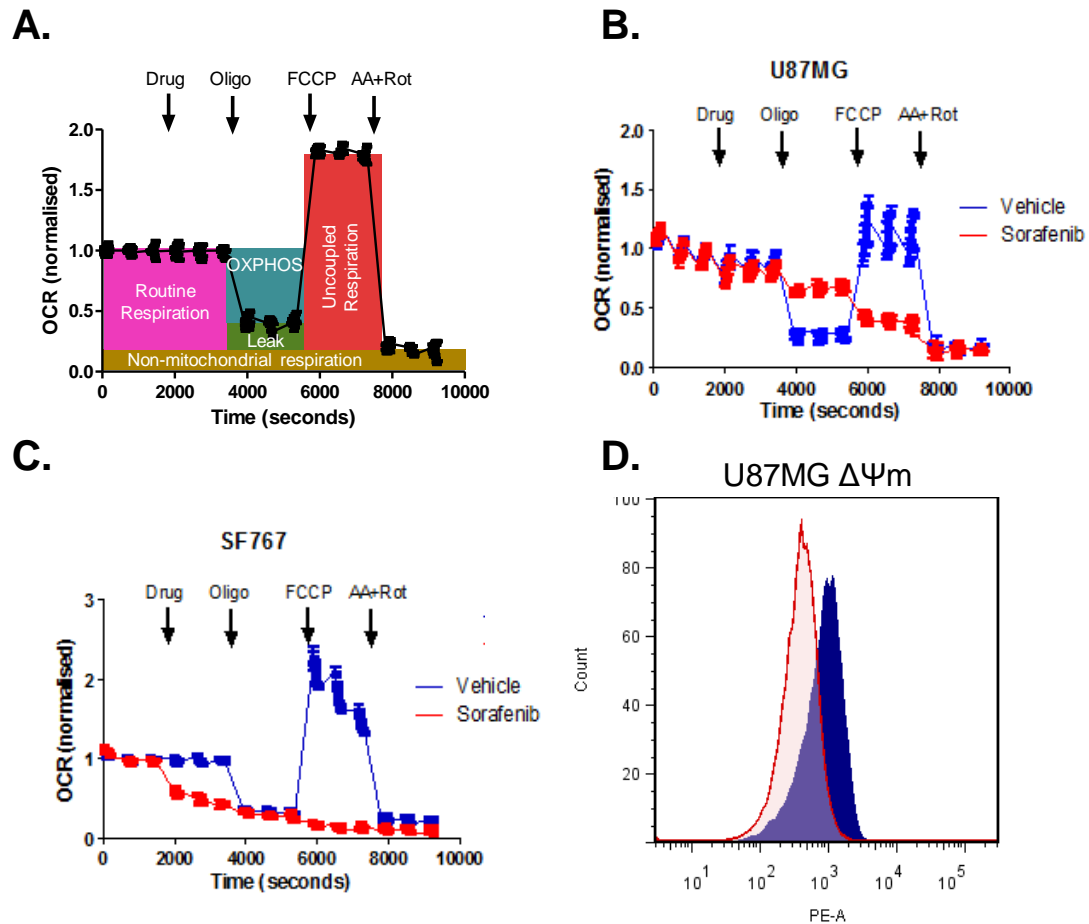


Figure 6.1. Disruption of mitochondrial function in whole cells treated with sorafenib. (A) Measurement of oxygen consumption with sequential addition of different mitochondrial poisons allows for the deduction of various parameters of mitochondrial function **(B, C)** Oxygen consumption rate (OCR) measured in U87MG **(B)** and SF767 **(C)** cells using the Seahorse XF Analyser. OCR was measured for three cycles prior to the addition of any compounds, then for three cycles following by the injection of 5 μM sorafenib or vehicle control (DMSO), 2.5 μM oligomycin, 500 nM FCCP, and 2.5 μM antimycin A plus 2.5 μM rotenone. **(D)** U87MG cells were cultured in the presence of 5 μM sorafenib (red) or vehicle control (blue) for 2 hours. Rhodamine 123 was added to a final concentration of 100 ng/ml for a further 2 hours to allow $\Delta\Psi_m$ dependent uptake of the dye before analysis by flow cytometry.

respiration. Remaining background oxygen consumption is therefore due to non-mitochondrial respiration.

Sorafenib produced slightly different effects on U87MG and SF767 (**Figure 6.1 B, C**). The basal respiration rate of SF767 cells was significantly reduced upon exposure of sorafenib while U87MG was unaffected. The addition of oligomycin demonstrated that 'proton leak' was significantly higher in U87MG cells treated with sorafenib compared to vehicle control, while there was no apparent difference in the SF767 cells.

Stimulation of uncoupled respiration resulted in a large increase in respiration in both cell lines, and was completely blocked by sorafenib treatment in both cell lines. These observations are consistent with sorafenib exerting two effects on mitochondrial function; inhibition of ETC activity, and uncoupling of oxygen consumption from ADP phosphorylation.

Exposure to sorafenib also resulted in dissipation of $\Delta\Psi_m$ in U87MG cells (**Figure 6.1 D**). U87MG cells in standard culture media were treated with 5 μM sorafenib or vehicle control for 1 hour prior to the addition of Rhodamine 123 to a final concentration of 100 ng/ml. After a further 2 hours, cells were harvested for analysis by flow cytometry. At this concentration of Rhodamine 123, $\Delta\Psi_m$ dependent uptake of the fluorescent dye results in increased fluorescence (at much higher concentrations, $\Delta\Psi_m$ dependent dye uptake results in reduced fluorescence due to quenching effects). Treatment with sorafenib reduced Rhodamine 123 fluorescence in U87MG cells, suggesting that this drug leads to loss of mitochondrial membrane potential.

High resolution respirometry

To gain a more detailed understanding of the mitochondrial targets of sorafenib, high resolution respirometry analysis using the Oroboros Oxygraph-2k was performed on digitonin permeabilised SF767 cells (**Figure 6.2**). Preliminary experiments had indicated that respiration of U87MG cells responded poorly to digitonin permeabilisation compared to SF767 cells (data not shown). The

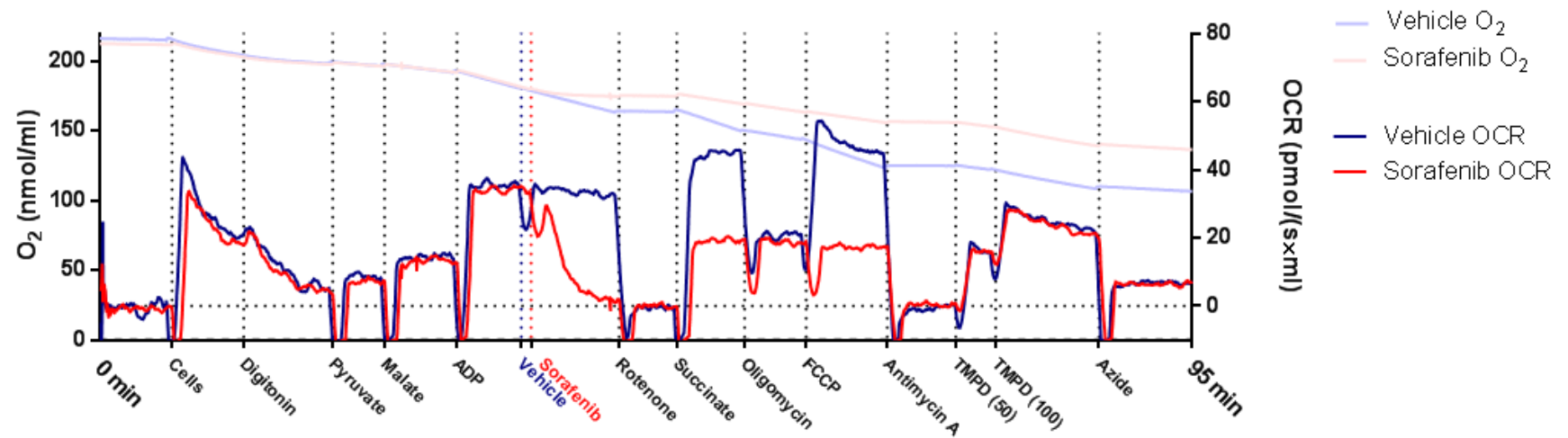


Figure 6.2. Detailed analysis of mitochondrial function in SF767 cells treated with sorafenib. 1.5×10^6 SF767 cells were injected into each oxygraph chamber containing 2 ml of respiration buffer. Cells were permeabilised with 9 μ g digitonin. 5 mM pyruvate, 2 mM malate, and 1 mM ADP were added to each chamber as substrates for complex I dependent, coupled respiration. 5 μ M sorafenib or vehicle control was added to each chamber. 1.25 μ M rotenone and 5 mM succinate were added to inhibit complex I and provide substrate for complex II dependent, coupled respiration. 1.25 μ M oligomycin was added to inhibit ATPsynthase and 500 nM FCCP added to stimulate uncoupled respiration. To inhibit complex III, 1.25 μ M antimycin A was added followed by 100 μ M TMPD as a substrate for complex IV. 40 mM of sodium azide was added to inhibit complex IV activity.

detergent digitonin allows for permeabilisation of the plasma membrane while preserving mitochondrial integrity. This allows for exogenous supply of substrates for specific complexes of the electron transport chain in a way not possible in intact cells.

1.5×10^6 SF767 cells were injected into each chamber of the oxygraph filled with 2 ml of digitonin respiration buffer, with cells respiring on endogenous substrates. The addition of 9 μg digitonin caused a gradual decline in respiration as permeabilisation of the plasma membrane results in loss of endogenous substrates and ADP (State 1). The addition of pyruvate and malate allows for progression of the TCA cycle, generating NADH as substrate for complex I (NADH dehydrogenase). Injection of ADP to 1 mM provides a substrate for complex V (ATP synthase) driving state III, complex I dependent respiration. After obtaining stable respiration in each chamber, vehicle control or sorafenib to a final concentration of 5 μM was added. The addition of sorafenib had an immediate inhibitory effect on respiration, with greater than 90% reduction in OCR approximately six minutes after exposure (**Figure 6.2**).

In order to assess complex II dependent respiration, rotenone (1.25 μM) was added to both chambers to inhibit complex I, and succinate (5 mM) was added as substrate for complex II (succinate dehydrogenase). Succinate stimulated respiration to a slightly higher rate than that seen with pyruvate and malate. Sorafenib treatment blunted complex II dependent respiration to about 45% of that observed in vehicle control treated permeabilised cells.

Effects on dyscoupling were evaluated by determining the respiratory control ratio in sorafenib and vehicle control treated cells. Oligomycin (1.25 μM) inhibits flux through complex V, resulting in state IV_o respiration supported by only proton leak across the inner mitochondrial membrane. The proton ionophore FCCP (500 nM) uncouples respiration from ATP synthase activity, theoretically facilitating maximal mitochondrial respiration, termed state III_u . The respiratory control ratio RCR is calculated from $\frac{\text{state } III_u}{\text{state } IV_o}$ and is a measure of uncoupling. There was considerable day to

day variability in the RCR of control treated cells, which reflects variation in the quality of mitochondria/permeabilised cell preparations, however the observed effects of sorafenib were consistent. In the example trace shown, the RCR was approximately 2.2. Treatment with sorafenib caused permeabilised cells to become non-responsive to oligomycin or FCCP, with a RCR close to 1 indicative of complete mitochondrial uncoupling.

To measure complex IV (Cytochrome c oxidase) activity directly, antimycin A (1.25 μ M) was added to inhibit complex III, followed by the addition of 100 μ M reduced TMPD, which donates electrons directly to cytochrome c, providing a substrate for complex IV. TMPD stimulated oxygen consumption identically in sorafenib and control treated cells suggesting that complex IV is not directly affected by sorafenib. Finally, sodium azide (40 mM) was added to inhibit complex IV for evaluation of non-specific oxygen consumption as a result of TMPD addition.

Using this experimental system, activity of complex I and complex II cannot be ascertained independent of complex III, nor can complex III activity be measured without utilising complex I or complex II to supply complex III with reduced ubiquinone. The following conclusions can be drawn from the above experiment; Complex I+III dependent respiration was completely and Complex II+III dependent respiration was partially inhibited by sorafenib. The activity of complex IV was not affected by sorafenib. Sorafenib caused mitochondria to become completely uncoupled. Due to this uncoupling, the effect on complex V activity cannot be determined.

Canonical targets of sorafenib cannot account for effects on mitochondria

As a multikinase inhibitor, sorafenib has numerous cellular targets. VEGF and PDGF receptors along with Raf family kinases are the best known targets of sorafenib, and their inhibition can lead to suppression of PI3K and MAPK signalling. Basal and uncoupled respiration of SF767 cells was assessed using the Oroboros Oxygraph following the addition of compounds with similar molecular targets.

To evaluate whether any of these targets could account for the effect of sorafenib on mitochondria, basal and uncoupled respiration of SF767 cells was assessed following the addition of compounds with similar molecular targets. Sunitinib inhibits VEGFRs, PDGFRs along with RET, CSF-1R and FLT3 but unlike sorafenib does not target Rafs. PLX4032 on the other hand is a specific inhibitor of Rafs. MAPK signalling was targeted using the MEK1/2 inhibitor U0126, and LY294002 was used to inhibit PI3K.

As was seen earlier, respiration in SF767 cells was robustly inhibited by sorafenib and could not be stimulated by the addition of FCCP (**Figure 6.3 A**). Targeting MAPK with U0126 resulted in only modest inhibition of respiration which was also less responsive to stimulation with FCCP compared to vehicle control (**Figure 6.3 B**). The PI3K inhibitor had no effect on routine or uncoupled respiration (**Figure 6.3 C**), nor did sunitinib or PLX4032 (**Figure 6.3 D**).

Sorafenib promotes dependence on glycolysis for ATP production

In both glioma cell lines, sorafenib causes a significant increase in glycolytic flux, as determined using the pH indicator based H⁺ production assay (**Figure 6.4**). 2-DG was able to significantly reduce glycolytic flux and profoundly blocked sorafenib stimulated glycolysis.

To evaluate the effect of simultaneous inhibition of mitochondrial respiration with sorafenib and glycolysis with 2-DG on cellular ATP, levels of the adenine nucleotide were measured using the Vialight HS kit, which uses ATP content as a proxy for cell viability (**Figure 6.5**). Sorafenib alone had no inhibitory effect on ATP levels, while 2-DG caused a significant drop in both glioma cell lines. The combination of both agents caused a synergistic drop in cellular ATP, far below that predicted by Bliss independence (95% confidence interval, red floating bars).

These treatments also induced morphological changes in both cell lines. This was more easily discerned in U87MG shown in (**Figure 6.6 A**). Sorafenib alone had apparent effect on cell

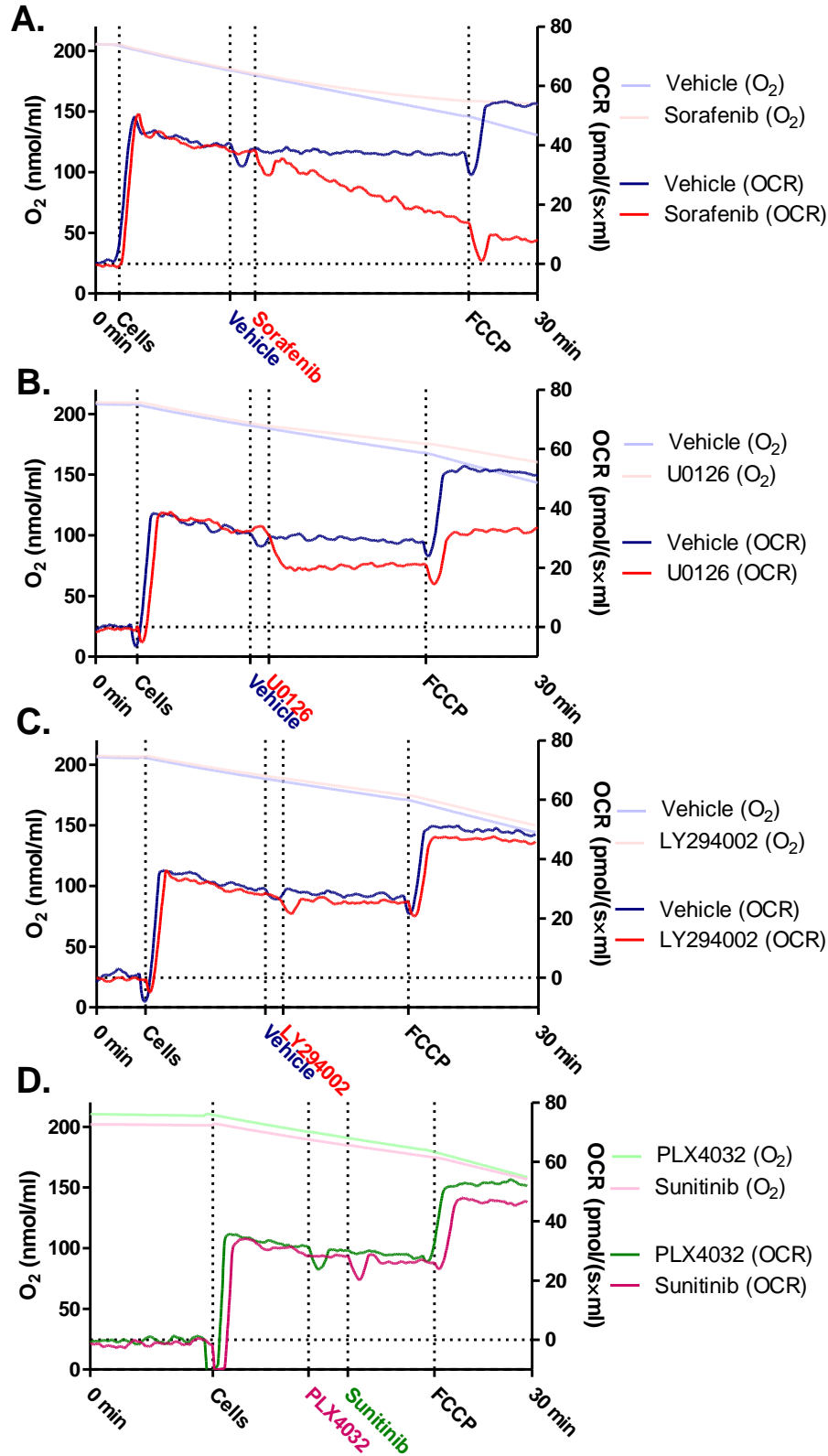


Figure 6.3. Respiration of SF767 cells treated with sorafenib and other tyrosine kinase inhibitors on routine and uncoupled respiration. 1.5×10^6 SF767 cells were injected into each oxygraph chamber containing 2 ml of glucose free DMEM. Cells were treated with inhibitors as indicated, followed by 500 nM FCCP to measure uncoupled respiration. A. 5 μ M Sorafenib and vehicle control. B. 10 μ M U0126 and vehicle control. C. 10 μ M LY294002 and vehicle control. D. 5 μ M PLX4032 and 5 μ M Sunitinib.

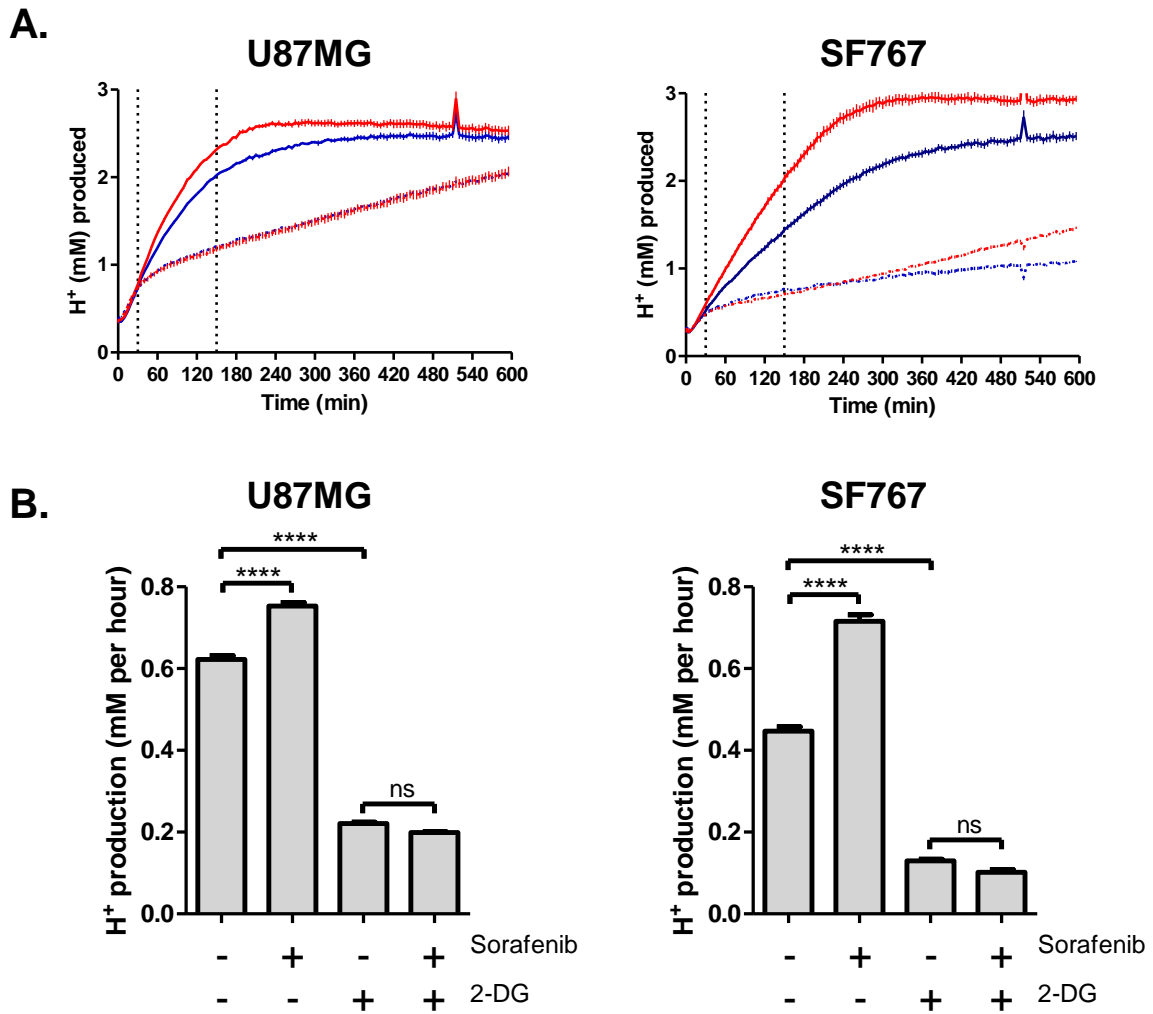


Figure 6.4. Sorafenib induced increase in glycolysis blocked by 2-DG **A.** U87MG and SF767 cells plated at 80,000 cells per well. H⁺ production monitored in assay media containing 17.5 mM glucose with vehicle control (blue) or 5 μM sorafenib (red) in the absence (solid) or presence (dashed) of 2-DG. **B.** Calculated glycolytic rates from 30-150 minutes post treatment.

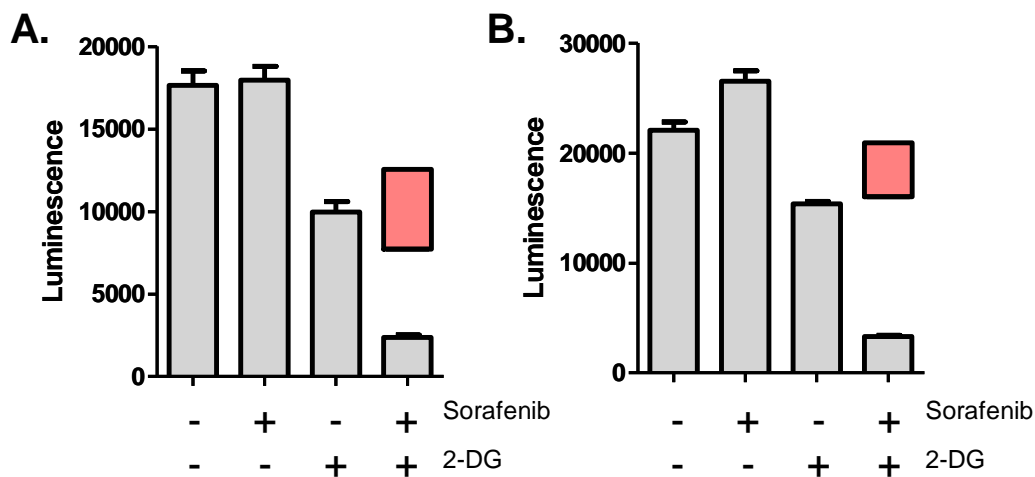


Figure 6.5. Synergistic Effect of Sorafenib and 2-Deoxyglucose on Intracellular ATP. **A.** U87MG cells plated at 10,000 cells per well and **B.** SF767 cells plated at 25,000 cells per well were treated with 5 μ M sorafenib, 25 mM 2-deoxyglucose or a combination of both for 1 hour and intracellular ATP content assessed using Vialight HS kit. The floating bars indicate the effect of both drugs combination, as predicted by Bliss independence to 95% confidence.

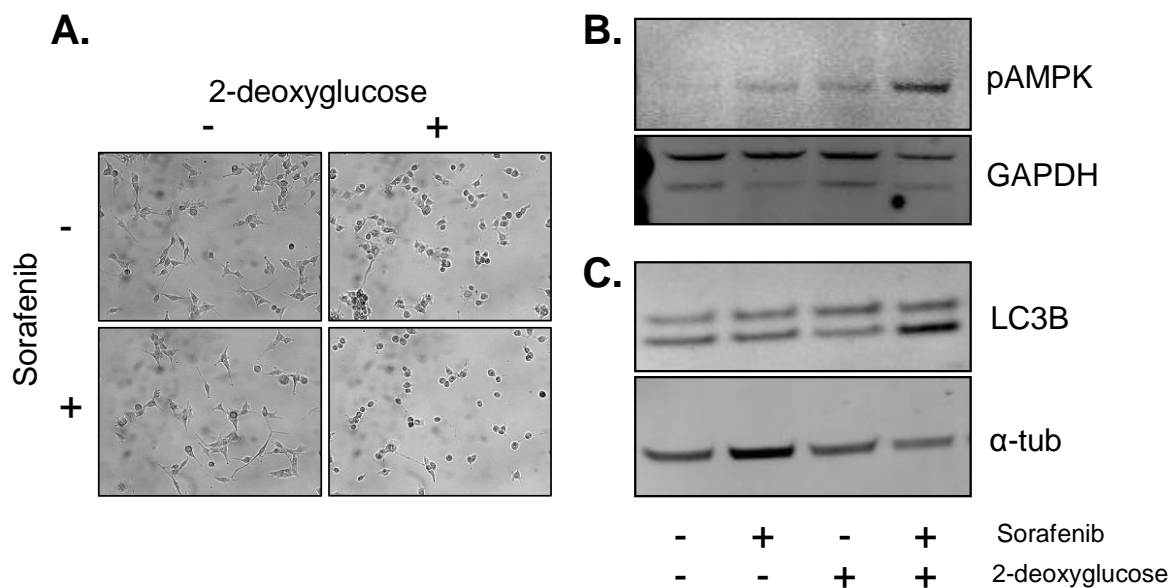


Figure 6.6. Promotion of an autophagic phenotype in U87MG cells with combination treatment. U87MG cells were treated with 5 μ M sorafenib or 25 mM 2-deoxyglucose overnight. **(A)** Brightfield images show changes in cell morphology following treatment. **(B)** Western blot of cell lysates probed for pT172 AMPK, as a marker of AMPK activation, and GAPDH loading control. **(C)** Western blot of cell lysates probed for LC3B, the lower (cleaved) band serving as a marker of autophagy, and α -tubulin loading control.

morphology, while 2-DG treated cells appeared rounded, with thinner dendritic processes than vehicle control treated cells. Combination treatment further promoted these morphological changes.

Suspecting that these morphological changes represent induction of autophagy, cell lysates of U87MG cells treated overnight were used for Western blot analysis of AMPK phosphorylation and LC3B cleavage. AMPK can be activated upon phosphorylation at Thr172 by LKB1 in response to a low ATP/AMP ratio. Treatment with sorafenib or 2-DG alone resulted in very weak phosphorylation of AMPK at Thr172, while both compounds together caused robust activation (**Figure 6.6 B**). Total AMPK was undetectable using an AMPK antibody (not shown).

LC3B is a marker of autophagy induction, becoming cleaved when active. The amount of cleaved LC3B, (lower band) was substantially higher in U87MG cells treated with both compounds (**Figure 6.6 C**), suggesting the combination of both agents, but neither agent alone resulted in induction of autophagy.

Sorafenib synergises with 2-DG to inhibit proliferation in vitro

To assess the effect of 2-deoxyglucose and sorafenib, both alone and in combination on cell proliferation, U87MG and SF767 cells seeded in 96 well plates were cultured for 4 days in the presence of each compound and cell viability assessed using the MTS assay. Both cell lines responded to sorafenib at low micromolar concentrations, and 2-DG at low millimolar concentrations (**Figure 6.7**). Based on these observations, checkerboard combination plates were prepared with the sorafenib concentration ranging from 0.625 μ M to 10 μ M and 2-DG ranging from 0.625 mM to 10 mM and MTS assays were performed after 4 days (**Figure 6.8 and Figure 6.9**).

The dose response curves of both drugs and their combination in each cell line fit well with the Hill model, all showing $r^2 > 0.95$. The Hill coefficient of sorafenib and 2-deoxyglucose were dramatically different, making the exclusivity of the two drugs ambiguous. A mutually non-exclusive interaction was assumed. The CI plots for U87MG and SF767 showed $CI > 1$ for all f_a values above

~0.25 and ~0.45 respectively suggesting that the two drugs were synergistic at higher effect levels. This interpretation is reinforced by isobolograms indicating synergy at IC₅₀, which becomes more apparent at IC₇₅. Bliss independence effect maps also indicated synergy over a range of dose combinations.

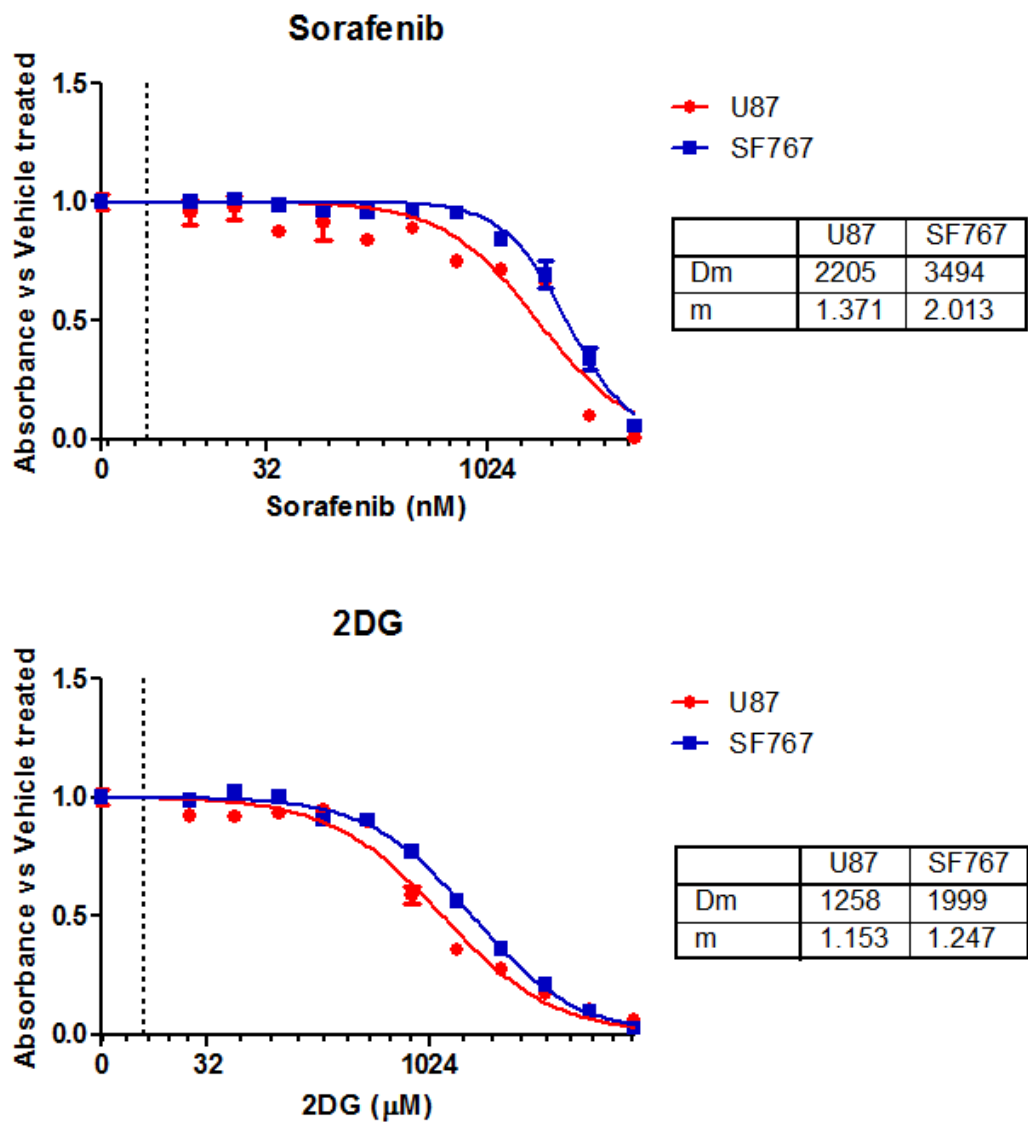


Figure 6.7. Effect of Sorafenib and 2-Deoxyglucose on cell proliferation in U87MG and SF767. U87MG cells plated at 1,000 cells per well and SF767 cells plated at 2,500 cells per well were treated with sorafenib or 2-deoxyglucose for 4 days and proliferation assessed using an MTS assay. Median effect dose (Dm, IC₅₀) and hill coefficient (m) calculated using median effects equation.

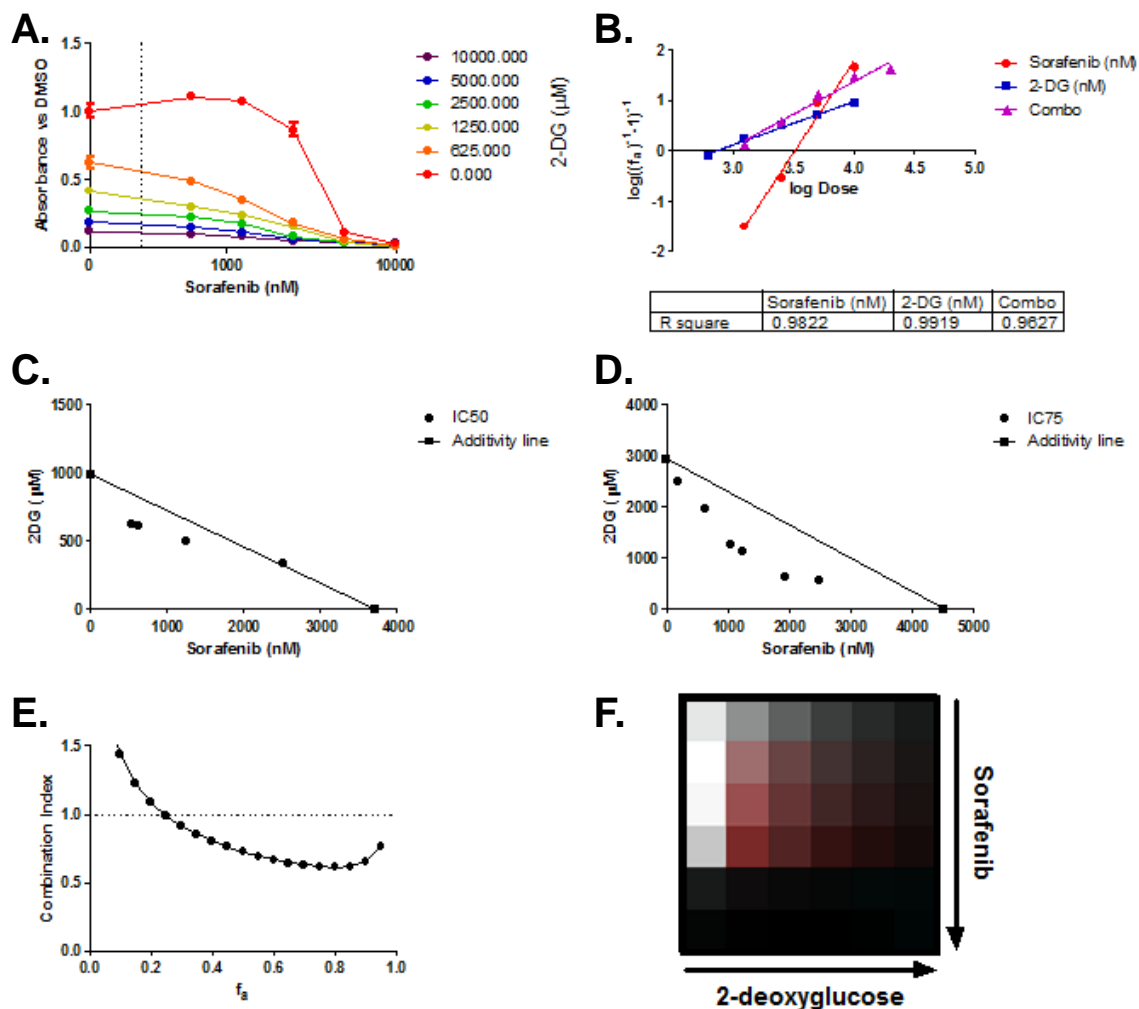


Figure 6.8. Interaction of sorafenib and 2-deoxyglucose on U87MG cell proliferation.

U87MG cells plated at 1,000 cells per well were treated with sorafenib and 2-DG in a checkerboard layout. Cell proliferation was assessed using an MTS assay. **A.** MTS reduction measured by change in absorbance. **B.** Linearisation of dose response curves using the Chou method. **C.** Isobologram at IC₅₀ effect level. **D.** Isobologram at IC₇₅ effect level. **E.** Combination Index plot of sorafenib and 2-DG. **F.** Bliss independence effect map.

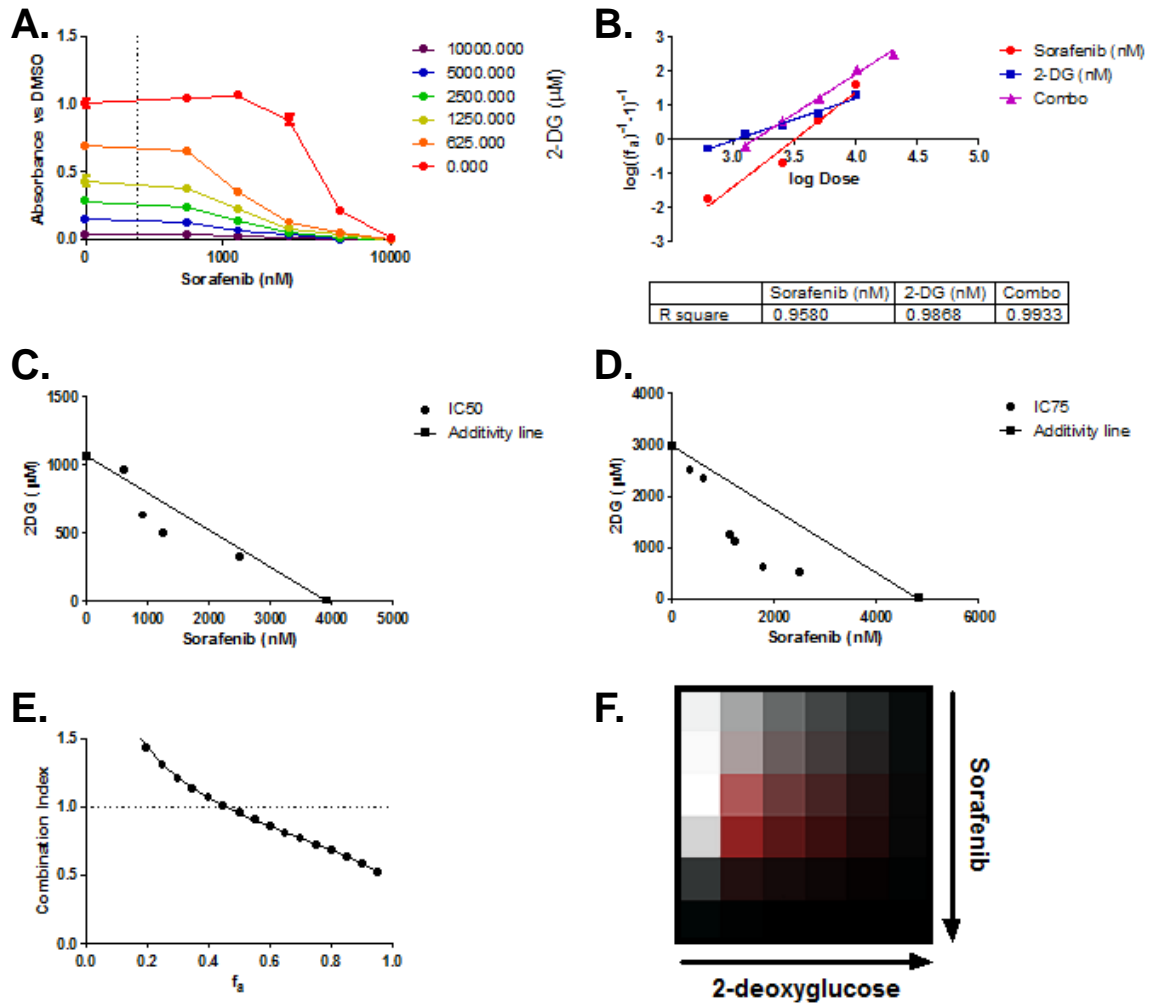


Figure 6.9. Interaction of sorafenib and 2-deoxyglucose on SF767 cell proliferation. U87MG cells plated at 1,000 cells per well were treated with sorafenib and 2-DG in a checkerboard layout. Cell proliferation was assessed using an MTS assay. **A.** MTS reduction measured by change in absorbance. **B.** Linearisation of dose response curves using the Chou method. **C.** Isobologram at IC₅₀ effect level. **D.** Isobologram at IC₇₅ effect level. **E.** Combination Index plot of sorafenib and 2-DG. **F.** Bliss independence effect map.

Combined Sorafenib and 2-DG treatment of U87MG xenograft tumours

Because the combination of sorafenib and 2-DG resulted in a synergistic depletion of cellular ATP and inhibition of proliferation, we evaluated the ability of these two agents to inhibit the growth of U87MG cells grown as xenografts tumours (**Figure 6.10**). Nude mice were injected with 10^6 U87MG cells subcutaneously into each flank. Treatment was initiated upon mean tumour size reaching 100 mm^3 on the 9th day following inoculation. The dosing schedule for 2-DG was based on that of Fath et al., 2009. Mice received 10 mg 2-DG per day (500 mg/kg assuming a weight of 20 g) by intraperitoneal injection, 5 days per week for two weeks. Mice also received either 0.6 mg sorafenib (30 mg/kg) or vehicle control by intraperitoneal injection following the same schedule. Daily injection of 100 mg/kg in mice harbouring intracranial U87MG tumours has been shown previously to completely prevent tumour growth during treatment (Siegelin et al., 2010). A reduced dose of 30 mg/kg was chosen to allow any synergising effect of 2-DG to become apparent.

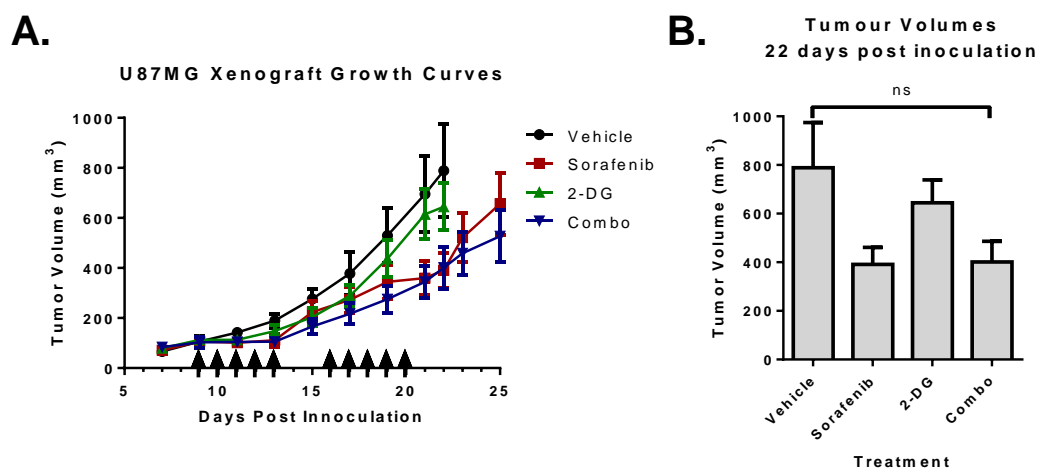


Figure 6.10. U87MG xenograft growth curves with sorafenib and 2-DG treatment. U87MG cells injected subcutaneously into the left and right flanks of nude mice, 10^6 cells per site. Injections of vehicle only (50% PEG400, 10% DMSO), Sorafenib (30 mg/kg/day), 2-DG (500 mg/kg/day) or combination commenced once mean tumour size reached 100 mm^3 , on day 9 post inoculation, and were performed 5 days per week for 2 weeks. 6 mice and up-to 12 tumours in each treatment group. **A.** Mean tumour volumes were determined until any one tumour in a group exceeded 1000 mm^3 at which point the mouse was sacrificed. **B.** Tumour volumes at day 22

Statistical analysis was performed on tumour volumes at day 22, following which mice were progressively sacrificed when tumour volume exceeded 1000 mm³ in accordance with Australian animal welfare guidelines. No treatment reached statistical significance compared to control using one way ANOVA. There was a trend of reduced tumour size in sorafenib treated mice compared to vehicle control (t-test p=0.061).

Discussion

The multikinase inhibitor sorafenib has previously been shown to have antiproliferative effects in a diverse range of cancer cell types including glioma, both *in vitro* and in animal xenograft models (Panka et al., 2006, Rahmani et al., 2007, Wilhelm et al., 2006, Yang et al., 2010, Gu et al., 2011). Because of the multitude of cellular targets, identification of the therapeutically relevant target presents a formidable challenge. In glioma cells, sorafenib has been shown to interfere with STAT3 signalling. However the ability of a constitutively active mutant STAT3 (STAT3-C) to only partially rescue proliferation calls into question the relevance of this target (Yang et al., 2010).

Here we show that sorafenib induces a severe loss of mitochondrial function in glioma cells. Because of the rapid onset of this effect, changes in gene expression or protein levels are unlikely to be driving this effect. As a lipophilic weak acid (Iyer et al., 2010), it is not unreasonable to expect that sorafenib can penetrate through cellular membranes to interact with organelles such as the mitochondria.

Detailed analysis of mitochondrial function using respirometry of digitonin permeabilised glioma cells has revealed multiple sites of inhibition. Respiration driven by complex I+II was completely blocked by sorafenib, while inhibition of complex II+III was partial.

Unfortunately, the current experimental setup did not allow us to determine function of complex III independently of both complex I and II. Both complex I and II supply complex III with

reduced ubiquinone. The addition of exogenous, reduced ubiquinone and/or a ubiquinone reducing system may allow for direct measurement of complex III activity using respirometry.

Sorafenib resulted in complete dyscoupling of mitochondria, which was accompanied by a loss of $\Delta\Psi_m$. It is not possible to determine complex V function in dyscoupled mitochondria using respirometry, however complex V ATPase activity has been shown to be inhibited by concentrations of sorafenib used here (Will et al., 2008).

The most widely recognised targets of sorafenib are RTKs of the PDGFR and VEGFR families, along with members of Raf family kinases (Wilhelm et al., 2006). Targeting a similar set of RTKs using sunitinib or Rafs using PLX-4032 did not elicit a similar response, suggesting that these targets cannot account for the observed effects. These experiments do not explicitly exclude the possibility that these observed effects are dependent on the combination of canonical sorafenib targets.

Because sorafenib has been shown to reduce signalling through both the PI3K/Akt and MAPK signal transduction pathways, the effect of inhibition of each of these pathways was evaluated. Inhibition of PI3K had no effect, while using U0126 to inhibit MAPK signalling had a moderate effect on respiration. Thus inhibition of MAPK may account for some of the mitochondrial effects of sorafenib.

As discussed in the introduction of this chapter, sorafenib has been shown previously to result in perturbations of mitochondrial function. Recently, (Zhao et al., 2013) showed that sorafenib not only induces mitochondrial fragmentation and mitochondrial cytochrome c release in HCC cells, but also in isolated mitochondria purified from such cells, indicating that plasma membrane proteins such as RTKs and cytosolic processes (such as PI3K and MAPK signalling pathways) are not necessary for sorafenib induced mitochondrial dysfunction. Levels of optic atrophy 1 (OPA1, a protein located in on the inner mitochondrial membrane involved in mitochondrial fusion, maintenance of mitochondrial cristae structure and suppression of cytochrome c release) declined rapidly in HCC

cells following sorafenib exposure. Knockdown of OPA1 expression by siRNA before sorafenib treatment resulted in enhanced cytochrome c release, implicating OPA1 as an important participant in sorafenib induced apoptosis (Zhao et al., 2013).

It is probable that down-regulation of OPA1 occurs as a consequence of disruption of mitochondrial respiratory function. Cardiac cells show a loss of OPA1 expression in heart failure. H9c2 embryonic cardiac cells engineered to overexpress OPA1 remain sensitive to ischemia/reperfusion (which results disrupts mitochondrial respiratory function) induced cytochrome c release, loss of mitochondrial tubular morphology and cell death (Chen et al., 2009).

While glioma cells already utilise glucose heavily for ATP production, perturbation of mitochondrial function by sorafenib induced a profound dependence on glycolysis for ATP production, resulting in an increase in the glycolytic rate. Sorafenib used in combination with the glycolysis inhibitor 2-DG resulted in a highly synergistic drop in ATP levels, accompanied by changes in morphology, and molecular indicators of autophagy induction.

Strategies utilising simultaneous targeting of both glycolysis and mitochondrial respiration have been evaluated previously and shown to produce synergistic responses both *in vitro* and *in vivo* (Fath et al., 2009, Fiume et al., 2011). The advantage of using sorafenib as the mitochondria targeting agent is that the drug has already been used in the clinic, both as an approved drug for HCC and RCC, and experimentally in glioma.

Both sorafenib and 2-DG produced dose response curves plateauing at 100% inhibition in cell proliferation assays, enabling the interaction of the two compounds to be evaluated using the checkerboard configuration. While combination index, isobologram and Bliss independence approaches all concluded a synergistic interaction of sorafenib and 2-DG, particularly at higher effect levels, the synergy is perhaps weaker than what would be expected given the substantial effect on cellular ATP levels.

Evaluating the combination of sorafenib and 2-DG in mouse xenografts failed to demonstrate a synergistic interaction *in vivo*. The effect of sorafenib alone was moderate. A sub-optimal dose of sorafenib was deliberately chosen in order to maximise the likelihood of observing an enhancing effect of 2-DG. Treatment with 2-DG had no effect, either alone or in combination with sorafenib. In other studies evaluating 2-DG used in combination with other cancer treatments, the glycolysis inhibitor shows no effect as a single agent. The dosing schedule and dosage of 2-DG used here was the same as that used by others who have demonstrated synergy *in vivo* when simultaneously targeting mitochondrial function (Fath et al., 2009).

While sorafenib is known to have excellent biodistribution *in vivo*, it is not clear whether sorafenib was present in xenograft tumours at a concentration sufficient to disrupt mitochondrial function. Assaying mitochondrial function in tumour explants would reveal whether sorafenib treatment *in vivo* produces the same effect on respiration as *in vitro*. The *in vitro* combination experiments suggested that synergy is greater at higher effect levels. This may mean that a synergistic effect of sorafenib with 2-DG may be more evident at higher dosing schedules.

Unfortunately, the availability of potent and specific inhibitors of glycolytic enzymes is currently quite limited. The alkylating agent 3-Bromopyruvate (3-BrP), while being substantially more potent than 2-DG, is also quite non-specific. While this may make it an inferior to 2-DG as a research tool for inhibiting glycolysis, this reduced specificity may actually enhance the efficacy of the compound as a therapeutic agent. While not a glycolysis inhibitor *per se*, DCA suppresses glycolysis in favour of respiration by increasing activity of PDH. DCA synergises with sorafenib to inhibit the growth of HCC cells both *in vitro* and *in vivo* (Shen et al., 2013).

Here, we identify mitochondrial function as a major site of inhibition in glioma cells by sorafenib. The degree to which the effect of sorafenib on mitochondrial function contributes to the drug's anti-proliferative effect is difficult to assess. Demonstrating that a particular targeted therapy exerts its effects through a particular pathway frequently involves expression of a mutant receptor or signal

transducer that is resistant to inhibition, and observing a reversal of the biological effects. For example, demonstrating that erlotinib inhibits cell proliferation through inhibition of EGFR would require showing that expression of an erlotinib resistant EGFR mutant receptor blocks the anti-proliferative effects of the drug.

Given the multitude of kinases identified as targets of sorafenib, as well as the multiple effects on mitochondrial function, identifying the biologically relevant target will be challenging. The next step will be identifying the mechanism by which sorafenib disrupts mitochondrial function.

While mitochondrial effects of sorafenib were first highlighted as an adverse side effect of the drug and something to be avoided in the development of future targeted therapies, these mitochondrial effects may yet prove to be at least partly responsible for the success of the drug in the clinic where other similar drugs (in terms of primary kinase targets) have failed.

References

- BULL, V. H., RAJALINGAM, K. & THIEDE, B. 2012. Sorafenib-induced mitochondrial complex I inactivation and cell death in human neuroblastoma cells. *J Proteome Res*, 11, 1609-20.
- CHEN, L., GONG, Q., STICE, J. P. & KNOWLTON, A. A. 2009. Mitochondrial OPA1, apoptosis, and heart failure. *Cardiovasc Res*, 84, 91-9.
- CHIOU, J. F., TAI, C. J., WANG, Y. H., LIU, T. Z., JEN, Y. M. & SHIAU, C. Y. 2009. Sorafenib induces preferential apoptotic killing of a drug- and radio-resistant Hep G2 cells through a mitochondria-dependent oxidative stress mechanism. *Cancer Biol Ther*, 8, 1904-13.
- CORIAT, R., NICCO, C., CHEREAU, C., MIR, O., ALEXANDRE, J., ROPERT, S., WEILL, B., CHAUSSADE, S., GOLDWASSER, F. & BATTEUX, F. 2012. Sorafenib-Induced Hepatocellular Carcinoma Cell Death Depends on Reactive Oxygen Species Production in vitro and in vivo. *Mol Cancer Ther*.
- EISEN, T., AHMAD, T., FLAHERTY, K. T., GORE, M., KAYE, S., MARAIS, R., GIBBENS, I., HACKETT, S., JAMES, M., SCHUCHTER, L. M., NATHANSON, K. L., XIA, C., SIMANTOV, R., SCHWARTZ, B., POULIN-COSTELLO, M., O'DWYER, P. J. & RATAIN, M. J. 2006. Sorafenib in advanced melanoma: a Phase II randomised discontinuation trial analysis. *Br J Cancer*, 95, 581-6.
- EISENMANN, K. M., VANBROCKLIN, M. W., STAFFEND, N. A., KITCHEN, S. M. & KOO, H. M. 2003. Mitogen-activated protein kinase pathway-dependent tumor-specific survival signaling in melanoma cells through inactivation of the proapoptotic protein bad. *Cancer Res*, 63, 8330-7.
- ESCUDIER, B., EISEN, T., STADLER, W. M., SZCZYLIK, C., OUDARD, S., SIEBELS, M., NEGRIER, S., CHEVREAU, C., SOLSKA, E., DESAI, A. A., ROLLAND, F., DEMKOW, T., HUTSON, T. E., GORE, M., FREEMAN, S., SCHWARTZ, B., SHAN, M., SIMANTOV, R. & BUKOWSKI, R. M. 2007. Sorafenib in advanced clear-cell renal-cell carcinoma. *N Engl J Med*, 356, 125-34.
- FATH, M. A., DIERS, A. R., AYKIN-BURNS, N., SIMONS, A. L., HUA, L. & SPITZ, D. R. 2009. Mitochondrial electron transport chain blockers enhance 2-deoxy-D-glucose induced oxidative stress and cell killing in human colon carcinoma cells. *Cancer Biol Ther*, 8, 1228-36.
- FECHER, L. A., AMARAVADI, R. K. & FLAHERTY, K. T. 2008. The MAPK pathway in melanoma. *Curr Opin Oncol*, 20, 183-9.

- FIUME, L., MANERBA, M., VETTRAINO, M. & DI STEFANO, G. 2011. Effect of sorafenib on the energy metabolism of hepatocellular carcinoma cells. *Eur J Pharmacol*, 670, 39-43.
- GOUGH, D. J., CORLETT, A., SCHLESSINGER, K., WEGRZYN, J., LARNER, A. C. & LEVY, D. E. 2009. Mitochondrial STAT3 supports Ras-dependent oncogenic transformation. *Science*, 324, 1713-6.
- GU, F. M., LI, Q. L., GAO, Q., JIANG, J. H., HUANG, X. Y., PAN, J. F., FAN, J. & ZHOU, J. 2011. Sorafenib inhibits growth and metastasis of hepatocellular carcinoma by blocking STAT3. *World J Gastroenterol*, 17, 3922-32.
- HAINSWORTH, J. D., ERVIN, T., FRIEDMAN, E., PRIEGO, V., MURPHY, P. B., CLARK, B. L. & LAMAR, R. E. 2010. Concurrent radiotherapy and temozolomide followed by temozolomide and sorafenib in the first-line treatment of patients with glioblastoma multiforme. *Cancer*, 116, 3663-9.
- HINGORANI, S. R., JACOBETZ, M. A., ROBERTSON, G. P., HERLYN, M. & TUVESON, D. A. 2003. Suppression of BRAF(V599E) in human melanoma abrogates transformation. *Cancer Res*, 63, 5198-202.
- IYER, R., FETTERLY, G., LUGADE, A. & THANAVALLA, Y. 2010. Sorafenib: a clinical and pharmacologic review. *Expert Opin Pharmacother*, 11, 1943-55.
- LIU, L., CAO, Y., CHEN, C., ZHANG, X., MCNABOLA, A., WILKIE, D., WILHELM, S., LYNCH, M. & CARTER, C. 2006. Sorafenib blocks the RAF/MEK/ERK pathway, inhibits tumor angiogenesis, and induces tumor cell apoptosis in hepatocellular carcinoma model PLC/PRF/5. *Cancer Res*, 66, 11851-8.
- LLOVET, J. M., RICCI, S., MAZZAFERRO, V., HILGARD, P., GANE, E., BLANC, J. F., DE OLIVEIRA, A. C., SANTORO, A., RAOUL, J. L., FORNER, A., SCHWARTZ, M., PORTA, C., ZEUZEM, S., BOLONDI, L., GRETEN, T. F., GALLE, P. R., SEITZ, J. F., BORBATH, I., HAUSSINGER, D., GIANNARIS, T., SHAN, M., MOSCOVICI, M., VOLIOTIS, D. & BRUIX, J. 2008. Sorafenib in advanced hepatocellular carcinoma. *N Engl J Med*, 359, 378-90.
- LYONS, J. F., WILHELM, S., HIBNER, B. & BOLLAG, G. 2001. Discovery of a novel Raf kinase inhibitor. *Endocr Relat Cancer*, 8, 219-25.
- PANKA, D. J., WANG, W., ATKINS, M. B. & MIER, J. W. 2006. The Raf inhibitor BAY 43-9006 (Sorafenib) induces caspase-independent apoptosis in melanoma cells. *Cancer Res*, 66, 1611-9.
- RAHMANI, M., DAVIS, E. M., CRABTREE, T. R., HABIBI, J. R., NGUYEN, T. K., DENT, P. & GRANT, S. 2007. The kinase inhibitor sorafenib induces cell death through a process involving induction of endoplasmic reticulum stress. *Mol Cell Biol*, 27, 5499-513.
- SCHMIDINGER, M., ZIELINSKI, C. C., VOGL, U. M., BOJIC, A., BOJIC, M., SCHUKRO, C., RUHSAM, M., HEJNA, M. & SCHMIDINGER, H. 2008. Cardiac toxicity of sunitinib and sorafenib in patients with metastatic renal cell carcinoma. *J Clin Oncol*, 26, 5204-12.
- SHEN, Y. C., OU, D. L., HSU, C., LIN, K. L., CHANG, C. Y., LIN, C. Y., LIU, S. H. & CHENG, A. L. 2013. Activating oxidative phosphorylation by a pyruvate dehydrogenase kinase inhibitor overcomes sorafenib resistance of hepatocellular carcinoma. *Br J Cancer*, 108, 72-81.
- SIEGELIN, M. D., RASKETT, C. M., GILBERT, C. A., ROSS, A. H. & ALTIERI, D. C. 2010. Sorafenib exerts anti-glioma activity in vitro and in vivo. *Neurosci Lett*, 478, 165-70.
- WEGRZYN, J., POTLA, R., CHWAE, Y. J., SEPURI, N. B., ZHANG, Q., KOECK, T., DERECKA, M., SZCZEPANEK, K., SZELAG, M., GORNICKA, A., MOH, A., MOGHADDAS, S., CHEN, Q., BOBBILI, S., CICHY, J., DULAK, J., BAKER, D. P., WOLFMAN, A., STUEHR, D., HASSAN, M. O., FU, X. Y., AVADHANI, N., DRAKE, J. I., FAWCETT, P., LESNEFSKY, E. J. & LARNER, A. C. 2009. Function of mitochondrial Stat3 in cellular respiration. *Science*, 323, 793-7.
- WILHELM, S., CARTER, C., LYNCH, M., LOWINGER, T., DUMAS, J., SMITH, R. A., SCHWARTZ, B., SIMANTOV, R. & KELLEY, S. 2006. Discovery and development of sorafenib: a multikinase inhibitor for treating cancer. *Nat Rev Drug Discov*, 5, 835-44.
- WILHELM, S. M., CARTER, C., TANG, L., WILKIE, D., MCNABOLA, A., RONG, H., CHEN, C., ZHANG, X., VINCENT, P., MCHUGH, M., CAO, Y., SHUJATH, J., GAWLAK, S., EVELEIGH, D., ROWLEY, B., LIU, L., ADNANE, L., LYNCH, M., AUCLAIR, D., TAYLOR, I., GEDRICH, R., VOZNESENSKY, A., RIEDL, B., POST, L. E., BOLLAG, G. & TRAIL, P. A. 2004. BAY 43-9006 exhibits broad spectrum oral antitumor activity and targets the RAF/MEK/ERK pathway and receptor tyrosine kinases involved in tumor progression and angiogenesis. *Cancer Res*, 64, 7099-109.
- WILL, Y., DYKENS, J. A., NADANACIVA, S., HIRAKAWA, B., JAMIESON, J., MARROQUIN, L. D., HYNES, J., PATYNA, S. & JESSEN, B. A. 2008. Effect of the multitargeted tyrosine kinase inhibitors imatinib, dasatinib, sunitinib, and sorafenib on mitochondrial function in isolated rat heart mitochondria and H9c2 cells. *Toxicol Sci*, 106, 153-61.
- YANG, F., BROWN, C., BUETTNER, R., HEDVAT, M., STARR, R., SCUTO, A., SCHROEDER, A., JENSEN, M. & JOVE, R. 2010. Sorafenib induces growth arrest and apoptosis of human glioblastoma cells through the dephosphorylation of signal transducers and activators of transcription 3. *Mol Cancer Ther*, 9, 953-62.

ZHAO, X., TIAN, C., PUSZYK, W. M., OGUNWOB, O. O., CAO, M., WANG, T., CABRERA, R., NELSON, D. R. & LIU, C. 2013. OPA1 downregulation is involved in sorafenib-induced apoptosis in hepatocellular carcinoma. *Lab Invest*, 93, 8-19.

Chapter 7 – General Discussion

Modulation of PKM2 in glioma	227
Effects of temsirolimus on glycolysis	231
Effects of sorafenib on mitochondrial respiration.....	232
Combined inhibition of glycolysis and respiration.....	233
References.....	235

The treatment of glioblastoma has seen a slow and modest improvement over the past 50 years, however clinical outcomes remain dismal. The nature of the disease makes glioblastoma highly refractory to the standard surgical modalities of surgery, chemotherapy and radiation therapy. A significant research effort is now dedicated to develop targeted therapies designed to target specific signalling pathways that are dysregulated in glioblastoma. Despite a detailed understanding of the signalling pathways involved and the development of potent inhibitors that effectively disrupt these pathways in model systems, the targeting of signalling pathways in glioblastoma has so far failed to produce any consistent improvements in outcome. Some explanations for this disappointing outcome include a failure of these agents to reach their intended target through the action of the blood brain barrier and drug transporters, innate and acquired resistance to targeted therapeutics, and perhaps most importantly, the complexity and heterogeneity (both across patients and within individual tumours) of the driving mutations that support tumour growth.

A promising alternative approach for the treatment of many cancer types including glioblastoma is to target cancer metabolism. The metabolism of cancer cells is often portrayed as highly distinct to that of normal cells. The cornerstone of cancer metabolism, the Warburg Effect otherwise known as 'aerobic glycolysis', describes how cancer cells have an inherent propensity to produce energy primarily through glycolysis rather than mitochondrial respiration even in the presence of ample oxygen. As described in Chapter 1, an evaluation of the literature reveals that there is surprisingly little experimental evidence in support of the Warburg Effect despite its widespread acceptance in the field. Rather than being cancer specific, aerobic glycolysis is a feature common to all proliferating cells, normal and cancerous alike. Why glycolysis is the preferred mechanism of ATP production in proliferating cells is still a mystery, especially considering the observation that glycolysis, but not respiration is dispensable for proliferation.

Even if assertions of the uniqueness of cancer metabolism are overstated, targeting cancer metabolism remains a viable strategy for cancer therapy. Just like chemotherapy and radiation

therapy are effective cancer treatments because they target rapidly proliferating cells, the potential success of novel metabolism based therapies would likely be due to their ability to perturb the metabolic requirements of proliferating cells in general.

The overall aim of this thesis was to explore the utility of therapeutic interventions targeting cancer cell metabolism. The metabolic effects of three distinct small molecules were described in *in vitro* systems. After describing their immediate effects on metabolism, experiments were performed in an effort to identify potential therapeutic strategies that could be used to exploit these changes in metabolism.

While the serum free cell lines used in Chapter 3 may be more representative of glioma cells *in vivo*, the principles and processes of cancer cell metabolism are likely to be conserved regardless of the culture conditions. Indeed similar metabolic effects of sorafenib and temsirolimus have been observed in a diversity of cancer cell lines (not shown). With this in mind, the FCS based cell lines U87MG and SF767 were used in Chapters 4, 5, and 6 instead of the serum free lines because they are better described in the literature, proliferate much faster and as adherent monolayers.

Modulation of PKM2 in glioma

One of the prime candidate metabolic targets for cancer therapy is the glycolytic enzyme pyruvate kinase M2 (PKM2), considered to be a key mediator of the Warburg Effect. A widely held view in the literature is that a key feature of oncogenesis is the reversion of pyruvate kinase isoforms from the tissue specific adult isoforms (such as PKM1 and PK-L) to the embryonic isoform (PKM2).

Like the Warburg Effect, this core belief is supported by surprisingly little evidence and has been refuted by a significant body of research including recent quantitative analysis at both the transcript (Desai et al., 2013) and protein level (Bluemlein et al., 2011). PKM2 is the dominant PK isoform in not only cancer tissues, but is also the dominant PK isoform in most normal tissues. Unlike its constitutively active splice variant PKM1, PKM2 interacts with a range of proteins that promote post-

translational modifications that lead predominantly promote dissociation of the active tetramer to the inactive dimer. PKM2 also performs roles beyond that of its canonical catalytic role, particularly in its dimeric form, functioning as a transcriptional activator and a protein kinase, which are likely to be important in cancer cell biology.

Expression of high levels of dimeric PKM2 as opposed to PKM2 specific isoform expression per se, does indeed appear to be specific to cancer cells (Eigenbrodt et al., 1997). Expression of PKM2 but not PKM1 is necessary for tumour growth. Critically, exogenous expression of constitutively active PKM1, even in the presence of endogenous PKM2 is sufficient to block tumour growth. Critically, this suggests that gain of function of tetrameric pyruvate kinase (canonical PK activity) rather than loss of function of dimeric PKM2 (non-canonical PKM2 activity) can lead to anti-cancer effects and highlights the potential for PKM2 activation as a therapeutic strategy.

These observations formed the rational basis for the development of a novel PKM2 activator, which was evaluated in Chapter 4. We hypothesised that a variety of biological conditions would lead to changes in tetramer formation and catalytic activity of the enzyme. Further, we anticipated that the pharmacologic activation of PKM2 under conditions that normally induce inactivation would compromise the biology of the cancer cell in a manner specific to the PKM2 inactivating conditions.

As expected, PKM2 tetramer formation was highly dependent on glucose concentration. This can be explained by allosteric regulation of PKM2 by the glycolytic intermediate F-1,6-BP. Of note, significant levels of tetrameric PKM2 were only observed above 4.4 mM glucose, i.e. at supra-physiological concentrations of glucose. Standard culture media such as DMEM typically contains 17.5 mM glucose, a concentration which would be considered extremely hyperglycaemic *in vivo*. At this glucose concentration, which would be used by the majority of cancer biologists, PKM2 activation is probably far higher than would be the case under more physiologically relevant conditions.

PKM2 was primarily dimeric in proliferating U87MG cells, while growth arrested cells showed a higher fraction of the active tetrameric enzyme. This suggested that dimeric PKM2 is important for cell proliferation. However pharmacologic activation had no observable impact on cell cycle or proliferation. This is consistent with the findings of others, who have shown that PKM2 activity has no impact on proliferation under highly facultative conditions *in vitro*.

Under all conditions evaluated in this study, the PKM2 activator WAY677099 was able to induce robust formation of catalytically active tetrameric PKM2 except in cells deprived entirely of glucose for a prolonged period. If similar conditions occur *in vivo*, such as within specific tumour niches, tumour cells may be able to escape PKM2 activation by WAY677099 or similar compounds.

Exposure to oxidative stress resulted in PKM2 inactivation, suggesting that this is an adaptive response to promote survival during potentially harmful conditions. Inactivation during oxidative stress is believed to promote survival by redirecting flux to the pentose phosphate pathway to drive regeneration of NADPH. However again we were unable to demonstrate any compounding effects of pharmacologic PKM2 activation and exposure to oxidative stress on cell survival or NADPH regeneration.

The effect of PKM2 activation on aerobic glycolysis was also evaluated. While there are no obvious implications for therapeutic potential of PKM2 activators by exploring these effects, aerobic glycolysis is considered to be a cornerstone of cancer biology and dimeric PKM2 is frequently cited as a key mediator of this phenomenon. How suppressed activity of a rate limiting enzyme of glycolysis can lead to increased glycolysis and decreased respiration (conversely increasing enzyme activity suppresses glycolysis and increases respiration) is a paradox that is difficult to explain.

The results presented here remove the paradox by showing that increasing activity of the enzyme does not in fact shift energy production from glycolysis to respiration but in fact does the

opposite. This is in line with what one would predict based on our current understanding of the relationship of glycolysis and respiration.

However upon further interrogation, this understanding could not account for the decrease in respiration observed. The predominant explanation for the Crabtree effect posits that glycolysis and respiration are mutually exclusive processes, in that they are both rate limited by demand for ATP (or supply of ADP) and this mutual exclusivity can be ameliorated by uncouplers such as FCCP. Here, FCCP could not reverse the suppression of respiration induced by PKM2 activation. Further, the suppression of respiration by PKM2 activation was most profound in the absence of glucose. Therefore, although the effect of PKM2 activation on respiration is in line with what one may logically expect, the logical explanation is insufficient to account for the effects observed.

Here we were unable to demonstrate any therapeutically useful effects of pharmacologic PKM2 activation. Another group has shown therapeutic efficacy of PKM2 activators, including *in vivo* (Anastasiou et al., 2012). Of course it is always possible that differing results are due to differences in cell lines, experimental conditions or differing behaviour of experimental compounds.

However it should be noted that this group has also uniquely observed PKM1/PKM2 isoform switching during breast cancer development (Christofk et al., 2008), inconsistent with the results of others showing no PKM1/PKM2 isoform switching in breast cancer (Bluemlein et al., 2011, Ibsen et al., 1982, Desai et al., 2013)).

The same group also uniquely demonstrated that increasing pyruvate kinase activity (through PKM1 over-expression or other means) leads to reduced glycolysis and increased respiration (Christofk et al., 2008, Hitosugi et al., 2009, Anastasiou et al., 2012), in contrast to the results of many others who have shown that PKM1 expression or other means of increasing pyruvate kinase activity leads to increased glycolysis and reduced respiration (Gosalvez et al., 1975, Gruning et al., 2011, Chen et al., 2012, Kosugi et al., 2011, Chen et al., 2011, Chiavarina et al., 2011). Despite the

majority of evidence demonstrating the contrary, the dominant view in the literature is that low PKM2 activity promotes aerobic glycolysis, while high PKM2 activity promotes respiration (Wong et al., 2013). Perhaps the data presented here will help to correct this misconception that PKM2 inactivity promotes aerobic glycolysis.

Effects of temsirolimus on glycolysis

Regardless of the controversy surrounding PKM2 and aerobic glycolysis in cancer, and despite no convincing explanation as to why proliferating cells undergo aerobic glycolysis, the glycolytic pathway remains a promising target for cancer therapy. Unfortunately the number of agents that can effectively inhibit glucose metabolism is rather limited. As shown in Chapter 5, inhibition of glycolysis may be an important mechanism of action for the TORC1 targeting drug Temsirolimus.

The effects of temsirolimus on glycolysis were initially identified while testing small molecule inhibitors for effects on PKM2 tetramer formation. Treatment with temsirolimus resulted in suppression of PKM2 tetramer formation and catalytic activity, and also robustly inhibited glycolysis. Treatment with WAY677099 restored PKM2 activity but did not restore glycolysis, indicating that loss of PKM2 activity was a consequence and not the cause of glycolysis inhibition by temsirolimus. We were unable to identify the specific point of inhibition along the glycolysis pathway, however the data presented suggests that this point lies above the branch-point of glycolysis and the oxidative arm of the pentose phosphate pathway.

While rapalogs such as temsirolimus are considered to be highly specific to inhibition of TORC1 via binding to the TORC1 antagonist FKBP12, our results do not exclude the possibility that Temsirolimus is inhibiting glycolysis independently of its actions on TORC1. One method for evaluating this possibility would be to silence expression of FKBP12 in glioma cells using siRNA. This would render TORC1 insensitive to inhibition by rapalogs. Thus any continued inhibition of glycolysis would suggest effects independent of TORC1 inhibition.

In Chapter 4, it was shown that the availability of glucose was a major determinant in the sensitivity of U87 cells to oxidative stress induced cell death. Treatment with temsirolimus, like glucose withdrawal, potentially sensitised U87 cells to the oxidative stress induced by diamide resulting in perturbations in NADPH levels followed by cell death. The use of diamide was a proxy for oxidative stress induced by radiation therapy.

These results have implications for the manner in which temsirolimus can be used for glioma therapy. Clinical trials involving a novel cancer therapeutic typically involve complementing the experimental treatment with the standard of care therapy. In the case of temsirolimus, the likelihood of observing a synergistic effect may be improved by treating with temsirolimus before and during radiation therapy such that its effects on glycolysis and sensitivity to oxidative stress are being exerted during the radiotherapy course.

Effects of sorafenib on mitochondrial respiration

Like temsirolimus, our investigation into the metabolic effects of sorafenib in glioma cells also originated from preliminary experiments investigating factors influencing PKM2 function in Chapter 4. Raf family kinases have previously been implicated in regulation of PKM2, leading us to evaluate the effect of sorafenib, a known inhibitor of Raf family kinases on PKM2 tetramer formation. Treatment of U87 cells with sorafenib promoted a dramatic reduction in tetrameric PKM2, while PLX4032, a potent and more specific inhibitor of Raf family kinases had no effect (data not shown). Also apparent was an increased acidification of culture media from U87 cells treated with sorafenib suggestive of an increased rate of glycolysis. These initial observations prompted us to further investigate the effects of sorafenib on glioma cells.

Exposure of glioma cells to sorafenib had immediate and profound effects on mitochondrial function. These effects were complex and were not similar to any other described mitochondrial poison. Collapse of $\Delta\Psi_m$ and the loss of responsiveness of sorafenib treated cells and mitochondria to oligomycin and FCCP indicate complete uncoupling of mitochondria. Further, complex I and III as

well as complex II and III dependent respiration was compromised. It would be expected that mitochondria under such conditions would be completely incapable of ATP generation. Indeed sorafenib treated glioma cells were entirely reliant on glycolysis for ATP generation.

The MEK inhibitor U0126 had some effect on respiration in SF767 cells suggesting that at least some, but certainly not all of the effects of sorafenib on mitochondrial respiration are governed by the MAPK signalling pathway.

While the data presented in Chapter 6 convincingly demonstrates that mitochondrial function is severely compromised by sorafenib, these results do not explicitly demonstrate that mitochondrial effects are responsible for the anti-proliferative effects of the drug. One approach to evaluate this would be to generate U87MG cells lacking functional mitochondria through chronic ethidium bromide exposure, so-called p^0 cells. A precedent of this approach can be found in the literature; the proliferation of p^0 yeast cells was shown to be unaffected by mitochondria targeting compounds including antimycin A that profoundly affect the proliferation of wild-type, mitochondrially competent yeast cells (Kemmer et al., 2009).

Combined inhibition of glycolysis and respiration

Because of the profound impact of sorafenib on mitochondrial function and the reliance of treated glioma cells on glycolysis for ATP production, we anticipated that the combination of sorafenib with a glycolysis inhibitor would result in a strong synergistic response. Along with a collapse in cellular ATP levels, sorafenib in combination with the glycolysis inhibitor 2-DG caused a significant change in cell morphology. Activation of AMPK as well as cleavage of LC3B indicated that cells were responding to energetic stress through activation of autophagy. The combination of these agents produced a synergistic response in inhibiting the proliferation of glioma cells *in vitro*.

Induction of autophagy is known to be a survival mechanism that can allow glioma cells to survive anti-cancer therapy (Fan et al., 2010). It is possible that the addition of an autophagy inhibitor may be able to potentiate the effectiveness of this combination.

Simultaneous inhibition of respiration and glycolysis was presented as a potential cancer therapy in Warburg's original landmark publication (Warburg et al., 1927), and since then others have demonstrated the feasibility of this approach *in vitro* and in animal models. Two clinically approved drugs, temsirolimus and sorafenib have been shown here to potently inhibit glycolysis and respiration respectively in glioma cells making them obvious candidates for combination therapy in glioblastoma.

The combination of these drugs was recently evaluated in a phase I/II clinical trial. Unfortunately the maximum tolerated dosage (MTD) of temsirolimus was extremely low (25 mg, once weekly vs. 170-250 mg, once weekly as a single agent) when used in combination with sorafenib (800 mg, daily) due to high grade thrombocytopenia. When used at MTD, the combination of these drugs had minimal activity (Lee et al., 2012).

As both temsirolimus and sorafenib exhibit effects on both cell signalling and metabolism, it is possible that anti-tumour activity and dose limiting toxicities of each drug are governed by distinct mechanisms of action. For instance, the anti-cancer effect of sorafenib may be primarily mediated by mitochondrial effects, while its toxicity due to cell signalling inhibition or vice versa. Derivatives of each compound that retain only their cell signalling or metabolism effects could hopefully allow one to distinguish the therapeutically relevant mechanism of action *in vivo*, and may also display a distinct toxicity profile. This may allow such derivatives to be used at elevated dosages in patients and may even allow their use in combination without the toxic interaction observed with the parent compounds.

References

- ANASTASIOU, D., YU, Y., ISRAELSEN, W. J., JIANG, J. K., BOXER, M. B., HONG, B. S., TEMPEL, W., DIMOV, S., SHEN, M., JHA, A., YANG, H., MATTAINI, K. R., METALLO, C. M., FISKE, B. P., COURTNEY, K. D., MALSTROM, S., KHAN, T. M., KUNG, C., SKOUMBOURDIS, A. P., VEITH, H., SOUTHALL, N., WALSH, M. J., BRIMACOMBE, K. R., LEISTER, W., LUNT, S. Y., JOHNSON, Z. R., YEN, K. E., KUNII, K., DAVIDSON, S. M., CHRISTOFK, H. R., AUSTIN, C. P., INGLESE, J., HARRIS, M. H., ASARA, J. M., STEPHANOPOULOS, G., SALITURO, F. G., JIN, S., DANG, L., AULD, D. S., PARK, H. W., CANTLEY, L. C., THOMAS, C. J. & VANDER HEIDEN, M. G. 2012. Pyruvate kinase M2 activators promote tetramer formation and suppress tumorigenesis. *Nat Chem Biol*.
- BLUEMLEIN, K., GRUNING, N. M., FEICHTINGER, R. G., LEHRACH, H., KOFLER, B. & RALSER, M. 2011. No evidence for a shift in pyruvate kinase PKM1 to PKM2 expression during tumorigenesis. *Oncotarget*, 2, 393-400.
- CHEN, J., JIANG, Z., WANG, B., WANG, Y. & HU, X. 2012. Vitamin K(3) and K(5) are inhibitors of tumor pyruvate kinase M2. *Cancer Lett*, 316, 204-10.
- CHEN, J., XIE, J., JIANG, Z., WANG, B., WANG, Y. & HU, X. 2011. Shikonin and its analogs inhibit cancer cell glycolysis by targeting tumor pyruvate kinase-M2. *Oncogene*, 30, 4297-306.
- CHIAVARINA, B., WHITAKER-MENEZES, D., MARTINEZ-OUTSCHOORN, U. E., WITKIEWICZ, A. K., BIRBE, R., HOWELL, A., PESTELL, R. G., SMITH, J., DANIEL, R., SOTGIA, F. & LISANTI, M. P. 2011. Pyruvate kinase expression (PKM1 and PKM2) in cancer-associated fibroblasts drives stromal nutrient production and tumor growth. *Cancer Biol Ther*, 12, 1101-13.
- CHRISTOFK, H. R., VANDER HEIDEN, M. G., HARRIS, M. H., RAMANATHAN, A., GERSZTEN, R. E., WEI, R., FLEMING, M. D., SCHREIBER, S. L. & CANTLEY, L. C. 2008. The M2 splice isoform of pyruvate kinase is important for cancer metabolism and tumour growth. *Nature*, 452, 230-3.
- DESAI, S., DING, M., WANG, B., LU, Z., ZHAO, Q., SHAW, K., YUNG, W. K., WEINSTEIN, J. N., TAN, M. & YAO, J. 2013. Tissue-specific isoform switch and DNA hypomethylation of the pyruvate kinase PKM gene in human cancers. *Oncotarget*.
- EIGENBRODT, E., BASENAU, D., HOLTHUSEN, S., MAZUREK, S. & FISCHER, G. 1997. Quantification of tumor type M2 pyruvate kinase (Tu M2-PK) in human carcinomas. *Anticancer Res*, 17, 3153-6.
- FAN, Q. W., CHENG, C., HACKETT, C., FELDMAN, M., HOUSEMAN, B. T., NICOLAIDES, T., HAAS-KOGAN, D., JAMES, C. D., OAKES, S. A., DEBNATH, J., SHOKAT, K. M. & WEISS, W. A. 2010. Akt and autophagy cooperate to promote survival of drug-resistant glioma. *Sci Signal*, 3, ra81.
- GOSALVEZ, M., LOPEZ-ALARCON, L., GARCIA-SUAREZ, S., MONTALVO, A. & WEINHOUSE, S. 1975. Stimulation of tumor-cell respiration by inhibitors of pyruvate kinase. *Eur J Biochem*, 55, 315-21.
- GRUNING, N. M., RINNERHALER, M., BLUEMLEIN, K., MULLEDER, M., WAMELINK, M. M., LEHRACH, H., JAKOBS, C., BREITENBACH, M. & RALSER, M. 2011. Pyruvate kinase triggers a metabolic feedback loop that controls redox metabolism in respiring cells. *Cell Metab*, 14, 415-27.
- HITOSUGI, T., KANG, S., VANDER HEIDEN, M. G., CHUNG, T. W., ELF, S., LYTHGOE, K., DONG, S., LONIAL, S., WANG, X., CHEN, G. Z., XIE, J., GU, T. L., POLAKIEWICZ, R. D., ROESEL, J. L., BOGGON, T. J., KHURI, F. R., GILLILAND, D. G., CANTLEY, L. C., KAUFMAN, J. & CHEN, J. 2009. Tyrosine phosphorylation inhibits PKM2 to promote the Warburg effect and tumor growth. *Sci Signal*, 2, ra73.
- IBSEN, K. H., ORLANDO, R. A., GARRATT, K. N., HERNANDEZ, A. M., GIORLANDO, S. & NUNGARAY, G. 1982. Expression of multimolecular forms of pyruvate kinase in normal, benign, and malignant human breast tissue. *Cancer Res*, 42, 888-92.
- KEMMER, D., MCHARDY, L. M., HOON, S., REBERIOUX, D., GIAEVER, G., NISLOW, C., ROSKELLEY, C. D. & ROBERGE, M. 2009. Combining chemical genomics screens in yeast to reveal spectrum of effects of chemical inhibition of sphingolipid biosynthesis. *BMC Microbiol*, 9, 9.

- KOSUGI, M., AHMAD, R., ALAM, M., UCHIDA, Y. & KUFE, D. 2011. MUC1-C oncoprotein regulates glycolysis and pyruvate kinase M2 activity in cancer cells. *PLoS One*, 6, e28234.
- LEE, E. Q., KUHN, J., LAMBORN, K. R., ABREY, L., DEANGELIS, L. M., LIEBERMAN, F., ROBINS, H. I., CHANG, S. M., YUNG, W. K., DRAPPATZ, J., MEHTA, M. P., LEVIN, V. A., ALDAPE, K., DANCEY, J. E., WRIGHT, J. J., PRADOS, M. D., CLOUGHESY, T. F., GILBERT, M. R. & WEN, P. Y. 2012. Phase I/II study of sorafenib in combination with temsirolimus for recurrent glioblastoma or gliosarcoma: North American Brain Tumor Consortium study 05-02. *Neuro Oncol*, 14, 1511-8.
- WARBURG, O., WIND, F. & NEGELEIN, E. 1927. The Metabolism of Tumors in the Body. *J Gen Physiol*, 8, 519-30.
- WONG, N., DE MELO, J. & TANG, D. 2013. PKM2, a Central Point of Regulation in Cancer Metabolism. *Int J Cell Biol*, 2013, 242513.